

Advanced Nuclear Fuel Cycle Systems Analyses for FY 2002

C. G. Bathke^(a), R. A. Krakowski^(a), H. R. Trellue^(b),
A. M. Spearing^(c), and C. M. Lovejoy^(d)

Los Alamos National Laboratory
Los Alamos, New Mexico 87545
25 October 2002

^(a)Group D-3, Systems Engineering and Integration

^(b)Group D-10, Nuclear Systems Design and Analysis

^(c)Group CNC-12, Scientific Software Engineering

^(d)Group AFC-TDO, AFC Technology Development Office

This page is intentionally left blank.

TABLE OF CONTENTS

ABSTRACT	v
1 OVERVIEW.....	1
2 DELTA EQUILIBRIUM NFC MODEL	5
2.1 Overview	5
2.2 Summary Results.....	11
2.3 NFC Scenario Down Selection	12
3 FCOPT OPTIMIZATION MODEL.....	15
3.1 Model Description.....	15
3.1.1 General Considerations	15
3.1.2 Specific Considerations.....	19
3.1.2.1 Objective Functions.....	20
3.1.2.1.1 Cost-Based Objective Function.....	20
3.1.2.1.2 Proliferation Risk Objective Function.....	20
3.1.2.2 Constraints.....	22
3.2 Interim Results	23
3.2.1 Scope of Analyses	23
3.2.2 Parametric Results.....	25
3.2.2.1 Time Evolution of Generation Mixes and Key Material Inventories and Flows Rates	29
3.2.2.2 Cost and Capacity of Interim SNF Storage (<i>is</i>).....	33
3.2.2.3 Cost and Capacity of Direct-Disposal Repository (<i>dd</i>).....	39
3.2.2.4 Cost and Capacity for Reprocessing (<i>rp</i>)	43
3.2.2.5 Optimizations that Reduce Proliferation Risk <i>versus</i> Cost	47
3.2.2.6 Capital Cost and Generation Mix.....	49
3.3 Summary Conclusions and Future Work	54
4 nuclear fuel cycle SIMULATION (NFCsim) MODEL	55
4.1 Introduction	55
4.2 Model Description.....	55
4.2.1 Object-Oriented Aspects of the Model.....	56
4.2.2 Simulation Aspects of the Model	59
4.3 Interim Results	64
4.3.1 Scenarios	64
4.3.2 Nuclear Phase-Out Scenario.....	64
4.3.3 Nuclear Resurgence Scenario.....	68
4.4 Summary Conclusions and Future Work	71
5 NEUTRONIC ANALYSES.....	73
5.1 Model Development.....	73
5.2 Results	76
5.2.1 Multi-Recycling MOX Fuel.....	78
5.2.2 Addition of Actinide Material Other Than Plutonium to MOX.....	81
5.2.3 Performance of ADS with Various Feed Streams.....	84
5.3 Coupling of Neutronics with NFC Simulation Model NFCSim	88
6 Waste Separation to Benefit Repository Capacity	91
6.1 The Present YM “Viability Assessment” Design	91

6.2	Separating Waste to Benefit Repository Capacity	92
6.3	Summary of Calculations	94
6.4	Results	98
6.5	Handling of Separated Wastes	102
6.6	Economics of Increasing Repository Capacity	103
6.7	Conclusions	106
7	SUMMARY AND FUTURE DIRECTIONS	107
7.1	Model Integration	107
7.2	Future Directions	109
7.2.1	DELTA Equilibrium Model	110
7.2.2	FCOPT Optimization Model	110
7.2.3	NFCSim Simulation Model	111
7.2.4	MARKAL General-Energy Optimization Model	111
7.2.5	Yucca Mountain Emplacement Model	112
7.2.6	Neutronics Support and Core Concepts Development	112
	REFERENCES	115
	NOMENCLATURE ^(a)	123
	Appendix A: Summary of Material (<i>m</i>) and Process (<i>p</i>) Definitions Used in the FCOPT Optimization Model	131
	Appendix B: Key Input Parameters Used in Evaluating the FCOPT Optimization Model	135
	Appendix C: Description of Cost- and Proliferation-Based Objective Functions	137
	C.1 Cost-Based Objective Function	137
	C.2 Proliferation Risk Objective Function	140
	Appendix D: Qualitative Description of Key FCOPT Constraints	149
	D.1 Mining and Milling (<i>mm</i>)	149
	D.2 Conversion (<i>cv</i>)	149
	D.3 Enrichment (<i>er</i>)	149
	D.4 Fuel Fabrication (<i>ffxxx</i> ; <i>xx</i> = <i>ux</i> , <i>mx</i> , <i>mt</i>)	149
	D.5 Blending (<i>bl</i>)	150
	D.6 Depleted Uranium Storage (<i>dus</i>)	150
	D.7 Weapons Uranium Storage (<i>wus</i>)	150
	D.8 Weapons Plutonium Storage (<i>wps</i>)	150
	D.9 Separations (<i>sep</i>)	151
	D.10 Electricity Generation [<i>gen(nucl,t)</i>]	151
	D.11 FBR Blanket Replenishment (<i>bks</i>)	153
	D.12 Cooling Storage (<i>cs</i>)	154
	D.13 Interim Storage (<i>is</i>)	154
	D.14 Reprocessing	155
	D.15 MOX Recycle Limits	155
	D.16 Other Material Storages (<i>rus</i> , <i>pus</i> , <i>wps</i> , <i>mas</i> , <i>fps</i>)	155
	D.17 Direct Disposal in Repository (<i>dd</i>)	156

Appendix E: Summary and Synopsis of Key Constraints (Mass and Energy Balances, Capacity Limits, <i>etc.</i>)	157
Appendix F: Elaboration of Vintaging and Discounting for the Cost-Based Objective Function.....	181
Appendix G: Correspondence Map of Material(<i>m</i>)/Process(<i>p</i>) Combinations	183
Appendix H: Summary of FCOPT Input Data (Supplement to Table B-I)	189
Appendix I: Benchmarking of Neutronics Methods (Monteburns Code).....	193
Appendix J: Calculation of Neutronic Safety Parameters.....	197
Appendix K: Spallation Product Radioactivity	201
Appendix L: Sample OREGIN2.1 Input for Use in NFCSim Nuclear Fuel Cycle Simulation Model.....	207
Appendix M: Design Parameters of the Yucca Mountain Repository.....	209
M.1 Details of the Yucca Mountain “Viability Assessment” Design..	209
M.2 Low and High Thermal Load Operating Modes.....	210
M.3 Higher Density Emplacement Methods for Low Heat Release Radionuclides	210
M.4 Extended Cooling Periods for Existing Spent Nuclear Fuel.....	210
Appendix N: Details of Thermal Heat Load Calculations for Section 6	213
N.1 Standard LWR.....	215
N.2 Extended LWR.....	223
N.3 MOX-Fueled LWR	231
Appendix O: Separations Processes and Error Analysis for Thermal Calculations	241
O.1 Separations Processes.....	241
O.2 Error Analysis.....	242

This page is left blank intentionally.

ABSTRACT

Reported herein are Fiscal Year 2002 (FY02) developments and results from the nuclear fuel cycle (NFC) Systems Analysis task. This task supports the Los Alamos perspective of the then Advanced Accelerator Applications (AAA) Program and the present Advanced Fuel Cycle Initiative (AFCI) of US Department of Energy. The AAA/AFCI Systems Analysis Task is based largely on the development and implementation of computer models that reflect and enlighten complex economic, technological, environmental, and societal trade-offs associated with future, advanced paths to sustainable nuclear energy. While only approximating reality, these system models aid in reflecting complex systems in an understandable form while providing a consistent framework for testing hypotheses and related scenarios for the future. Hence, while these computer models represent imperfectly a range of possible futures, they importantly provide a framework for organizing large amounts of data in a scientifically disciplined framework to provide options to decision makers for R&D allocations in an iterative process of attempting to influence that future through planning.

The FY02 efforts reported herein divide almost equally between the development of NFC models and the use of these models to assess and evaluate a range of NFC scenarios. The general approach followed during these FY02 AAA/AFCI Systems Analysis efforts was as follows:

- Scope scenario options and related impacts using equilibrium (steady-state), “top-level” (aggregated processes) NFC Model;
- Evaluate scenarios based on a range of performance indicators or metrics (*e.g.*, cost, waste mitigation, proliferation risk, resource utilization);
- Build scenarios based on coupled nuclear-generation technologies presented in a multi-tiered configuration;
- Based on equilibrium analyses, perform dynamic *simulations* and *optimizations* on limited number of scenarios

The scoping of NFC scenario options and associated impacts first used the equilibrium (steady-state), “top-level” (aggregated processes) DELTA model, which was originally developed to support cost analyses of a range of fast-spectrum reactor (FR) and accelerator-driven system (ADS) transmutation schemes (OECD, 2002; Brogli, 2002). This equilibrium NFC model was used to evaluate scenarios based on a range of performance indicators or metrics (*e.g.*, cost, waste mitigation, proliferation risk, resource utilization), as well as to build scenarios based on coupled technologies presented in a multi-tiered [Once-Through Light Water Reactor (LWROT) → N-Recycle LWRs (LWRMX(N)) → Fast-Spectrum Burner (FSB)] configurations. The results from these equilibrium analyses (Krakowski, 2002) were used to provide a technical basis for a USDOE Report to Congress on this AFCI program (USDOE, 2002a). Based on these equilibrium NFC analyses using the DELTA model, it became apparent that a clearer understanding of the dynamics of achieving any given equilibrium scenario is crucial,

particularly with respect to whether a desired equilibrium condition could actually be achieved, and if so, at what cost in terms of dollar expenditures, added waste inventories, and added environmental, proliferation, and economic risk. To this end a multi-pronged attack was launched to understand these temporal aspects of the NFC using both dynamic *simulations* and *optimizations*. While a major part of FY02 was devoted to the development of the requisite modeling capability embodied in the NFC simulation model NFCSim and the NFC optimization model FCOPT, preliminary applications of both models to a number of NFC scenarios were made. The NFCSim simulation model is the focus to these efforts, with the FCOPT optimization model being more developmental and providing directions for the application of the significantly more detailed and data-intensive NFCSim model. In addition, a commercial simulation tool (Extend, 2002) was used for early scoping of the three-tiered NFC scenarios developed as part of the DELTA-based equilibrium analyses. On the optimization front, the applicability to a broader understanding of NFC scenarios in the context of a full-energy optimization model, MARKAL (Fishbone, 1981) was explored. In critical support of all NFC modeling efforts, a state-of-the-art neutronics (burn-up, depletion, reactivity, *etc.*) analysis was pursued. This effort was supported by parametric studies of a wide range of fueling/burn-up/safety(reactivity) computations using the MCNP-based (Briesmeister, 1980) reactor-physics burn-up code Monteburns (Trellue, 1998). This integrated neutronics/reactor-core-physics support is crucial at all levels of AFCI modeling activity and integration of a part of this larger neutronics effort, ORIGEN2.1 burn-up/depletion calculations, is proposed to be integrated into the NFCSim simulation model in the future. In particular, the neutronic efforts focused on developing the optimum combination of Light Water Reactors to burn plutonium and Accelerator-Driven Systems to burn minor actinides. Lastly, towards the end of the FY02 work period, the issue of the Yucca Mountain (YM) “business model” surfaced (YMBM), wherein a question was raised of a YM capacity increase and YM Total System Life Cycle Cost (TSLCC) decrease if spent nuclear fuel (SNF) were first to pass through a range of possible processing or mass-and-volume reduction operations. To this end a simplified repository emplacement and cost model was developed and evaluated as a means to guide the use of NFCSim into a more detailed evaluation of this near-term problem and opportunity.

This FY02 progress report, therefore, elaborates progress made in the five technical areas described above:

- Steady-state *equilibrium* DELTA nuclear fuel cycle modeling efforts, as performed in support to the Report to Congress (Sec. 2);
- Temporal *optimization* modeling effort embodied in FCOPT, with an emphasis placed on model development, limitations, advances, and preliminary results (Sec 3);
- Time-dependent simulation modeling effort embodied in NFCSim, also with an emphasis placed on model development, limitations, advances, and early results (Sec 4);

- Progress in neutronics support provided to the above-listed NFC modeling effort, as well as intrinsic advances in the crucial area of reactor-physics (Sec. 5);
- Early results from the “top-level” YM repository business model (YMBM, Sec. 6).

An emphasis is placed on descriptions and documentation of the FCOPT and NFCSim models, with only sample, interim results being present. The description of progress in neutronics support combine with the FCOPT and NFCSim descriptions to present an integrated NFC modeling effort that will be further integrated, and broadly benchmarked and exercised in FY03, including the provision of detailed assessment of the efficacy of the YMBM. Sec. 7 concludes with encapsulated summary of the FY02 AAA/AFCI Systems Studies task and a description of future work.

This page is left blank intentionally.

1 OVERVIEW

The advanced nuclear fuel cycles (NFC) being investigated over the course of FY02 have evolved considerably, as have the analytic and computer models used to assess each. This study year began with the concepts and associated computational database that resulted from investigations made during the previous fiscal year and reported in (Van Tuyle, 2001). The Systems Analyses FY02 effort focused on understanding quantitatively the economic, proliferation, and waste-mitigation risk associated with the NFC scenarios reported in (Van Tuyle, 2001), and a complementary scenario set reported by a separate but closely related OECD study that emerged on the same timescale (OECD, 2002). The costing and proliferation model developed to support the latter study was expanded and modified first to perform an NFC study at the Paul Scherrer Institute (Brogli, 2002), and then adopted to the specific FY02 needs of the (then) AAA Program, as defined in (Van Tuyle, 2001). This steady-state (equilibrium, *per-TWeh*) DELTA model, along with the results generated there from, is reported in detail in (Krakowski, 2002). Early into FY02, the need to provide technical support to the USDOE Report to Congress (RTC) on this subject (USDOE, 2002a) became apparent, and many of the results and investigations reported in (Krakowski, 2002) reflect this requirement.

In addition to providing technical support to the DOE as it prepared the RTC, the down selection of six NFC examined with the DELTA model encompasses a second major FY02 Systems Analysis activity. This scenario down selection was made to give focus to more-detailed, time-dependent (temporal) NFC analyses needed to address key issues of R&D, technology-deployment, and spent-nuclear-fuel (SNF) disposition schedules. While equilibrium models (*e.g.*, DELTA) are valuable for scoping and comparing key sustainability metrics (*e.g.*, economics, ecology, society) for a broad range of possible scenarios on a *per-TWeh* basis, the following concerns drive the need for temporal models:

- Equilibria for long-term energy scenarios rarely exist, and if so these “equilibria” are transient;
- Even if achievable, the time and resource allocations required to reach such a (desired) steady state can not be determined from an equilibrium analysis;
- Related to the last point, equilibrium analysis cannot determine the progression of technology developments and deployments needed to achieve a given (desired) state, nor can the life-cycle costs incurred be determined with any accuracy;
- The evolution and competition among technologies leading to a desired equilibrium scenario can be elucidated only through temporal analyses; this condition holds both within the nuclear-energy enterprise and for conditions where that enterprise must compete with other energy technologies.

Hence, only temporal models can address the feasibility and cost of achieving some desired end state. These temporal models divide into two broad classes:

- Simulation models [NFCSim (a Los Alamos product being developed as part of the AAA/AFCI Program), and a commercial product EXTEND[®] (1999)]; generally, simulations models allow full external scenario control with significant technical detail (and database requirements);
- Optimization models [FCOPT (a Los Alamos product focused on NFC, developed initially as part of an LDRD project and being adapted to the needs of the AAA Program), MARKAL (world-class general energy model where nuclear energy competes with other energy carriers to satisfy an exogenous end-use energy demand), (Fishbone, 1981)];

For both simulation and optimization models, as applied to the AAA Project needs, demand for nuclear energy is provided as exogenous input. Coupled energy-economy models are also available where demand *per se* is endogenous and driven by productivity (GDP), population, energy resource and prices, endogenous technological learning (ETL), *etc.*; for example, these include:

- “Top-down” econometric models (ERB, SGM) (Edmonds, 1985; Baron, 1992);
- “Bottom-up” technology models energy-economy coupling (MARKAL-MACRO) (Manne, 1992; Kypreso, 1996);

Both approaches have single- or multiple-region capabilities, which is important for including impacts of flow (trade) among regions of energy sources, technology, *and nuclear materials*, and impacts of technology mixes thereon. Figure 1-1 gives a graphical perspective of this temporal modeling potential and the relationship with the models adopted for development to meet the AAA/AFCI Project needs.

In summary, NFC systems analyses began in early FY02 with the DELTA equilibrium model being applied to scenarios generated by the AAA Program in FY02 (Van Tuyle, 2001) and augmented by a more recent OECD study (OECD, 2002). The technical results based on cost, proliferation, and waste-mitigation risks were used primarily to support the RTC (USDOE, 2002a) and to provide grounds for NFC scenario down selection. This process led to candidates for more detailed analyses using temporal models that focused on the NFC (rather than broader issues/scope, Figure 1-1) in the context of both simulation (NFCSim, EXTEND[®]) and optimization (FCOPT) models; the former is developed to provide significant time-dependent technological detail, and the latter is developed as an aid in guiding the former. The results from the equilibrium DELTA model have been reported in a separate report (Krakowski, 2002), and only a synopsis is reported herein (Sec. 2). This description also includes suggestions for the NFC scenario down selection. The major part of the FY02 effort was devoted to both FCOPT and NFCSim models and was developmental, with only interim results for a direct LWR-based scenario being reported, respectively, in Secs. 3 and 4.

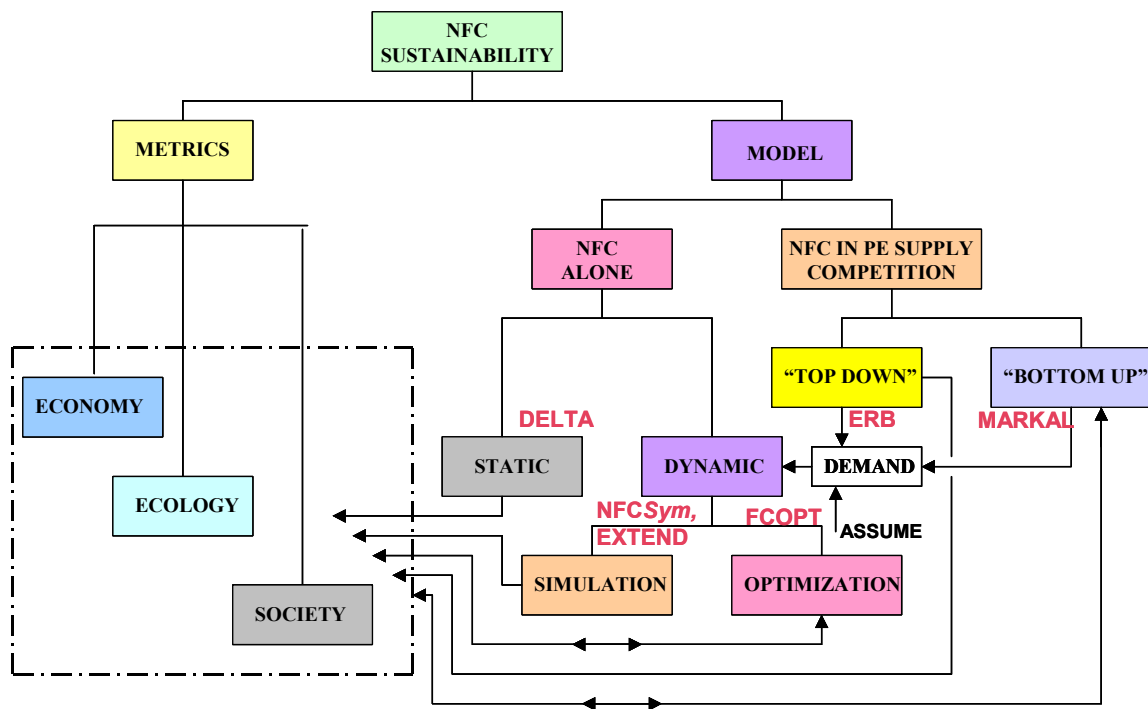


Figure 1-1. Spectrum of NFC Modeling Options showing the relationship between the models used to meet AAA Program needs and others available to address simulation-versus-optimization and econometric (“top-down”)-versus-technological (“bottom-up”) issues.

While nominal estimates of key neutronics parameter (*e.g.*, burn-up, input and output concentrations from various processes, including critical or driven reactors) were used in the equilibrium scenario analyses made by the DELTA model, considerably greater neutronics detail is necessary for the temporal analyses, particularly for the detailed NFCSim simulations. The credibility of any simulation depends crucially on the credibility of the time-dependent and time-evolving neutronics parameters, particularly for highly recycling systems, where neutron-spectral impacts on cross-section sets and attendant reaction rates can be significant. This credibility issue also connects with the reactivity swings and criticality margins allowed by safety-related considerations, and for this detailed neutronic support is required by the temporal NFC modeling activity, particularly for the simulation modeling. To this end, these systems analyses were heavily supported by state-of-the-art neutronics computations and model development; results from this activity in FY02 are reported in Sec. 5.

Lastly, since a key focus of equilibrium, simulation, or optimization NFC modeling is to assess the economic, proliferation, and environmental impacts on the repository for each scenario investigated, some attention must be given to the repository, in so far as heat-and mass-loading constraints apply. Understanding this all-important repository response became even more important towards the end of FY02, when interest in the degree to

which repository efficiency (*e.g.*, mass- and heat-loading for a given total dollar expenditure) can be impacted in the nearer-term by SNF preconditioning over a range of treatments that vary from selective preprocessing with little or no transmutation to more advanced NFC scenarios that resemble closely those down selected from the equilibrium analyses. This repository analysis activity was of necessity small, but was conducted in response to near-term interest and requests dealing with the efficacy of the Yucca Mountain (YM) “Business” Model (YMBM) and is reported in Sec. 6. Finally, a brief summary of FY02 activities and findings is given in Sec. 7, which also describes work planned for FY03.

2 DELTA EQUILIBRIUM NFC MODEL

Details of the DELTA model, its application, and a wide range of parametric results can be found in (Krakowski, 2001); only an executive overview of approach, a summary of results, and scenario down selection are reported here.

2.1 Overview

The equilibrium-NFC assessment was conducted for two of the main technologies [critical fast reactors (FRs) and sub-critical accelerator-driven systems (ADSs)] envisaged to provide the energetic (fast) neutrons needed to transmute completely the transuranic (TRU) materials created by existing thermal-spectrum commercial nuclear power plants. A limited range of scenarios, wherein existing thermal-reactor technologies are used in conjunction with these fast-spectrum burners (FSBs: FRs or ADSs), was investigated in terms of total system-wide energy costs, *COE (mill/kWeh)*, and in terms of average system-wide proliferation attractiveness level, $\langle AL \rangle$; both of these metrics were evaluated relative to the once-through, light-water-reactor (LWR) based commercial fuel cycle. In addition, two “self-sustained” nuclear fuel cycles that do not depend on the once-through fuel cycle are included in the scenario set investigated by this study (a highly plutonium-recycling LWR that feeds a minor-actinide consuming ADS, and a Fast Breeder Reactor, FBR). All analyses are based on an equilibrium (*per-TWeh* steady-state) mass/energy-flow model, which alleviates the need for specific demand and deployment assumptions. Figure 2-1 summarizes graphically the key scenarios examined and the relevant notion used to designate them.

The system-wide cost of electricity for scenarios that use the intrinsically more-expensive ADS-base transmuters benefit from fissioning much of the plutonium feed emanating from the once-through LWR fuel cycle in a thermal-spectrum reactor (also an LWR) interposed in a *first-tier* role (Figure 2-1) that is positioned above the *second-tier* FSB; the commercial once-through LWR driver is termed “*tier-zero*” in this *multi-tier* hierarchy. This dual-tier structure also benefits the FR-based transmuter; this benefit derives not so much from economic reasons, but for reasons of improved ratio of electricity generation from the FR to that from the (LWR) client reactor, thereby reducing infrastructural impacts and minimizing the perturbation to the overall electric-generation network and mix that is assumed to remain dominated by the once-through LWR reference fuel cycle. This infrastructure or “support-ratio” (SR) issue for the FR transmuter derives from the need for these critical systems to dispose of self-generated plutonium, which translates into a potential disadvantage only for a relatively stagnant, business-as-usual (BAU) nuclear-growth scenario.

The relative integrated cost of the single-tier FR transmuter is found to be approximately 10% higher than a once-through LWR fuel cycle, while the cost of a single-tier ADS-driven transmuter is 30% higher. The relative costs in either case, however, can be reduced by fissioning a portion of the plutonium in plutonium-recycling LWRs prior to irradiation in FSBs of either kind. In the limit of complete destruction of the (intrinsic)

plutonium in advanced highly recycling LWRs, the cost of a second-tier minor-actinide-consuming ADS transmuter tends towards that of either the single-tier or the double-tier FR approach ($\approx 10\%$ of the once-through LWR reference case). Generally, a much stronger reduction of energy costs is observed for the ADS-based transmuter systems as more of the plutonium is consumed by the less-expensive first-tier commercial LWR technology.

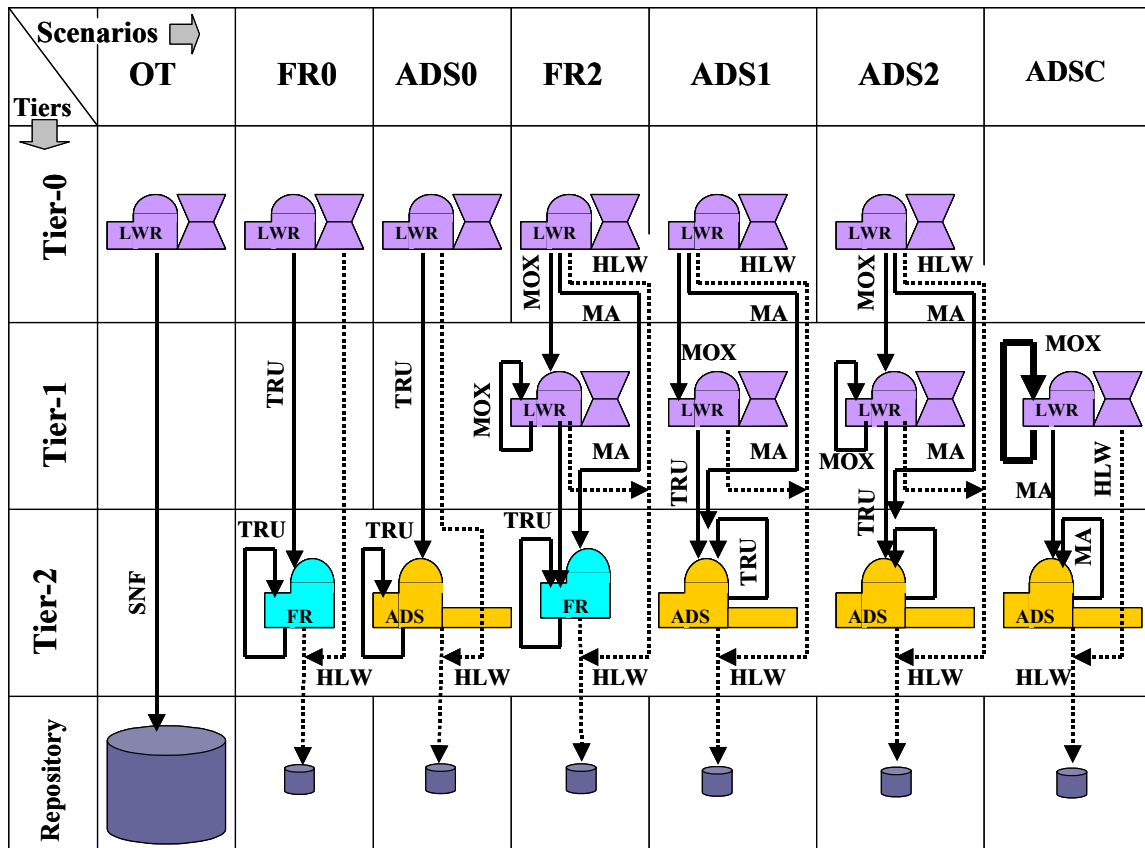


Figure 2-1. Key NFC scenarios and related material flows investigated by the equilibrium DELTA model (Krakowski, 2002).

The net cost of a unit mass of transuranic material that is not directed to the geologic repository represents another economic measure used for inter-scenario comparison. An approximate measure of this “marginal cost” is the ratio of the difference in system-wide cost of electricity between a given transmutation scenario and that of the reference once-through LWR divided by the corresponding differences in transuranic material per unit of generated energy for the scenario in question and that of the reference scenario. This ratio has the units of $\$/kgTRU$ of transuranic material not sent to the repository. This marginal cost, $MC(\$/kgTRU)$, is compared to the direct cost of spent-nuclear-fuel disposal in geologic repositories and, therefore, provides a relatively transparent means to establish a trade-off between the direct-disposal and transmutation-based alternatives being examined. Figure 2-2 compares the marginal cost of transuranic mitigation for the key

NFC scenarios depicted in Figure 2-1, as well as giving the fraction, f_{GEN2} , of the total (equilibrium) electrical generation provided by the second (FSB) tier.

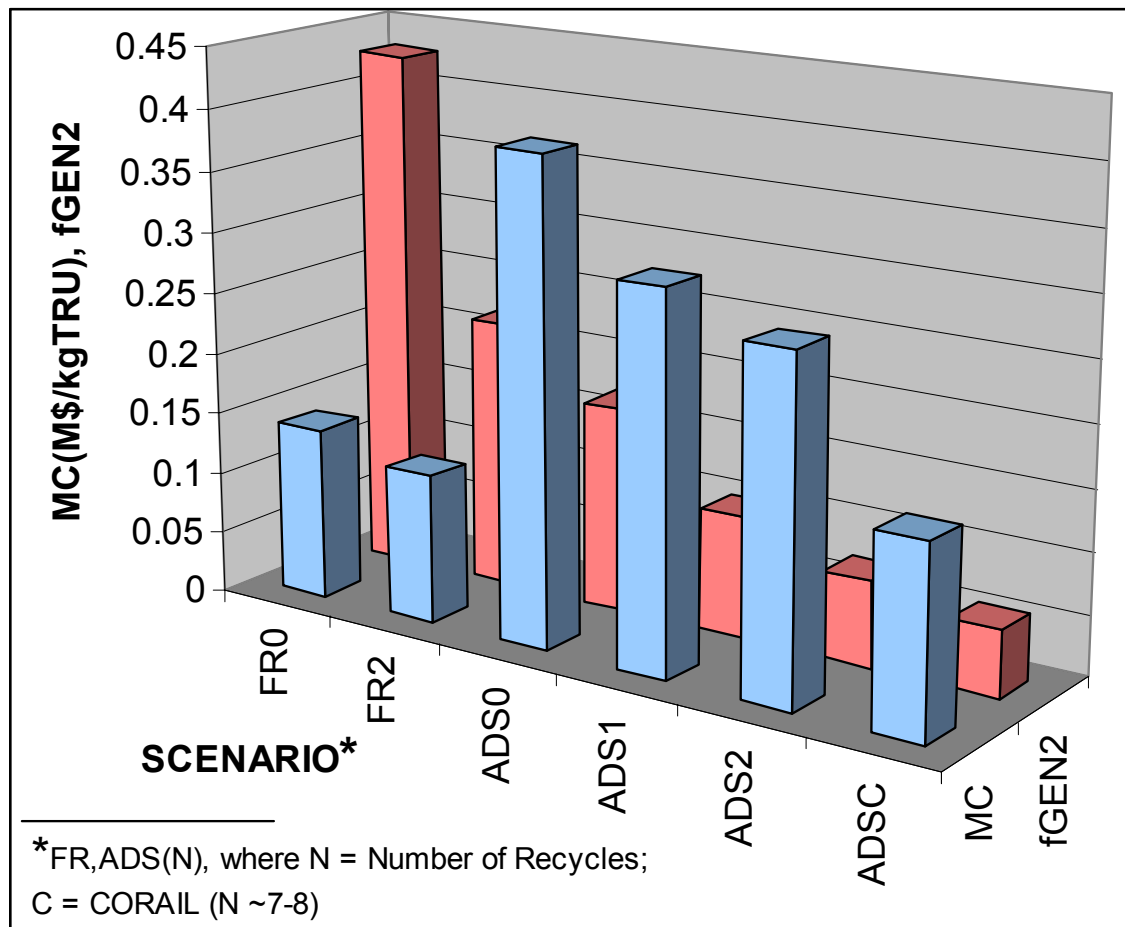


Figure 2-2. Variation of marginal cost for transuranic mitigation, $MC(\$/kgTRU)$, and fraction of tier-two electricity generation, f_{GEN2} , with key NFC scenarios (Figure 2-1).

A more thorough comparison made on this marginal-cost basis must also account for the indirect external benefits of transmutation portended by the removal of this waste-disposal barrier to the broader implementation of nuclear power [e.g., reduced greenhouse-gas (GHG) emissions, increased energy security, reduced adverse health effects associated with breathing the products of fossil-fuel combustion, redirection of dwindling fossil-fuel reserves to other high(er)-end uses, *etc.*]. For the most economical FR- or ADS-based scenarios, the cost per unit mass of transuranic material avoided is a little more than 2,000 $\$/kgSNF(eq)$ for the former and more than 2,500 $\$/kgSNF(eq)$ for the latter. Again, each transmutation scenario provides the additional benefits noted above, and any final assessment must be based on the incremental $\$/kgSNF$ costs of

accruing these benefits. This dependence of COE on SNF repository disposal cost is illustrated in Figure 2-3.

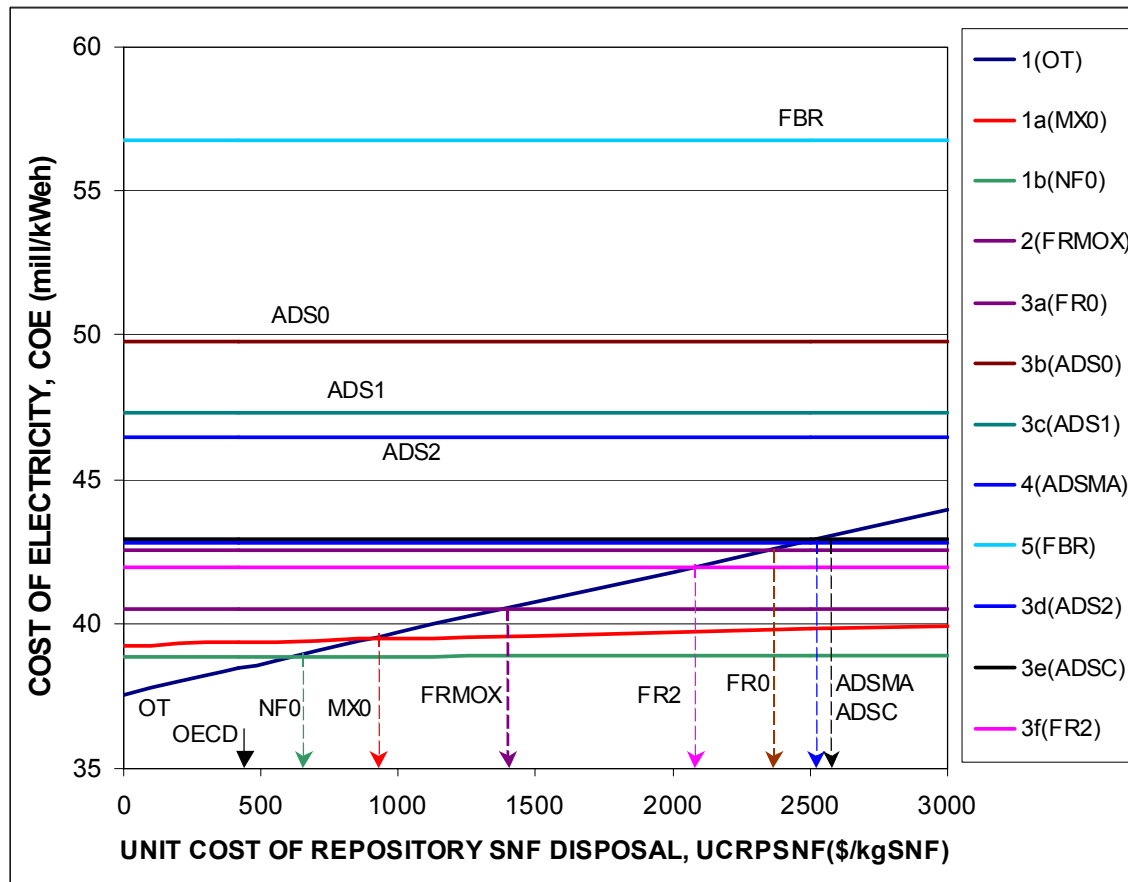


Figure 2-3. Dependence of COE on unit cost of SNF repository disposal, UCRPSNF(\$/kgSNF), for all scenarios considered in this study; points of economic breakeven for each qualifying scenario is shown [please note that more NFC scenarios than indicated on Figure 2-1 are included; refer to (Krakowski, 2002; Brogli, 2002) for details)].

Two economically preferred scenarios emerge from these equilibrium studies: a) a FR-based approach that would utilize existing, but not commercialized, reactor technology, but would require a fuel-cycle demonstration program; and b) a minor-actinide-burning ADS with deep (total) burn of (intrinsic, as a minimum) plutonium in thermal-spectrum reactors. The latter scenario would require the development and demonstration of ADS technologies, as well as deep-burn plutonium technologies as applied to otherwise conventional LWRs. Finally, a support ratio that is based on the ratio of energy generated from the thermal-spectrum systems (both the once-through and the MOX recycling LWRs) to that generated by the fast-spectrum system, is calculated to be ≈ 2 for the FR-based scenarios and ≈ 15 for the ADS-based scenario, indicating considerably different infrastructure impacts, and hence deployment strategies, for these two

approaches having comparable cost-of-energy impacts ($\approx 10\%$ relative to the reference once-through LWR).

Compared to the once-through LWR reference scenario, all transmutation-based scenarios show some increase in the system-wide proliferation attractiveness metric, $\langle AL \rangle$ [refer to (Krakowski, 2002) or Sec. C.2], even accounting approximately for increases in long-term “plutonium-mine” proliferation risk for the reference case. The increase in $\langle AL \rangle$, however, is not large and, furthermore, indicates only a need for increased extrinsic and/or intrinsic protective barriers to achieve similar levels of (acceptable) proliferation risk. The economic impacts of the need for increased protective barriers have not been assessed, but if these barriers are primarily intrinsic (e.g., associated with inherently high radiation barriers or poor source-material quality), the direct economic impacts should be negligible. Generally, the stand-alone scenarios (e.g., no tier-zero once-through LWR technology) have higher $\langle AL \rangle$ values compared to those scenarios that are driven by the reference once-through LWR (scenario $nsc = lwrot$) technology, with this increase driven by the higher rates of TRU material handling (mainly fuel fabrication and limited amounts of post-processing plutonium storage) *per-TWeh* for these self-sustained systems.

A limited amount of single-point Parametric Systems Analyses (PSA) were performed on those variables that either could be strong drivers of cost and/or have large uncertainties. Parameters of interest for impacts on system-wide cost of electricity include: ADS electricity generation option; accelerator unit capital cost; process losses; and burn-up fraction. The option not to generate electricity for the ADS-base transmuter scenarios increased the $\langle COE \rangle$ by 10-15%; changes in the unit capital cost of the accelerator amount to $1.3\% / (\$/Wb)$ or an “elasticity” of $0.2(\%COE/\%UTCACC)$ for the most expensive ADS scenario (e.g., no tier-one technology). Process loss fractions (to a repository) for TRU much greater than $f_{Lj} = 0.002-0.003/pass$, depending on scenario, will jeopardize the goal of >100 reduction in repository-directed TRU compared to the once-through LWR reference scenario; and $\langle COE \rangle$ increases rapidly for *per-pass* burn-up fractions $BUf < 0.10$, with the repository TRU reduction factor of 100 becoming unattainable for $BUf < 0.05-0.10$ for the base-line value of $f_{Lj} = 0.001/pass$, with specifics again depending on scenario.

Finally, a composite relative figure-of-merit metric, $RFOM$, based on the relative cost, $RCOST$, the relative (TRU) loss, $RLOSS$, the relative proliferation attractiveness, $RPAL$, and tier-two electricity-generation fraction, f_{GEN2} , was formulated to provide insight into the changes in scenario ranking as one or the other of the component metrics (cost, loss, proliferation, infrastructure impacts) were de-emphasized. This simplified relative [to $nsc = lwrot$] figure of merit, $RFOM$, has been defined in terms of relative cost increase, $RCOST - 1$, the relative reduction in TRU vectored to the repository, $1 - RLOSS$, and a measure of relative proliferation attractiveness level, $1 + \log(RPAL)$ and is given below:

$$RFOM = \frac{RCOST - 1}{1 - RLOSS} [1 + \log(RPAL)]. \quad (2-1)$$

The form of the cost component adopted for inclusion in $RFOM$ emphasizes relative competitiveness; the form of the (TRU) waste-mitigation term reflects a point of diminishing return when $RLOSS$ is very small (as is the case in most of the scenarios considered); and the logarithmic form for $RPAL = \langle AL \rangle(nsc) / \langle AL \rangle(lwrot)$ returns the numerical assignment of each $AL(nrx, npr)$ value from the original decadal assignment back to the original A \rightarrow E description of proliferation Attractiveness Levels (Krakowski, 2001; USDOE, 1999; Sec. C.2). Figure 2-4 displays $RFOM$ for each of the scenarios described on Figure 2-1, in addition to a scenario base solely on an FBR. It is also noted that, as defined, $RFOM$ is driven largely by cost considerations, and in this definition large values imply unattractiveness; in a sense, $RFOM$ is a figure of “demerit”. Figure 2-4 also shows the impact of removing the proliferation-risk metric $RPAL$; also shown is the impact of including a demerit for large infrastructural impacts associated with low support ratios, SR , by displaying the modified figure of merit $f_{GEN2} * RFOM$.

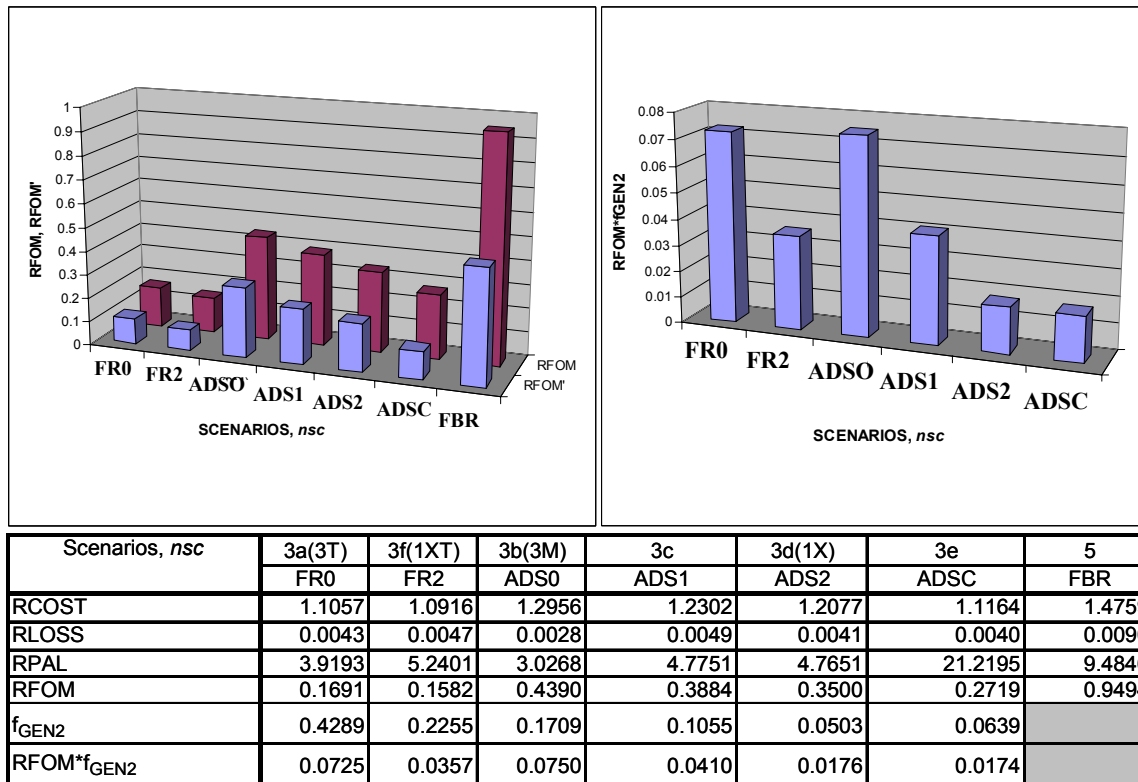


Figure 2-4. Comparison of relative figures of merit with ($RFOM$) and without ($RFOM'$ inclusion of the proliferation metric ($RPAL$)); according to this definition, lower values of $RFOM$ are better. The right frame attempts to illustrate the shift in preferences when $RFOM$ is multiplied by the fraction of total generation supplied by the Tier-2 technology, f_{GEN2} , to penalize those scenarios with low support ratios, $SR \sim 1/f_{GEN2}$; the scenario notation is that described on Figure 2-1.

In summary, for the transmutation-based scenarios examined and the linearly multiplicative $RFOM$ formulation used (Krakowski, 2002), the costing metric dominated the ranking, the ranking did not change when stakeholders having little interest in

proliferation where considered, but significant shifts in the rank ordering are observed depending on the inclusion or exclusion of the infrastructure impacts *vis-à-vis* support-ratio considerations.

2.2 Summary Results

The findings from the study based on an equilibrium DELTA model are recapitulated as follows in terms of the four main issues being investigated (proliferation, waste-mitigation, electricity-generation costs, and infrastructure impacts):

- *Proliferation*: Near-term proliferation attractiveness levels increase only moderately relative to the once-through LWR reference scenario for all P&T scenarios investigated; the cost associated with mitigating these moderate increases in proliferation attractiveness levels to acceptable levels remains to be quantified, but is expected to be small for any approach that emphasizes intrinsic barriers to theft or diversion of source material. At the level of these analyses, (steady-state, minimal modeling of transportation) proliferation risk is not a scenario discriminator.
- *Waste Mitigation*: All P&T scenarios considered meet the somewhat arbitrary goal of reducing repository-directed TRU relative to the once-through LWR reference scenario by over a factor of one hundred, for the *per*-pass process loss rates and burn-up fractions assumed, and under steady-state equilibrium conditions. While less-optimistic assumptions may drive this TRU-reduction goal below 100, significant reductions are still expected. The reduction of repository-directed TRU is not a scenario discriminator under the conditions and assumption of these analyses.
- *Generation Cost*: System-wide generation costs are higher for ADS-based transmutation scenarios compared to FR-based scenarios, with significant reductions in this cost metric occurring for the ADS transmuters that are aided by high-recycle (or possibly deep burn) tier-one thermal-spectrum reactors. The lower system-wide generation costs for FR-based transmuters is not reduced significantly by interposing similar tier-one thermal-spectrum burners. Cost is a strong scenario discriminator under the conditions and assumptions of these analyses.
- *Infrastructural Impacts*: The fraction of the total system-wide electricity generation supplied by the tier-two fast-spectrum transmuter is larger for the FR-based systems for the level in internal conversion of uranium to plutonium assumed, whereas this fraction is considerably smaller for the non-fertile-fueled ADS-based transmutation systems. Depending on the transmuter deployment scheme and the degree to which the generation capacity for the present inventory of commercial nuclear reactors is allowed by market forces to be impacted by the

transmutation technology, infrastructure impacts as determined by the magnitude of f_{GEN2} can be an important scenario discriminator.

The results reported from this multi-tiered, equilibrium analysis, as summarized above, support the limits of: a) elimination of tier-one for the FR-based scenarios (FR0); or b) the melding of tier-zero with tier-one for the ADS-based scenario (ADSC). In either limit, a temporal evolution leads to a simplified single-tier architecture, depending on the overall long-term demand for nuclear energy and the time required to develop and deploy all aspects of all technologies associated with either FR0 or ADSC scenarios.

While the major components of the life-cycle costs (LCC) can be estimated from the COE-based cost metric, given some assumption on demand for nuclear energy, the equilibrium assumptions upon which this model is based represents the greatest impediment to a full LCC analysis. To this end, dynamic optimization and/or simulation models based on specific demand and deployment schedules and scenarios are required. These more advanced and realistic modeling approaches would include appropriate RD&D constraints and related uncertainty assessments, and are recommended for any future work aimed at charting the course of transmutation-based scenario analyses, specifically, and the assessment of nuclear-energy sustainability, in general.

2.3 NFC Scenario Down Selection

On the basis of these equilibrium DELTA model results, a reduced set of NFC scenarios was to be selected for more detailed analyses using the time-dependent simulation (NFCSim) and optimization (FCOPT) models. In actuality, only a general direction for such a down selection is indicated in this section, in that a broader community involvement with this process than is represented by the Los Alamos Systems Analysis team is required. This broader input, in fact, has been derived and is reported herein (Salvatores, 2002).

Figure 2-5 suggests a process for reducing or focusing the number of possible NFC scenarios based on the economic results derived from the equilibrium NFC analyses. These scenarios divide according to whether the future demand for nuclear energy in the US is large or small. For the latter, the use of high-recycle LWRs to consume (fission or transmute to higher actinides) intrinsic (CORAIL) or extrinsic + intrinsic (MIX) plutonium restricts new/advanced technologies to a relatively minor role as an MA-burning ADS. The economic impact on the composite generation system would be minimal, as is indicated on Figure 2-3 [or its COE-based counterpart (Krakowski, 2002)], and a significant (again, in terms of f_{GEN2}) new technology (*e.g.*, FRs) would not have to be introduced. The major “new” technology in terms of electricity generation would be the advanced (CORAIL, MIX) LWRs. On the other hand, for high-demand scenarios, the introduction of LWR-displacing FRs could be better justified on the basis of both TRU removal (mainly by fissioning) in early times and LWR displacement at later times. Figure 2-5 also includes a deep-burn HTGR leg supported by either an ADS or an FR,

with longer-term, high-demand scenarios probably leading to an HTGR *versus* FR “shoot out” (e.g., the “fbr or htgr” endgame shown on Figure 2-5).

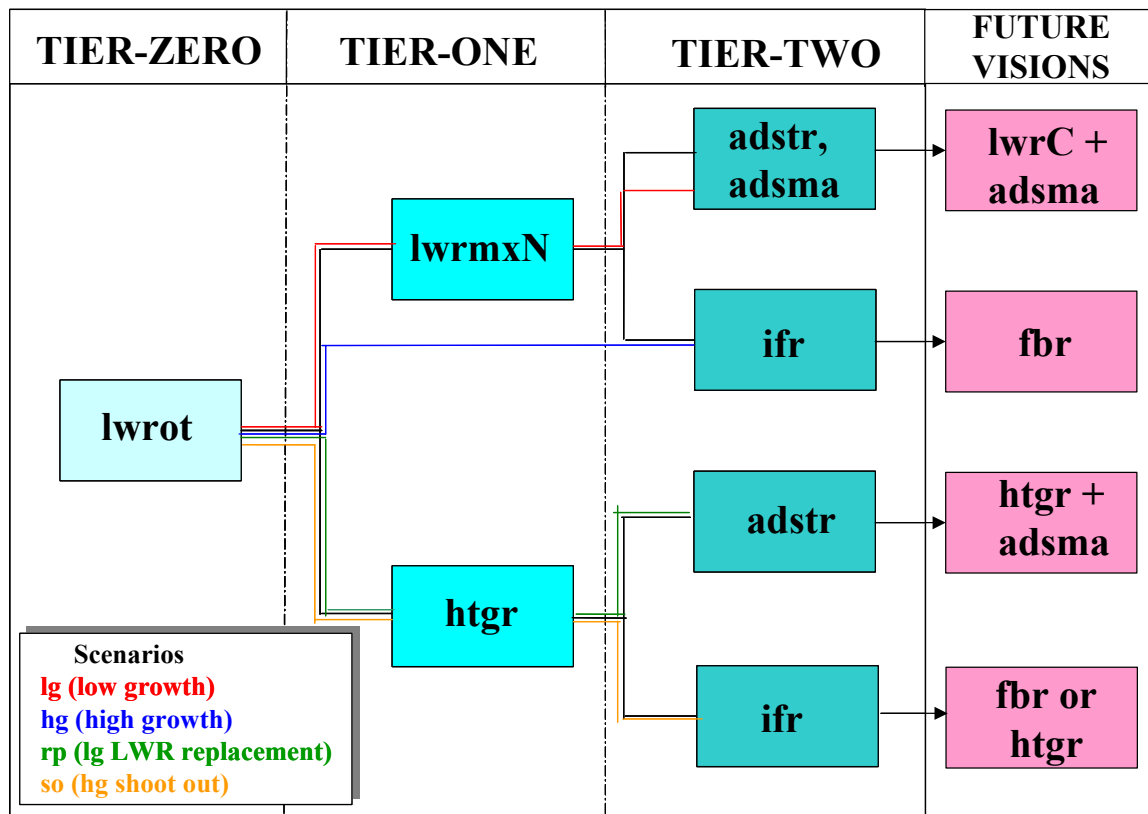


Figure 2-5. Suggested “roadmap” for NFC scenario down selection base largely on a high- *versus* low-demand scenario for nuclear electricity in the US; the deep-burn HTGR leg is include for completeness (fairness), in that this range of scenarios was not considered in this study and the “htgr *versus* fbr” endgame requires a more profound (temporal, optimization) analysis.

On the basis of this recapitulation and synthesis, as well as discussion with colleagues at ANL (Salvatores, 2002), four scenarios (and attendant minor variations) evolve as a down-selection set for consideration in subsequent temporal (simulation + optimization) analyses using the NFCSim and FCOPT models, respectively, described in the following two sections. This collaborative distillation of possible advanced NFCs is summarized in Figure 2-6.

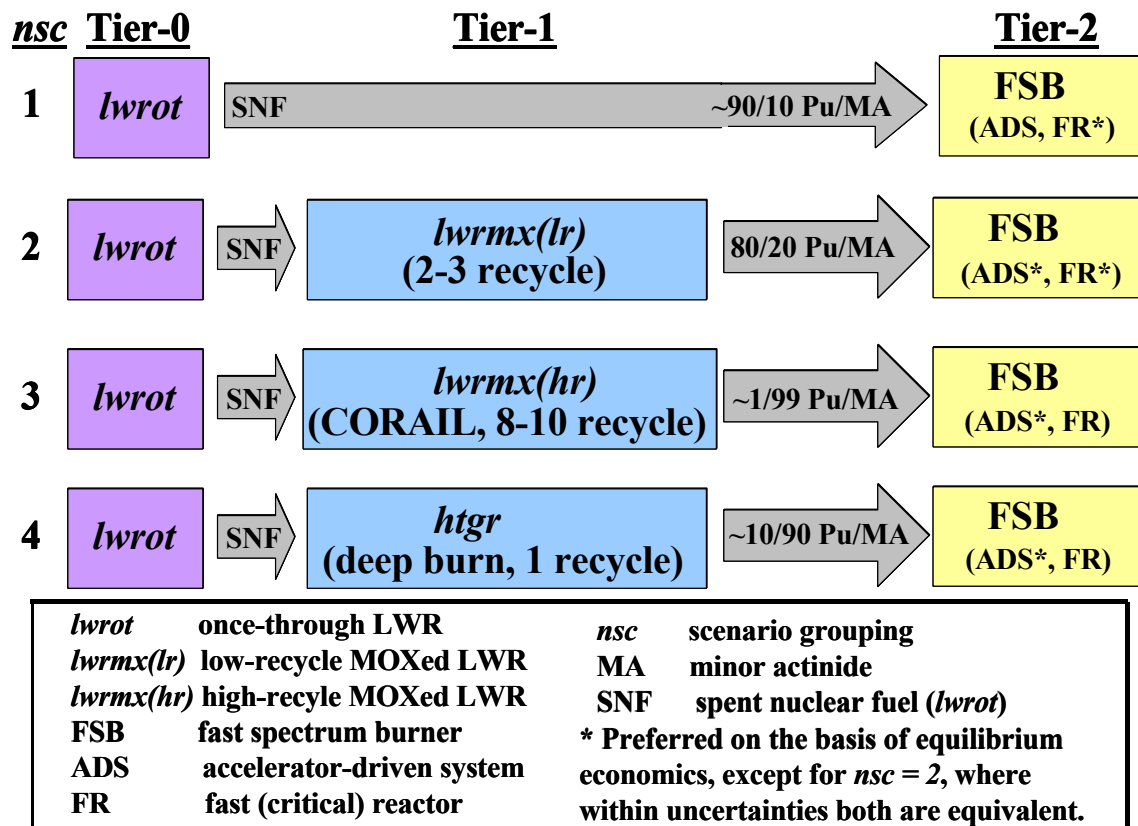


Figure 2-6. Collaborative (Krakowski, 2002; Salvatores, 2002) distillation of possible advanced NFC scenarios adopted for temporal (simulation + optimization) analyses.

3 FCOPT OPTIMIZATION MODEL

3.1 Model Description

3.1.1 General Considerations

The FCOPT model uses Linear Programming (LP) methods to optimize a comprehensive set of nuclear fuel cycle (NFC) options. Within the context of LP models, FCOPT is time dependent (t) and tracks a range of ($m = 20$) nuclear materials and related processes ($p = 55$). Process material flows (kg/yr) and inventory (kg) are represented by the vector $x(m,p,t)$, which is followed over a 2000-2100 time frame in one-year increments. The model is driven by an exogenous demand for nuclear-electric energy. Using this exogenous nuclear-energy demand, the FCOPT model expands the nuclear-energy option and in the version reported herein follows six (electricity) generation technologies that include one sub-critical accelerator-driven transmuter and one critical fast-spectrum transmuter, along with four commercial nuclear power plant (NPP) options. Multiple processing/reprocessing and repository/depository options can be modeled, as well as a range of uranium-enrichment technologies. The simplified version described herein, however, aggregates these technology options for enrichment and disposition into one each, except for processing/reprocessing, wherein “separations” are defined as the purview of the transmuting technologies and “reprocessing” is associated with the commercial power-producing technologies. In Appendix A, Table A-I lists the material options, and Table A-II summarizes the process options presently modeled by FCOPT; Appendix B lists typical input required of the FCOPT model; objective functions are described quantitatively in Appendix C; a qualitative description of key constraints that drive FCOPT is found in Appendix D; and Appendix E lists the $nc = 95$ constraint equations that form the overall description of mass balances, electrical-energy generation requirements (needed to meet the aforementioned exogenous demand for nuclear energy), technology (electricity generation, reprocessing/separation, storage, repository, *etc.*) capacity constraints, and technology deployment-rate limits. Figure 3-1 depicts a generalized mass/power flow diagram around which the FCOPT model is built. While the use of LP optimization models is not new, past work (Pavelescu, 1982; Ursu, 1986, 1990) has focused on a much higher level of NFC aggregation.

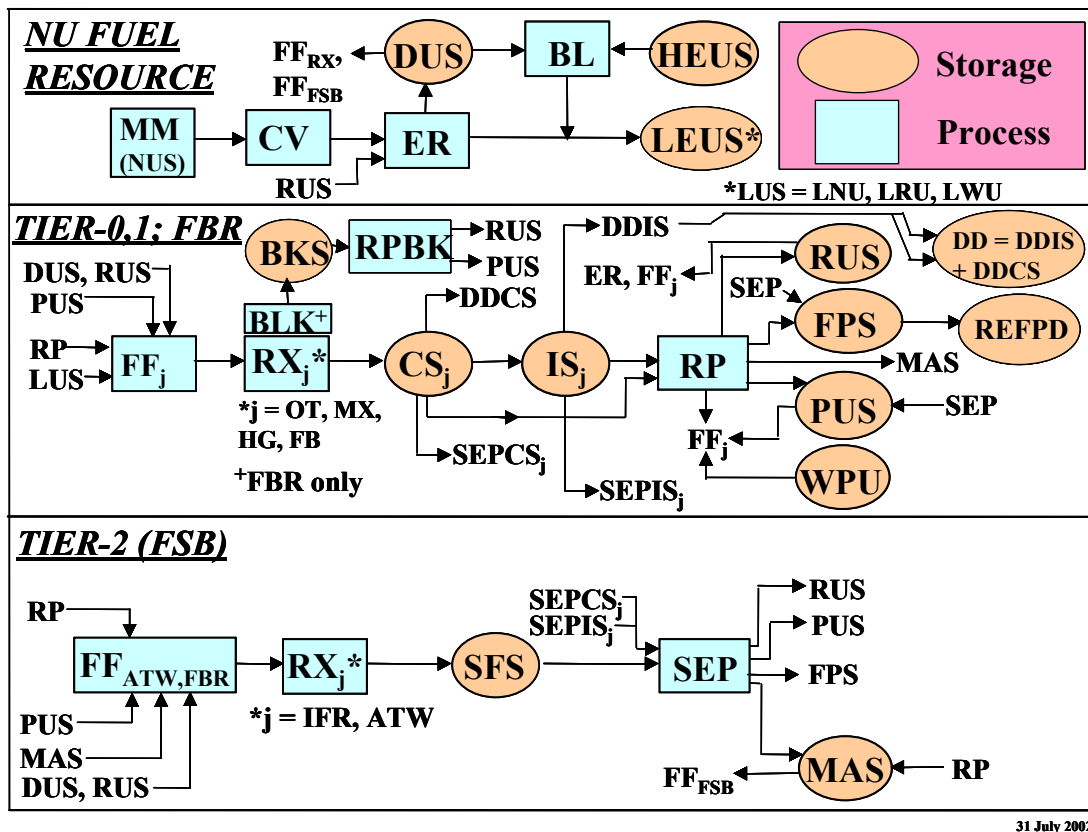


Figure 3-1. Generalized NFC mass/power-flow diagram around which the FCOPT model is built.

The structure of the LP model on which FCOPT is based reflects three “top-level” operational elements: *Objective Function*; *Decision Variables* (or Activities); and *Constraints*, as is elaborated below:

- **Objective Function:** an LP is designed to find the best or “optimal” solution (e.g., best combination of materials and processes for all time steps in the case of the FCOPT model), where “best” is described in terms of life-cycle cost; minimum repository impact; minimum operational worker radiation dose; minimum proliferation risk (as defined by a range of criteria); *etc.*
- **Activities or Decision Variables:** alternative approaches that give what to do, how to do it, and how much of it to do in order to minimize or maximize a given Objective Function; in the context of FCOPT, the Activity or Decision Variables are inventories (kg) or flow rates (kg/yr), $x(m,p,t)$, or electricity generation in units of MW $_{yr}/yr$, $gen(nucl,t)$, for given sets of materials $\{m\}$, processes $\{p\}$, and times $\{t\}$, where $\{nucl\}$ is the generation subset of $\{p\}$;
- **Constraints:** specify the conditions under which combinations of Activities can be selected, and reflect: overall demand rates; technology deployment rates;

storage or processing capacity limits; material availability; Endogenous Technical Learning (ETL, but not modeled here) impacts on cost and deployment, *etc.*

The material, process, and time sets, $\{m\}$, $\{p\}$, and $\{t\}$, respectively, elements of which are listed in Table A-I and Table A-II, define the activity vector $x(m,p,t)$, which in turn is related by the series of constraint equations or inequalities listed in Appendix E. These constraints take the following general form:

$$\sum_{\{m\},\{p\}} a(m,p) * x(m,p,t) \leq b(t), \quad (3-1)$$

where the parameters $a(m,p)$ and $b(t)$ are derived from essential input that defines or constrains the search for the vectors $x(m,p,t)$ that minimize the Objective Function. In the case where the total discounted cost over the time set $\{t\}$ is to be minimized, the objective function takes the following form:

$$OBJ_{COST} = \sum_{\{m\},\{p\},\{t\}} UC(m,p) * x(m,p,t) / (1+r)^{t-t_o}. \quad (3-2)$$

In this expression, $UC(p,m)$ represents a unit cost and has units (\$/kg, \$/kg/yr, \$/We, *etc.*) that depends on the particular vector $x(m,p,t)$ or $gen(nucl,t)$ being evaluated, r (1/yr) is a discount rate, and t_o is a reference year to which the cost-based objective function is referenced. When the unit cost is effectively time dependent, as in the case of a depletable resource like mined and milled ($p = mm$) natural uranium ($m = nu$), $UC(nu,mm)$ (\$/kgNU) depends on the cumulative resource use and, hence, indirectly on time; in this case, the problem becomes nonlinear (NLP). Lastly, a nonnegativity constraint is generally applied, wherein:

$$x(m,p,t), gen(nucl,t) \geq 0, \quad (3-3)$$

where the set of electrical generation technologies, $\{nucl\}$, is a subset of the parent process technologies, $\{p\}$.

Other objective functions can be considered, with a measure of proliferation propensity or risk being one of particular interest to this study, and is designated by OBJ_{PROL} . Both OBJ_{COST} and OBJ_{PROL} are elaborated in Appendix C. Combinations of these objective functions can (and are) be considered:

$$OBJ = OBJ_{COST} + pro * OBJ_{PROL}, \quad (3-4)$$

where pro represents an importance or connectivity parameter used in such linear multi-criteria optimizations and must assume compatible units [*e.g.*, with OBJ_{COST} having units of US dollars (USD) and OBJ_{PROL} is expressed in “exposure” (to theft or diversion) units (*e.g.*, kgPu-yr, refer to Appendix C.2), pro would assume the units of \$/kgPu/yr].

It should be emphasized that FCOPT is not a time-dependent model *per se* in the sense that the problem is not recursively advanced in time according to the dictates of some ordinary or not-so-ordinary differential equation, nor is time advanced numerically in accordance with the dictates of some clock ticking in the background, as in the case of a simulation model like NFCSim (Sec. 4.). Instead, the LP (or NLP) model treats $x(m,p,t)$ as a separate variable, x_j , for each element of the set $\{m,p,t\}$; with i identified with the subset union $\{m,p\}$, the problem assumes the following standard LP form (Brinkman, 1989):

$$\text{maximize } f(x_1, \dots, x_n) = \sum_{j=1}^n c_j x_j ,$$

subject to the constraints;

$$\sum_{j=1}^n a_{ij} x_j \leq b_i \text{ for all } i, \quad 1 \leq i \leq m , \quad (3-5)$$

and the nonnegativity constraints;

$$x_j \geq 0 \text{ for all } j, \quad 1 \leq j \leq n .$$

Hence, the primary aim of the FCOPT model is to find the vector $x(m,p,t)$ that minimize the designated objective function, and in the course of finding a feasible solution FCOPT assures that all the m constraints are met while minimizing $f(x_1, \dots, x_n)$. The actual time evolution reported for any of the $x(m,p,t)$ vectors may not be as smooth as if it were determined from a direct time-dependent simulation; this time-dependence is determined largely by the details enforced through the nc constraint relationships (Appendix E). In any case, the optimization is conducted in a multi-dimensional feasibility space of dimension $(t = 100) * (m = 20) * (p = 60) \sim 120,000$; of course, many of these combinations are null, in that material m may be allowed to reside in or flow to a limited number of processes p , and for those processes p dealing with material m , this co-existence may not exist for all times t ; Appendix H gives an m versus p “map” for the problem investigated in this study.

The FCOPT model, as originally formulated, was evaluated as either a Fortran 90 program with some C functionality associated with the optimizer or on a GAMS (Brooke, 1988) mathematical programming platform. Both versions use the CPLEX (ILOG, 1999) LP software to optimize (minimize) the total discounted energy cost over the specified time frame (typically, 2000 \rightarrow 2100, or 100 years) in one-year increments. This optimization is performed using a set of constraints (material flow balances, energy balances related to exogenous demand constraints, growth rate and capacity constraints, *etc.*) applied between various materials/processes and input parameters specifying the cost per unit of each material or process production capacity, as is summarized in Sec.

3.1.2 and elaborated in Appendix E, and depicted graphically in Figure 3-1 in terms of the material and energy flows that are followed. The model as presently formulated has ~80 active constraints, but in more extended versions has over 100 constraints that relate the flow of material between key NFC processes. Some of these constraints are time-dependent, and the balance for one time may depend on variables evaluated in the previous time (*e.g.*, lag times between connected processes are included). If parameter values are required during the historical times before the period of optimization, data are provided for past (historically, starting in 1990) material flows or inventories. Non-linearities occurring in the objective function (*e.g.*, when unit costs depend on the activity level being determined) require computationally time-consuming nonlinear procedures, which were circumvented in the analyses reported herein by either specifying nominally constant coefficients (*e.g.*, unit costs), or adopting an iterative procedure. Investigation of non-linear problems requires another optimizer, and is left as a topic for future study.

Although not as data intensive as is the technology/process/procedurally-rich simulation model, NFCSim, described in Sec. 4, FCOPT nevertheless requires the specification of a non-trivial number of costing and process (including the power reactors *per se*) parameters. Before describing more specific aspects of FCOPT, some of these key parameters needed to evaluate both the b_i and a_{ij} parameters listed in Eq. (3-5), as well as the objective functions $OBJ_k (k = COST, PROL)$ described in the following subsections, are summarized in Table B-I (Appendix B). While not a complete parameter listing, the definitions and values given in Table B-I, along with the material and process definitions/notations given in Table A-I and Table A-II, are essential in describing more detailed aspects of the FCOPT model. It is noted that the last few entries in Table B-I express typical results for the parameters listed, which will be addressed parametrically in Sec. 3.2.

3.1.2 Specific Considerations

The objective functions that are to be minimized for the solution vector, $x(m,p,t)$, over this $(t = 100) * (m = 20) * (p = 60)$ -dimensioned feasibility space include: *economic* (total present-value of energy generation costs, including technology vintaging); *proliferation* [MAUA-based, multiple single-attribute utility functions (Krakowski, 1998); or Material Vulnerability Analysis, (MVA), based on numerical assignments (Brogli, 2002; Krakowski, 2001) of USDOE fissile-material Attractiveness Level (USDOE, 1999)]; and *environment* [operational (near-term) and repository (long-term) human radiation exposure] metrics. The focus of the present study is on the first two objective functions. These separate optimizations (minimizations) determined by the FCOPT model should then be evaluated in aggregate using one of a number of multi-objective/criteria analyses [Multi-Criteria Decision Analyses (MCDA) (Haldi, 2000), Multi-Criteria Mapping (MCA) (Sterling, 1997) or the use of membership functions (Silvennoinen, 1982)]. In the context of the present study, only the optimizations based on economic or proliferation-risk have been completed, and the latter has been evaluated only for the relatively simple, but transparently heuristic MVA methodology (Krakowski, 2001); the impact of linearly

combining the economic and proliferation objective functions according to Eq.(3-4) is reported, however (Sec. 3.2.2.5).

3.1.2.1 Objective Functions

The study evaluated two objective functions: one based on total present-value cost in the year 2000 summed over the period of optimization (2000-2100), OBJ_{COST} ; and one monitoring a proliferation risk metric, OBJ_{PROL} , based on an Attractiveness-Level-weighting of plutonium exposure to theft or diversion. Both metrics are described further in the following two subsections, with Appendix C elaborating on the computational details required for evaluation and subsequent minimization by the FCOPT model.

3.1.2.1.1 Cost-Based Objective Function

The cost-based objective function, $OBJ_{COST}(\$)$, is the sum of the discounted annual charges incurred in the course of operating each of the key NFC process $\{p\}$ over the time frame of the optimization (typically, for the period 2000 \rightarrow 2100). This sum over key accounts evaluated at a given time t is comprised of 18 contributions ranging over the entire fuel cycle depicted in Figure 3-1. Listed in Appendix I are the component annual charges that are then discounted to the reference year (2000) using a discount rate of r in the discounting term $pdr(t) = 1/(1 + r)^t$; Table A-I and Table A-II (Appendix A) should be consulted for material and process identifications, Table B-I (Appendix B) gives definitions for key unit costs, and the Nomenclature describes remaining variables.

Appendix F gives a further explanation of this capital costing procedure; as for all other terms in this costing objective function, $OBJ_{COST}(\$)$, these are discounted to the reference year (2000) using the discount rate dr and summed over the optimization period (2000,2100).

3.1.2.1.2 Proliferation Risk Objective Function

Numerous studies have been performed regarding how best to estimate quantitatively the proliferation risk of a certain fuel-cycle process, including Expert Delphi Group, Comparative Value Measures, Multi-Attribute Utility Analysis (MAUA), Risk/Consequence or Probabilistic Risk Analysis, and a range of Multi-Criteria Optimization techniques; these have all recently been reviewed (Krakowski, 2001). A highly subjective MAUA method for generating relative proliferation risk indices (pri) was applied to the E³ model (Krakowski, 1999a,b) that generates the exogenous demands used to drive FCOPT, and this model was coded as a post processor to FCOPT. This proliferation risk model is a hybrid of earlier work in this area (Silvennoinen, 1982; Papazoglou, 1978). Although this MAUA proliferation model was incorporated into FCOPT as a post-processing operation performed during the cost optimization, resources were insufficient to find a way for the resulting proliferation-risk index to be incorporated

linearly into a proliferation-risk objective function. The required development, the strong likelihood of a NLP problem resulting, and the incomplete understanding of FCOPT responses, even for linear problems, led to the adoption of a simpler, heuristic approach to proliferation-risk optimization (minimization) in FCOPT. Nonetheless, future efforts along this MAUA line using the approach (illustrated in Figure C-1, Appendix C), or more recent reincarnations (Charlton, 2002) thereof, will be pursued in the future.

One approach to developing a simpler approach to proliferation risk optimization examined (Brogli, 2001) a simplified and transparent “recipe” that might be used by nuclear utilities to classify related source materials. One approach evolved from this effort wherein the basic Attractiveness Level (*AL*) metric suggested by the USDOE (1999) was applied in setting protection Categories for various forms of SM. While the quantitative *AL* designations ranged from A through E, as described below, assignments of a numerical ranking and then assigning such a ranking to SM at particular locations in the NFC (Figure 3-1) gives a measure of importance with respect to proliferation potential/propensity/risk/*etc.* The use of *AL* values as weights that reflect the importance of fissile material in a given form at a given node in the NFC is described and applied in FCOPT as a proliferation objective function, OBJ_{PROL} , to be minimized. As with the MAUA methodology, only a relative (to a point-of-departure or POD case) proliferation metric results, which nonetheless is useful in assessing tradeoffs with economic or costing parameters, capacity limitations, technology deployment rates, *etc.* (Sec. 3.2.2.5). The approach behind these *AL* assignments is summarized in Appendix C (Sec. C.2), which describes the algebra of its application through FCOPT to the problem at hand.

The International Atomic Energy Agency (IAEA) has also recommended a set of criteria for the level of protection needed to assure fissile materials ^{233}U , ^{235}U , and plutonium isotopes are safe from illicit use through diversion or theft for the construction of nuclear explosive devices (IAEA, 1999). The USDOE guidance (USDOE, 1999) represents more elaborated and extended recommendations in the form of quantitative *AL* assignments (A \rightarrow E) and offers a more graded and hopefully useful/usable set of criteria. Both sets of protection categories are based on kind [^{233}U , ^{235}U , and Pu (all isotopes)], concentration (as in the case of ^{235}U), and mass of fissile material. A summary description of the USDOE recommended *AL* values, along with comparable, but less-detailed (graded) groupings suggested by the IAEA, is given in Table C-I (Appendix C). Each of the *AL* values associated with the USDOE guidelines and the “subclasses” for the comparable IAEA guidelines for a given mass of the respective weapons-usable material has associated with it a protection Category I, II, or III. The highest level of protection requires three barriers and corresponds to Category I. The lowest level of protection, Level III, corresponds to an unfenced, unbarred building.

By assigning decadal numerical values to the A \rightarrow E *AL* categories (*e.g.*, 10,000 \rightarrow 1, respectively), these *AL* assignments can be used as weighting factors to give an *AL*-weighted plutonium inventory, as follows:

$$p_{u\text{inval}}(t) = \sum_{mpu} \sum_{ppu} AL(mpu, ppu) * y_{pu}(mpu, ppu) * tres(ppu) * x(mpu, ppu, t) \quad (3-6)$$

The following integration over time gives a measure of exposure or vulnerability to theft or diversion:

$$xpospual(t) = \int_0^t puinval(t) dt \quad (3-7)$$

When evaluated at the last time period, $tmax$, a measure of OBJ_{PROL} in units of $kgPu\cdot yr$ results; $OBJ_{PROL} = xpospual(tmax)$ is to be minimized either directly or in the linear combination given in Eq. (3-4).

3.1.2.2 Constraints

The constraints used in FCOPT are summarized qualitatively in Appendix D and quantitatively in Appendix E. The purpose of these $nc \sim 80$ constraints is to assure in as general way possible the continuity of material flows between various steps (and process options) in the fuel cycle (Figure 3-1), and the accumulation of materials within key storage points are consistent. In addition, the summation of net annual energy generation from all *nucl* generation technologies allowed to contribute to the mix needed to satisfy exogenous demand, $gent(t)$, as well as the rate at which these technologies are deployed or removed, represent crucial constraints in the choice of each of the $x(m,p,t)$ plus $gen(nucl,t)$ variables in a way that is both feasible (*e.g.*, all constraint equations and inequalities are satisfied) and optimal (*e.g.*, minimized the objective function $OBJ = OBJ_{COST} + pro * COST_{PROL}$). In addition to assuring flexibility in meeting mass-flow conservation through the many technology options and combinations allowed by the problem statement, some of the constraints listed in Appendix E specify (possibly time-dependent) capacity limits imposed on both storage and reprocessing facilities, as well as the rate at which these capacities might be achieved in the future. The key to setting up an optimization problem of this kind is to assure the flexibility in technology choice (be it a storage system, a reprocessing system, an electrical generation system, a repository, *etc.*) is not so overly constrained as to convert the “optimization” into a “simulation”. Furthermore, this flexibility or breadth of technology choice must be preserved to an extent that feasible, and ideally optimally feasible, solutions can be found.

In formulating the FCOPT model, as embodied in the constraints listed in Appendix E, a number of process choices were made initially, some of which had to be relaxed to the set given in Appendix E in order to gain better control and understanding of the optimization problem being pursued. While the description of most of the storage facilities being considered is straightforward, the complexity and multiplicity of the various reprocessing technologies supporting the range of generation technologies considered, albeit in this study the set *nucl* is not large, forced a condensation and aggregation to the version of FCOPT reported herein. These limitations will be relaxed in future versions of FCOPT, once more experience is gained with an NFC optimizer of this kind.

For the purpose of the present study, two kinds of spent-fuel processing schemes were finally adopted: “reprocessing” for oxide-fueled, commercial generation technologies, $rx = \{rxot, rxmx, rxhg, rxfb\}$, and “separations” for the transmuting (and also power-

generating) technologies, $fsb = \{rifr, atw\}$. “Separations” was differentiated from “reprocessing” because both minor actinides and fission products were part of the waste stream leaving the “reprocessing” technology, whereas primarily fission products flow from the “separations” technology. Furthermore, the initial formulation of the FCOPT model made distinctions between four separate fast-spectrum burners [FSBs: an integral fast reactor (IFR) and three kinds of accelerator-driven systems (ADS)], three kinds of direct-disposal and fission-product geological repositories (e.g., bedded salt *versus* volcanic tuff *versus* granite), and three uranium enrichment schemes (diffusion, centrifuge, and laser-isotope separations). This overly ambitious attack on a difficult problem was reduced in scope through aggregation of these technology into two FSBs [an IFR (*rifr*) and an ADS (*atw*), with both burning plutonium of reactor (*rpu*) or weapons (*wpu*) origin, as well as minor actinides (*ma*)], one kind of repository [early differentiation based on geophysical characteristics proved unwarranted for the present level of analyses, particularly since the environmental metric is yet to be evaluated], and one uranium enrichment technology, (based largely on either diffusion or centrifugation technologies).

The reduced set of constraints given in Appendix E reflects the above-described aggregation, and even some of those listed have been reduced to inactive status to allow a firmer grasp on the complex interaction between mass and energy balance, technology deployment-rate limits, and time-dependent capacity limits. While the relationships given in Appendix E are largely self-evident, some description of the broad groups indicated is warranted. Appendix D gives a qualitative, equation-free description of the 17 generic kinds of constraints that comprise the FCOPT model, whereas Appendix E lists the equations actually programmed into the model, along with some narrative. The language of this description is that of the set-based notation described in Table A-I and Table A-II for materials m and processes p , respectively.

3.2 Interim Results

3.2.1 Scope of Analyses

The FCOPT model is driven by an exogenous demand for nuclear energy. The projected demand used over the period 2000-2100 for the results reported in this section is based on an assumption of a US growth rate of $dgrowth = 0.01/yr$. Other base-case NFC characteristics used to generate these interim results are as listed in Table B-I (Appendix B) and in more detail in Appendix G. In the course of understanding impacts on cost and generation mix, the following input conditions to FCOPT were varied:

- In concert with the exploratory nature of this interim evaluation of the FCOPT model, the focus of parametric studies reported in this section is the understanding of the trade-off between (relative) cost and proliferation risk, as measured by the two objective functions OBJ_{COST} and OBJ_{PROL} , when key capacity limits related primarily to repository (direct) disposal (*dd*), interim SNF storage (*is*), reprocessing (*rp*), and separated-plutonium storage (*pus*).

- Related to the understanding of the cost and proliferation impacts of the above-listed technology capacity constraints are the relative costs attendant to each of these key storage elements in the NFC; the impacts of changes in unit costs associated with each are subsequently explored.
- Unit Total Cost, $UTC(\$/We)$, associated with selected electricity-generation technologies, with the capital costs of the six generation technologies listed in Table B-I and Appendix G serving as consensus-generated (OECD, 2002) nominal or point-of-departure (POD) values for key cost estimating relationships (CER);
- Growth rate constraints through the $fgrow(nucl,t)$ parameter, as given in Constraint 39 listed in Appendix E, where $nucl$ is the set of all six generation technologies being considered. Actually, constraints were imposed on both the growth and the decrease of each technology, as given below:

$$dcap(nucl,t) < cap(nucl,t-1)*fgrow(nucl,t) + fseed(nucl)*gent(t), \quad (3-8)$$

$$dcap(nucl,t) > -fdecx(nucl)*cap(nucl,t), \quad (3-9)$$

where the capacity, $cap(nucl,t)$, is related to the generation, $gen(nucl,t)$ according to

$$gen(nucl,t) < cap(nucl,t)*avail(nucl,t). \quad (3-10)$$

The parameter $fseed(nucl)$ is a small fraction of the total demand $gent(t)$ needed to assure that a given technology that is initially zero (*e.g.*, all except $rxot$) has a chance to grow if it contributes to minimizing the respective objective function at some future time. The growth fraction, $fgrow(nucl,t) = fgrowrx(nucl)*fgrowmn(t)$, is taken as a factor $fgrowrx(nucl)$ times $fgrowmn(t) = eps(t)$, where $eps(t) = dln(gent(t))/dt$ is the overall growth of the total demand for nuclear energy. The factor $fgrowrx(nucl)$ was varied to show its significant impact on the cost-optimized generation mix, $gen(nucl,t)$.

- Two objective functions were evaluated; OBJ_{COST} : the present value of all (nuclear) energy costs over the period 2000-2100; and OBJ_{PROL} : the AL -weighted exposure ($kg\text{-}yr$) evaluated at the terminus year (2100). As described below, the ratio of OBJ_{COST} to the total discounted generation over the optimization period (2000,2100) results in an average cost of electricity,

$$< COE > (mill / kWh) = \frac{OBJ_{COST}}{hpy \int_{2000}^{2100} \frac{gen(t)}{(1-dr)^{t-2000}} dt} \quad (3-11)$$

where $hpy = 8,760$ h/yr.

When conducting parametric variations of unit costs, deployment-rate limits, or capacity limits, a base case is identified (unfortunately, not fully consistent among the full set of parametric studies conducted and reported herein), and results are presented in terms of $\langle COE \rangle$ and $pri = xpospual(2100)$ (Sec. C.1, Appendix C) values that are normalized to that base or point-of-departure case; these relative economic and proliferation metrics are labeled $rcoe$ and $rpri$, respectively.

As noted above, in additions to the time evolution of the generation mix, $gen(nucl, t)$, the average cost of energy, $\langle COE \rangle$, as measured by the total discounted energy cost divided by the total discounted energy generation over the same period, $\int gent(t)pdr(t)dt$, where $pdr(t) = 1/(1 + dr)^t$, is a discounting factor, and the system-averaged Attractiveness Level weighted plutonium exposure, $xpospual(t)$, as given in Sec. C.2 and is evaluated at the terminus year 2100, were monitored. Also computed from the optimized results is the undiscounted annual energy charge, $AC(t)$, which is comprised of 14 NFC sub-accounts (Sec. C.1, Appendix C). Dividing $AC(t)$ by $gent(t)$ gives an instantaneous (undiscounted) measure of the cost of electricity, $COE(mill/kWeh)$, which, depending on the tightness of the constraints imposed on the FCOPT material and energy balance and capacity constraints, can show fluctuations that reflect the looseness of the constraints that define the LP model searching for a global optimum solution over the complete variable set $\{m, p, t\}$.

3.2.2 Parametric Results

Before presenting these interim results, it must be emphasized the FCOPT model is not a time-dependent model in the sense of solving a forward-progressing differential equation. Each variable $x(m, p, t)$ or $gen(nucl, t)$ is chosen by the optimizer to minimize the objective function as $m * p * t$ separate entities are varied to achieve a minimum value of OBJ_k . The smoothness of the resulting time series for a given m or p [or in the case of $gen(nucl, t)$, $nucl$] is determined by the efficacy of the constraints imposed on this optimization in the search of “reality”. Furthermore, the search for an optimally feasible solution to the NFC problem described in Sec. 3.1.2 and Appendix E has not been straightforward. Appendix H gives a mapping of material m and process p for a given time t , the vector $x(m, p, t)$ is null for null entries into this map. This combination of searching for a physically realistic and optimally feasible solution has presented a challenging problem. The parametric results reported herein reflect more the difficulty of this search and a recipe for future work instead of presenting an end result that is immediately applicable to guiding the making of policy. The process of this search for a physically acceptable, optimally feasible solution to the NFC problem under the conditions of meeting an exogenously imposed nuclear-energy demand has led to important insights into the way in which the long-term nuclear enterprise might be conducted. Even for the relatively simplified NFC model posed herein, and the compactness of the option space being evaluated, the trade-off between storage and SNF disposal capacities allocated, rate of technology introduction imposed, and the desire to minimize (within the confines of the present study) both cost and proliferation risk presents a formidable challenge. The

interim results presented in the following subsections reflect the degree to which this challenge has been met, as well as the degree and direction of future work in this area.

Table B-I (Appendix B) lists key parameters for the point-of-departure (POD) adopted for this study. Starting with this input, $RS = 25$ Run Series were conducted to explore model sensitivities to key input, and to improve both model constraints and input data. Table 3-I describes these Run Series, each of which represents a number of FCOPT evaluations, depending on the degree of parametric systems analyses conducted. This table also lists the key input parameters varied in each Run Series. In the course of conducting this exploration, the POD cases were “refreshed”, as is indicated on Table 3-II. The key input defining these five main POD cases that have emerged from this exercise are listed in Table 3-II, which is an expansion of Table B-I; any blank entry in Table 3-II assumes the value of the preceding non-blanked entry.

In the course of these preliminary FCOPT runs, two overarching findings/observations emerged. Firstly, for the range of inputs listed in Table 3-II (Appendix G) and the array of constraints enforced (Appendix E), the *rxot* and (to a lesser extent) the *rxmx* generation technologies dominate the generation mix over the optimization time frame (2000,2100) for the fixed uranium price ($ucmm = 30$ \$/kgU) and $dgrowth = 0.01$ 1/yr growth rate assumed. The *rxhg* and/or *rxfb* technology under some circumstances entered the mix in the latter half of this century, but only as minor contributor to the overall nuclear demand (few percent total integrated generation); the transmuting technologies, $fsb = \{rxif, atw\}$, never entered the generation mix, whether that mix was optimized to minimize cost or proliferation risk. Secondly, although in almost all cases, unit costs, capacity limits, and deployment-rate constraints imposed on key front- and back-end technologies [e.g., interim SNF storage (*is*), direct-disposal repository (*dd*), reprocessing (*rp*) and separations (*sep*), separated plutonium storage (*pus*), etc.] exhibited only minor impacts on energy costs, the impacts on both the form and evolution of the stored inventories and process rates, as well as on the proliferation metric [either $pri = xpospual$ (kgPu/yr) or the POD-normalized value, $rpri$] were important. The trade offs between $rpri$ and $rcoe$ [the POD-normalized cost of electricity computed according to Eq. (3-11)] proved equally interesting. These “top-level” findings are elaborated in the following subsections that comprise the bulk of the interim FCOPT results reported herein.

These interim results are grouped into the following six subsections: generation mix and typical mass flows and inventories (Sec. 3.2.2.1); impacts of interim storage cost and capacity (Sec. 3.2.2.2); impacts of repository cost and capacity (Sec. 3.2.2.3); impacts of reprocessing cost and capacity (Sec. 3.2.2.4); cost *versus* proliferation risk (Sec. 3.2.2.5); impact of generation technology capital cost (Sec. 3.2.2.6).

Table 3-I. Description of RS = 25 Run Series Forming the Basis of this Study.

Run Series	Description/Comments	Parameter Varied
01	Initial point-of-departure (POD) case	starting set
02	Decrease <i>ru</i> versus <i>nu</i> relative processing costs from 100 to 1	<i>fruvsn</i>
03	Vary <i>dd</i> capacity,	<i>ddcapf</i>
04	Use proliferation objective function	<i>prolif</i> = 1
05	Vary cost/proliferation metric	<i>pro</i>
06	Vary <i>dd</i> , <i>pu</i> , and <i>ma</i> disposal unit costs	<i>ucddf</i> , <i>ucpud</i> , <i>ucmad</i>
07	Vary generation technology deployment-rate constraint	<i>fgrowrx</i> , <i>fseed</i>
08	Vary cost-proliferation coupling coefficient for new (lower) <i>frowrx</i> and <i>fseed</i> values	<i>pro</i>
09	Vary generation deployment rate with higher <i>ru</i> processing costs (<i>fruvsn</i> = 2) and lower seed parameter (<i>fseed</i>)	<i>fgrowrx</i>
10	Same as series Run 09 with cost-proliferation coupling parameter <i>pro</i> = 100 \$/kgPu/yr	<i>fgrowrx</i>
11	Vary cost-proliferation coupling parameter <i>pro</i> with higher <i>is</i> and <i>dd</i> capacity, for <i>bnisrx</i> (= 70) and <i>ddcapf</i> (<i>ym</i> = 10),	<i>pro</i>
12	Vary unit cost of <i>fp</i> storage for nominal POD parameters	<i>ucfps</i>
13	Vary <i>is</i> and <i>rp</i> capacities to search for feasibility limits	<i>bnisrx</i> , <i>ddcapf</i>
14	Vary <i>rp</i> capacity for <i>bnisrx</i> = 70; identify a new POD case as RUN 14a	<i>ddcapf</i>
15	Vary <i>dd</i> , <i>pu</i> , and <i>ma</i> disposal unit costs for new POD (RUN 14a), with <i>rp</i> deployment functionality (<i>exrp</i>) decreased to 1;	<i>ucddf</i> , <i>ucpud</i> , <i>ucmad</i>
16	Vary all reprocessing unit costs for all repository (<i>dd</i>) unit costs fixed at 500 \$/kg	<i>ucrpux</i> , <i>ucrpmx</i> , <i>ucrpbm</i> , <i>ucsep</i>
17	Vary <i>dd</i> unit cost for new POD case (RUN 17b)	<i>ddcapf</i>
18	Vary unit costs of interim SNF storage (<i>is</i>)	<i>ucisp</i> , <i>ucisu</i>
19	Vary cost-proliferation coupling coefficient for RUN19a POD	<i>pro</i>
20	Vary (enlarge) optimization time frame to test optimization results	<i>tmax</i>
21	Vary unit total cost of one generation technology (<i>rxhg</i>)	<i>uct(rxhg)</i>
22	Vary <i>is</i> and <i>dd</i> capacity limits, along with <i>pus</i> unit cost to map infeasibility limits	<i>bnisrx</i> , <i>ddcapf</i> , <i>ucpus</i>
23	Vary <i>is</i> , <i>pus</i> , and <i>dd</i> capacity limits to map infeasibility limits	<i>bnisrx</i> , <i>ddcapf</i>
24	Vary generation technology deployment rates again, settle on new POD (RUN 24c)	<i>Fgrowrx</i> , <i>fseed</i>
25	Vary unit total cost of one generation technology (<i>rxhg</i>) for new POD case (RUN 25c)	<i>utc(rxhg)</i>

Table 3-II. Listing of Key Input Parameters Defining the Evolving Point-Of-Departure Cases (POD) Used in this Study.

CASES/POD (RUN)			01	14a	17b	19a	24c
<i>Capacities/Limits</i>	<i>Symbol</i>	<i>Unit</i>					
Number of core loads in interim storage	bnisrx(nucl)	----					
o Once-through LWR (rxot)	bnisrx(rxot)	----	10	70			10
o MOX-fueled LWR (rxmx)	bnisrx(rxmx)	----	10	70			10
o MOX-fueled HTGR (rxhg)	bnisrx(rxhg)	----	10	70			10
o MOX-fueled FBR (rxfb)	bnisrx(rxfb)	----	10	70			10
o Metal-fueled IFR-based transmuter (rifr)	bnisrx(rifr)	----	10	70			10
o Metal-fueled ADS-based transmuter (atw)	bnisrx(atw)	----	10	70			10
Final repository capacity	ddcapf	kg(SNFeq)	7.0E(+07)	7.0E(+08)	7.0E(+07)	7.0E(+08)	7.0E(+07)
Reprocessing deployment-rate limit	rpratelim		2				
Reprocessing capacity limit							
o Initial capacity	rpcapi	kg/yr	0	0	0		
o Final capacity	rpcapf	kg/yr	1.0E(+08)	3.0E(+06)	1.0E(+08)		
o Initial time	trpi	----	11	11	11		
o Final time	trpf	----	21	31	31		
o Exponent	exprp	----	1	2	1		
Separated-plutonium storage capacity limit	bnpus	kg(Pu)	1.0E(+06)				1.0E(+07)
Separated minor-actinide storage capacity limit	bnmas	kg(Pu)	1.0E(+06)				
<i>Unit Costs</i>							
Mined and milled natural uranium	ucmm	\$/kg(NU)	30				
Relative process cost for ru versus nu	frvusnu	----	100				
Fuel Fabrication							
o Uranium oxide	ucffux	\$/kg(UOX)	250				
o Uranium-plutonium mixed oxide	ucffmx	\$/kg(MOX)	3000				
o Uranium-plutonium-zirconium metal	ucffmt	\$/kg(HM)	3000				
Storage							
o Cooling storage	uccs	\$/kg(SNF)/yr	60				
o Interim storage for rux	ucisu	\$/kg(SNF)/yr	60				
o Interim storage for rmx	ucisp	\$/kg(SNF)/yr	60				
o Reactor uranium storage	ucrus	\$/kg(HM)/yr	300				
o Separated-plutonium storage	ucpus	\$/kg(HM)/yr	300				
o Separated minor-actinide storage	ucmas	\$/kg(HM)/yr	300				
o Separated fission-product storage	ucfps	\$/kg(FPP)/yr	100				
Installed unit total capital costs	uct(nucl)						
o Once-through LWR (rxot)	utc(rxot)	\$/We	1.70				
o MOX-fueled LWR (rxmx)	utc(rxmx)	\$/We	1.70				
o MOX-fueled HTGR (rxhg)	utc(rxhg)	\$/We	2.30				
o MOX-fueled FBR (rxfb)	utc(rxfb)	\$/We	2.60				
o Metal-fueled IFR-based transmuter (rifr)	utc(rifr)	\$/We	2.60				
o Metal-fueled ADS-based transmuter (atw)	utc(atw)	\$/We	3.00				
Reprocessing and Separations							
o Reprocessing of UOX (rux)	ucrpx	\$/kg(HM)	1500				
o Reprocessing of MOX (rmx)	ucrpxmx	\$/kg(HM)	1500				
o Reprocessing of FBR blanket materials (bmx)	ucrpblmx	\$/kg(HM)	1500				
o Reprocessing of FSB materials (separations)	ucsep	\$/kg(HM)	4000				
Repository Disposal							
o Repository SNF direct disposal	ucddf	\$/kg(SNF)	1000		500		
o Repository separated-plutonium direct disposal	ucpud	\$/kg(HM)	1000		500		
o Repository minor-actinide direct disposal	ucmad	\$/kg(HM)	1000		500		
o Repository fission-product direct disposal	ucfpd	\$/kg(FPP)	100		500		

Table 3-II. Listing of Key Input Parameters Defining the Evolving Point-Of-Departure Cases (POD) Used in this Study (continued).

CASES/POD (RUN)			01	14a	17b	19a	24c
Generation Growth Constraint:	Symbol	Unit					
$d\text{cap} < \text{cap}(\text{nucl}, t-1) * f\text{grow}(\text{nucl}, t) + f\text{seed}(\text{nucl}) * g\text{ent}(t)$							
$f\text{grow}(\text{nucl}, t) = f\text{growrx}(\text{nucl}) * f\text{growmx}(t); f\text{griwnx} = \text{eps}(t)$							
$f\text{growrx}(\text{nucl})$							
o Once-through LWR (rxot)			2				
o MOX-fueled LWR (rxmx)			2	0.5			2
o MOX-fueled HTGR (rxhg)			2	0.5			2
o MOX-fueled FBR (rxfb)			2	0.5			2
o Metal-fueled IFR-based transmuter (rifr)			2	0.5			2
o Metal-fueled ADS-based transmuter (atw)			2	0.5			2
$f\text{seed}(\text{nucl})$							
o Once-through LWR (rxot)			0.01				
o MOX-fueled LWR (rxmx)			0.01	0.005			0.01
o MOX-fueled HTGR (rxhg)			0.01	0.0001			0.01
o MOX-fueled FBR (rxfb)			0.01	0.0001			0.01
o Metal-fueled IFR-based transmuter (rifr)			0.01	0.0001			0.01
o Metal-fueled ADS-based transmuter (atw)			0.01	0.0001			0.01
Proliferation Metric							
Object function	prolif		0	0	0	0	0
Multi-criterion unit cost	pro	\$/kg(AI)/yr	0	0	0	0	0

3.2.2.1 Time Evolution of Generation Mixes and Key Material Inventories and Flows Rates

As described above, the mix of generation technologies was found to be relatively insensitive to the range of capacity and deployment-rate constraints imposed. The time-series describing key front- and back-end inventories and mass flow rates, however, showed a greater sensitivity to the parameters varied. This behavior is exemplified by the corresponding results displayed in Figure 3-2 through Figure 3-7 for the respective Run 14a, 19a, and 24a POD cases listed in Table 3-II. It is noted that for these POD cases, unit costs of storage (*ucis*), disposal (*ucddf*), reprocessing, (*ucrp*) and capital cost of electricity generation (*utc*) were held constant; the impact on both *rcoe* and *rpri* of parametrically varying these key unit cost are examined in the following subsections.

The evolution of POD cases represented by Runs 14a → 19a → 24c was not systematic during this exploratory phase, but the differences in the time dependencies of the mass inventory and flow-rate observed in Figure 3-2 through Figure 3-7 reflect the large differences in repository capacity ($y_m = 10$ for Runs 14a and 19a, but $y_m = 1$ for Run 24, where y_m corresponds to Yucca Mountain equivalents, $7(10)^7 \text{ kgSNF}$). Run 14a was limited to a final (after a linear ramp over a period of $\text{trpf} - \text{trpi} = 10 \text{ yr}$) reprocessing capacity of $\text{rpcapf} = 3,000 \text{ tonneHM/yr}$, whereas Runs 19a and 23c have essentially unlimited reprocessing capability, but only after $\text{trpf} - \text{trpi} = 20 \text{ yr}$, with Run 19a achieving that final (large) capacity quadratically in time ($\text{exprp} = 2$) and Run 24c approached that repository capacity linearly ($\text{exprp} = 1$) in time. Lastly, the interim SNF storage for Runs 14a and 19a were set at the high value of $\text{bnixrx}(\text{nucl}) = 70 \text{ reactor-core-equivalents}$, but is reduced to 10 reactor-core equivalents for Run 24c. Achieving an optimally feasible solution to this problem depends sensitively on these parameters.

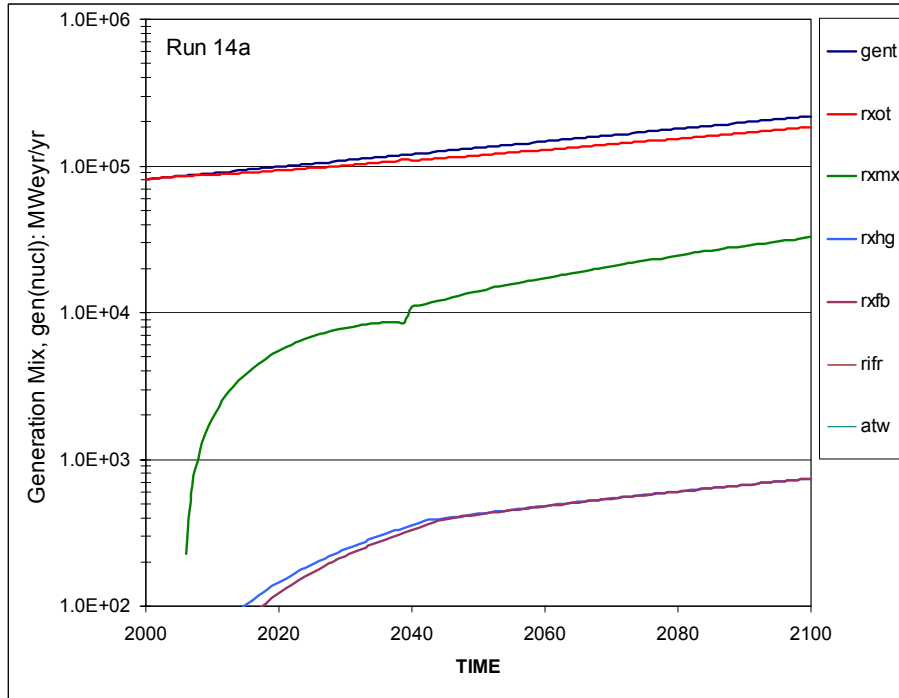


Figure 3-2. Time evolution of generation mix for Run 14a POD case (Table 3-II).

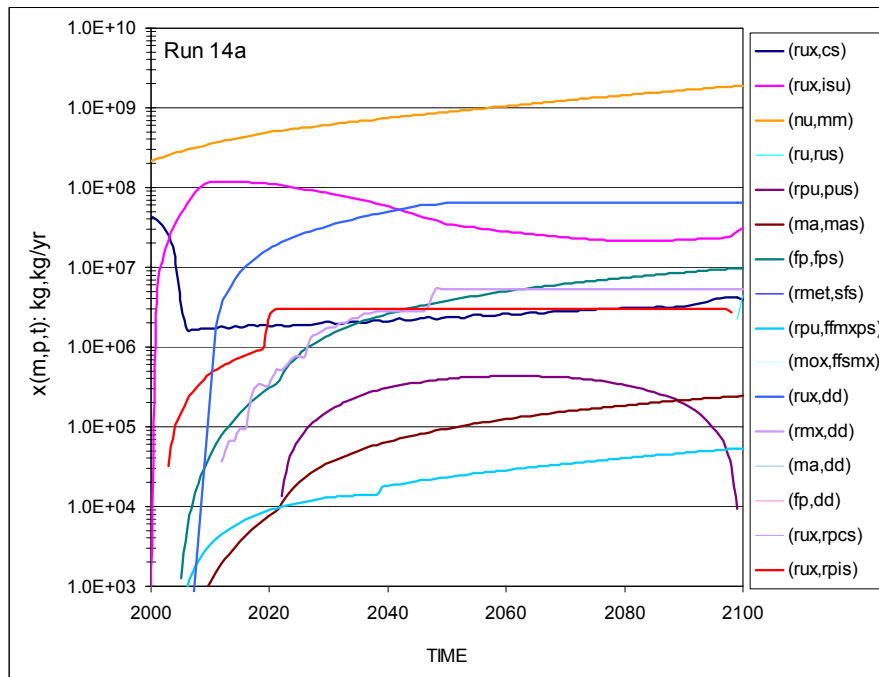


Figure 3-3. Time evolution of key NFC material inventories and flow rates for Run 14a POD case (Table 3-II).

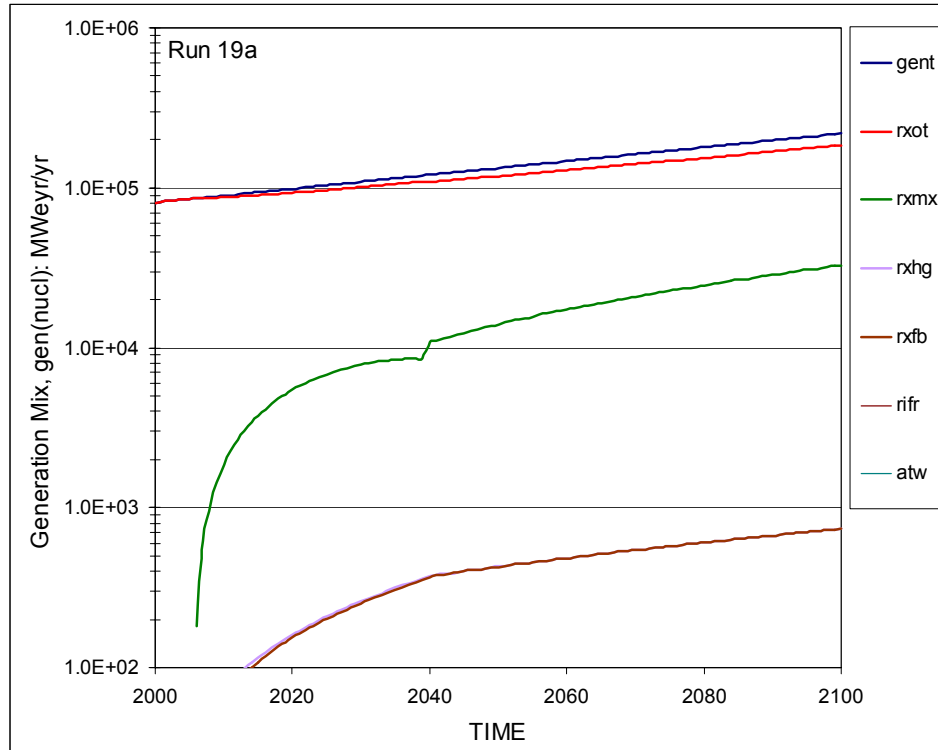


Figure 3-4. Time evolution of generation mix for Run 19a POD case (Table 3-II).

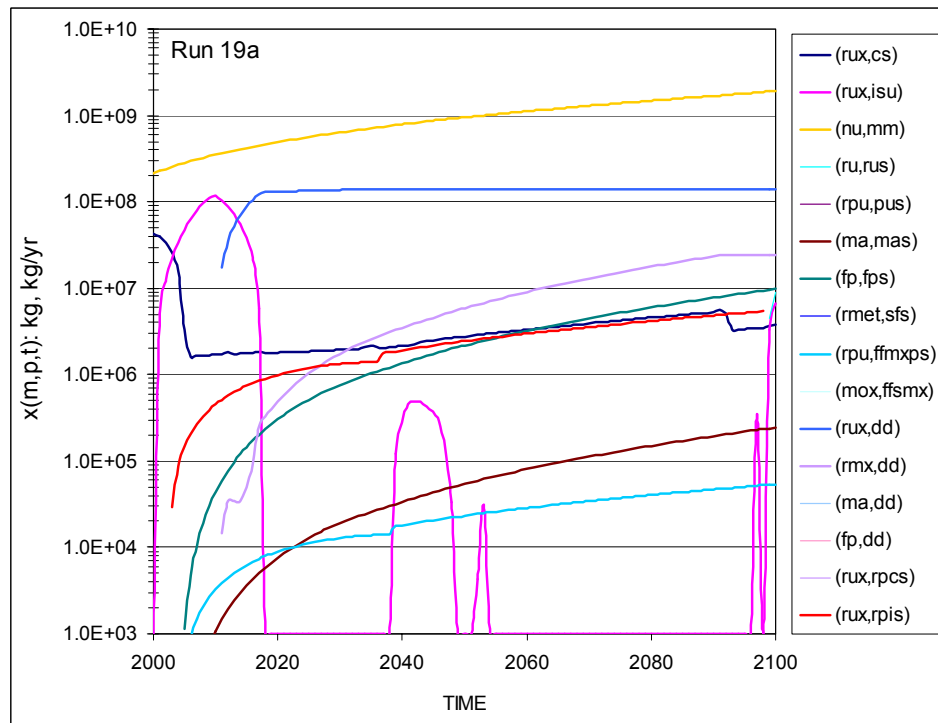


Figure 3-5. Time evolution of key NFC material inventories and flow rates for Run 19a POD case (Table 3-II).

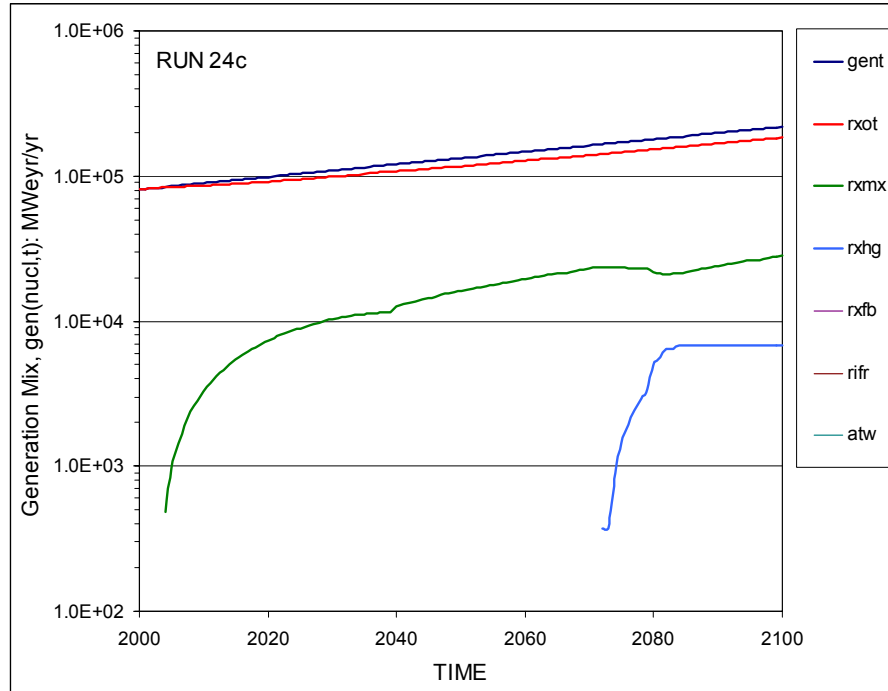


Figure 3-6. Time evolution of generation mix for Run 24a POD case (Table 3-II).

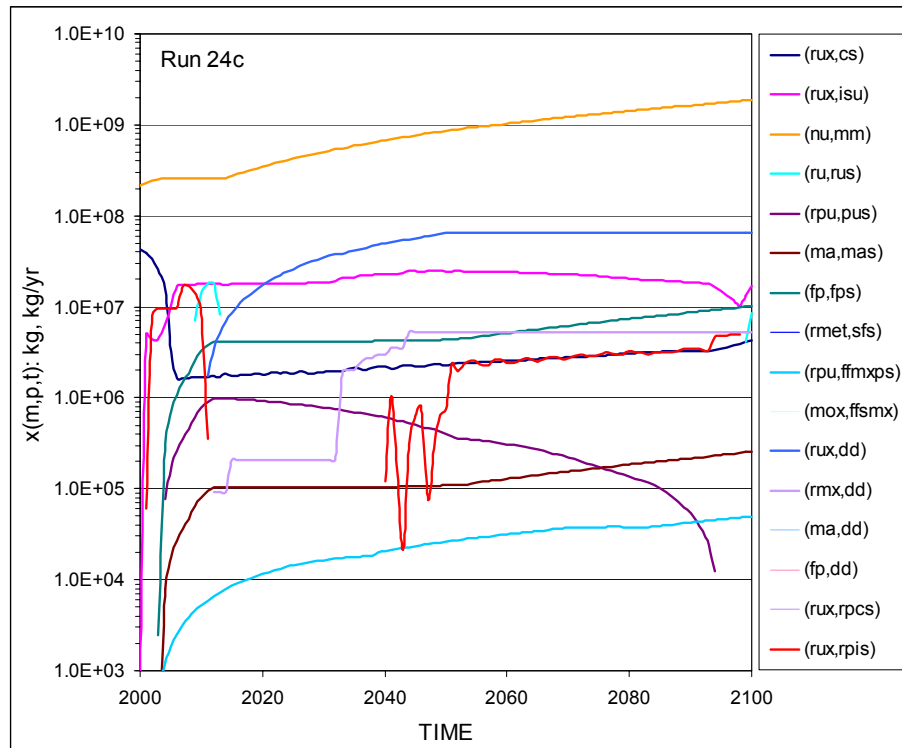


Figure 3-7. Time evolution of key NFC material inventories and flow rates for Run 24a POD case (Table 3-II).

Finally, while the capacity of the separated-plutonium storage (*pus*) was limited to 1,000 *tonnePu* for Runs 14a and 19a, this limit was increased by a factor of 10 for Run 24c; as seen from in Figure 3-2 through Figure 3-7, this higher *pus* limit was never met. While these differences have only a small impact on *COE*, the impact on *PRI* and the overall dynamics depicted in Figure 3-2 through Figure 3-7, are larger. Table 3-III summarizes a few key, “top-level” parameters that quantify these findings for the POD cases listed in Table 3-III; the *COE* and *pri* values listed in Table 3-III provide the normalizations for *rcoe* and *rpri* reported subsequently.

Table 3-III. “Top-Level Results for thePOD Cases Represented by Runs 14a, 19a, and 24c.

CASES/POD (RUN)			01	14a	17b	19a	24c
<i>Top-Level Results</i>	Symbol	Unit					
Cost of electricity	coe	mill/kWeh	46.11	43.82	43.15	41.11	44.35
Fraction once-through LWR/OT generation technology	fGEN(rxot)	---	0.8791	0.8880	0.8880	0.8880	0.8791
Proliferation metric	pri	kgPuyr	4.85E+10	3.00E+10	7.66E+09	7.75E+09	4.88E+10
Present value of total cost	pvtot	\$	8.83E+11	8.39E+11	8.26E+11	7.87E+11	8.49E+11
Cost/proliferation metric	pvtot/pri	\$/kgPu/yr	18.20	27.91	107.85	101.50	17.40

The capacity limits and unit costs for interim SNF storage (*is*), repository direct disposal (*dd*), and reprocessing (and separations) (*rp*, *sep*) technologies play an important role in the dynamics of material inventories and flow-rate; these dependencies have been examined parametrically in Run Series $RS = \{17,18,23\}$, $\{15,17\}$, and $\{13,14,16\}$, respectively. In addition, the trade off between cost and proliferation risks *vis-à-vis* the connection parameter *pro* [Eq. 3-4] is examined in Run Series 19, and the single example of the response and impact of shifts in the unit total cost of a selected generation technology (*rxhg*) is examined in Run Series {24c,25}; the results of these five parametric systems analyses (*is*, *dd*, *rp*, *pro*, and *utc*) are reported in the following subsections.

3.2.2.2 Cost and Capacity of Interim SNF Storage (*is*)

The unit cost for interim storage (*is*) for both spent UOX (*ru*x placed in *isu*) and spent MOX (*rm*x placed in *isp*) is taken at $ucisu = ucisp = 60$ \$/kgSNF/yr, and the capacity is set at $bnisrx(nucl) = 70$ reactor-core equivalents for all generation technologies (for Runs 14a and 19a; Run 24c *is* capacity is set at $bnisrx = 10$ reactor core equivalents). Either reducing the *is* capacity or increasing the cost of using whatever capacity exists is expected to exert pressure on either the direct-disposal repository (*dd*), or reprocessing for plutonium burning in $rx = \{rxmx, rxhg, rxfb\}$ technologies. Reprocessing (*rp*) in turn produces separated plutonium that must either be stored in *pus* and/or burned in *rx* or *fsb* technologies, given that the respective capacities and/or costs allowing. Depending on the respective costs (including that of *rp*, as well as the rate at which reprocessing capacity is introduced, *rpratelim*) and the overall impact on energy cost as well as the magnitude of inventories of plutonium with high proliferation proneness (high *AL*) leads to interesting cost-proliferation (*rcoe-rpri*) tradeoffs, as noted earlier. This subsection begins the exploration of these tradeoffs.

Run Series $RS = \{17,18,23\}$ address the $ucisu$, $usisp$, $bnisrx(nucl)$ impact analyses. Increasing interim storage unit costs, $ucis(u,p)$, combines with the search for a feasible optimum solution to push SNF into the direction of dd (as long as the price is right and the capacity exists to handle the SNF ingress), as well as shifting SNF material flows into reprocessing. For the present conditions driving FCOPT, it appears to be more cost-optimal to process the SNF and store it as separated plutonium in pus , with some this separated reactor-plutonium material supporting the growing $rxmx$ technology. The growing plutonium inventories in pus are expected to increase $rpri$, since this form has been assigned a high AL value (Sec. C.2, Appendix C). The introduction of rp capability and the attendant increase in pus inventories switches on for a narrow range of $ucis(u,p)$ values, which are designated as $ucis^*$ in Figure 3-8 and Figure 3-9, both of which give the dependence of $rcoe$ and $rpri$ on $ucis(u,p)$; these frames show both a direct and a correlative dependence of these parameters. Figure 3-10 depicts the time evolution of separated-plutonium inventory, $x(rpu,pus,t)$, and the rate of rux SNF reprocessing, $x(rux,rpis,t)$, for a range of unit costs of holding SNF in interim storage, $ucis(\$/kgSNF/yr)$; the point where the “critical” value $ucis^*$ is transcended indicates a significant change in the inventory $x(rpu,pus,t)$, as driven by the large (early) increase in SNF reprocessing rate of rux SNF from interim storage is , $x(rux,rpis,t)$ ($kgSNF/yr$). These increases in turn drive a sudden increase in the normalized proliferation risk index, $rpri$, because of the high AL rating of this material form in this process. The peculiar sudden fall and dips in the $x(rux,rpis,t)$ transients cannot be explained, and must be addressed by the addition of rate-limiting constraints and/or cost penalties for reprocessing capacity that goes unused after reprocessing has shown a large production rate; the interest and capital on such an underutilized plant must be paid, and these kinds of costs are not yet included in the objective function, OBJ_{COST} .

The interim-storage capacity constraint, $bnisrx(nucl)$, expressed here in reactor-core equivalents, represents a second driver of plutonium into other parts of the NFC in search for a minimum-cost configuration. Using Run 17b as a POD case, $bnisrx(nucl)$ was varied over a wide range, wherein all generation technologies $nucl$ shared the same values of $bnisrx$. The dependence of $rcoe$ and $rpri$ on $bnisrx$ in both comparative and correlative forms is shown on Figure 3-11 and Figure 3-12, respectively; the cost impacts of reducing interim storage capacity are weak, but the impact on pri is significant. The reason for this behavior is illustrated by the Figure 3-13 and Figure 3-14 time-dependent depiction of SNF inventory in is as well as the separated-plutonium inventory in pus . As expected, $x(rux,is,t)$ diminishes with decreased capacity allocation, $bnisrx$, but the increased storage of separated-plutonium shown in Figure 3-14 strongly drives an increase in pri because of the high AL assignment to this plutonium form. This strong- $rpri$, weak- $rcoe$ impact of allocated is capacity is dependent on the characteristics of the Run 17a POD case used, wherein the repository capacity is set at $ddcapt = 7(10)^7 kgSNF (ym = 1)$. For most of the $bisrx$ cases considered, the repository reaches this capacity limit, but interestingly the full limit is reached only for the higher values of $bnisrx$, as is shown in Figure 3-15, which gives the dependence of $x(rux,dd,2100)$ on $bnisrx$; it is unclear whether this unintuitive result is a failure of the model or the modeler.

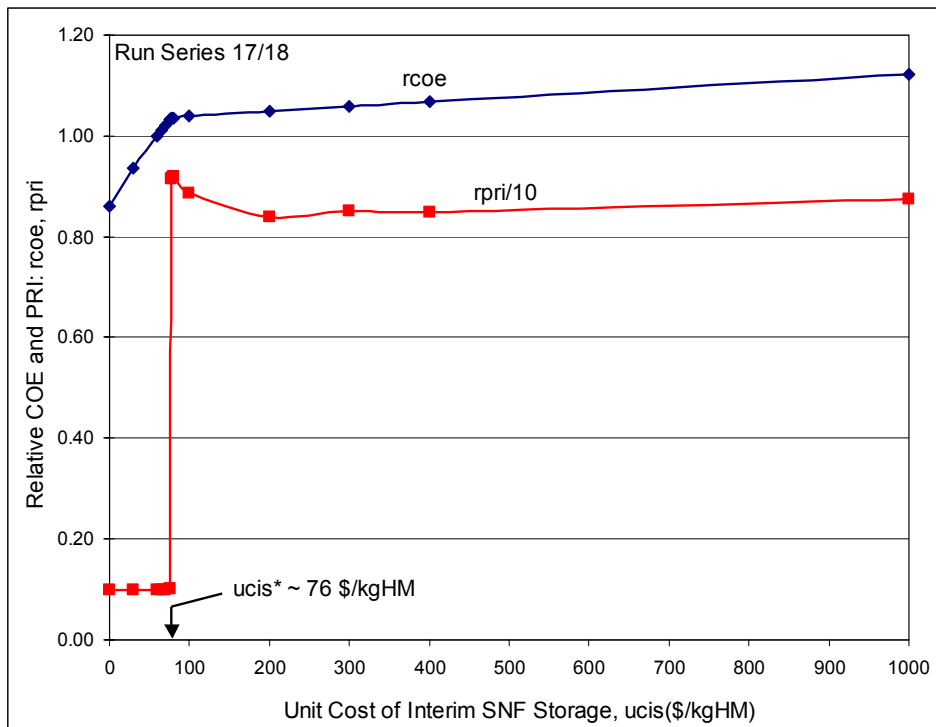


Figure 3-8. Impact of interim storage costs, $ucis(u,p)$, on relative cost and proliferation risk index: direct individual plots (Run 17b is POD case, Table 3-II).

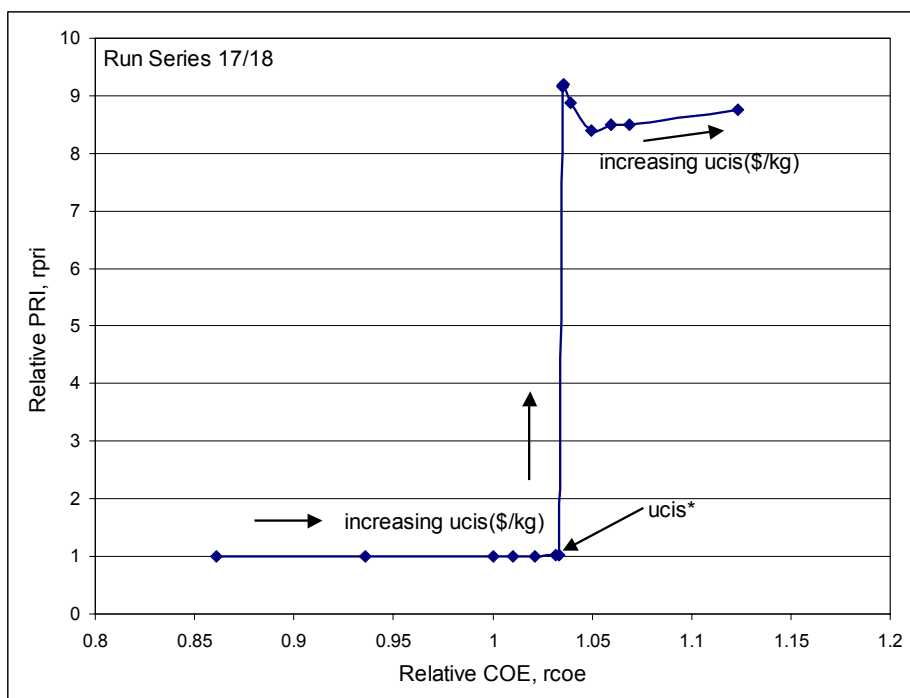


Figure 3-9. Impact of interim storage costs, $ucis(u,p)$, on relative cost and proliferation risk index: cross-correlative plots (Run 17b is POD case, Table 3-II).

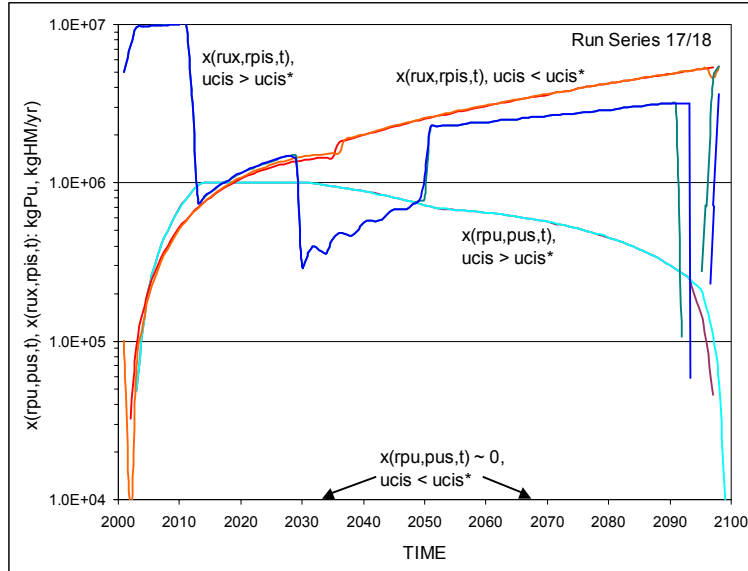


Figure 3-10. Time evolution of separated-plutonium inventory, $x(rpu, pus, t)$, and the rate of SNF reprocessing, $x(rux, rpi, t)$, for a range of unit costs of SNF storage in interim storage, $ucis (\$/\text{kgSNF}/\text{yr})$; the point where the “critical” value $ucis^*$ is transcended indicates a significant change in the inventory $x(rpu, pus, t)$, which drives a sudden increase in $rpri$ because of the high AL rating of this material form in this process.

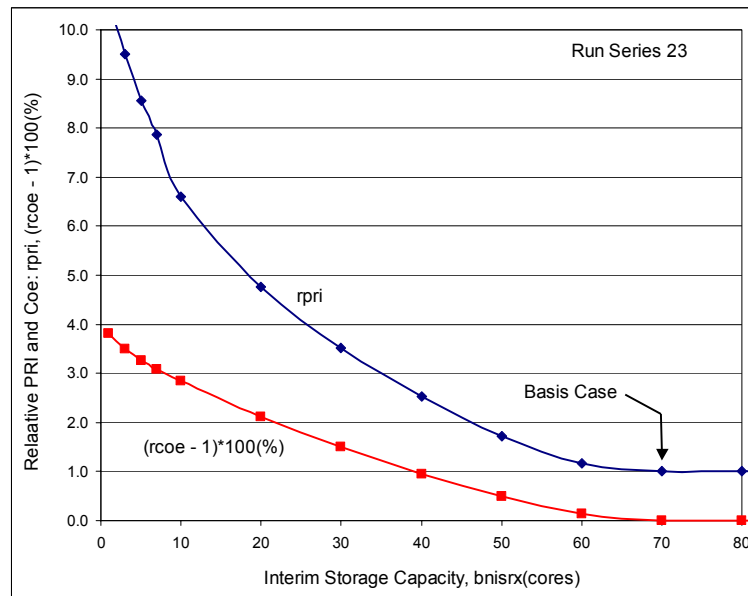


Figure 3-11. Dependence of relative COE and PRI on interim storage (is) capacity, $bnisrx(\text{nucl})$, which is expressed in reactor-core equivalents, for this case, the POD is provided by Run 17a (Table 3-II).

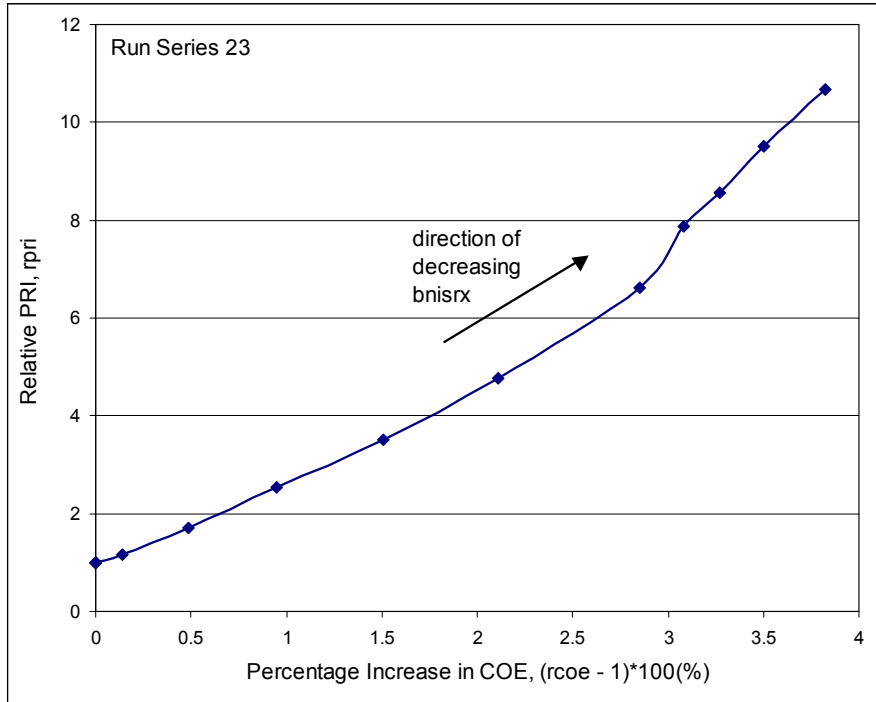


Figure 3-12. Dependence of relative COE and PRI on interim storage (*is*) capacity, $bnisrx(nucl)$, which is expressed in reactor-core equivalents, for this case, the POD is provided by Run 17a (Table 3-II); in this frame, a $rcoe-rpri$ cross correlation is depicted.

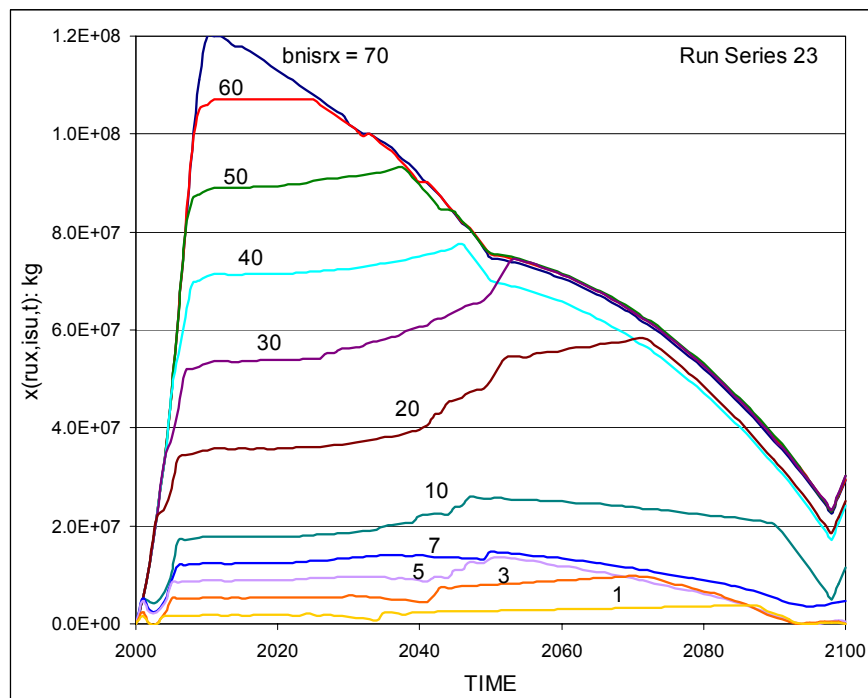


Figure 3-13. Time evolution of interim storage SNF inventory, $x(rux, is, t)$, as interim storage capacity, $bnisrx(nucl)$ is varied.

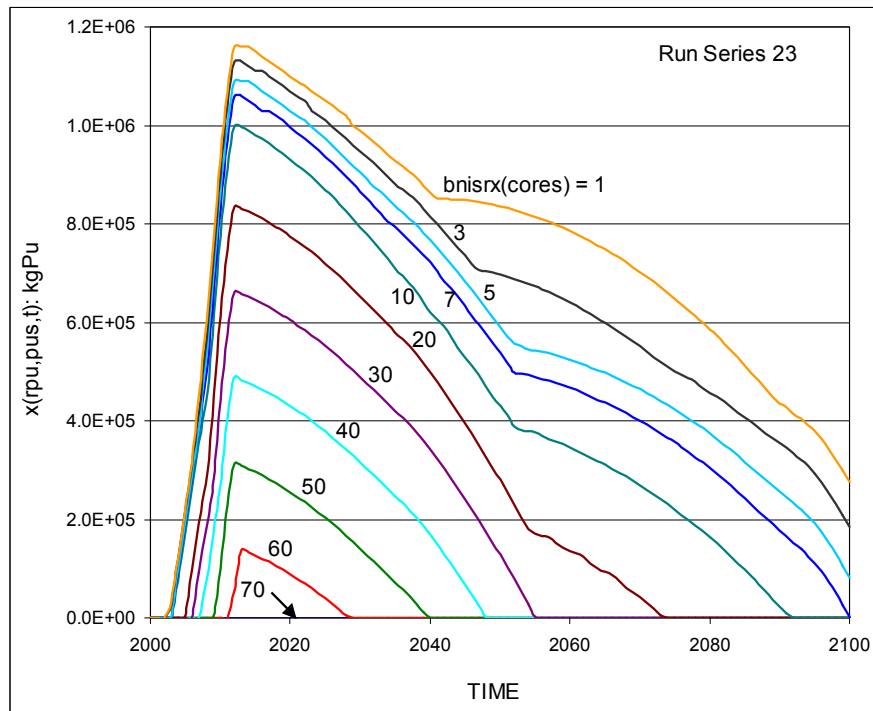


Figure 3-14. Time evolution of separated-plutonium storage inventory, $x(rpu,pus,t)$, as interim storage capacity, $bnisrx(nucl)$ is varied.

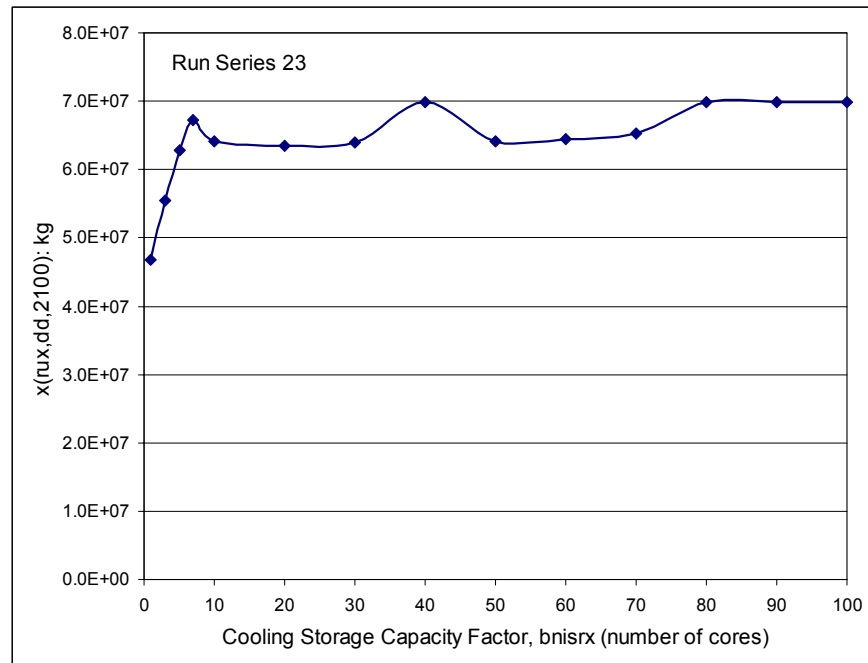


Figure 3-15. Dependence of repository rux inventory at the end of the optimization period, $x(rux,dd,2100)$, on the assigned interim-storage capacity, $bnisrx(nucl)$, where the latter is expressed in reactor-core equivalents; the POD case (Run 17b, Table 3-II) has the final repository capacity at $ddcapf = 7(10)^7 \text{ kgSNF}$ ($ym = 1$).

3.2.2.3 Cost and Capacity of Direct-Disposal Repository (*dd*)

For the unit costs assumed for both interim storage [$ucis(u,p) = 60 \text{ \$/kgSNF/yr}$] and repository disposal ($ucdd = 500 \text{ \$/kgSNF}$) in the POD case used for this analysis (Run 17b), neither NFC elements are expected to exhibit strong cost impacts. Neither will the impact on *pri* be strong for the *AL* assignments made to these systems (Sec. C.2). Nevertheless, using Run 17b as a POD case, $ucdd(\text{\$/kgSNF})$ and $ddcapf(\text{kg})$ were subject to single-point variations. The result for the variation of *rcoe* and *rpri* as $ucdd$ is varied show (the POD for this variation is based on Run 14a parameters) no impact on *pri*, with the small impacts on *COE* shown in Figure 3-16. This figure also depicts SNF inventories in both the repository (*dd*), and interim storage (*is*), $x(rux,dd,2100)$ and $x(rux,is,2001)$, respectively, at the end of the optimization period (2100) as the unit cost of repository disposal, $ucdd(\text{\$/kgSNF})$ is varied; for these variation, the cost of interim storage is fixed at $ucis(u,p) = 60 \text{ \$/kgSNF/yr}$. The behavior depicted on Figure 3-16 is expected: a) increased repository rent, $ucdd$, shifts the preferred SNF residency to the interim storage (*is*); b) the proliferation impacts **for the assigned *AL* values in this region of the NFC** are nil, and c) the economic impacts are also small as long as a relatively cheap alternative SNF dwelling place of reasonable capacity is available.

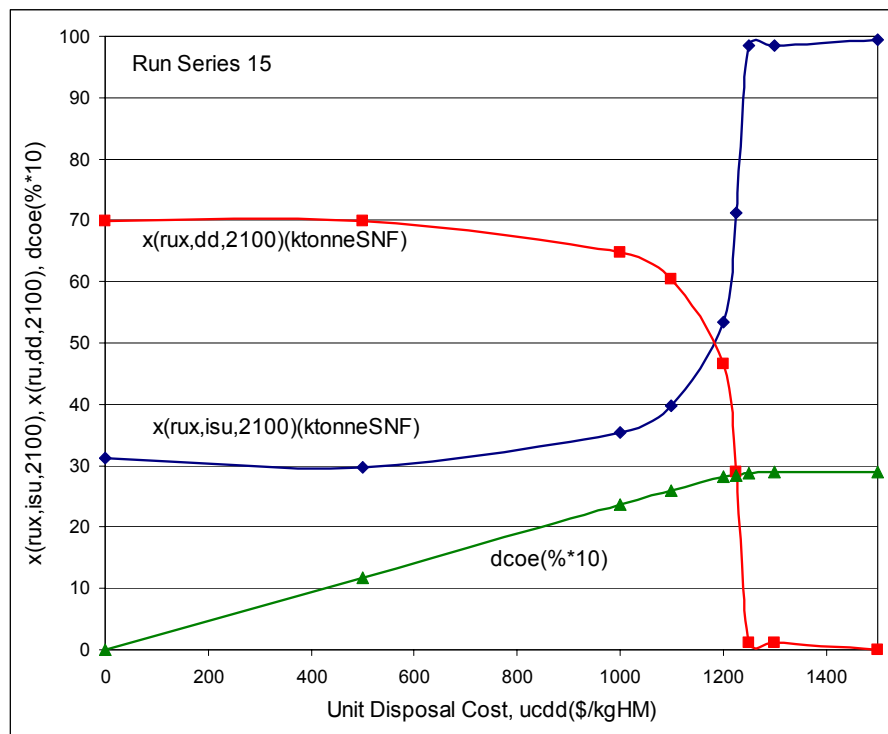


Figure 3-16. Variation of relative COE and SNF inventories in both the repository (*dd*), and interim storage (*is*), $x(rux,dd,2100)$ and $x(rux,is,2001)$, respectively, at the end of the optimization period as the unit cost of repository disposal, $ucdd(\text{\$/kgSNF})$ is varied; for these variations, the cost of interim storage is fixed at $ucis(u,p) = 60 \text{ \$/kgSNF/yr}$.

Using Run 17a as a POD case, the variation of the final repository capacity, $ddcapf(kgSNF)$, that is increased linearly in time over a period $tddf - tddi = 20\text{ yr}$ starting in the year 2010, the cost and proliferation impacts are expected to be small for the reasons cited above. Figure 3-17 and Figure 3-18 show the dependence of $rpri$ and $rcoe$ as $ddcapf$ is varied over a range of Yucca Mountain equivalents, ym ($ym = 1$ corresponds to $70,000\text{ tonneSNF}$); both comparative and correlative plots are shown. The trends indicated on Figure 3-17 and Figure 3-18 are expected, and the impacts are small, as long as alternatives (e.g., interim storage) of acceptable cost and capacity are available; this situation may not be achievable in the world outside that modeled by FCOPT in its present form. This SNF “cat-and-mouse” game played by SNF ($m = rux$) between dd and is is illustrated in Figure 3-19 and Figure 3-20.

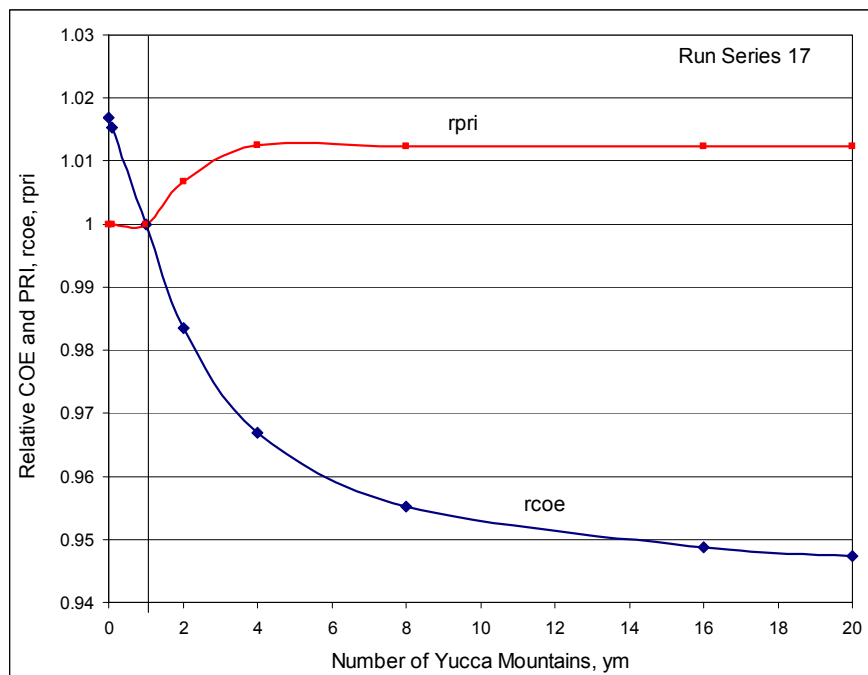


Figure 3-17. Comparative dependence of relative cost and proliferation indices, $rcoe$ and $rpri$, as the final repository capacity, $rpcapf(kgSNF)$, is varied, where ym is expressed in $70,000\text{ tonneSNF}$ equivalents.

It is noted that, for each final repository capacity constraint, a time exists for which the spent fuel contained therein is equal to the SNF inventory contained in interim storage. The dependence of this “equi-partition” time, $t^*(yr)$, on the repository capacity limit expressed in ym units is shown on Figure 3-21. This correlation is possible over such a wide range of ym because of the large interim storage capacity limit, $bnismx = 70\text{ reactor-core-equivalents}$, assumed for this parametric analysis.

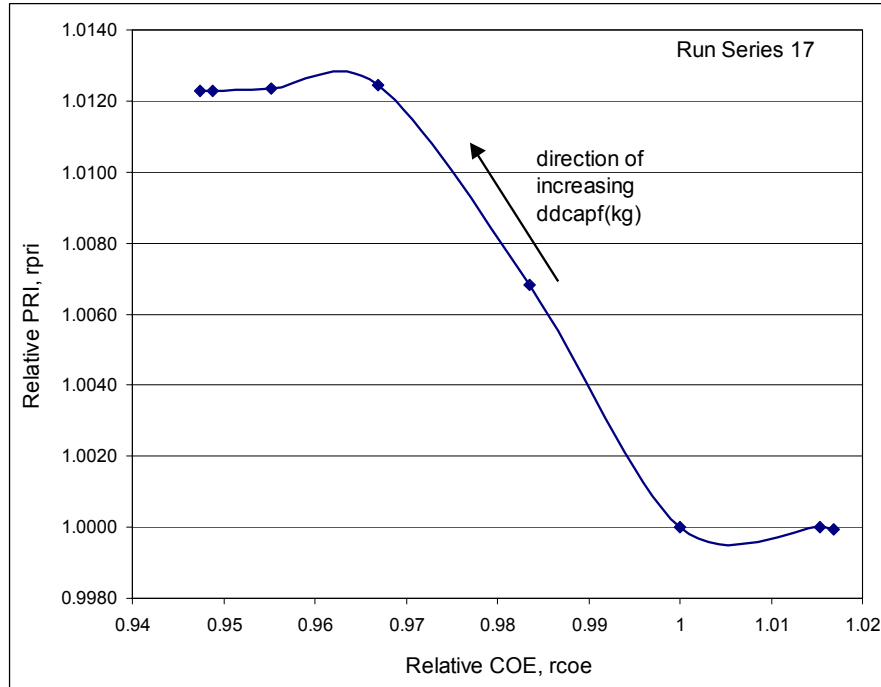


Figure 3-18. Correlative dependence of relative cost and proliferation indices, $rcoe$ and $rpri$, as the final repository capacity, $ddcapf(kgSNF)$, is varied., where ym is expressed in 70,000 tonneSNF equivalents.

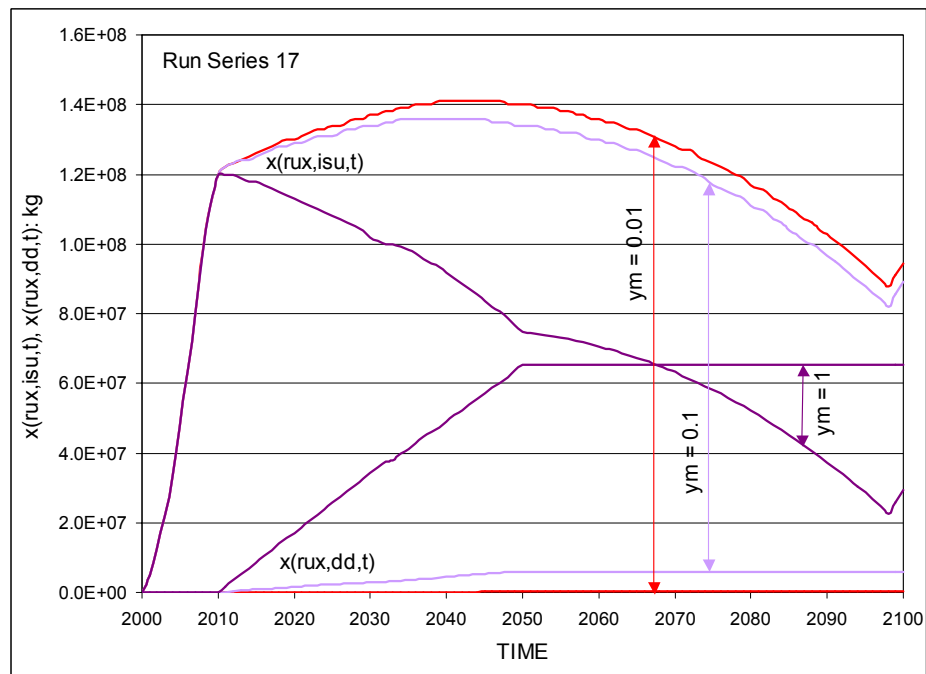


Figure 3-19. Time-dependence of SNF ($m = rux$) inventories in interim storage, $x(rux,is,t)$, and the direct-disposal repository, $x(rux,dd,t)$, for a range of final repository capacity limits, $ddcapf(kgSNF)$, expressed in Yucca Mountain equivalents, ym ($ym = 1$ corresponds to 70,000 tonne SNF).

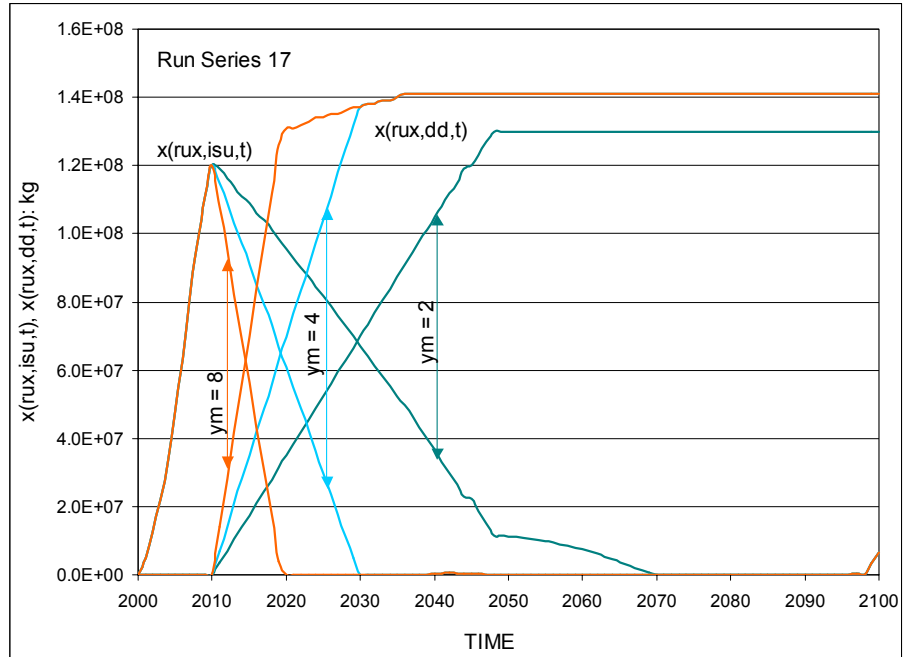


Figure 3-20. Time-dependence of SNF ($m = rux$) inventories in interim storage, $x(rux, is, t)$, and the direct-disposal repository, $x(rux, dd, t)$, for a range of final repository capacity limits, $ddcapf(kgSNF)$, expressed in Yucca Mountain equivalents, ym ($ym = 1$ corresponds to 70,000 tonne SNF).

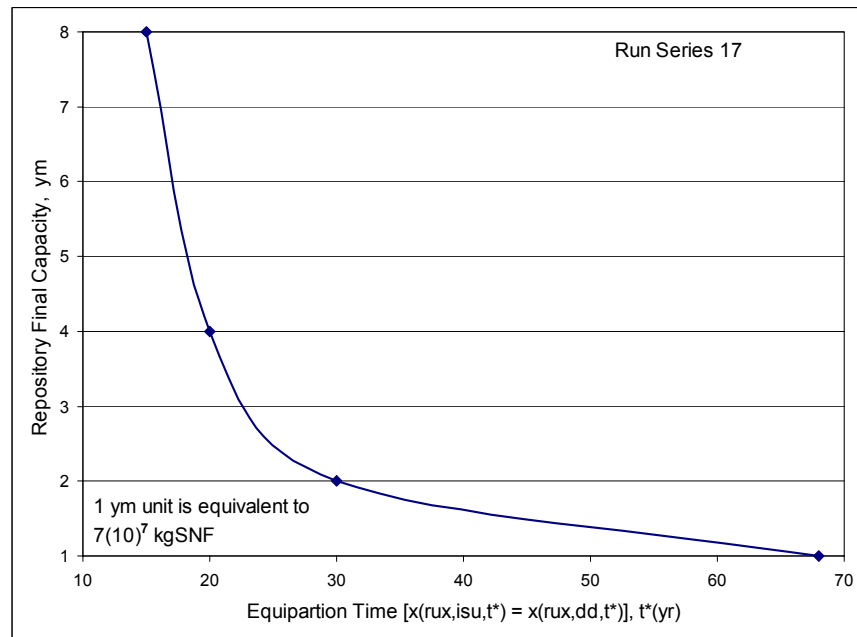


Figure 3-21. Correlation of repository capacity with equi-partition time t^* , which is defined as the time where $x(rux, is, t^*) = x(rux, dd, t^*)$; this correlation holds only for an interim storage capacity of $bnisrx = 70$ reactor-core-equivalents.

3.2.2.4 Cost and Capacity for Reprocessing (*rp*)

The POD case for the cost and capacity variations applied to the reprocessing technology (*rp*) is that provided by Run 14a. Generally, for the large repository and interim storage capacity limits that characterize this POD case, increased processing costs, $ucrp(\$/kgSNF)$, will increase the relative cost of energy, but this increase will not be large because reprocessing for this POD case is not a major cost component. Correspondingly, decreased values of $ucrp(\$/kgSNF)$ will also decrease $rcoe$, but not by a significant factor. Increased $ucrp$ should reduce the amount of reprocessing and, hence, the amount of separated plutonium stored in pus , so the relative proliferation risk, $rpri$, is expected to decrease, or at least hold constant if it is already low for the POD case selected.

Decreased $ucrp$ will increase the level of reprocessing, and if this increase leads to an increase in the amount of separated plutonium in storage, pus , then $rpri$ is expected to increase. Figure 3-22 and Figure 3-23 show this behavior for both $rcoe$ and $rpri$ in both a comparative and a correlative format, respectively. That the transition to higher $rpri$ systems occurs just below the $ucdd$ values ($1,500 \text{ } \$/kgSNF$) adopted for the POD case is considered coincidental. The time evolution of the separated-plutonium storage inventory, $x(rpu, pus, t)$, for the range of reprocessing costs considered is shown on Figure 3-24; $x(rpu, pus, t)$ generally increases as $ucrp$ decreases, and because of the high AL value assigned in this model to plutonium in this form at this NFC node, the relative proliferation index, $rpri$, increases as is indicated.

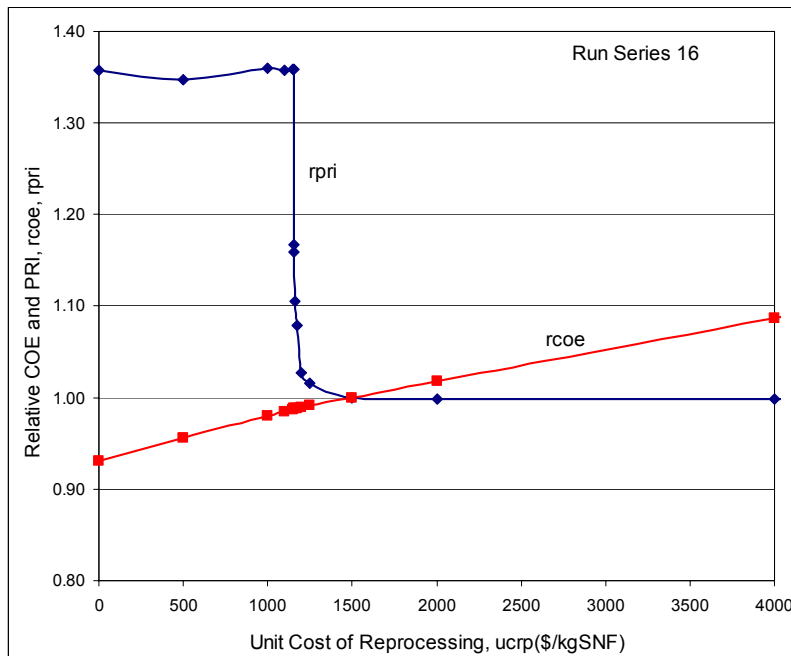


Figure 3-22. Comparative plot of the dependence of relative cost, $rcoe$, and proliferation risk index, $rpri$, on reprocessing unit cost, $ucrp(\$/kgSNF)$, for a POD case based on Run 14a (Table 3-II).

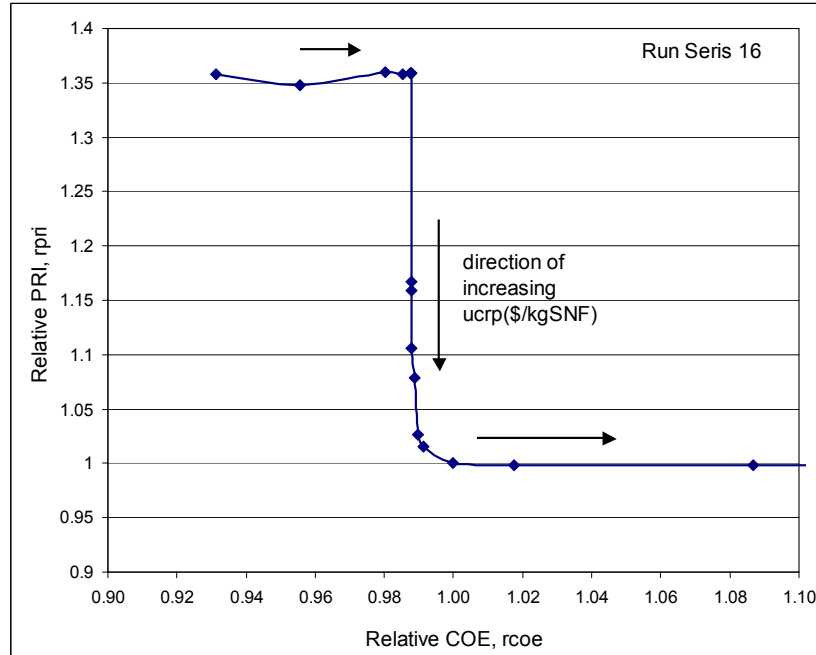


Figure 3-23. Correlative plot of the dependence of relative cost, r_{coe} , and proliferation risk index, r_{pri} , on reprocessing unit cost, $ucr p(\$/kgSNF)$, for a POD case based on Run 14a (Table 3-II).

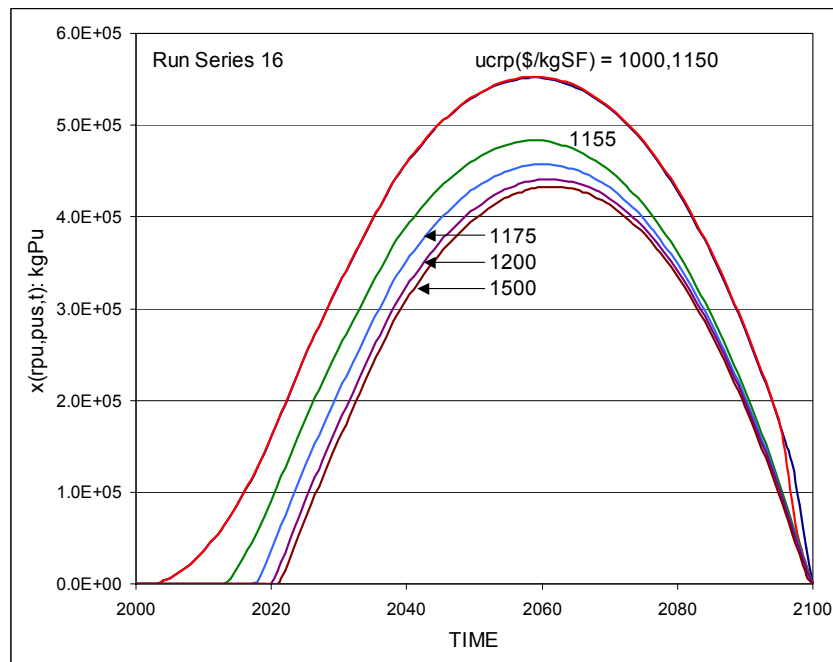


Figure 3-24. Time dependence of separated-plutonium inventories, $x(rpu,pus,t)$ for a range of reprocessing unit costs, $ucr p(\$/kgSNF)$, for a POD case based on Run 14a (Table 3-II).

Like the opening of the repository, reprocessing capacity is assumed to ramp linearly starting at time $trpi$ to a final capacity $rpcapf(kgSNF/yr)$ at time $trpf$; for the Run 14a POD case, $trpt - trpi = 20\text{ yr}$, starting in the year 2010. The dependence of $rcoe$ and $rpri$ on $rpcapf$ for these conditions, as illustrated in Figure 3-25 is not fully explicable at this time. Significant problems were encountered in achieving an optimal feasible solution for values of $rpcapf$ below $3(10)^6\text{ kgSNF/yr}$ and for introduction times much later than those listed in Table 3-II. This POD case resides at the edge of feasibility space for reasons not fully understood. Figure 3-26 gives the rate of reprocessing, $x(rux, rpis, t)$ as a function of time and $rpcapf$, as reported by FCOPT and this series of parametric studies. While the decrease in $rpri$ with increasing $rpcapf$ results in large part from the decrease in separated-plutonium inventories, as is illustrated in Figure 3-27, why $x(rpu, pus, t)$ should decrease with increased reprocessing capacity is not understood at present.

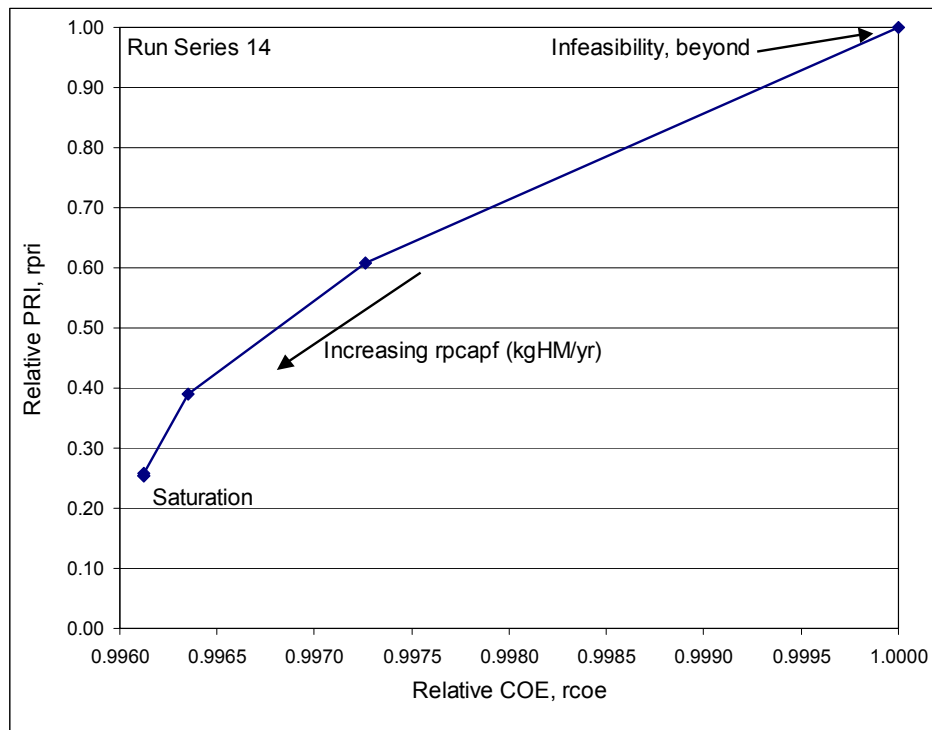


Figure 3-25. Correlative dependence of $rpri$ and $rcoe$ on $rpcapf$ for a POD case based on Run 14a (Table 3-II).

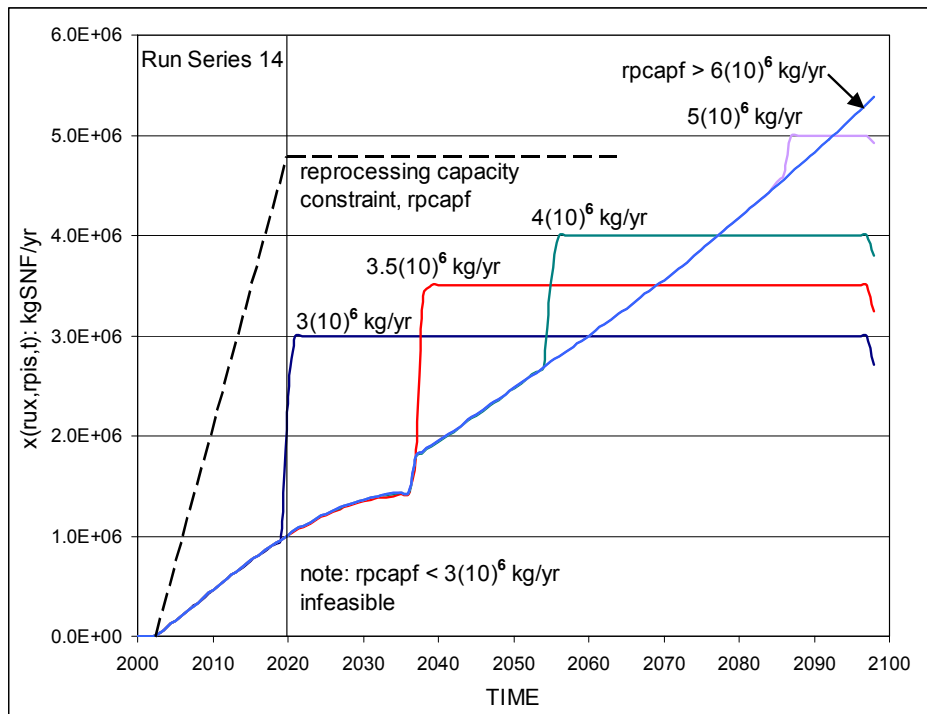


Figure 3-26. Time dependence of SNF reprocessing rate for a range of reprocessing capacity limits $rpcapf$, as imposed by the linear ramp indicated by the dashed curve.

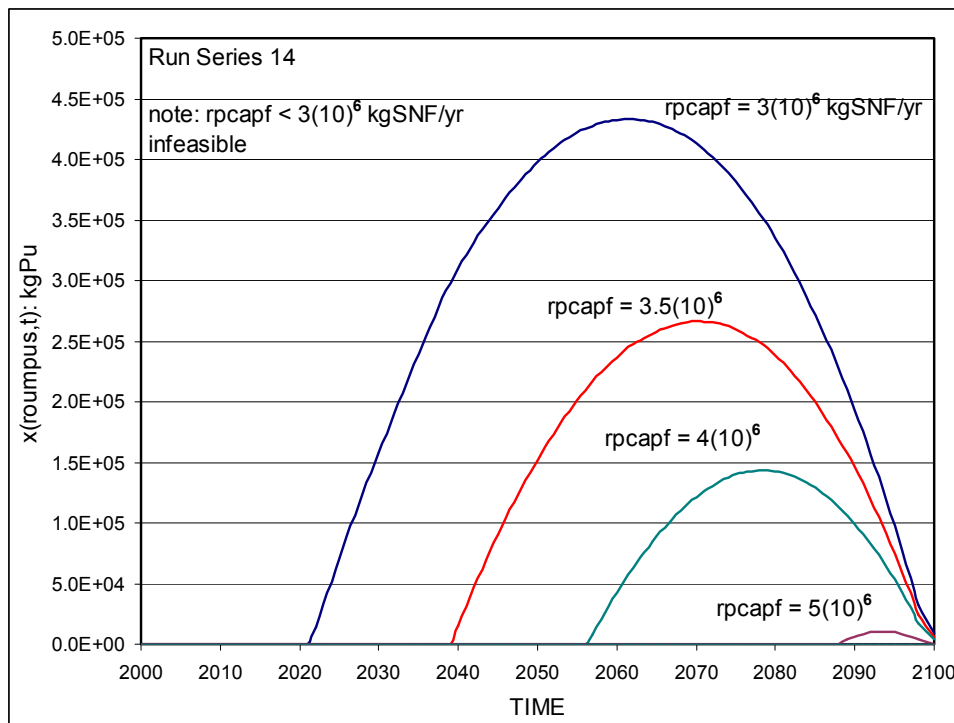


Figure 3-27. Time dependence of the separated-plutonium inventory for a range of reprocessing capacity limits $rpcapf$.

3.2.2.5 Optimizations that Reduce Proliferation Risk *versus* Cost

Equation (3-4) indicates a direct means to combine the cost and proliferation objective functions by means of a linear coupling coefficient pro (\$/kgPu/yr), which assigns a dollar cost to the risk of theft or diversion associated with a given level of integrated exposure of plutonium in its various forms and inventories. For small values of pro capital and operating costs dominate the optimization process; for large values of pro , the effective cost of proliferation or the risks related thereto dominate the objective function as the FCOPT model searches for the feasible set of $x(m,p,t)$ vectors that would minimize the Eq. (3-4) objective function in terms of material and process selection for all times within the time frame of the optimization. More so than any of the previously reported single-point parameter studies, the selection of the POD case from which such a parametric study departs determines the trends that result. For this parametric variation of the cost-proliferation coupling coefficient, pro , Run 19a serves as the POD case. This POD case is characterized by a large final repository capacity ($ym = 10$), and an equally large (eventual) deployment of reprocessing capability ($rpcapf$). The ultimate level of interim storage capacity is also large ($bnisrx = 70$ reactor-core-equivalents), the reprocessing charges are moderate-to-high ($ucrp = 1,500$ \$/kgSNF), and the direct disposal charges by any standard are low ($ucdd = 500$ \$/kgSNF), at least for moderate-sized repositories. Finally, the base pri that results from these configuration-determining economic and capacity input, along with the AL weightings given to each (m,p,t) coordinate of the NFC undergoing optimization (Table 3-III), determine the dependencies of $rcoe$ and $rpri$ on pro reported below.

Although a strong negative correlation of relative proliferation risk with relative energy cost is revealed in Figure 3-28 and Figure 3-29 (e.g., reduced proliferation risk is accompanied by an increased energy cost), these cost increases and (particularly) proliferation-risk reductions are small. Again, this behavior may be dependent on the POD chosen for these parametric analyses. More importantly, however, is the strongly non-linear, almost discontinuous, interaction between cost and proliferation metrics as the relative importance of each in optimizing a given NFC configuration varies. The initial reductions in $rpri$ can be achieved for only minor relative cost increase, but beyond a threshold reduction in $rpri$, the relative costs increase rapidly. Lastly, although not explicitly shown, the generation mix for all cases examined undergoes relatively little change; most of the variations occurring as the cost-proliferation centrum is shifted by increasing or decreasing pro occur within the NFC with relatively little impact on the mix of generation technologies used to meet the exogenous demand.

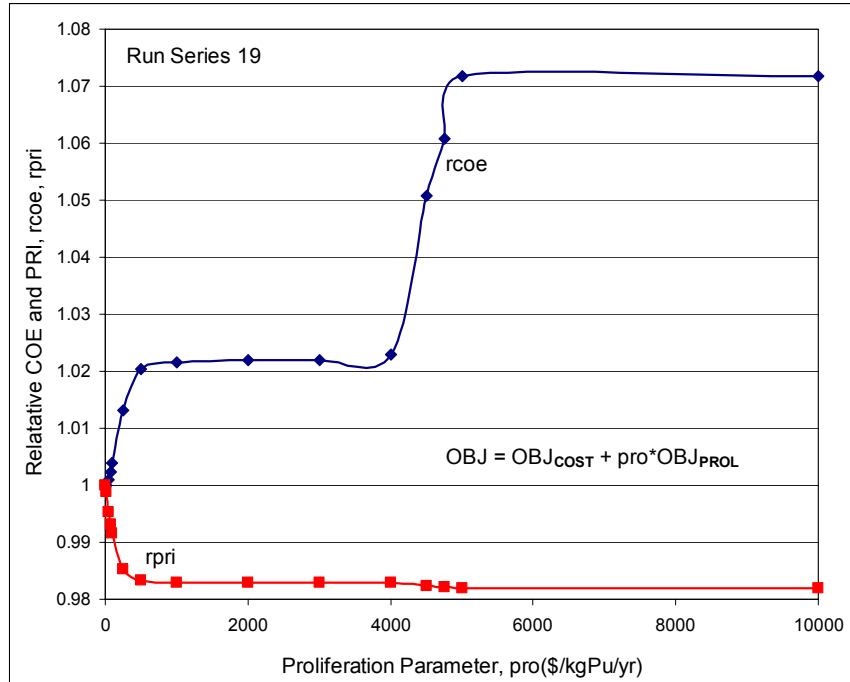


Figure 3-28. Comparative dependence of the relative cost and relative proliferation risk, $rcoe$ and $rpri$, on the cost-proliferation coupling coefficient pro , as defined on this chart; the POD case is that reflected in the Run 19a parameter list (Table 3-II).

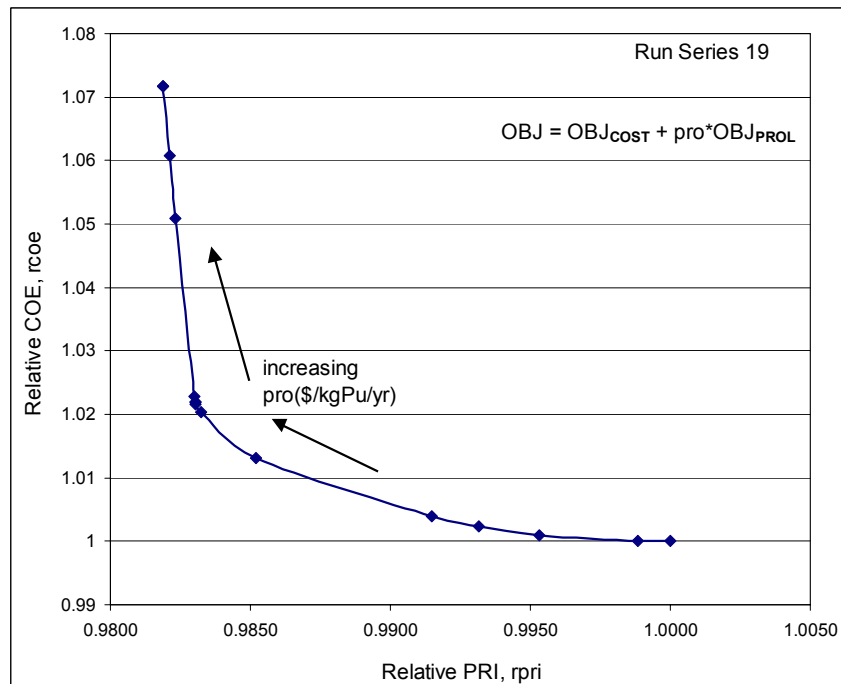


Figure 3-29. Correlative dependence of the relative cost and relative proliferation risk, $rcoe$ and $rpri$, on the cost-proliferation coupling coefficient pro , as defined on this chart; the POD case is that reflected in the Run 19a parameter list (Table 3-II).

3.2.2.6 Capital Cost and Generation Mix

The last probe into the merits and demerits of the FCOPT model, as it is presently constituted, examined the impact of diminishing capital costs, through the unit total cost, $utc(nucl)$ (\$/We). Since the $rxhg$ (MOX-fueled HTGR) technology appears as a minor player in most of the POD cases used in this study, the impact of decreasing $utc(rxhg)$ on generation mix, energy cost, and proliferation risk was investigated. As has been the case for the other results reported herein, FCOPT yielded a number of surprises. Firstly, since the plutonium that fuels the $rxhg$ technology is expensed as part of the other LWR technologies or in costs estimated for the overall NFC, it is expected that significant market share would be subsumed by the $rxhg$ technology once $utc(rxhg)$ was lowered below the 2.3 \$/We value that forms the basis for all POD databases in general; the Run 24c POD case was used specifically for this parametric study. The surprise was that the appetite of the $rxhg$ technology for “free” plutonium was so great that for very low $utc(rxhg)$ values the market share taken by this generation technology appeared to exceed the rate at which plutonium is produced by the LWR technologies. This “loophole” must be closed by introducing an appropriate set of constraints into future versions of FCOPT, but this discovery should not impact results reported up to this point.

Figure 3-30 through Figure 3-33 depict the time-dependence of the generation mix for this Run-24 (again, Run 24c provides the POD case) series of FCOPT optimizations using a cost-based objective function. Relatively minor changes in $utc(rxhg)$ are required for this HTGR/MOX technology to penetrate, particularly since the MOX fuel is relatively cost-free to that generation technology. This penetration occurs first at the expense of the LWR/MOX technology ($rxmx$), and then for even lower values of $utc(rxhg)$ further market penetration occurs at the expense of the plutonium-generating LWR/OT technology ($rxot$). The transition to higher market share with diminished $utc(rxhg)$ is not smoothly presented by the FCOPT model in its present form, as is illustrated in Figure 3-34 and Figure 3-35 by the dependence of total generation fraction determined over the optimization periods (2000,2100). Again, the discontinuous nature of this $rxhg$ market “take over” as $utc(rxhg)$ is decreased is evident in Figure 3-35. Finally, the dependence of relative cost and proliferation-risk indices, $rcoe$ and $rpri$, on $utc(rxhg)$ is illustrated in Figure 3-34. In addition to illustrating this non-uniform market takeover, in the early stages of this takeover, as the $rxhg$ technology begins its rise to prominence, the fuel cycle passes through a (cost-minimizing) configuration where significant quantities of separated plutonium become part of the minimum-cost solution, and the relative proliferation-risk index exhibits a “resonance” at about $utc(rxhg) = 2.1$ \$/We. This behavior is illustrated in Figure 3-36 and Figure 3-37. The realism of these kinds of effects and the need for additional constraints to control them is a topic for future work.

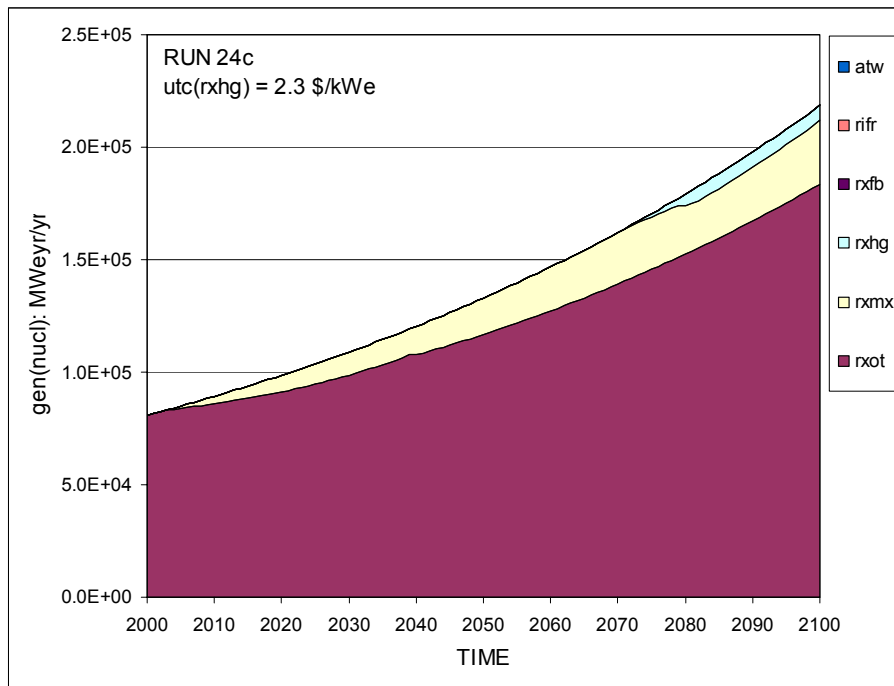


Figure 3-30. Time-dependent generation mix for the Run-24c POD case, where $utc(rxhg) = 2.3 \text{ \$}/\text{kWe}$.

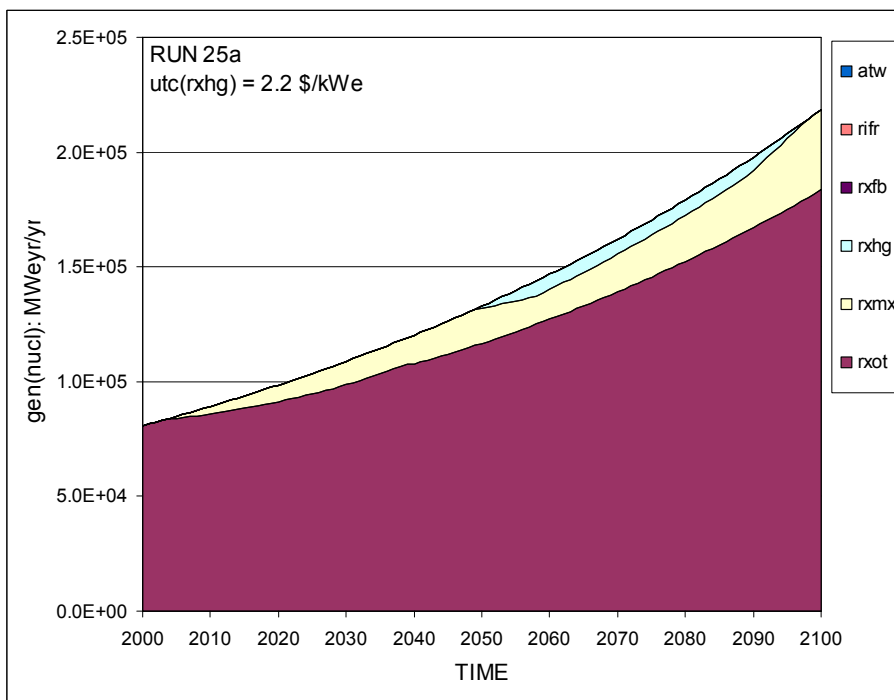


Figure 3-31. Time-dependent generation mix for the Run-24c POD case, where $utc(rxhg)$ is reduced to $2.2 \text{ \$}/\text{kWe}$.

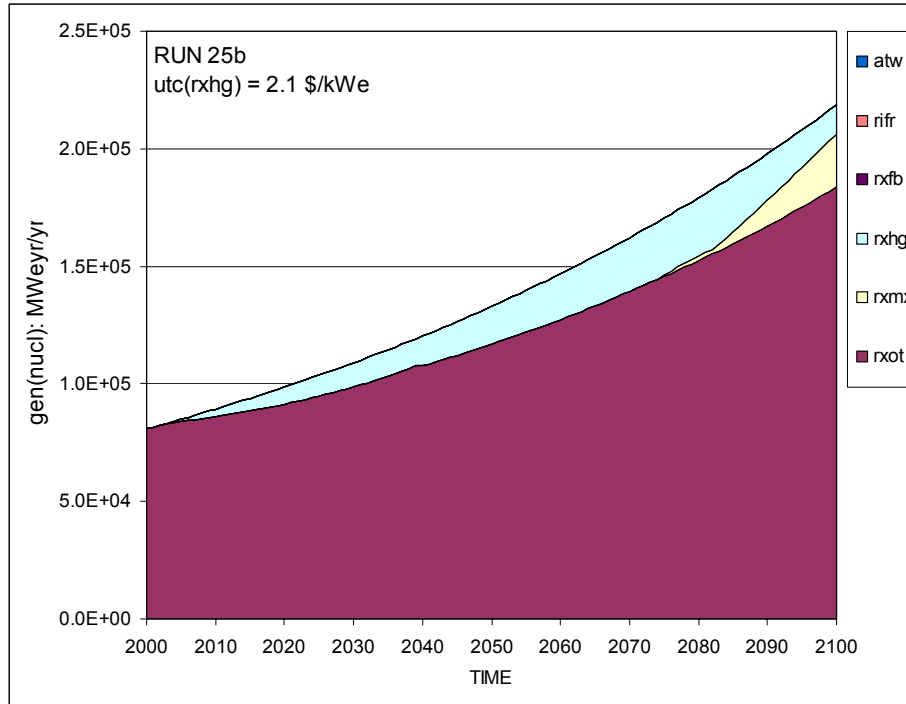


Figure 3-32. Time-dependent generation mix for the Run-24c POD case, where $utc(rxhg)$ is reduced to 2.1 $\$/We$.

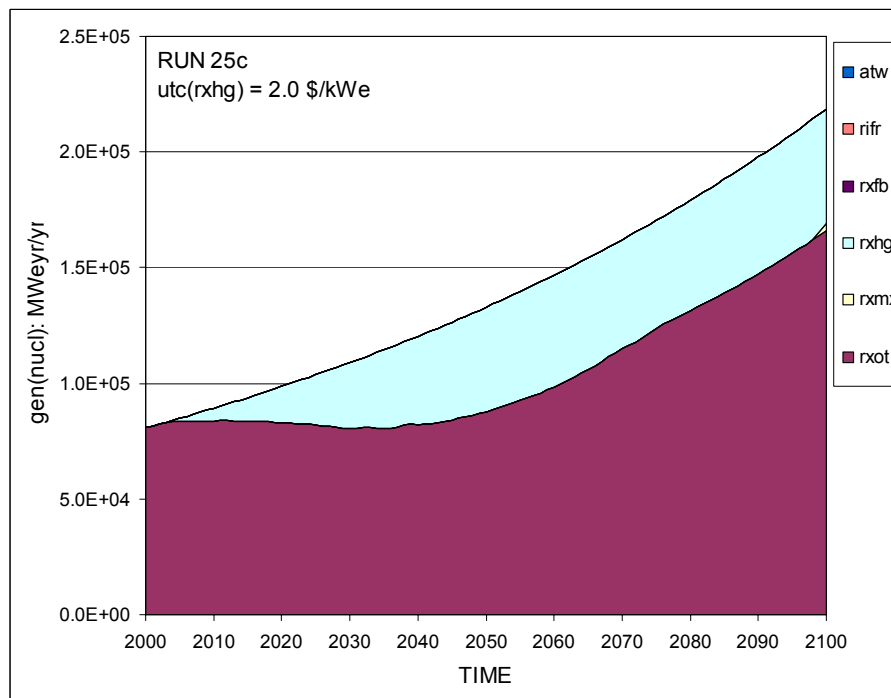


Figure 3-33. Time-dependent generation mix for the Run-24c POD case, where $utc(rxhg)$ is reduced to 2.0 $\$/We$.

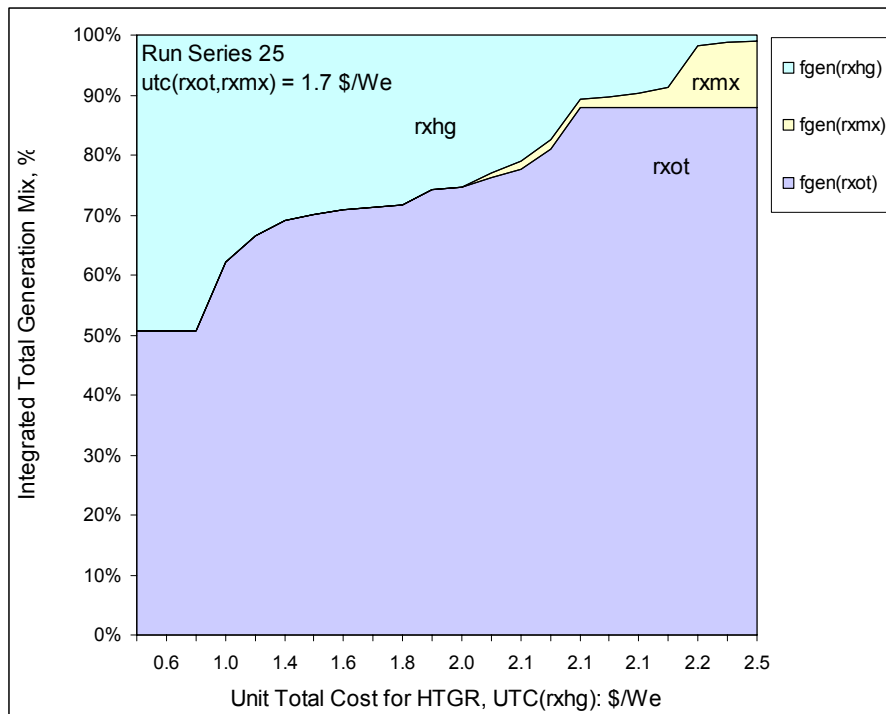


Figure 3-34. Integrated generation mix as a function of HTGR unit total cost, $utc(rxhg)$, expressed in terms cumulative percent.

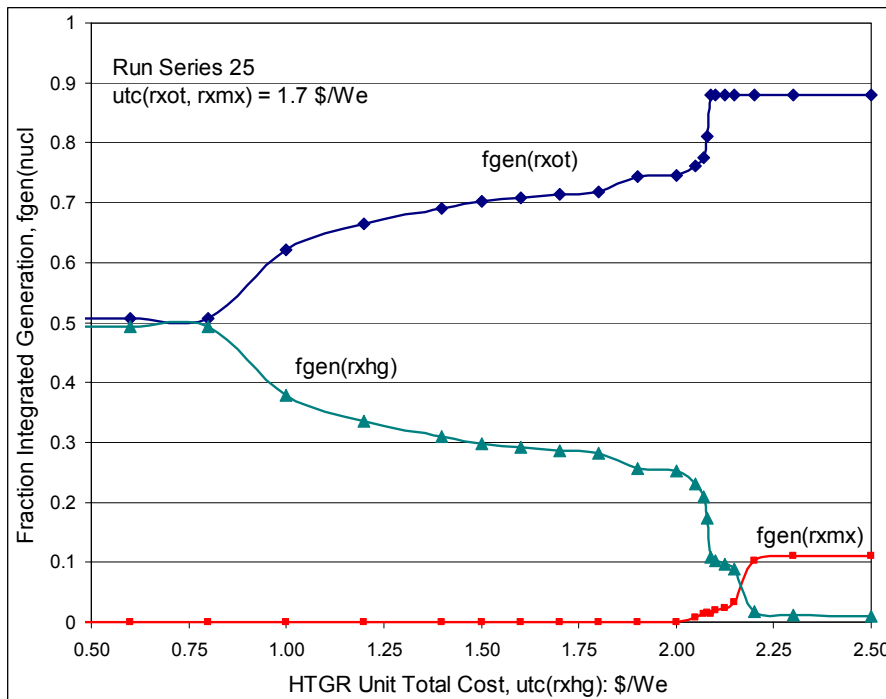


Figure 3-35. Integrated generation mix as a function of HTGR unit total cost, $utc(rxhg)$, expressed as a fraction of respective contribution, $fGEN(nucl)$.

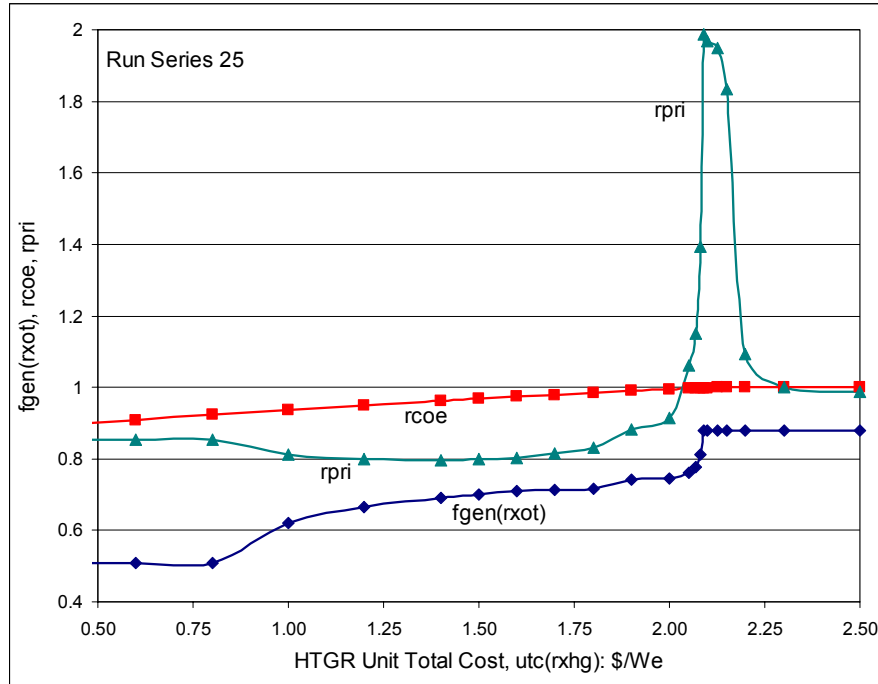


Figure 3-36. Comparative dependence of integrated generation fraction for the (initially) dominant LWR/OT technology, $f_{GEN}(rxot)$, along with the relative generation cost and proliferation risk index, $rcoe$ and $rpri$, on the unit total cost ascribed to the HTGR/MOX technology, $utc(rxhg)$.

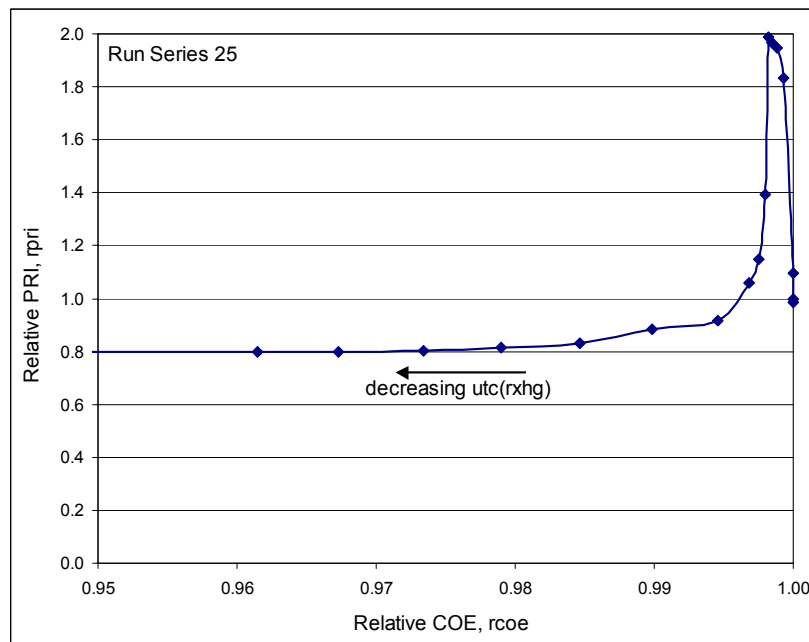


Figure 3-37. Correlative dependence of the relative generation cost and proliferation risk index, $rcoe$ and $rpri$, as the unit total cost ascribed to the HTGR/MOX technology, $utc(rxhg)$, is varied.

3.3 Summary Conclusions and Future Work

The application of LP optimization methods using a range of objective functions represents a new development, although use of LP models as a design and decision aid to select and optimize “top-level” reactor characteristics on the basis of core physics and performance has been reported nearly two decades ago (Pavelescu, 1982; Ursu, 1986; Ursu, 1990). To some extent, new ground has been broken by the present, more detailed and comprehensive NFC optimization study, with some success and some shortfalls (and some mysteries) being reported. The primary aim of this detailed reporting of the FCOPT model is to derive collegial and community feedback on the technical aspects of this NFC modeling approach, the efficacy and realism of the constraints that comprise this model, and ways in which transparency of both input and output can be enhanced in order to utilize more fully the power of these optimization methods. The results from a narrowly defined set of parametric analyses reported herein indicate that when pushed in certain directions the model generally responds in a way that is intuitively expected. Sometimes, however, this is not the case, and for these conditions the capabilities of the model must be more carefully examined. At the highest level, the FCOPT model performs the useful functions of quantitatively expressing complex (full NFC) systems in understandable form by providing a consistent framework in which to probe possible solutions and tentative hypotheses while organizing the necessarily large amounts of data needed to attack such complex problems. The FCOPT model described herein is a good start in this direction, but a number of necessary improvements, advancements, and clarifications need to be addressed; these set the agenda for future work in this area, which includes:

- Improve the technical fidelity of the fairly simple description of the reactor technologies presently included in FCOPT, particularly as related to the neutronics database and the technical detail used to describe each generation technology;
- Incorporate more precise mass-balance constraints at the elemental, if not isotopic, level, while assuring that the fuel-consuming technologies cannot expand beyond the level of resource available without incurring appropriate penalties associated with the use of so-called “backstop” resources.
- Include non-linear (economy-of-scale, EOS) scalings in the cost estimating relationships (CERs) used to estimate annual charges, and eventually the present value of total costs used in the cost-based objective function, OBJ_{COST} ; inclusion of resource depletion costing for uranium heads the top of the list for improvements in this area, which is followed closely by capacity scaling of both generation, reprocessing, and disposal technologies.
- Develop costing algorithms that respond to the under-utilization of certain capital stocks (e.g., reprocessing plants that in earlier periods may have provided larger output) with appropriate cost penalties.

4 NUCLEAR FUEL CYCLE SIMULATION (NFCSim) MODEL

The bulk of the FY02 effort in NFC simulation modeling activities was devoted to the development of a JAVA™-based, detailed simulation of the full NFC, along with the construction of supporting databases. Preliminary exploration of a commercial product, EXTEND™, was also conducted. This section describes the role of the JAVA™-based NFCSim model that resulted (Sec.4.1), a working description of NFCSim (Sec. 4.2), and first results from NFCSim (Sec. 4.3); Sec. 4.4 gives an agenda for future work in both development and application to immediate questions at hand.

4.1 Introduction

The NFC Simulation model (NFCSim) completes the troika of systems models used to analyze the myriad of possible NFC scenarios; the DELTA equilibrium model of Sec. 2 and the FCOPT optimization model of Sec. 3 are the two other systems models. The DELTA model has been the systems-analysis workhorse, because it can be used to compare scenarios in the shortest amount of time of the three NFC systems models reported herein. Ignoring most temporal effects gives the DELTA model its ease of development and speed. For example, when comparing two scenarios with the DELTA model, no heed is given to whether the technologies used in the scenarios can be deployed at the same time nor to the consequences of delayed deployment (*e.g.*, the need for interim storage, or utility disenchantment with nuclear power).

Temporal effects are included in both the FCOPT optimization model and the NFCSim simulation model. Therefore, both of these latter two models can be used to address deployment issues. Whereas the FCOPT model selects from a menu of available technologies to determine the optimal (using cost, proliferation-risk, or a combination of both as a figure of merit) NFC scenario, NFCSim evaluates scenarios the details of which users must significantly delineate. The user of the FCOPT model surrenders the responsibility for making the best or optimal decisions to the mathematical algorithms and constraints of FCOPT, while the user of the NFCSim must rely on his judgment and select all the options when composing a scenario that may not even be close to optimal. This control afforded by NFCSim comes at the expense of both the time to setup a simulation and the time to simulate a scenario. Generally, simulation models tend to be more technology-rich, and the results are more easily understood and conveyed to others compared to optimization models, which in turn point unequivocally in the direction of optimality; both approaches are complementary in their application to understanding complex, far-horizon technological scenarios that is needed for prudent planning and policy making.

4.2 Model Description

The NFCSim model simulates complex nuclear-fuel-cycle (NFC) scenarios characterized by a large array of interacting components of the NFC; NFCSim is written in an object-

oriented language, Java™. Taken together these statements have pronounced implications on how the simulation model is constructed. First, the object-oriented aspects of the model are discussed, followed by a discussion of the simulation aspects of the model.

4.2.1 Object-Oriented Aspects of the Model

Every simulated element of the NFC is represented in the model as an object.* For example, the Palisades nuclear power plant is one such object. Likewise, separate objects are defined for the three Palo Verde plants, the three Oconee plants, the two Surry plants, the two Limerick plants, *etc.* Objects with similar properties, features, and/or functions are grouped into classes in Java™. Classes contain fields that are the class properties and methods that modify fields or return the results of calculations. The aforementioned 11 reactors all consume low-enriched uranium oxide (UOX) fuel [~17-27 tonne of Initial Heavy Metal (IHM)/yr], produce power (~800-1,200 MWe), and discharge spent fuel (~17-27 tonne IHM/yr). These common features permit the formation of a Reactor class, as is shown in Figure 4-1. Each object represents a unique copy or “instance” of its class.

* The reader uninitiated with the basic concepts of object-oriented programming is referred to any of the introductory textbooks on Pascal, C/C++, Ada, or Java™, such as (Bishop, 1998). Most Java™ textbooks are written for programmers familiar with C/C++. For those readers with some familiarity with object-oriented programming, (Flanagan, 1997) or one of its later editions would be an excellent Java™ reference. A very brief description of some basic Java™ features is given in this footnote.

A class is the elemental programming unit in Java™ and represents an assembly of data and methods. Data is referred to as fields. Methods are generally used to manipulate fields and are analogous to FORTRAN subroutines. An object is an instance of a class. For example, Oak could be a class of oak trees, whereas the particular oak tree in your front yard is an instance of the Oak class. Objects are created in a process called instantiation.

Another important Java™ concept is that of subclasses and inheritance. A common programming practice for large Java™ programs is to establish a class structure that proceeds from the general to the specific. For example, the aforementioned Oak class could be a subclass or extension of Deciduous, a superclass that could contain several subclasses of deciduous trees. A field denoting a general property of deciduous trees, such as the number of leaves on a deciduous tree, should belong in the Deciduous superclass. A field denoting the number of acorns produced by an oak tree would properly belong in the Oak class. Every instance of an oak tree (*e.g.*, the object in your front yard) inherits its own copy of the leaf-number and acorn-number fields upon instantiation that are initially set to zero. A method to set the number of leaves belongs in the Deciduous superclass, whereas a method that modifies the acorn-number field and is itself used in a method for counting acorns belongs in the Oak class. Without getting into naming conventions and method invocation procedures, suffice it to say that both of these methods are readily available to modify the number of leaves and acorns of any particular tree (*i.e.*, object).

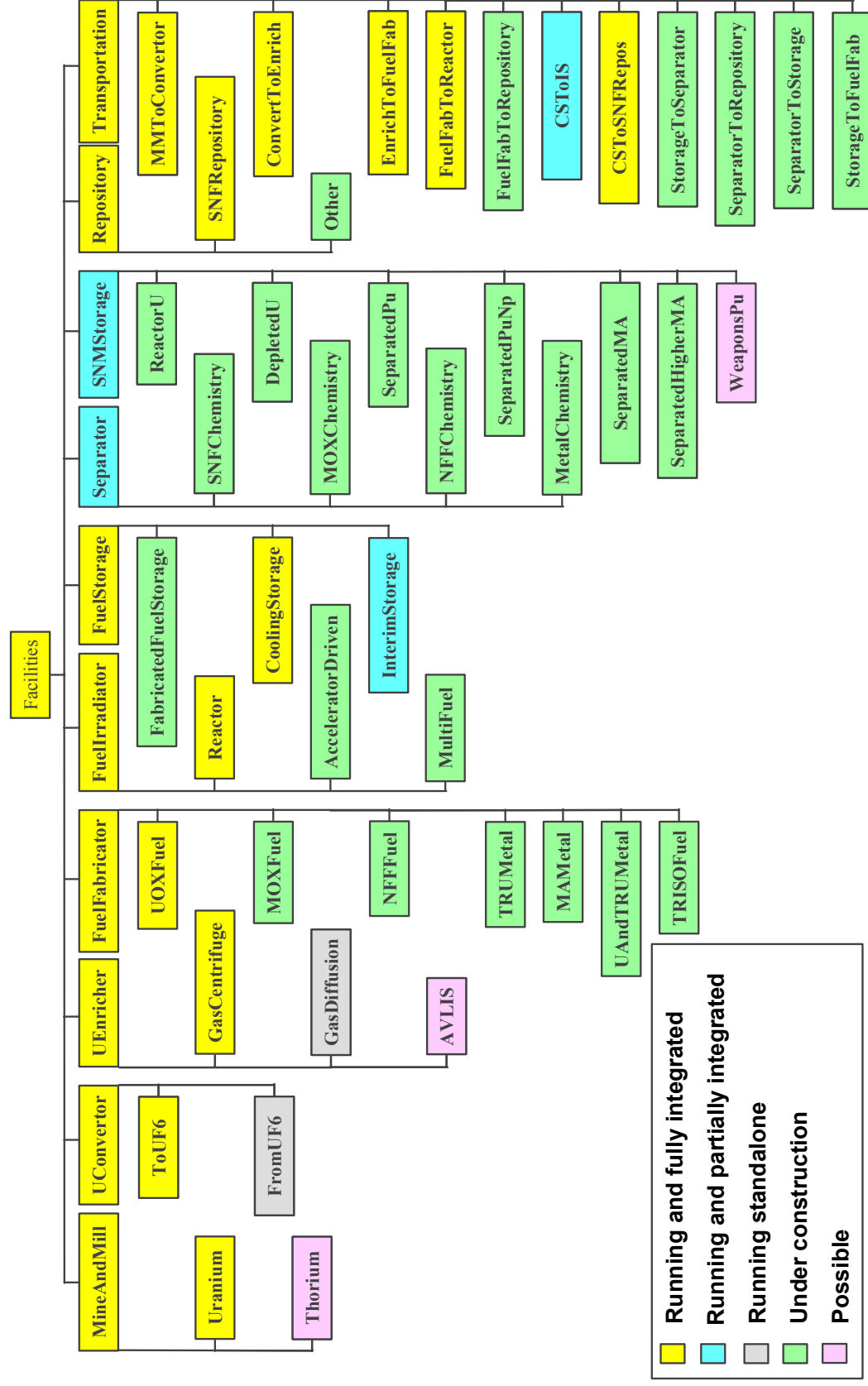


Figure 4-1. The class hierarchical structure used in the NFCSim simulation model.

Classes can be grouped together to form a superclass. For example, one such superclass in Figure 4-1, FuelIrradiator, is formed from the aforementioned Reactor class, the AcceleratorDriven class for accelerator driven systems, and the MultiFuel class for reactors that are designed to burn simultaneously more than one fuel type. Examples of this latter class are the two-region gas-cooled reactor (GCR) being proposed by General Atomic (GA) (Venneri, 2001) and an ALWR that burns MOX and UOX fuels simultaneously.

Nine other superclasses exist at the same level as the FuelIrradiator class (Figure 4-1). These nine superclasses are organized according to function or process. For example, the MineAndMill superclass encompasses all subclasses whose functions are mining and milling.

A naming convention has been adopted for the lowest-level subclasses in which the name indicates the function to be performed by objects in that class. The subclasses of the MineAndMill superclass are named according to the type of ore mined. The names of the UConverter subclasses indicate whether the feedstock is being converted to or from UF₆. The subclasses of the UEnricher superclass are categorized by the enrichment method: gas centrifuge, gaseous diffusion, or laser separation. The FuelFabricator subclass names denote which fuel type is fabricated. The names of the FuelStorage subclasses suggest the storage type. The names used for Separator subclasses provide clues as to the intended use of the separated nuclear materials. The subclasses of the SNMStorage superclass are named for the component of spent nuclear material for which storage is provided. The Transportation subclass names are of the form originating facility plus “To” plus destination (e.g., FuelFabToReactor). At the present only one subclass of the Repository superclass is provided, and it is named for the type of material to be interred. Possible Repository subclasses are envisioned for long-lived fission products and irradiated uranium. The rationale for naming the FuelIrradiator subclasses was described above.

The ten superclasses described in the previous paragraphs are themselves a subclass of a single superclass, Facilities, as is shown in Figure 4-1. The Facilities superclass houses the simulation clock and those properties that are common to all subclasses. Examples of common properties are start and termination dates for each nuclear facility, days until and type of the next event, and the material list. The material list dictates the level of detail at which the flow of material is followed in a simulation. Specifically, the material list delineates what elements and/or isotopes are followed throughout the NFC and can be as simple as $\vec{M} = \{U, Pu, MA\}$ or as complicated as $\vec{M} = \{^{233}U, ^{235}U, ^{238}U, ^{237}Pu, ^{239}Pu, \dots\}$.

The implementation of the elemental and/or isotopic delineation occurs at the lowest class level (e.g., GasCentrifuge, Reactor, or SNFRepository). Every object in these classes receives nuclear material, performs some operation on the material, and/or sends the material to the next object in the NFC. The mass flow through all objects except those derived from the subclasses of the MineAndMill, FuelIrradiator, and Repository superclasses can be represented as $m_{in} \Rightarrow m_{out} + m_{waste}$, where m_{in} corresponds to the mass of feedstock into the object, m_{out} is the mass of the product from the object, and

m_{waste} is the mass of waste, if any, from the object that needs to be tracked and ultimately interred in a repository. The tracking and internment of this waste is particularly relevant to objects from the FuelFabricator and Separator superclasses. When instantiating one of these objects, three vectors \vec{f}_{in} , \vec{f}_{out} , and \vec{f}_{waste} must be specified that give the fractions of m_{in} , m_{out} , and m_{waste} that correspond to the elements and/or isotopes of the material list. Also, the ratios m_{out}/m_{in} and m_{waste}/m_{in} are specified upon instantiation. Only \vec{f}_{out} and \vec{f}_{waste} are specified for the subclasses of the MineAndMill superclass, and only \vec{f}_{in} is specified for the subclasses of the Repository superclass. The objects derived from the FuelIrradiator superclass use a mass balance of the form $m_{in}(1 - f_b) = m_{out}$, where f_b is the burn fraction. For these objects (*i.e.*, reactors) only \vec{f}_{in} , \vec{f}_{out} , and f_b need be specified. Typically, $f_b = 0.05$ in an LWR. For the same LWR and $\vec{M} = \{U, Pu, MA\}$, $\vec{f}_{in} = \{1, 0, 0\}$ and $\vec{f}_{out} = \{0.98577, 0.01266, 0.00157\}$, which indicates destruction of U and creation of Pu and MA.

At present, the costing model follows that used in a recently completed OECD study, as extended to the DELTA equilibrium NFC model (OECD, 2002 and Krakowski, 2002). The unit costs are properties of the lowest subclasses, but the annual and total costs are associated with their superclasses. For example, the unit cost of enrichment (\$/SWU) is a property of the GasCentrifuge class and is set upon instantiation of a gas centrifuge plant (*i.e.*, a GasCentrifuge object). However, the annual cost of enrichment is a property of the UEnricher class.

The calculation of annual costs is based upon the general principle that a cost should be assessed at the time a service is rendered. To facilitate annual costing, the receiving and shipping dates and masses are properties of the middle-level classes (*e.g.*, FuelFabricator or FuelStorage). For most functions, therefore, the cost is incurred at the time the product is shipped. Some costs, however, are assessed partially on the time spent in residence, which is a property of the lowest subclass. One such example is cooling storage, which is assessed on a \$/kg/yr basis. Costs with a time component are apportioned to the appropriate years based on knowledge of the receiving and shipping dates.

4.2.2 Simulation Aspects of the Model

At the most elemental level, NFCSim is a simulator of the flow of reactor fuel charges through the NFC on a daily basis. A fuel charge is taken here to be the mass of fuel that is loaded into a reactor during a scheduled power outage for refueling. A reactor core consists of several charges; an LWR typically has three charges. The mass and composition of a charge is changed appropriately as it moves through each process that comprises the overall NFC.

One class not shown in Figure 4-1 simulates the movement of charges; namely, the DemandSimulator class. This class is primarily a repository of the methods needed to

simulate fuel charge movement. The most important of these methods is one called timeDependence. This method cycles through the time loop that is the heart of the simulation and is shown diagrammatically in **Figure 4-2**. At each time step, this method interrogates the NFC objects depicted on Figure 4-1 (*e.g.*, reactors, enrichment facilities, fuel fabrication plants) in search of “events” that should occur on the current time step. A list of possible events is given in Table 4-I. All NFC objects have a facility opening and closure date, which is determined at the time of instantiation and from the setting of an object’s lifetime. The appropriate setting of these dates is how options (*e.g.*, open Yucca Mountain in 2010) are switched on or off in the NFCSim model.

Table 4-I. Listing of Possible Events and the Corresponding Classes.

Event	Class
Plant opening	All NFC classes
Plant closure	All NFC classes
Ship charge(s)	All NFC classes except Repository
Receive charge(s)	All NFC classes except MineAndMill
restart	FuelIrradiator
shutdown	FuelIrradiator
Meet capacity	All NFC classes except FuelIrradiator

Shipping and receiving are the primary events simulated in NFCSim. When the DemandSimulator detects an object with a shipping date equal to the date on the simulation clock, the DemandSimulator consecutively runs two of the methods associated with that object: 1) a method to get the current properties of the fuel charge (*e.g.*, mass, composition, an identification number of the reactor for which the fuel charge is destined or from which the spent-fuel charge originated) and 2) a method that accumulates statistics related to the presence of the fuel charge in the object (*e.g.*, costs) and then “erases” the fuel charge from the object. The DemandSimulator then runs a method of the next object in the chain of NFC processes that effectively transfers the fuel charge (*i.e.*, sets the properties of the charge). This method not only sets the date this next object received the fuel charge, but invokes other methods that set the date when the fuel charge is to be shipped again and what its properties will be upon shipping.

The concepts of shipping and receiving used in NFCSim are easily confused with real-world transportation shipments. Within NFCSim even the objects of the Transportation subclasses have shipping events. These shipping events correspond to the unloading of a train, truck, barge, *etc.* Similarly, receiving events correspond to the loading of a train, truck, barge, *etc.*

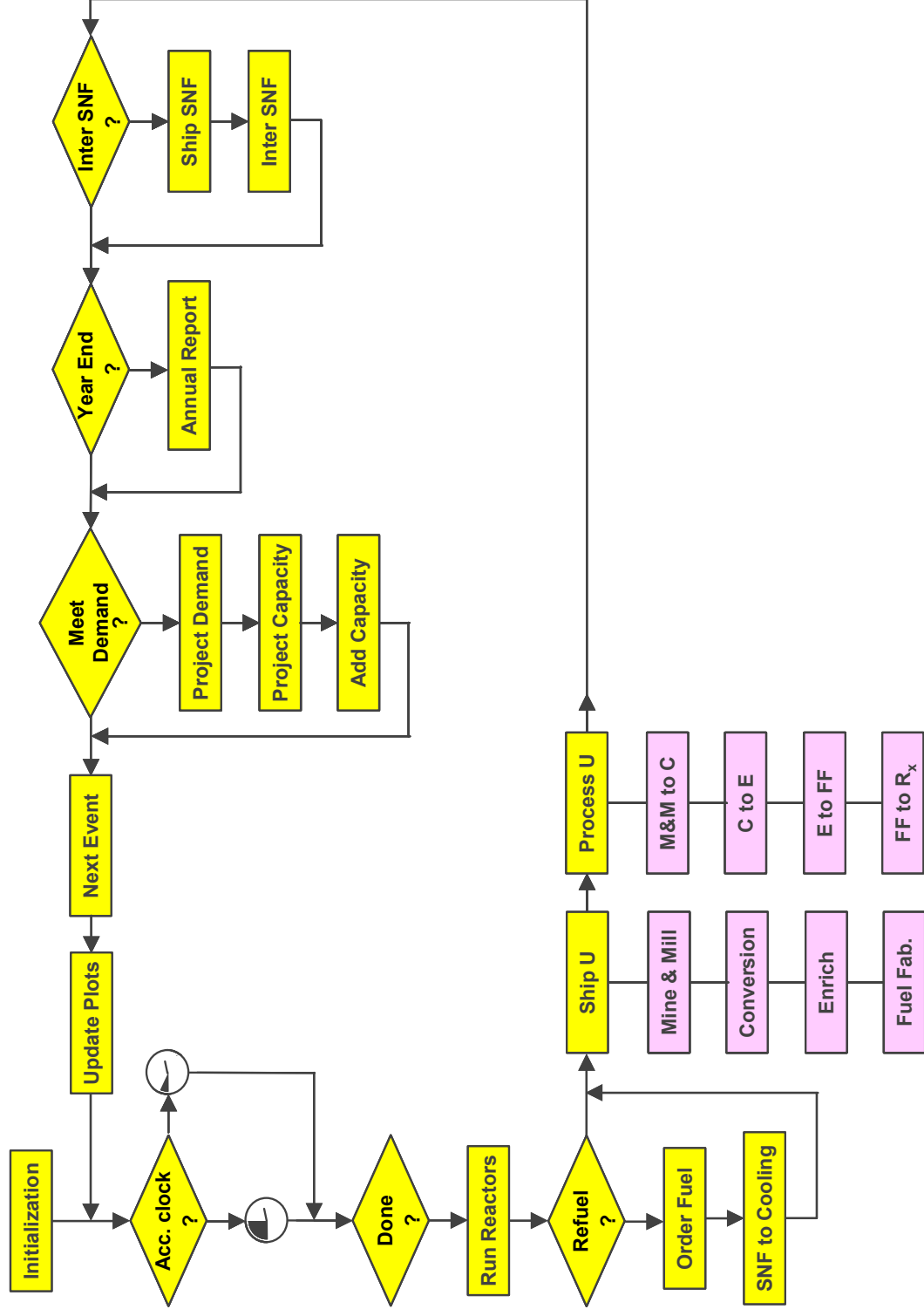


Figure 4-2. Flow diagram of the NCSim program is shown above.

The remaining events are of minor importance and serve only to maintain simulation fidelity at a high level. The meet-capacity events are used to signal the need for additional capacity (e.g., the opening of a second repository). The FuelIrradiator restart and shutdown events are included primarily to provide accurate dating of discharged fuel, although these events also permit accurate calculation of power generation, which can exhibit large fluctuations. At the time when a FuelIrradiator is restarted, a Boolean field in the FuelIrradiator is set to true so that the DemandSimulator can later detect and, if warranted, reset the status of this Boolean field and then start a charge on its way from a mine to the reactor on the same time step that the Fuel Irradiator is restarted.

As is shown in Figure 4-2, a simulation run in the timeDependence method of the DemandSimulator class begins with initialization, wherein the present-day fleet of nuclear reactors is instantiated and their properties (e.g., burn fraction, burn-up, days up and down, power, startup date, *etc.*) are set. Presently, NFCSim must re-enact the history of these reactors from their respective startup dates to the date selected for the simulation to “begin.”

Within the time loop of the timeDependence method, the first operation is to increment the simulation clock. The minimum time step in NFCSim presently is one day, which corresponds to the minimum resolution of all time scales in NFCSim. The only restriction on time scales is one imposed by Java™, which cannot resolve dates below a millisecond. Sub-day time scales may be needed to model the projected high availability of next generation reactors; a plant availability of 90% corresponds to a downtime of 36 ½ days. Even a time step of one day is CPU intensive for a NFC with a hundred reactors and associated support facilities. Jumping from event to event is a means to accelerate the time loop. The time to the next event is determined at the end of the time loop by interrogating the shipping date of each object in the entire NFC for the earliest shipping date. For accounting reasons (*i.e.*, calculation of annual costs), the time loop begins on January 1 of the year the simulation begins, and is exercised every subsequent January 1 and December 31 (*i.e.*, accounting is treated like an event).

After the simulation clock is incremented, all members of the FuelIrradiator class (*i.e.*, reactors) are “run” from the previous date to the current date on the simulation clock. Running the reactor objects has the effect of starting up, shutting down, restarting, or decommissioning those reactor objects whose time for these events has come, while doing nothing to those reactor objects in the middle of the power-producing portion of a cycle or in the middle of a power outage for maintenance and refueling (objects of other classes are “run” by subsequent operations within the time loop). For those reactors restarting power production, the DemandSimulator initiates an order for ore so that a freshly fabricated fuel charge is delivered to the reactor just in time to begin the next power production cycle. For those reactors shutting down for maintenance and refueling, the DemandSimulator transfers an irradiated charge just discharged from the reactor to its associated cooling storage facility (*i.e.*, cooling pond). At present, this transfer does not use a transport object and is both free and instantaneous.

The next operation in the time loop is to interrogate all “front-end” facilities to determine if the uranium product from that facility should be shipped. The DemandSimulator then transfers said product to the appropriate transportation media. The DemandSimulator follows with yet another interrogation, this time of the transportation media. If warranted, the DemandSimulator transfers the transportation load to the appropriate front-end facility for processing or to a reactor.

Next the DemandSimulator inters SNF in a repository, provided one is open. The DemandSimulator abides by the Yucca Mountain shipping schedule of 4,300 shipments over 24 years. Within that framework, the shipping schedule in NFCSim ramps up according to a displaced, half period sinusoid over 4 years from 0 shipments *per* year to 200 shipments *per* year. The ramp-up period covers 300 shipments. The DemandSimulator searches all cooling storage facilities for the oldest irradiated fuel charges to ship first. In NFCSim SNF must be older than seven years to be shipped from cooling storage.

After having performed all of the time simulating tasks, the DemandSimulator turns to “housekeeping” chores. The first such chore is the generation of an annual report, if the date on the simulation clock is December 31. This report consists of a tabulation of the masses handled at the middle-class level (*e.g.*, Uconvertor, FuelFabricator, Transportation), the total energy produced, and the total costs incurred in the current annum. The annual costs and annual energy production are then used to calculate an instantaneous cost of electricity, $COE(mill/kWeh)$.

The DemandSimulator next checks whether the simulation has entered the period in which an exogenous demand for nuclear electricity is imposed. The demand at some future time t is assumed to be of the form: $D(t) = P(t_0)[1 + growth]^{Y(t)}$, where $P(t_0)$ is the installed capacity at the time t_0 when enforcement begins, *growth* is the rate at which demand changes, and $Y(t) = t - t_0$ is the real number of years since time t_0 . Inherent to the NFCSim model is the assumption that no response is instantaneous (*i.e.*, new capacity only appears after some delay for installation and/or other reasons). Consequently, the DemandSimulator looks at the demand appropriately shifted into the future. Similarly, the DemandSimulator interrogates all objects of the FuelIrradiator subclasses for closure dates to predict the amount of installed capacity that will still be operating at the appropriate time in the future. It also interrogates these same objects for startup dates to project that capacity that has been ordered but not yet installed. The difference between the projected demand and the combination of capacities that are installed and will still be running and capacities that have been ordered and will be running yields the capacity that needs to be ordered immediately for future operation. The DemandSimulator then instantiates the largest integer number of reactor objects that will not exceed the projected demand with the appropriate startup date and also initiates the production chain for producing the necessary number of charges to startup each new reactor. Consequently, the DemandSimulator will always slightly undershoot the demand curve.

Finally, the DemandSimulator determines the number of days until the next event to which the time step for the next cycle of the time loop can be safely set. The

“housekeeping” chores are complete when the time-dependent plots are updated with the latest results. Examples of the types of plots available in NFCSim are presented in the next section.

4.3 Interim Results

4.3.1 Scenarios

The results of two scenarios are presented in the next sections to illustrate the capability of the NFCSim model. Both simulations start with the present-day nuclear industry legacy of 104 operating reactors and the associated SNF generated from startup to the beginning of the simulation (*i.e.*, 38,900 tonne SNF for an assumed burn-up of 40 MWt d/kg IHM and burn fraction of 5%). All but 38 reactors are assumed to shut down after a nominal plant life of 40 years. These 38 reactors either have or have applied for (and, it is assumed, will be granted) life extensions. The names of these 38 reactors and the length of the life extension is given in Table 4-II. Also, a SNF repository (*i.e.*, Yucca Mountain) is assumed to open in both scenarios on Monday, January 4, 2010. As previously described, transportation of SNF to the repository is assumed to ramp up over the course of four years from 0 to a maximum of 200 shipments *per* year (for a total of 300 shipments during the ramp period). However, NFCSim will not ship SNF with an age that is less than seven years. The first repository (*i.e.*, Yucca Mountain) is assumed to stop receiving shipments after 24 years and a total of 4,300 shipments. In NFCSim a shipment is assumed to be a single charge discharged from a reactor, and the oldest SNF is shipped first. For these conditions NFCSim calculates a capacity of 77,000 tonne SNF for the first repository, consistent with projections for Yucca Mountain.

4.3.2 Nuclear Phase-Out Scenario

The results of an NFCSim simulation of the phase out of nuclear power in the US are shown in Figure 4-3 and Figure 4-4. The instantaneous power (that power being delivered to the grid) can be as low as 75% of the installed capacity. With the life extensions of Table 4-II, the last plant, Beaver Valley 2, shuts down in November 2047. The total SNF generated is estimated to be ~103,000 tonne SNF; 77,000 tonne SNF fill the first repository (*i.e.*, Yucca Mountain) and 25,600 tonne SNF are stored in a second repository. Without these life extensions, a second repository with a capacity of only 10,000 tonne SNF is needed by the year 2032. Some nuclear utilities are upgrading reactor cooling systems and applying for a license to increase their reactor’s power-generating capacity by as much as 25%. If these licenses are granted, then the necessary capacity of a second repository will be even larger than the 25,000 tonne SNF estimated herein.

Table 4-II. Reactors with a Plant Life in Excess of 40 Years.

Reactor	Plant Life (yr)
Brunswick 1	60
Brunswick 2	60
Robinson 2	60
Calvert Cliffs 1	60
Calvert Cliffs 2	60
Palisades	44
North Anna 1	60
North Anna 2	60
Surry 1	60
Surry 2	60
Catawba 1	60
Catawba 2	60
McGuire 1	60
McGuire 2	60
Oconee 1	60
Oconee 2	60
Oconee 3	60
Pilgrim	60
Arkansas 2	60
Peach Bottom 2	60
Peach Bottom 3	60
Beaver Valley 1	60
Beaver Valley 2	60
St. Lucie 1	60
St. Lucie 2	60
Turkey Point 3	60
Turkey Point 4	60
Cooper	60
Point Beach 1	60
Point Beach 2	60
Fort Calhoun	60
Summer	60
Farley 1	60
Farley 1	60
Hatch 1	60
Hatch 2	60
Browns Ferry 2	60
Browns Ferry 3	60

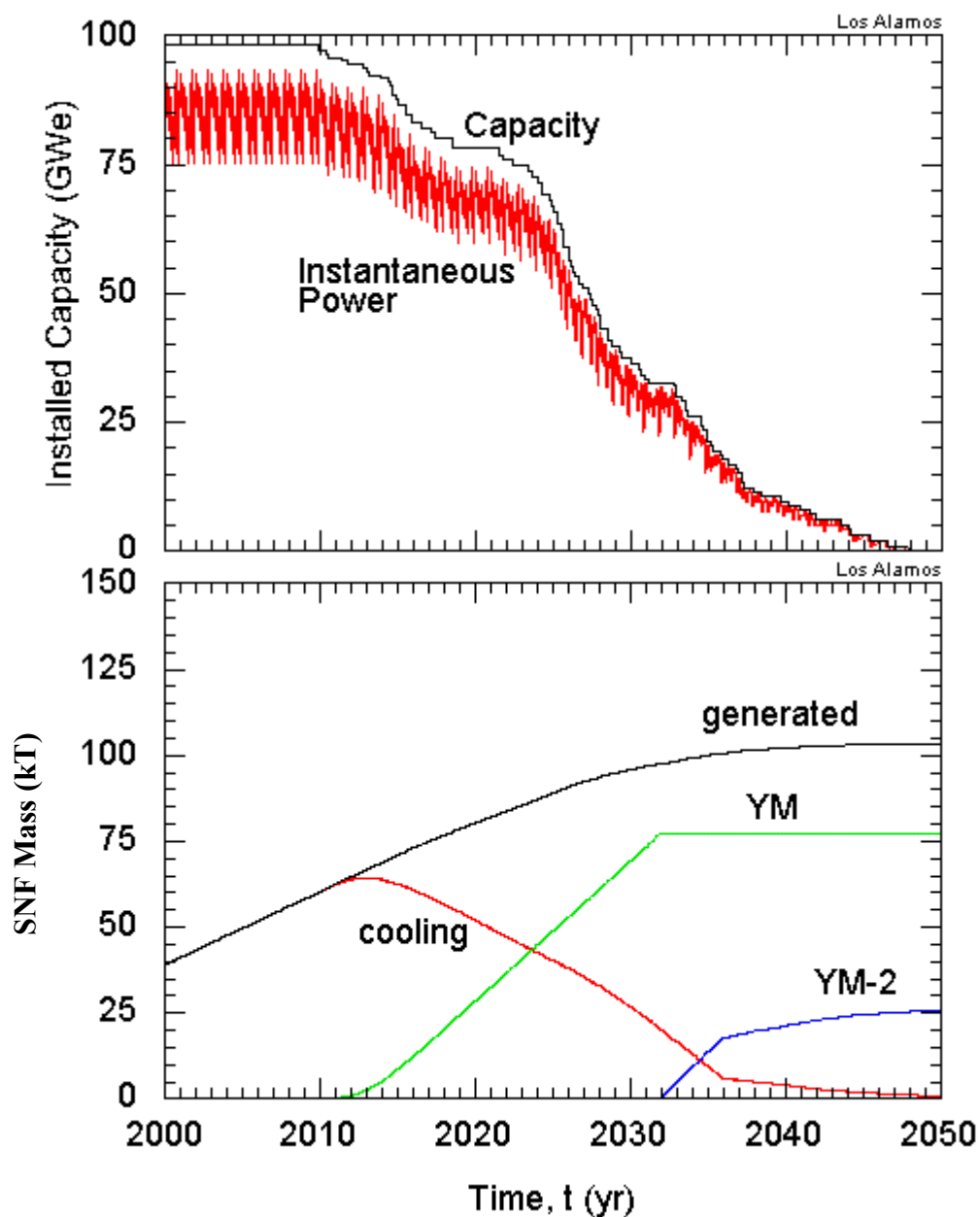


Figure 4-3. The installed capacity for generating power and the instantaneous power are shown above for a nuclear phaseout scenario, and the mass of SNF generated, stored in cooling ponds, and interred in Yucca Mountain and a second repository are shown below.

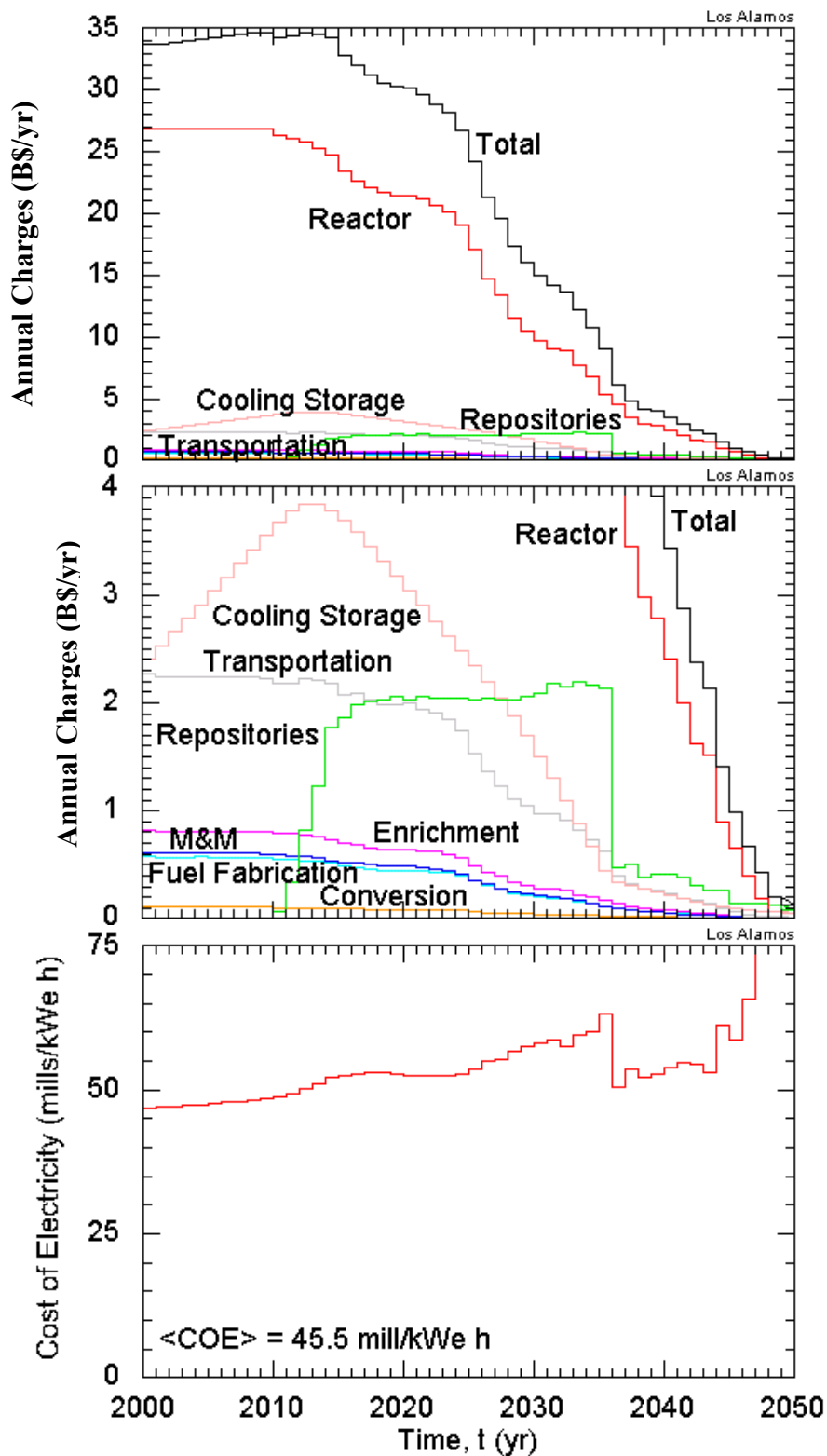


Figure 4-4. The undiscounted annual charges (top two plots) and COE are plotted as a function of time for a nuclear phaseout scenario. The discounted COE , $\langle COE \rangle$, is also given in the bottom plot.

Using in NFCSim the costing model from the steady-state DELTA model [Sec. 2, (Krakowski, 2002)] and the costing data from Appendix H yields the results for undiscounted annual charges (undiscounted annual charges are presented here, because inflation and escalation are not included in these results and, hence, the undiscounted annual charges directly correlate with facility usage) and *COE* shown in Figure 4-4. As expected, the annual capital charge of the reactors dominates the cost. The annual cost of cooling storage rises linearly during the period between 2000 and 2010 when the capacity is constant. In the DELTA model the annual cost for cooling storage is charged at 60 \$/kg/yr, as if the cooling storage facility were charging a rental fee. A more accurate costing model would charge a levelized cost based only on capacity. Although the cost of transporting nuclear material throughout the NFC is relatively inexpensive at 50 \$/kg, the transportation costs are nearly 2.3 B\$ in 2000, because of the large masses that must be transported between the mine and the converter and between the converter and the enrichment plant. The repository cost ramps up starting in 2010, as expected, but sharply drops in 2036 when repository shipments finally catch up to the backlog of SNF older than seven years. The annual enrichment, mining and milling, fuel fabrication, and conversion costs are small compared to the other costs. The *COE* starts fluctuating after 2024 as the revenue stream dries up, but costs for repository internment, cooling storage, and transportation continue even after electricity production ceases. Such costs would normally be paid from an escrow account, which presently is not but should be included in the NFCSim costing model. A discounted *COE* for the simulation period $\langle COE \rangle$ is also calculated and presented on Figure 4-4 that is the ratio of the sum of the discounted annual charges for the simulation period and the sum of the discounted energy produced in the same period.

4.3.3 Nuclear Resurgence Scenario

The results of an NFCSim simulation wherein an exogenous demand for nuclear power that increases at 1% per annum beginning September 1, 2012 and that is met with ALWRs are shown in Figure 4-5 and Figure 4-6. Small deviations of the installed capacity from the demand curve for short periods of time are observable for the combination of reasons given in Sec. 4.2.2. These deviations are small compared to the fluctuations in instantaneous power. The energy produced displays a step-function approximation to an exponential (demand) curve after the year 2012.

As with the nuclear-phaseout simulation (Sec. 4.3.2), the reactor capital costs dominate the annual charges. The cooling storage cost rises until a repository opens, for the same reasons as given for the nuclear-phaseout simulation (Sec. 4.3.2, *i.e.*, cooling storage is costed at 60 \$/kg-yr, as if the cooling storage facility were charging a rental fee). The transportation cost starts to rise after 2012 primarily because of the transport of uranium before enrichment occurs. In this scenario, repositories shipments do not catch up to the backlog of SNF older than seven years until 2042, when the repository cost drops to a nearly constant value for the rest of the simulation.

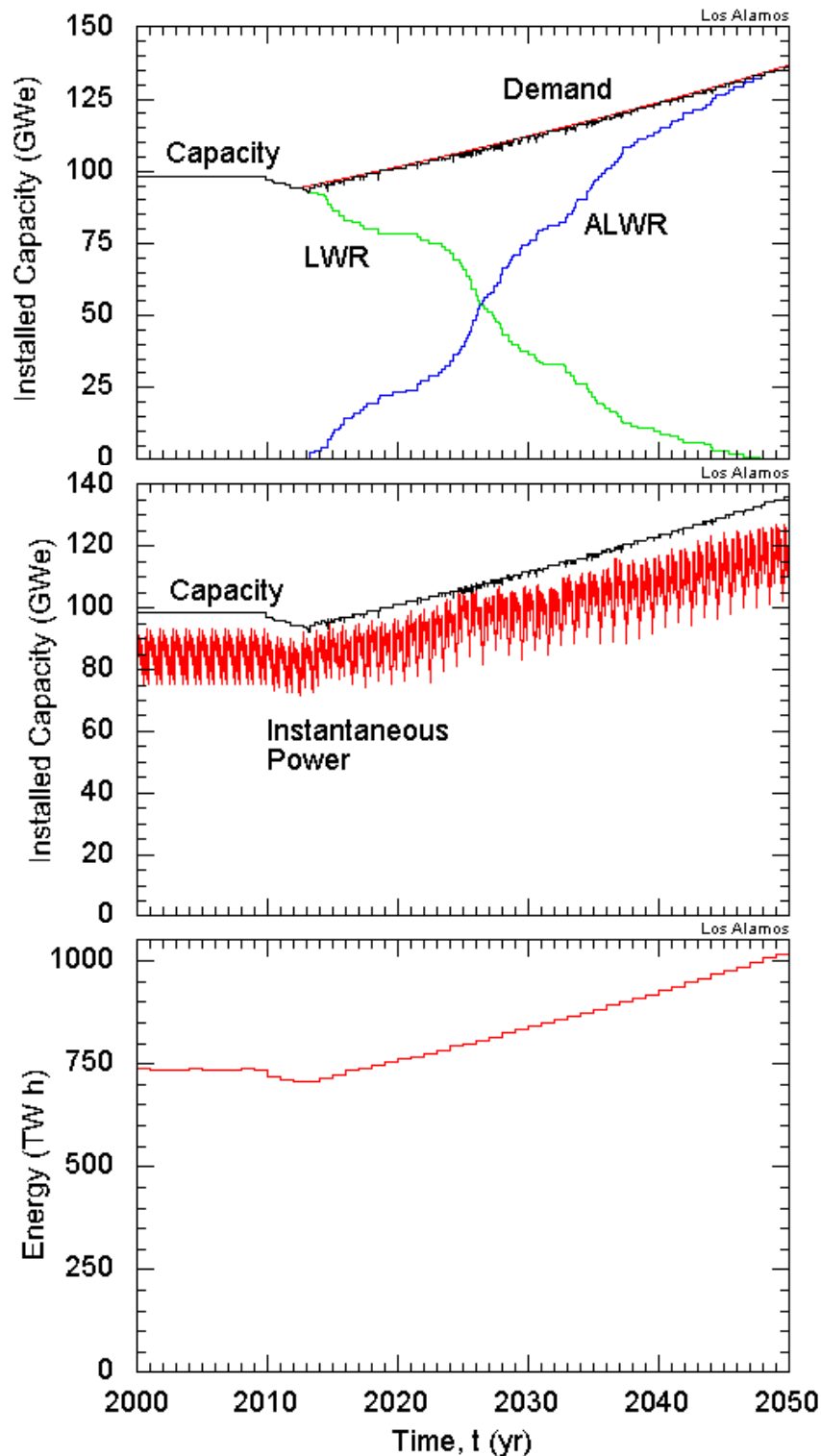


Figure 4-5. The total installed capacity, the exogenously imposed demand, and the LWR and ALW capacities are shown in upper plot for a nuclear resurgence scenario based on ALWRs. The installed and instantaneous capacities are shown in middle plot. The energy production is shown in bottom plot.

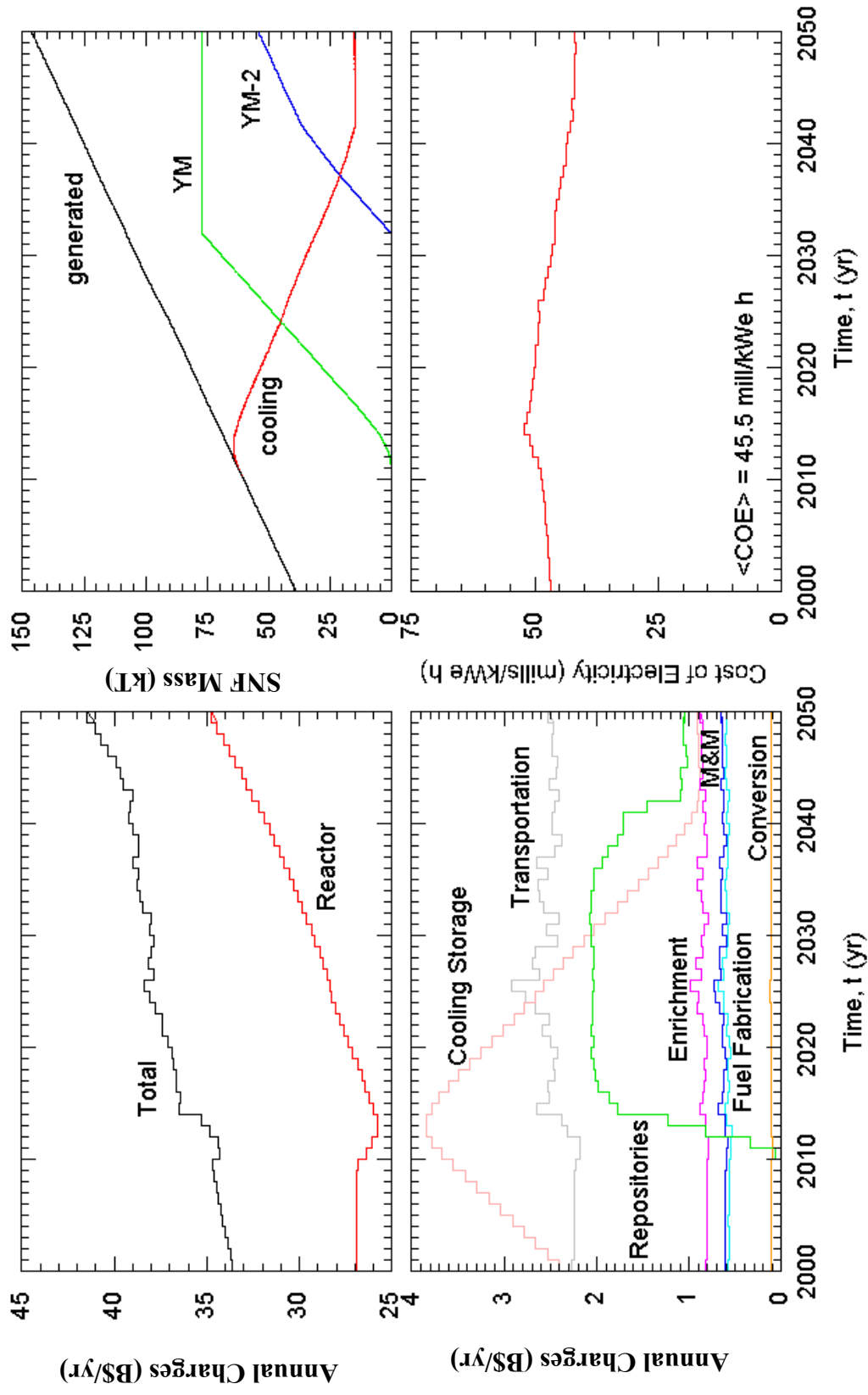


Figure 4-6. The annual costs are shown on the left for a nuclear resurgence scenario based on ALWRs. The mass of SNF generated, stored in cooling ponds, and interred in Yucca Mountain and a second repository are shown in the upper right. The COE is plotted as a function of time in the lower right. The discounted COE , $\langle COE \rangle$, is also given in the lower-right plot.

The SNF waste generated increases nearly linearly, and reaches a maximum of 146,000 tonneSNF in 2050. The mass in cooling storage appears to bottom out in 2042, because the backlog of SNF in cooling storage that is seven years old or older has been eliminated and the demand growth is small.

There is at most a ± 5 -mills/kWe-h swing in the instantaneous, undiscounted *COE* that is driven by the changes in the annual cost of cooling storage and repository internment. The *COE* is lower in 2050 than in 2000, because the mass stored in and cost of cooling storage has been reduced to the minimum possible. For all the differences in the instantaneous, undiscounted *COE* for the nuclear phase-out and nuclear resurgence scenarios, the discounted *COE* for these two scenarios are not discernibly different (Figure 4-4 and Figure 4-6, respectively).

4.4 Summary Conclusions and Future Work

The results of Section 4.3 demonstrate the capabilities and readiness of NFCSim to serve as a focus of the AFCI Systems Analysis effort at Los Alamos. The FY03 program will continue with minor development of this model to address the costing issues raised by these results as well as complete the integration of the Separator class. These development issues can be easily and quickly resolved, permitting the early use of NFCSim to address key AFCI issues. Key elements of this task includes:

- Integrate/normalize NFCSim and FCOPT models using a relatively simple, LWR-based NFC scenario.
- Benchmark NFCSim with the CEAs COSI simulation model, once a benchmark case is identified that covers both the NFCSim model scope (US nuclear economy) and the COSI model scope (French nuclear economy).
- Benchmark NFCSim model with other NFC models currently being developed, such as the OECD dynamic simulation NFC model presently under development (Bertel, 2002) and/or the MIT model (Golay, 2002).
- Incorporate into NFCSim and apply a Yucca Mountain “Business” model based on the work proposed in Sec. 7.2.5.
- Incorporate into NFCSim and apply a proliferation model based on the extensive body of past work to evaluate the NFC *versus* NFF (non-fertile-fuel) approaches.
- Develop a capability to analyze in a complete NFC context the most promising reactor concepts produced by the Generation IV roadmapping efforts.

This page intentionally left blank.

5 NEUTRONIC ANALYSES

The main goal of the neutronic analyses for system studies this year was to explore one multi-tier concept in detail: the use of Light-Water Reactors (LWRs) to burn plutonium as mixed oxide fuel (MOX) in Tier-1 systems (Figure 2-1) and the use of Accelerator-Driven Systems (ADSs) to burn the remaining plutonium and minor actinides (MA) in Tier-2 systems. In this study, the LWR use of full cores of MOX fuel with an enriched uranium support as a function of multi-recycling of plutonium [the MIX concept developed in France, (Barbrault, 1996; Youinou, 1990b)] was chosen for investigation. A detailed Monte Carlo burn-up code and 3D model were used for these analyses and are discussed in Sec. 5.1. The base case that was examined for irradiation in Tier 1 uses only plutonium, after it is separated from the other elements in spent nuclear fuel (SNF). A separated plutonium stream, however, can be considered a proliferation hazard, so two other cases were examined in which this hazard can be reduced: in one case a large amount of Cs and Sr is retained with the plutonium, and in another the plutonium is not separated from the MA in SNF. In both cases, the plutonium-containing stream is fabricated as MOX fuel and burned in an LWR. The remaining material not irradiated in the LWR in all cases is sent to an ADS for complete destruction. Each of these material streams were run through ADS burn-up calculations to determine how performance can be enhanced in Tier 2. The results from all these calculations, including the recommended multi-tier system, are given in Sec. 5.2. Finally, Sec. 5.3 describes how the results from detailed burn-up studies conducted, are proposed to be incorporated into the NFCSim code (Sec. 4).

5.1 Model Development

To perform neutronics studies for the transmutation of SNF, an appropriate irradiation code must be used. As part of the Accelerator Transmutation of Waste project in the past, the code Monteburns was developed (Trellue, 1998; Poston, 1999). Monteburns is a code that links the Monte Carlo transport code MCNP (Briesmeister, 1980) and the isotope depletion and decay code ORIGEN2.1 (Croff, 1980) that can be used to perform automated burn-up calculations. Monteburns can be used for both LWR and ADS calculations and has been benchmarked for the types of analyses examined here, as described in Appendix I.

The geometric MCNP model used to perform burn-up calculations in the LWR was a reflected 1/8 core with three fuel regions, as shown in Figure 5-1. Each assembly was irradiated for a total of three cycles, but the calculations performed here were modeled for four cycles using Monteburns to obtain more representative material compositions in each region. The initial composition of the material irradiated one and two cycles was estimated based upon results from previous runs, but by the fourth cycle should have represented an accurate equilibrium model. Each irradiation consisted of a 203-d burn period, a 39-d cooling time (for routine maintenance of the reactor), another 203-d burn period followed by a 64-d cooling time during which the most irradiated assemblies were

removed and fresh assemblies were replaced in the reactor. The once- and twice-irradiated assemblies were moved (shuffled) to different locations so that fresh fuel is always added to the same assemblies. The center assembly of the reactor was replaced with a thrice-irradiated fuel assembly, but since this accounts for only one of 193 assemblies in the entire core (3 regions of 8 assemblies plus 1/8 the center assembly in the 1/8 core model), this procedure should have had little impact on the results. The results reported in this research reflect the average of the fuel rods removed from the eight twice-irradiated assemblies removed each cycle in the 1/8 core model. The average soluble boron concentration in the cooling-water was maintained around 600 ppm, and the uranium enrichment in the MOX was adjusted so that the beginning of cycle (BOC) k_{eff} was about 1.035 and the end of cycle (EOC) k_{eff} was about 1.0. It was assumed that the boron concentration would be increased and/or control rods would be added to decrease the k_{eff} to around 1.0 at the beginning of cycle. Each placement of fresh MOX fuel in a reactor is called a “pass” in this study; therefore, the total number of recycles should be equal to one minus the total number of passes.

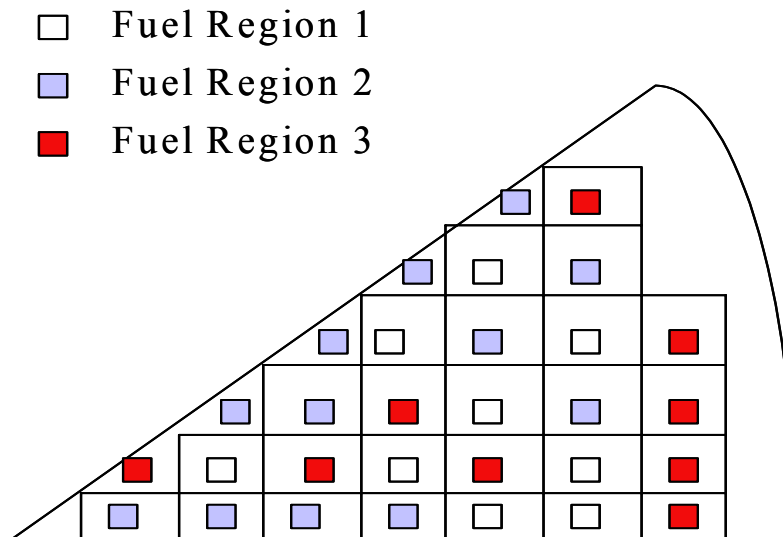


Figure 5-1. Location of different regions in a 1/8 core LWR model.

The main goal of the Tier-1 calculations was to design an LWR system that could burn a full core of MOX fuel while meeting neutronic safety constraints. To burn a majority of the plutonium in LWRs within a reasonable number of license extensions, it was found that 8-9w% plutonium in heavy metal (HM) is required in the MOX fuel (Trellue, 2001). Using full cores of MOX fuel with this relatively large plutonium fraction presented a design challenge, but neutronic safety conditions with 8.3w% Pu in heavy metal were met with only a few design modifications, as shown in Table 5-I and Appendix J, which give a description of parameters and results. These modifications include the use of additional water holes in place of fuel rods, slightly enriched soluble boron in the water (25% ^{10}B), and the use of boron carbide control rods instead of silver-indium-cadmium loaded control rods that are commonly used. As the number of recycles of plutonium

increased, so does the required enrichment of uranium. Additionally, the boron efficiency slightly decreased with subsequent recycles, but the condition of 4 pcm ($\Delta k = 10^{-5}$)/ppm (parts per million) is still met in all cases. Table 5-I shows results for the first three passes (two recycles); subsequent recycles only changed these parameters slightly. The total rod worth, however, should be greater than 5,000 pcm, so the enrichment of boron in the control rods had to be increased to about 33% if more than one recycle is performed for spent MOX fuel. The fuel assembly design used for these calculations was that for a 15x15 H.B. Robinson PWR with both water holes and burnable poison rods (Hermann, 1995). Preliminary calculations show that as long as the ratio of fuel rods to control rods remains constant, neutronic safety parameters should be met for the use of other assemblies, such as the 17x17 PWR assemblies.

Table 5-I. Neutronic Safety Cases for Multi-Recycling of Plutonium.

	Pu from SNF	(Natural Uranium)	After 1 st Recycle	(2% ²³⁵ U)	After 2 nd Recycle	(2.4% ²³⁵ U)
	BOC	EOC	BOC	EOC	BOC	EOC
Doppler coefficient (pcm/degree K)	-3.16	-2.94	-2.72	-2.44	-2.65	-2.75
Moderator coefficient (pcm/degree K)	-47.13	-51.99	-44.28	-50.33	-44.42	-49.26
Boron worth (pcm/ppm)	4.96	5.22	4.84	5.01	5.25	4.77
Void coefficient (pcm/degree K with 25% coolant reduction)	-199	-217	-184	-201	-186	-201
Total Rod worth (pcm)	5092	5083	4866	4817	4835	4695
Initial Boron concentration (ppm)	1,733	-	1,600	-	1,480	-

The safety calculations show that the initial plutonium-only and the plutonium plus cesium and strontium cases also met most neutronic safety conditions, as shown in Table 5-II. The case with plutonium and minor actinides, however, did not meet the required safety margins. The enrichment of the soluble boron had to be increased again to 33% to yield an acceptable boron efficiency, and the addition of four more control rods at a boron enrichment of 25% led to an acceptable (*i.e.*, > 5000 pcm) total rod worth.

Table 5-II. Neutronic Safety Calculations for the Three Multi-Recycling Cases.

	Pu-only BOC	Pu-only EOC	Pu+Cs+Sr BOC	Pu+Cs+Sr EOC	Pu+MA BOC	Pu+MA EOC
Doppler coefficient	-3.155	-2.94	-2.60	-2.13	-2.13	-1.80
Moderator coefficient	-47.13	-51.99	-46.02	-48.59	-38.92	-65.65
Boron worth	4.96	5.22	6.64	4.41	3.2	3.7
Void coefficient	-199	-217	-192	-210	-153	-170
Total rod worth	5092	5083	5119	5244	4881	5016

5.2 Results

To reduce the radiotoxicity of SNF to less than that of natural-uranium ore in less than 1,000 years, a > 99.75% burn rate is required. Such a burn rate is probably not achievable using MOX fuel in a commercial LWR, but one question that must be answered is: how much plutonium can be burned in various passes in a LWR as MOX fuel? The first step to performing such a calculation was to determine what isotopic vector of plutonium from SNF would be fabricated into MOX fuel. As the burn-up of UO₂ fuel increases, the quantity of fissile ²³⁹Pu relative to other plutonium isotopes decreases, and a large variety of burn-ups exist in present-day SNF. The ²³⁹Pu will burn the fastest, so the most conservative plutonium vector to consider would be one with the least amount of ²³⁹Pu. This vector would be associated with a high burn-up case, such as extended burn-up for a LWR fueled with UO₂. Thus, a case was run using the Monteburns code discussed in Sect. 5.1 for an extended LWR burn-up (60 GWtd/tonneIHM with 4.2w% enriched uranium fuel) with an average cooling time of one decade. The resulting plutonium vector that was used in multi-recycling calculations appears in Table 5-III.

Table 5-III. Isotopic Plutonium Vector for MOX Calculations.

Pu Isotope	Weight Fraction in Pu
Pu238	0.038229
Pu239	0.500503
Pu240	0.259054
Pu241	0.100855
Pu242	0.101358

Plutonium from UO₂ spent nuclear fuel is recycled as MOX fuel in LWRs worldwide, but recycling MOX fuel is more complicated than recycling regular SNF because its heat load and activity is larger. To recycle spent MOX fuel in processes that are similar to those used for UO₂ SNF, the activity and heat load should be similar. Table 5-IV shows the activity and heat load of SNF from UO₂ fuel with a standard burn-up, UO₂ with an

extended burn, and from MOX fuel with separated plutonium and a burn-up of ~50 GWtd/tonneIHM for both the beginning and end of an average operating cycle (BOC and EOC respectively). The larger the burn-up of the MOX fuel, the more plutonium can be burned each cycle. The maximum burn-up currently achieved in Europe for MOX fuel is around 50 GWtd/tonneIHM, so a similar burn-up is used in this research.

Table 5-IV. Activity and Heat Load of SNF as a Function of Cooling Time.

Activity (Ci) # years of cooling	Standard Burn-up for UO ₂ Fuel Actinides	Total	Extended Burn-up for UO ₂ Fuel Actinides	Total	MOX Fuel Actinides)	Total
1	5.75E+05	8.72E+06	8.06E+05	9.73E+06	4.11E+06	1.24E+07
3	4.85E+05	3.35E+06	6.66E+05	4.42E+06	3.47E+06	6.52E+06
5	4.42E+05	2.13E+06	6.07E+05	3.10E+06	3.18E+06	4.96E+06
7	4.04E+05	1.73E+06	5.56E+05	2.61E+06	2.91E+06	4.30E+06
10	3.54E+05	1.46E+06	4.89E+05	2.24E+06	1.92E+06	2.83E+06
Heat Load (W)						
1	2.84E+03	3.75E+04	6.04E+03	4.51E+04	2.92E+04	6.48E+04
3	1.20E+03	1.24E+04	3.01E+03	1.80E+04	1.66E+04	2.86E+04
5	1.13E+03	6.92E+03	2.80E+03	1.16E+04	1.56E+04	2.18E+04
7	1.12E+03	5.25E+03	2.71E+03	9.28E+03	1.51E+04	1.94E+04
10	1.11E+03	4.36E+03	2.60E+03	7.84E+03	1.32E+04	1.57E+04

From Table 5-IV, it is deduced that after seven years of cooling, the activity of spent MOX fuel is approximately equal to that of UO₂ fuel after three years, but the heat load is still greater. A breakdown of the actinide isotopes contributing to this heat load is given in Table 5-V. Along with ²³⁸Pu, which is a common concern for spent MOX reprocessing (Baetsle, 1997), the isotopes ²⁴¹Am and particularly ²⁴⁴Cm contribute significantly to the heat load. ²⁴⁴Cm has an 18.1-yr half-life, so a longer cooling time would reduce the heat load from this isotope. Nonetheless, the half-lives of ²³⁸Pu and ²⁴¹Am are about 90 and 430 years respectively, and their contributions keep the heat load in spent MOX fuel above that seen from spent UO₂ SNF for many decades, so hot cells or at least increased neutron shielding would probably have to be used to keep the cooling time reasonable. It is also impractical to let the material cool much longer than seven years in any case because the ²⁴¹Pu rapidly decays to ²⁴¹Am, increasing the plutonium depletion rate, as shown in Table 5-VI, but a valuable fissile plutonium isotope is lost in the process. A cooling time of seven years, therefore, was chosen for all spent MOX recycles of plutonium and is assumed to be the most optimistic case in terms of time required for the mission

Additional results from three different categories of calculations are presented in the following sections: the multi-recycling of plutonium as MOX fuel, the use of plutonium plus minor actinides or fission products in MOX fuel to decrease proliferation risk, and the performance of the ADS using different actinide feed streams with and without the Tier- 1 irradiations.

Table 5-V. Heat Load (watts) of Various Isotopes in MOX after Seven Years *versus* Extended Burn-up UO₂ After Three Years SNF.

	Spent MOX Fuel	Spent UO ₂ Fuel
Pu238	6390	905
Pu239	188	39.1
Pu240	591	72.8
Pu241	103	18.2
Pu242	4.39	0.454
Am241	2000	137
Am242m	0.334	0.0324
Am243	57.9	7.88
Cm242	27.1	128
Cm243	34.2	5.23
Cm244	11100	1710
Cm245	3.27	0.275
Cm246	0.386	0.0819

Table 5-VI. Percent Plutonium in Transuranic Material as a Function of Decay Time.

Years of Cooling	Percent Plutonium
1	27.6
3	28.6
5	29.5
7	30.4
10	33.6

5.2.1 Multi-Recycling MOX Fuel

Assuming a cooling time of seven years, the depletion of plutonium in one “pass” of MOX fuel is about 30%. Unfortunately, the depletion is insufficient to reduce significantly the mass or radiotoxicity of SNF sent to the repository. Spent MOX fuel, therefore, must be reprocessed and re-fabricated into fresh MOX fuel rods for further reactor irradiation. As the number of recycles of plutonium in MOX fuel increases, the fissile content of the plutonium decreases because the most fissile isotopes are preferentially depleted. The reactivity of the fuel at the end of a MOX irradiation, therefore, is less than that at the beginning. If this fuel is taken as is and directly re-fabricated into MOX fuel rods, the reactor would not be critical. Therefore, one or more of several procedures or alterations must occur to make the reactor critical. First, the plutonium content in heavy metal can be increased in subsequent recycles, but the additional plutonium must come from somewhere. With the first irradiation, 30% of the plutonium is already destroyed, so unless the amount of plutonium in two reactors (or

assemblies) can be combined into one reactor (assembly), the amount of plutonium needed for a second pass is insufficient. Requiring the number of reactors (or assemblies) needed for burning a select set of plutonium to decrease with the number of recycles would complicate licensing and logistics. It would be more straightforward through mass conservation to have all plutonium from one reactor being burned in the same reactor through various numbers of recycles. In addition, licensing fuel types that have varying amounts of plutonium *versus* uranium in heavy metal would be expensive and time consuming. An alternative technique for multi-recycling of plutonium would be to increase the enrichment of the uranium in the MOX fuel as the number of recycles increases to keep the reactivity greater than unity. The uranium-to-plutonium ratio would remain the same to ease the task of fuel licensing.

Even with keeping the amount of plutonium in the MOX fuel constant, another source of plutonium is still required to make up for that which is burned each cycle. This situation is where plutonium from original (legacy) SNF could be important. This legacy plutonium has a higher fissile plutonium content than spent MOX fuel, so not only would it help mass conservation issues, it would also help boost the reactivity of the system with multiple recycles. Therefore, if one starts with 100 grams of plutonium for MOX irradiation and 30% of it is depleted, only about 70 grams remains after reprocessing. Hence, 30 grams of plutonium from legacy SNF is added to the 70 grams to again make 100 grams. If 30% of this plutonium is depleted, then 60 of 130 grams of total legacy plutonium is destroyed, which corresponds to a depletion rate of about 46% after the second “pass.” This plutonium depletion rate per pass, however, actually decreases as the number of recycles increases because the fissile quality of the plutonium decreases. Figure 5-2 shows the cumulative percentage of initial plutonium that is depleted as the number of recycles increase, as well as showing the relative percentage of minor actinides that build up and the uranium enrichment for each pass. Table 5-VII gives more information about each recycle, and Table 5-VIII displays the activity and heat load as a function of cooling time for the second and third relative to the first recycle of MOX. Note that the uranium enrichment does not rise above 3 w% for any of the passes, which is well within current enrichment limits.

Table 5-VII. Detailed Results for Each Plutonium Recycle as MOX.

Pass number	% Pu burned per cycle	Cumulative Pu put into system	Cumulative %Pu burned	MA's built up per cycle	Cumulative %MA Burned	Fraction Pu depleted to MA's built up	Uranium enrichment (% ²³⁵ U)
1	30.4	100	30.4	8.31	8.3	3.7	0.72
2	27.1	130.4	44.1	9.03	13.3	3.3	2.0
3	26.2	157.5	53.1	9.42	17.0	3.1	2.4
4	25.7	183.7	59.6	9.47	19.7	3.0	2.6
5	25.2	209.4	64.3	9.58	21.9	2.9	2.8
6	24.5	234.6	67.8	9.61	23.6	2.9	2.95
7	24.5	259.1	70.9	9.71	25.1	2.8	3.0

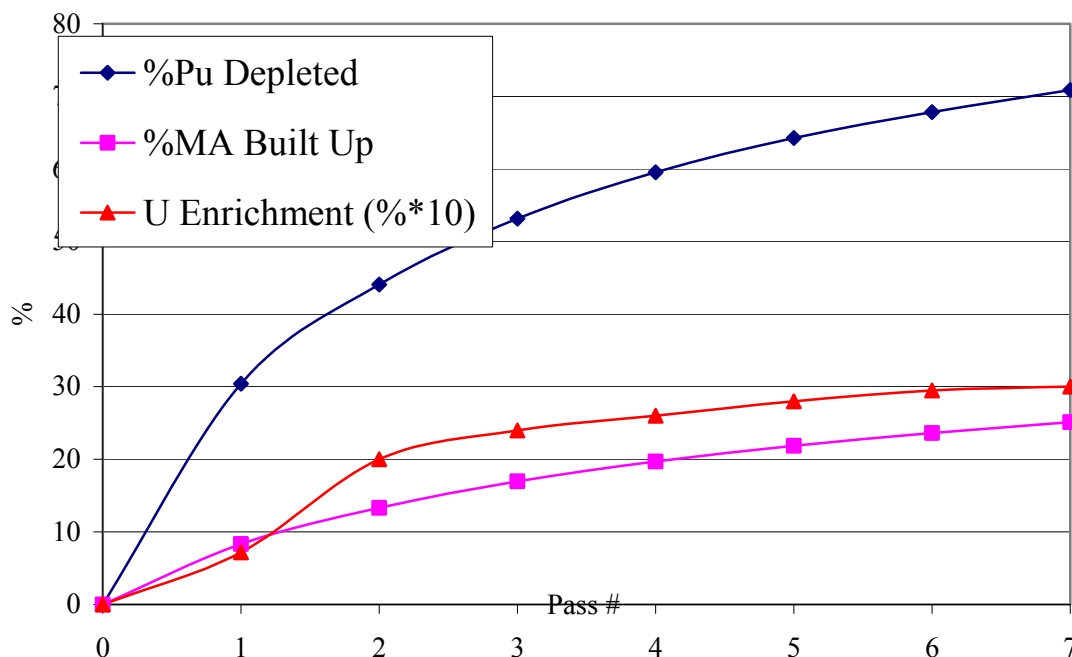


Figure 5-2. Multi-Recycling of Pu as MOX fuel in LWRs.

Table 5-VIII. Activity and Heat load of Spent MOX Fuel as a Function of Cooling Time.

Activity (Ci) # years	First Recycle Actinide	Total	Second Recycle Actinide	Total	Third Recycle Actinide	Total
1	4.11E+06	1.24E+07	4.31E+06	1.25E+07	4.31E+06	1.25E+07
3	3.47E+06	6.52E+06	3.64E+06	6.71E+06	3.65E+06	6.72E+06
5	3.18E+06	4.96E+06	3.33E+06	5.16E+06	3.33E+06	5.18E+06
7	2.91E+06	4.30E+06	3.06E+06	4.48E+06	3.06E+06	4.50E+06
10	1.92E+06	2.83E+06	2.01E+06	2.96E+06	2.02E+06	2.98E+06
Heatload (W)						
1	2.92E+04	6.48E+04	3.12E+04	6.64E+04	3.21E+04	6.72E+04
3	1.66E+04	2.86E+04	1.83E+04	3.02E+04	1.91E+04	3.11E+04
5	1.56E+04	2.18E+04	1.72E+04	2.34E+04	1.80E+04	2.43E+04
7	1.51E+04	1.94E+04	1.66E+04	2.10E+04	1.74E+04	2.19E+04
10	1.32E+04	1.57E+04	1.44E+04	1.70E+04	1.50E+04	1.76E+04

Both the heat load and the activity of the spent MOX fuel increase slightly with the number of recycles, but not significantly enough that reprocessing the second or third pass would be too much different than recycling the first pass of spent MOX fuel. Figure 5-3 shows the ending actinide isotopic concentrations in the spent MOX fuel after each pass.

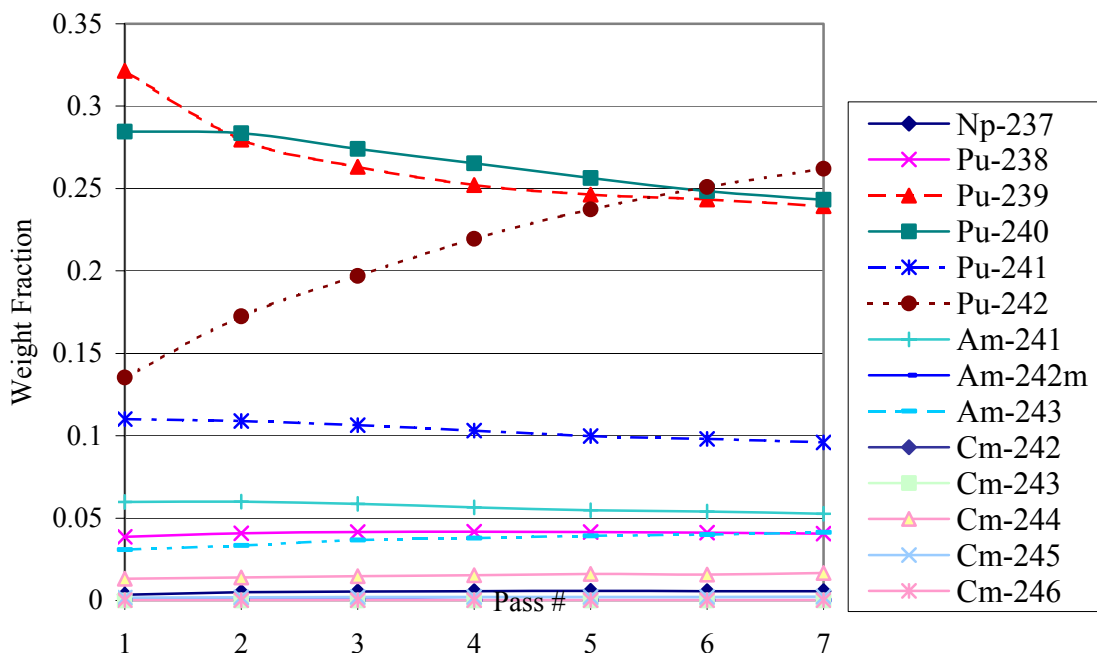


Figure 5-3. Change in actinide isotopic content as the number of passes in MOX Fuel increases.

As expected, the concentrations of ^{239}Pu and ^{241}Pu decrease as the number of recycles increase whereas ^{242}Pu increases significantly (*i.e.*, the fissile quality decreases). The ^{238}Pu content is around 4-5w% for all cases (including the initial high burn-up UO_2 fuel for the first pass), which well exceeds the current fabrication limit of 2.1 w% and demands the use of hot cells, or remote handling, as assumed previously. The main decision that has to be made in this research was how many recycles of plutonium should really be performed. With only two recycles (three passes), over 50% of the plutonium can be depleted, which was the goal. Therefore, it must be determined whether further recycles offer any additional advantage to the ADS operations. This issue will be explored further in Sec. 5.2.

5.2.2 Addition of Actinide Material Other Than Plutonium to MOX

The first problem that must be overcome before any transmutation of SNF can occur is overcoming the political directive of the 1970s stating that no reprocessing will be performed in the United States (CARTER, 1977). The motivation of this decision was to start a trend of not having separated plutonium streams being created worldwide, meaning that there would be no separated plutonium streams in the U.S. Of course, most of the rest of the world chose not to follow. The current political atmosphere of the US, however, still does not favor (or even allow) the separation of plutonium. It would be less of a proliferation risk and possibly make reprocessing more favorable if the plutonium did not exist as a pure product in any stream. Instead, assuming appropriate separation processes exist, the plutonium could be kept with the minor actinides and/or certain fission products. The presence of minor actinides in SNF, however, would decrease the

amount of plutonium that could be burned each pass (in a thermal neutron spectrum) and will lead to significant Am and Cm buildup. The effects of the burn are examined further in this section. In addition, a case was briefly considered in which plutonium is kept with the fission products strontium and cesium to increase the activity of the material stream, thereby reducing the proliferation attractiveness of this material. Plutonium contributes to ~26% of the activity of SNF after 10 years, and ⁹⁰Sr and ¹³⁷Cs comprise ~36% of the total activity. By keeping these selected fission products with the plutonium and doubling their presence from other Sr and Cs sources, MOX fuel could have about the same activity as SNF, which would represent an added nonproliferation benefit. The added activity, however, would make the fuel more difficult to fabricate, but with the use of hot cells and/or remote handling of the material (as may already be required for spent MOX fuel), such a proposal is not completely out of the question. However, developing a separations process that does not separate fission products from plutonium before the uranium will be difficult (the current PUREX process separates fission products first before the actinides, so strontium and cesium cannot be kept with the plutonium), but these materials could be combined at the separations facility, which would reduce the necessary transport of pure plutonium.

The nonproliferation advantage of keeping minor actinides or fission products with the plutonium is that the activity and/or heat load of the MOX fuel would be increased, but unfortunately, it also makes MOX fabrication more complicated. The activity for the minor actinide case after ten years reaches less than that of the plutonium-only case after seven years, but the heat load remains more than twice that of plutonium only, as is illustrated in the summary given in Table 5-IX. The case with strontium and cesium retention has a much higher activity and heat load than the plutonium-only case (which is the point of adding them in the first place). For subsequent calculations, it was assumed that the spent fuel with MAs was reprocessed after ten years and the spent fuel with strontium and cesium after seven years, since the activity will not decrease for hundreds of years, and the assumption is that special handling is required anyway.

Table 5-IX. Activity and Heat Load of Eight Assemblies of Modified MOX Cases to Decrease Proliferation Risk.

Activity (Ci) # of years cooling	Pu only in MOX 1 st pass Actinide	Total	Pu plus MAs in MOX Actinide	Total	Pu plus Sr and Cs in MOX Actinide	Total
1	4.11E+06	1.24E+07	6.39E+06	1.46E+07	1.57E+07	3.53E+07
3	3.47E+06	6.52E+06	4.95E+06	8.01E+06	1.45E+07	2.84E+07
5	3.18E+06	4.96E+06	4.52E+06	6.35E+06	1.37E+07	2.59E+07
7	2.91E+06	4.30E+06	4.16E+06	5.60E+06	1.30E+07	2.42E+07
10	1.92E+06	2.83E+06	2.84E+06	3.79E+06	9.92E+06	1.86E+07
Heatload (W)						
1	2.92E+04	6.48E+04	8.55E+04	1.20E+05	4.18E+04	1.29E+05
3	1.66E+04	2.86E+04	4.55E+04	5.72E+04	2.91E+04	9.07E+04
5	1.56E+04	2.18E+04	4.21E+04	4.82E+04	2.75E+04	8.10E+04
7	1.51E+04	1.94E+04	4.04E+04	4.47E+04	2.65E+04	7.60E+04
10	1.32E+04	1.57E+04	3.35E+04	3.62E+04	2.20E+04	6.04E+04

The difference in the depletion rate of plutonium in MOX fuel both by itself and with MAs and Cs/Sr is shown in Table 5-X. The addition of strontium and cesium has little affect on the depletion at a given burn-up because the actinide composition is the same. However, when minor actinides become part of the MOX fuel, the plutonium depletion for the first pass decreases significantly (from about 30% to 20%). Many more recycles would have to be performed to achieve the same destruction of plutonium, but MAs are being depleted as well (there is not a net buildup of MAs because some of the ones initially present do fission and are destroyed), it does benefit overall actinide transmutation. After ten years of cooling, however, MAs do start building up, primarily due to the decay of ^{241}Pu (with a 14.4 year half-life) to ^{241}Am .

Table 5-X. Comparison of Plutonium Depletion and MA Buildup *per*-Pass When Fission Products or MAs are Added to Plutonium in MOX Fuel.

Case	Pu Depletion	MA Buildup
Plutonium Only	30.3	8.58
Plutonium Plus Sr and Cs	30.6	8.35
Plutonium Plus MAs	20.7	--- ^(a)

^a The buildup of MAs after seven years was approximately equal to MA depletion.

Multiple recycles of plutonium plus MAs in MOX fuel do pose a challenge. To meet reactivity constraints, the amount of TRU contained in the heavy metal of MOX fuel was raised to 12.55 %, which was shown to be the largest possible in previous calculations (Van Tuyle, 2001). In addition, even with the increase in TRU concentration, the uranium enrichment was still required to be 2.7 w% for the first pass. By the second pass, the necessary enrichment became 6 w% and significant safety concerns existed (Appendix J). Commercial enrichment plants today usually produce a product that is less than 5 w% ^{235}U , although higher enrichments are technically feasible. For the purpose of this research, however, it is assumed that 6 w% would not be economically achievable and that it is not possible to perform multi-recycling of the plutonium with minor actinides in MOX, so the remaining 80% of the plutonium and minor actinides are sent to the Tier-2 ADS technology. From the ending isotopic mixes after the first and second passes displayed in Figure 5-3, the ^{238}Pu concentration in particular significantly increases in the second pass, which makes the heat load much larger. Additionally, the ^{239}Pu concentration decreased, which is the reason for the increased uranium enrichment.

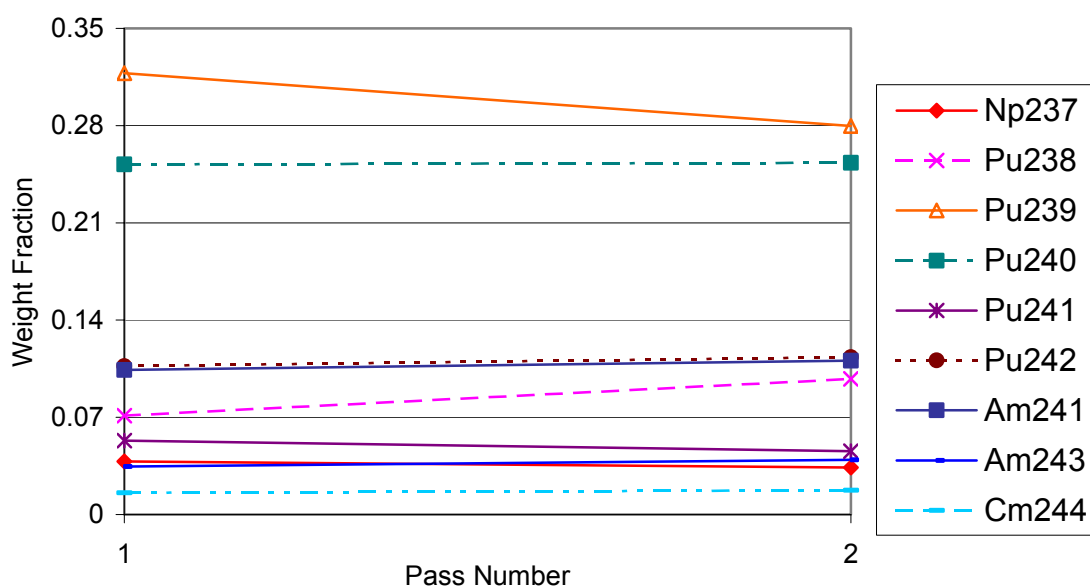


Figure 5-4. Isotopic composition of actinides in MOX fuel with Pu + MA Stream.

5.2.3 Performance of ADS with Various Feed Streams

An important issue to be addressed for an ADS system is whether it creates more waste than it destroys (*i.e.*, do the spallation products produced when the proton beam hits a target have a radiotoxicity larger than that of the SNF itself?). Previous studies have shown that spallation products pose a significant radiotoxicity problem, but these results were based on *inhalation* radiotoxicity, and not ingestion radiotoxicity; the latter is more important for the geological repository. Studies performed this fiscal year showed that spallation products do not pose a greater ingestion radiotoxicity hazard than fission products from SNF after about the first ten years, but the inhalation radiotoxicity associated with spallation products can be important shortly after removal from the ADS, as is shown in Appendix K (Trellue, 2002).

Five different cases were chosen for assessment of the ADS neutronic performance: one without a Tier-1 technology, one where plutonium and minor actinides are irradiated for one pass in an LWR, and three cases corresponding to plutonium irradiated for 3, 4, and 5 passes in an LWR as MOX fuel (2, 3, and 4 recycles). For each of the ADS cases examined, it is assumed that the uranium separations efficiency is 99.9%. Therefore, as the number of recycles increase, the uranium content in the feed also increases. After the initial separations process, about 10% of the actinide stream is uranium, which is fairly significant. The amount of uranium increases slightly with the number of recycles of MOX fuel.

The actual ADS design that was used for these calculations consisted of a LBE (lead-bismuth eutectic) target and a sodium-cooled blanket and produced about 840 MWt of fission energy. Two main regions of fuel were considered: one on the outside with a

higher actinide enrichment and one on the inside (*i.e.*, closer to the target) with a lower actinide enrichment. Within each region, either 7 or 8 inner zones of fuel were modeled, one of which (the most irradiated) was replaced with fresh fuel at the end of each cycle, which was typically about six months. The fuel rods were contained in hexagonal assemblies and consisted of zirconium metallic fuel with an actinide volume fraction of less than 50% (Yang, 2000). Each rod is irradiated for about three to four years, at which point it is removed from the system because the fast fluence limit on the cladding (a form of stainless steel) is about $4(10)^{23}$ n/cm². After appropriate cooling, the fuel is separated, the actinides (and possibly long-lived fission products if they are to be transmuted or stored separately) are retrieved, and they are mixed with “fresh” fuel and recycled back in the ADS during a later cycle.

The difficult part of performing these calculations is related to the fact that Monteburns calculates a time-dependent, non-equilibrium, depletion scenario. What this means is that when the system first starts up, the composition of fuel in each zone must be estimated, because only the fresh fuel composition is known. Until at least ten cycles are run, it is not known what the actual composition in each region really is (*i.e.*, what fission products and minor actinides are present and in what concentration). At equilibrium, the overall composition material in the system is fairly consistent from one cycle to the next. Hence, approximately the same amount of each isotope that is added at the beginning of each cycle is depleted during the course of the cycle. Therefore, the amount of material that should be added is approximately equal to the fission rate, or about one kg/GWtd of irradiation. A thermal power production of 840 MWt, yields to a feed rate of about 0.840 kg/d. As higher actinides are built into the system initially, however, the feed rate per cycle is much higher because additional neutron absorptions occur relative to fissions. Up to several decades may be required for a system to reach equilibrium, but the smaller the amount of plutonium in the feed material, the faster equilibrium is reached. Figure 5-5 shows the feed rate as a function of the number of cycles for different feed compositions coming into the ADS.

Table 5-XI displays the resulting reactivity swing for the four different feed streams delivered to the Tier-2 ADS compared to the base case of all material going to the ADS (*i.e.*, no Tier-1 LWR) along with the actual isotopic vectors entering the ADS and the initial TRU volume percent in the fuel.

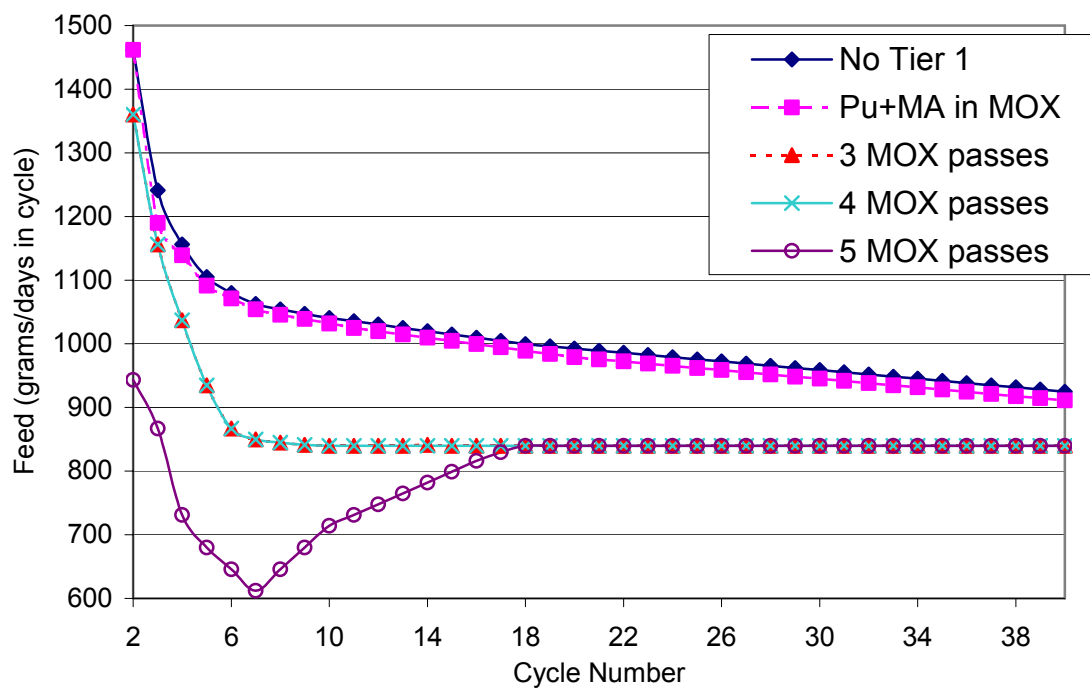


Figure 5-5. Feed Rate as a function of cycle in the Tier-2 ADS.

Table 5-XI. Isotopic Vector Entering the Tier-2 ADS and the Resulting Reactivity Swing for the Different Cases.

	No Tier 1	Pu+MA MOX	3 MOX passes	4 MOX passes	5 MOX passes
U235	0.000	0.001	0.001	0.001	0.001
U236	0.000	0.000	0.001	0.001	0.001
U238	0.064	0.081	0.109	0.116	0.121
Np237	0.055	0.038	0.082	0.086	0.090
Pu238	0.030	0.065	0.024	0.021	0.019
Pu239	0.396	0.289	0.151	0.129	0.115
Pu240	0.205	0.229	0.157	0.136	0.119
Pu241	0.080	0.048	0.061	0.053	0.046
Pu242	0.080	0.097	0.112	0.112	0.110
Am241	0.055	0.098	0.174	0.194	0.209
Am242m	0.000	0.001	0.001	0.001	0.001
Am243	0.024	0.033	0.088	0.103	0.115
Cm244	0.009	0.015	0.036	0.041	0.046
Cm245	0.001	0.004	0.005	0.005	0.006
Cm246	0.000	0.001	0.000	0.000	0.001
Vol.% Act.	11	14.5	21.6	22.5	27
delta k-eff	0.07	0.06	0.035	0.03	0.025

It is apparent from the results given in Figure 5-5 that it takes much longer to reach equilibrium in the case without Tier-1 systems, and the case where only a small amount of plutonium and minor actinides are depleted in Tier 1 than the cases with multi-recycling in Tier 1. Additionally, little difference in the feed rate of the ADS for material that has been irradiated 3 and 4 passes in Tier 1 is observed. However, once material has been irradiated for five passes as MOX, the initial minor actinide fraction increases significantly because so much plutonium has been irradiated as MOX fuel. Hence, the plutonium fraction in the fuel actually increases with the equilibrium feed rate in the first 15 or so cycles as more plutonium builds in, and, because of this increase in fissile quality, the actual feed rate must go below 0.840 kg/day to keep the system from going critical. This behavior results from insufficient plutonium starting in the system (the feed is <15% fissile plutonium), and may be considered undesirable from a safety standpoint. Therefore, it is recommended that no more than three recycles should be performed when an ADS is used in Tier-2, and it was concluded that four passes of MOX fuel is the optimum when the remainder of the material is sent to an ADS. This approach maximizes the amount of plutonium burned in Tier 1 without significantly affecting the Tier-2 ADS. If four passes become unreasonable 30 years later, then three passes should also be acceptable in the ADS, but less plutonium would be consumed and more ADSs would be required.

For one region in 1/8 of a LWR core, the mass of initial plutonium irradiated was 278 kg. Since the amount of plutonium burned each recycle is replaced with “fresh” SNF, the actual amount of plutonium added during four passes was 1.84×278 kg, or 511.5 kg (the depletion rate during the first pass was 30.4%, the second was 27.1%, and the third was 26.2% for a total of 84%), or about 4 tonnes of plutonium for a full core. Assuming that the irradiation time is about four years (for three cycles in the reactor) and that seven years of cooling and one year of time for fabrication is required, then “new” fuel is required for nine different loads (cycles) in the reactor. Therefore, about 36 tonnePu can be irradiated per reactor over the course of 48 years. To burn the approximately 830 tonne of plutonium from legacy SNF ($0.0119 \times 70,000$ tonne SNF = 833 tonne Pu), then about 23 reactors are required.

About 60% of the plutonium is depleted during four passes in an LWR, including 20% converted to minor actinides (Figure 5-1). Therefore, about 40% of the plutonium is actually destroyed and does not need to be processed in Tier-2 technologies. Additionally, for every 100 kg of plutonium to feed Tier-1 LWRs, about 18 kg of minor actinides from SNF are separated, and the resulting MA stream must be irradiated in Tier-2 systems. The amount of material that is sent to an ADS with three recycles of MOX fuel, therefore, amounts to about 590 tonnes, as is indicated below:

$\sim 70,000 \text{ tonneSNF} \times 0.0119 \text{ tonnePu/tonneSNF} \times 0.60 \text{ (1 - fraction of Pu fissioned in Tier 1)} \times 1.18 \text{ (1 + MA/Pu in SNF)} = 590 \text{ tonne to ADS.}$

The initial actinide inventory in a fast-spectrum ADS is about 2.2 tonne, and the feed rate is about 0.840 kg/d for a 840 MWt system. Over the expected operation period of

60 years, about 20 tonne of actinides can be burned, requiring about 30 ADS to complete the mission.

5.3 Coupling of Neutronics with NFC Simulation Model NFCSim

Another goal of system studies neutronics support in FY02 was to develop a way to incorporate neutronic calculations into the NFC simulations model NFCSim. In particular, one goal of the simulation calculations was to track the irradiation of fuel in all past and future US nuclear reactors. The ability to calculate the isotopic and/or elemental vectors of material streams after irradiation in an LWR (using UO_2 or MOX fuel), a gas-cooled reactor, and/or fast-spectrum critical reactor or ADS is also desired for a more robust simulation of advanced nuclear fuel cycles. The Monteburns code is a (computer) time-intensive burn-up model that requires considerable disk space and is, therefore, not practical for a real-time simulation. However, the main isotope decay and depletion calculation in Monteburns is performed using the burn-up/depletion code ORIGEN2.1 (ORNL, 1999) (or ORIGEN2.2, which is a slightly updated version but functions similarly). If the appropriate cross sections are applied to ORIGEN2.1, an accurate burn-up calculation can be performed in minutes for the burn-ups of interest in this project. In order to represent accurately the cross sections for a particular system, a transport code must be run to develop the one-group cross section as a function of neutron spectrum to be used in ORIGEN2.1. The Monte Carlo transport code MCNP (Briesmeister, 1996) uses continuous energy cross sections and can derive one-group cross sections based upon the flux of neutrons at various energies. One purpose of the Monteburns code (Trellue, 1998; Poston, 1999) is to process this cross section and flux output from MCNP into a format that can be used by ORIGEN2.1 and then to run ORIGEN2.1 with this data. The Monteburns code keeps the ORIGEN2.1 input files (including composition, burn-up information, and cross sections) from each burn-up step so that the user can process the data further and separately. For the neutronic coupling proposed to NFCSim, the average cross section data files (taken about halfway through the burn-up step) for numerous cases were obtained using Monteburns, and a compatible ORIGEN2.1 input file with the burn-up and composition information was developed for each case to be used along with the corresponding cross section file.

The cases for which cross section information was generated using Monteburns are listed in Table 5-XI. The ORIGEN2.1 default library identifiers for each case are also listed, along with the burn-up and initial enrichment of uranium used (if relevant). The default MOX cases are those that recycle plutonium only (no other fission products or minor actinides). The IFR case is that for a representative fast reactor in ORIGEN2.1 (*i.e.*, FFTF), and it is not known how this cross section set was generated so little data appears for this case. The Monteburns cases that were run were developed as part of the systems studies in both FY01 and FY02. A sample ORIGEN2.1 input file (named TAPE5.INP) is listed in Appendix L. This file would accompany the file (TAPE9.INP) generated for each case. Preliminary comparisons showed that using this average cross section file and ORIGEN2.1 for a case typically generated results that were within 5% of those calculated by a detailed Monteburns run, as shown in Appendix L.

Table 5-XII. Description of Cases for NFCSim Simulation Model.

Case	Burn-up (GWd/MTHM)	Uranium enrichment (% ²³⁵ U)	ORIGEN2.1 library identifiers
Low Burn-up UO ₂ in a LWR	27	2.56	204, 205, 206
Medium Burn-up UO ₂ in a LWR	38	3.2	219,220,221
High Burn-up UO ₂ in a LWR	60	4.2	219,220,221
First Pass MOX in a LWR	50	0.72	210,211,212
Second Pass MOX in a LWR	50	1.8	210,211,212
Third Pass MOX in a LWR	50	2.4	210,211,212
Fourth Pass MOX in a LWR	50	2.7	210,211,212
Fifth Pass MOX in a LWR	50	2.9	210,211,212
Sixth Pass MOX in a LWR	50	3.0	210,211,212
Seventh Pass MOX in a LWR	50	3.1	210,211,212
First Pass MOX w/ MAs in a LWR	50	2.7	210,211,212
Representative ADS Case with 3 recycles of MOX in Tier 1	~200	-	381,382,383
Representative IFR Case	-	-	381,382,383

Future neutronic work for the AFC systems effort will be to not only provide simplified data that can be used in the simulations model, but also to further advanced fuel cycle design as new reactors are examined in future studies.

This page is intentionally left blank.

6 WASTE SEPARATION TO BENEFIT REPOSITORY CAPACITY

By separating certain components of spent nuclear fuel (SNF), it may be possible to increase the capacity of a long-term geological repository (*e.g.*, Yucca Mountain, YM or its successor, called herein YM2, which according to statute cannot be at the present YM site) by a factor of ~ 10 or more. Additionally, retrievable storage is required for the separated components (cladding, uranium, high-heat-load fission products, transuranic elements), and transmutation of transuranic (TRU) elements would be required for a permanent solution. Only the heat load of repository waste and its volume are herein considered to be design constraints. Specifically, the statutory limit of YM capacity (70,000 tonneHM of SNF and defense waste, prior to opening YM2) is ignored; indeed it is the goal of this study to investigate ways to exceed that capacity and thereby delay the need for YM2.

6.1 The Present YM “Viability Assessment” Design

The present concept for SNF storage at YM, as described in the Yucca Mountain Viability Assessment (YMVA), involves emplacing the waste in 157 km of horizontal tunnels or drifts that form a thin horizontal layer covering 741 acres several hundred meters below the surface (USDOE, 1988). The SNF is contained within multiple “barriers”, including: 1) the original fuel package, 2) a double-walled, cylindrical metal waste package (WP), 3) (possibly) backfill that surrounds the WP in the emplacement drift, 4) the tuff that composes YM, and 5) a layer of zeolitized tuff that acts as a permeation barrier for dissolved metals. Over several hundreds or thousands of years, the waste package and the original fuel packages will corrode and release radioactive wastes that have not yet decayed, which then will migrate slowly through the rock and perhaps into the groundwater over 10^4 - 10^7 years. The multiple-barrier design attempts to maximize the time before release, consistent with the constraint that the spent fuel is not reprocessed. Details of the current WP, YM tunnel spacing, and other parameters are listed in Appendix M.

One would like to employ high packing densities per unit area simultaneously to minimize the cost of YM and to maximize its capacity and therefore to delay the need (and the political costs) for YM2, YM3, *etc.* However, the packing density for SNF in YM (a statutory 70,000 tonneHM of all waste types in a designed 741 acres \rightarrow 94 tonne/acre, (USDOE, 1988)) is limited by the allowed temperature rise in the near-field geological structure, which in turn is determined by the decay heat released by the waste.

Several repository temperature constraints have been identified (USDOE, 1988) that limit the permissible density of this decay heat, and hence the emplacement density of the waste. Considering only limiting cases, the first constraint is that the temperature of the original fuel package (*e.g.*, fuel-pin cladding) should be maintained below 350°C to prevent damage to the cladding. This limit is set by the internal pressure caused by volatile fission products inside the SNF and, therefore, will be lower for higher burn-up fuel characterized by a given cooling time. For waste emplaced after 10 years cooling,

this is the most restrictive constraint. For reprocessed fuel, where the cladding has been removed, and the waste form is now vitrified high-level waste (VHLW); this is not a concern, but the temperature constraint now is replaced by the VHLW centerline temperature, as is discussed below.

Secondly, the temperature of the rock adjacent (~1 m) to the WP should not exceed 200°C to prevent fracturing and subsequent increased leach rates after the WP is breached (~10,000 yr after emplacement). Three-dimensional, time-dependent finite-element thermal analysis has shown that this constraint is set by the total heat release in the initial ~40 yr after emplacement (USDOE, 1988; Bechtel, 2002)

Thirdly, the temperature of the zeolite layer, which is located approximately 60 m below the waste emplacement level, should not exceed 90°C. Time-dependent thermal analysis has shown that this temperature is controlled by the total heat release in the initial ~300 yr after waste emplacement.

Fourthly, the waste centerline temperature for the VHLW should not exceed 400 – 500° C to prevent crystallization that would reduce the retention of radioisotopes. The VHLW canister described by Croft (Croft, 1994) was shown to meet this limit assuming the second and third constraints are met. This modified canister contained waste producing 4.74 kW in a double-walled package 3.66 meters long translates into a linear heat release (including 0.1 meter canister spacing) of 1.26 kW/m, which is approximately the same as the YMVA design of 1.45 kW/m for packaged SNF. The VHLW package contains ~400 l (1 tonne, assuming a specific gravity of 2.5) of vitrified high-level waste.

A fifth constraint imposed on waste packing density is set by assuming a conservative maximum waste composition of 25% by weight in the vitrified waste. Waste fractions (WF) of up to 50% have been demonstrated, but a more common and conservative assumption is 20%. For the given VHLW package design, the 25% limit sets a constraint of no more than 250 kg of separated waste per waste package (WP). Larger-diameter packages may relax this constraint, but this option is not a considered herein. As shown below, the waste packing density can be the limiting constraint for optimally reprocessed waste, so larger-diameter VHLW packages or higher waste weight fractions should be considered in further study.

Finally, it is noted that alternative plans for low-thermal-loading configurations exist (Bechtel, 2002; USNWTRB, 1999; USDOE, 2002) that would reduce the permissible temperatures and, therefore, reduce the waste packing density below the YMVA design values. These options are described in Appendix M.

6.2 Separating Waste to Benefit Repository Capacity

Analyses leading to the present repository design (USDOE, 1988) have all assumed that the SNF would remain intact inside its original fuel and waste packages. However, a number of authors (Croft, 1994; WHC, 1990; Forsberg, 2000) have recognized that

certain isotopes contribute the majority of the heat released from SNF. Removing those isotopes from SNF would greatly reduce the decay heat of the waste and, therefore, in principle would greatly increase the capacity of a geological repository (*e.g.*, YM or YM2). The separated components would be handled separately, as is described in Sec. 6.5.

As shown in Fig. 6-1, for times less than ~65 yr after irradiation, the major contributors to decay heat are isotopes of cesium and strontium (^{137}Cs with half-life $t_{1/2} = 30.2$ yr, and ^{90}Sr with half-life $t_{1/2} = 29$ yr), and their short-lived decay products $^{137\text{m}}\text{Ba}$ and ^{90}Y , respectively. After this time, the major heat releases come from the actinides, primarily the various isotopes of the TRU elements plutonium, curium, and americium (Pu, Cm, and Am). The remaining isotopes in SNF contribute ~3.7% to the heat load at 10 yr after irradiation.

The present study examines a number of reprocessing schemes that remove various fractions of the waste, and then package the remainder as VHLW for emplacement in the repository tunnels or drifts. Alternative, higher-density emplacement methods have been proposed (Bechtel, 2002; USNWTRB, 1999; USDOE, 2002) that could improve on this packaging method; these are described in Appendix M.

It is noted that reprocessing spent nuclear fuel potentially offers other benefits. In particular, removing from SNF those species with high radiotoxicity promises long-term, but difficult-to-quantify merit. The radioisotopes with the highest contribution to radiotoxicity for future inhabitants of Yucca Mountain are ^{129}I , ^{99}Tc , and several isotopes of the various actinide decay chains (*e.g.*, ^{237}Np) (van Tuyle, 2001), with the latter dominating the very long-term radiotoxicity. These species are all readily separated from SNF using aqueous separations such as those proposed herein. The iodine is recovered as a volatile species during the decladding/dissolution step; soluble technetium is co-extracted with uranium and can be later separated; and the removal of actinides is discussed in greater detail below in Sec. 6.3. The iodine and technetium are candidates for destruction by transmutation in reactors or in accelerator-driven transmuters, as of course are the actinides, with thermal neutron spectra more efficiently destroying the former and fast neutron spectra more efficiently destroying the latter. The relatively small masses and volumes of iodine and technetium also make encapsulation relatively simple. Then disposal of these species in waste forms specifically optimized for their containment is possible, rather than disposal in a general waste package intended for unseparated SNF. The relatively high thermal-neutron cross section for ^{99}Tc opens the possibility of using this material as a burnable poison in thermal reactors. However, the present study only investigates the potential thermal benefits to the repository of waste separation, not the simultaneous reduction of radiotoxicity that results from that separation; the latter remains as future work for the systems analyses task.

6.3 Summary of Calculations

The present study examines the effects on YM or YM2 of removing various constituents from the SNF. Seven cases or scenarios are considered for different levels of cleanup, as is listed in Table 6-I. Scenarios II-VII investigate removal of the actinides U, Pu, and the minor actinides MA = Cm + Am. Scenarios III, IV, and VII also consider the removal of the high heat release (HHR) fission products ^{137}Cs and ^{90}Sr . It is noted that Scenario VII describes the most complete cleanup, and the base case Scenario I has no cleanup and, therefore, represents the present emplacement plan. Table 6-I uses the acronyms HHR, LHR, and VLHR for high, low, and very low heat release fractions, as introduced by Croft (Croft, 1994), to facilitate comparison to this important previous study.

It is assumed that fission products other than those listed here are not removed, except that any reprocessing step (*i.e.*, Scenarios II-VII) will necessarily release the “volatile” fission products (*e.g.*, tritium, carbon, krypton, xenon, bromine, and iodine). These volatile elements can be trapped and processed separately, and, as shown in Fig. 6-1, they represent only a small fraction of the total decay heat.

The decay heat from SNF depends primarily on the fuel composition and burn-up. For these analyses, the burn-up/depletion behavior of the fuel during the irradiation period has been modeled using the Monteburns computer code (Trellue, 1998), as described in Sec. 5 (Neutronics Analysis). The output from Monteburns provides the “initial” isotopic distribution of the SNF. The output from Monteburns is then used as input to ORIGEN2.1 (ORNL, 1999), which calculates the decay heat and isotopic composition as a function of time during the cooling period.

Three cases were calculated for light water reactor (LWR) burn/irradiation cycles using different fuels and burn-up levels. These cases are summarized in Table 6-II. All cases considered represent reactors generating a thermal power of approximately 3,400 MWt. The Monteburns-generated decay heats reported herein are normalized to SNF mass in units of tonne of Initial Heavy Metal (*tonneIHM*). Details of these computations are summarized in Appendix N.

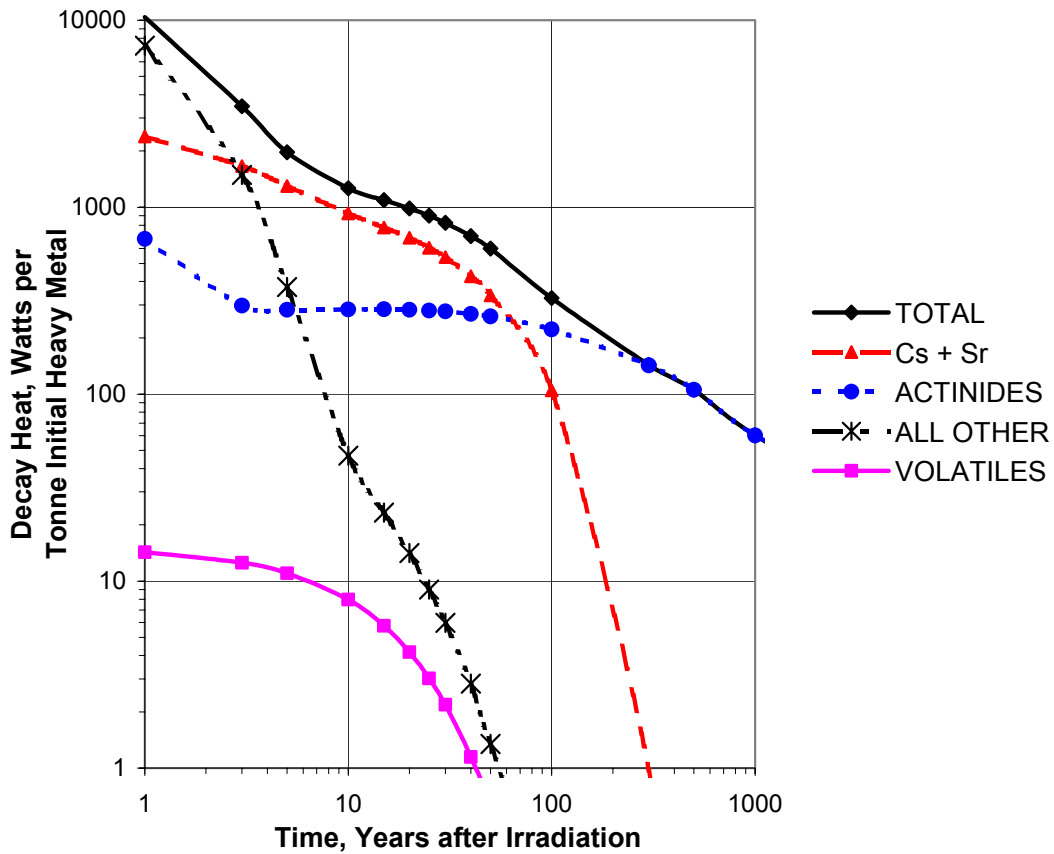


Figure 6-1. Spent Nuclear Fuel Decay Heat, Light Water Reactor at Burn-up of 38 GWd/tonneIHM.

Although various benefits may ensue from increasing or decreasing the cooling period prior to waste emplacement or reprocessing followed by emplacement, a period of 10 yr has been used for consistency with previous studies.

Table 6-I. Summary Description of Seven Scenarios Based on Different Degrees of Activation and Fission-Product Removal.

	Short Description	Elaborated Description of Material Form	Presumed Advantage of Scenario
I	Base Case	Direct disposal of SNF fuel assemblies	Base- or Point-of-Departure (POD) case: direct disposal of SNF fuel assemblies, including VFPs.
II	I – U(ranium)	Vitrified [MA + Pu + NVFP]	Reduce mass but must deal with full short- and long-term heat load, which establishes limits on the degree to which the volume of the waste form can be reduced.
III	II – {Cs,Sr}	Vitrified [MA + Pu + VLHR = LHR]	Reduce mass, as well as short-term heat load associated with HHRs, but with full (TRU = Pu + MA) long-term heat load and proliferation risk.
IV	III - Pu	Vitrified [1 - U - HHR - Pu = MA + VLHR = LHR]	Similar to <i>nsc</i> = <i>III</i> , with some reduction in long-term heat load through the removal of Pu (and reduced long-term proliferation risk).
V	II - Pu	Vitrified [1 - U - Pu = MA + NVFP]	Not unlike <i>nsc</i> = <i>II</i> , but with some reduction in long-term heat load resulting from Pu removal (and reduced long-term proliferation risk).
VI	V - MA	Vitrified [1 - U - Pu - MA = NVFP]	Reduce mass with full short-term heat load, but with significantly reduced long-term heat load.
VII	IV - MA	Vitrified [1 - U – HHR - Pu – MA = VLHR]	The best it gets; volume and mass reduction along with reductions in both short-term and long-term heat loads
MA = minor actinides Np,Cm, Am		VFP = volatile fission products	LHR = Low heat release radionuclides
TRU = MA + Pu		NVRP = non-volatile fission products	HHR = high heat release radionuclides
			VLHR = very low heat release radionuclides

Table 6-II. Three Irradiation Cases That Produce Different SNF Isotopic Compositions.

Name	Initial Enrichment (percent ^{235}U or Pu)	Burn-up Level (GWd /tonneIHM)	Total Reactor Fuel Mass, tonneIHM
Standard LWR	3.2 (^{235}U)	38	84.8
Extended LWR	4.2 (^{235}U)	60	84.8
Mixed-Oxide fueled LWR	9.0 (Pu)	49	80.2

Existing SNF represents a wide range of burn-up, with values that are often substantially lower than the “Standard LWR” case considered here (Table 6-II), and extended cooling periods (25-45 yr; Appendix M) compared to the 10 yr used in these studies. The decay heat from the existing SNF, therefore, is often substantially lower than assumed in most analyses, including those presented herein. For this reason, the areal packing density of 94 tonneIHM/acre calculated from the statutory capacity and planned emplacement area (USDOE, 1988) is larger than the oft-quoted value 57 tonneIHM/acre for 10-yr-cooled spent fuel.

Of the various temperature constraints listed in Sec. 6.1, only the VHLW centerline temperature, the near-field tunnel-wall temperature, and far-field zeolite temperatures have to be considered in setting areal limits for the scenarios that invoke SNF component separation through reprocessing; the cladding temperature is not of concern since the cladding must be removed to accomplish any reprocessing step.

A number of detailed three-dimensional finite-element, time-dependent thermal analyses have been performed for the YM repository (USDOE, 1988; Bechtel, 2002; USDOE, 2002) to determine the maximum thermal capacity. For 10-yr-cooled SNF loaded at an initial linear density of 1.45 kW/m with a drift tunnel spacing of 81 m, it is found that the tunnel wall temperature peaks at ~40 yr after emplacement, and the far-field temperature peaks in a few hundred years. For maximum precision, it would be necessary to repeat these calculations with each specific isotopic mix used in the present calculations, including all separation schemes II-VII (Table 6-I), to determine the peak temperatures and, therefore, to determine the allowable areal loadings for each of the six reprocessing cases.

Instead, a linear waste packing density has been assumed that produces equivalent total heat release in a given time frame (40 yr or 300 yr for the near-field tunnel-wall and far-field zeolite layer temperature rises, respectively). This condition is predicted to generate a temperature profile similar to those of the detailed studies and, therefore, leads to similar maximum temperatures. For 10-yr cooled SNF emplaced at 1.45 kW/m in the emplacement drifts specified in the YMVA design, both the 40 -yr and 300- yr total heat loads produce temperatures that are close to the maximum allowable values. It is assumed that these constraints equally limit the maximum allowable waste packing density. As a substitute for detailed 3-D, time-dependent thermal calculations, therefore, the heat released in a given time period by a given quantity of the reprocessed fuel (Scenarios II-VII of Table 6-I) is matched to the heat released by the un-reprocessed fuel (Scenario I) over that time period. Because the reprocessed fuel has a lower

heat release on a *per-tonneIHM* basis than the un-reprocessed fuel, a larger quantity of the reprocessed fuel can be stored in the waste package designed for un-reprocessed fuel (Scenario I). Depending on the isotopic composition of the reprocessed fuel, either the short-time (40-yr integration) or long-time (300-yr integration) heat ratio may limit the maximum permissible packing density. Integrated heat releases are determined by numerical integration of the instantaneous heat releases calculated by ORIGEN2.1; single-exponential decay is assumed to describe the period between adjacent time steps.

To calculate the constraints that follow from the HLW centerline temperature limit, which occurs at short periods after vitrification /emplacement, we determine the increased packing density from the instantaneous heat release at vitrification/emplacement. The ratio of the instantaneous heat release from unprocessed fuel to that of reprocessed fuel (for separation schemes II-VII) is used, even though the unprocessed fuel is not vitrified, because the total heat limits of the unprocessed SNF waste package and the VHLW waste packages are nearly identical. Reprocessed waste is vitrified at 25% waste by weight, which in many cases limits the decay heat in a WP and, therefore, limits the linear packing density for reprocessed waste with the high-heat-release elements removed.

Separations using aqueous processes are assumed (Appendix O). These technologies have been demonstrated, at bench and often on industrial scales, with recoveries above 99.9% for all processes modeled herein. For these calculations the efficiencies are assumed to be 100%; this assumption is examined in Appendix O, and is shown to have negligible effect on the conclusions. Separation at 10-yr cooling is assumed to be followed with immediate vitrification and emplacement.

6.4 Results

Figure 6-2 shows the integrated heat release for several of the scenarios listed in Table 6-I. As expected, the highest heat release comes from Scenario I (base case, no reprocessing), and the lowest heat release comes from Scenario VII [all HHR species (TRU and Cs, Sr) removed]. Scenario II (removal of uranium only) is omitted from Figure 6-2 because in terms of heat load reduction this scenario cannot be distinguished from Scenario I on the scale of this figure. Two vertical dashed lines on Figure 6-2 indicate the points at which the integrated heats are compared for the short-time (tunnel-wall temperature) and long-time (zeolite layer temperature) thermal constraints, as scaled according to the procedure described in the previous section. The results presented in Figure 6-2 were compared to the published results of Croft (1994), and agreement is within a few percent.

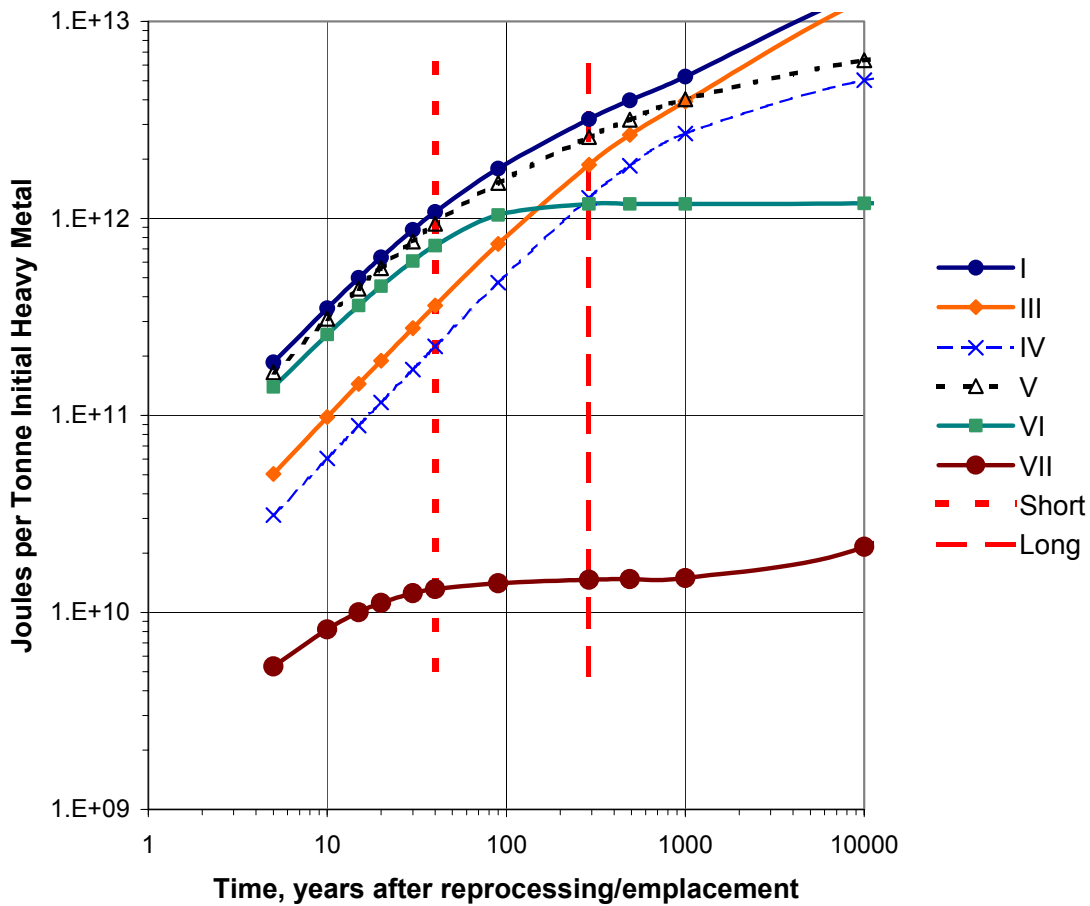


Figure 6-2. Integrated thermal energy released from reprocessed SNF with different reprocessing scenarios.

The calculated repository capacity ratios for the Standard LWR fuel (Table 6-II) are presented in Table 6-III. Results for “Extended-LWR” and “MOX-Fueled-LWR” fuel/burn-up cycles are given in Appendix N. For each reprocessing scenario, Scenarios II-VII (Table 6-I), increased packing densities (expressed as a ratio to that of un-reprocessed SNF, Scenario I) are calculated for the short-term integrated, long-term integrated, and “instantaneous” (10 yr after irradiation) conditions. The fourth column in Table 6-III gives the density limit imposed by the waste fraction in VHLW (assumed 25%); this value varies directly with the mass of the remaining fission products after the separation process is performed. The fifth column repeats the lowest (limiting) value of the four constraints. Figure 6-3 gives a graphical display of the YM capacity enhancement ratios listed in Table 6-III.

Table 6-III. Repository Capacity Ratios Calculated on the Basis of Scenario-Dependent Heat Loads (Figure 6-2).

Scenario <i>nsc</i>	Standard LWR				
	Short-Term Benefit ^(a)	Long-Term Benefit ^(b)	Waste Package Limit ^(c)	Waste Fraction Limit ^(d)	Least Limit ^(e)
II	1.00	1.00	1.01	6.8	1.00
III	2.99	1.71	3.82	7.4	1.71
IV	4.82	2.51	6.09	9.6	2.51
V	1.15	1.23	1.12	8.6	1.12
VI	1.48	2.7	1.30	9.0	1.30
VII	82.2	218	26.9	10.1	10.1
^(a) Short-Term Benefit: Ratio of heat releases for Scenario I compared to Scenario <i>nsc</i> , integrated over first 40 years after separation/emplacement. ^(b) Long Term Benefit: Ratio of heat releases for Scenario 1 compared to Scenario <i>nsc</i> , integrated over first 290 years after separation/emplacement. ^(c) Waste Package Limit: Ratio of heat releases for Scenario 1 compared to Scenario <i>nsc</i> ; instantaneous heat release controlling waste package centerline temperature for vitrified HLW. ^(d) Weight Fraction Limit: Limit assuming VHLW is no more than 25% HLW by weight. ^(e) Lesser of first four values.					

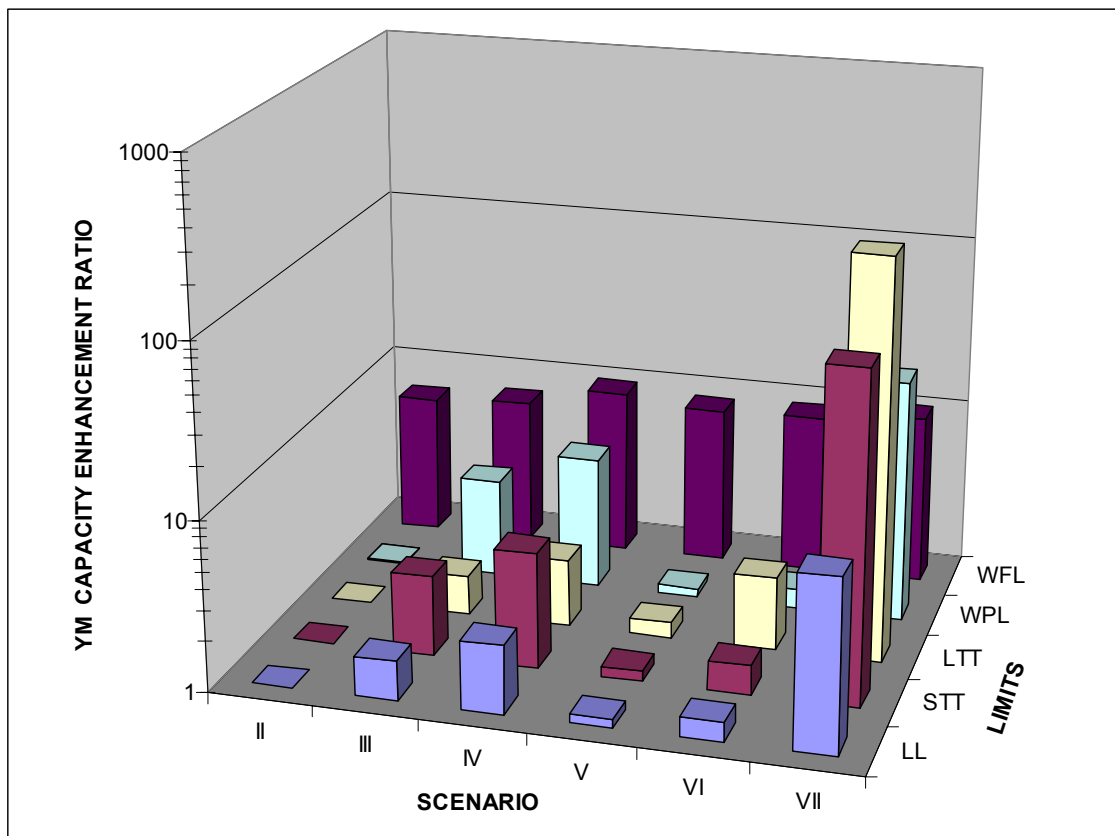


Figure 6-3. Yucca Mountain capacity enhancement ratios versus Scenarios ncs (Table 6-I) and limiting constraints (Table 6-III), where LL = Least Limit; STT = Short-Term Thermal; LTT = Long-Term Thermal; WPL = Waste Package Limit; and WFL = Waste-Fraction Limit.

The limiting ratio for Scenario II is 1.0, which shows no gain from a heat-load viewpoint for uranium separation alone. Although the volume of the waste is reduced by removing the ~85% of mass that is uranium and the ~11% of the mass that is cladding and supporting structure, the heat release is essentially unchanged; for these reasons the waste emplacement is not improved compared to unprocessed SNF (Scenario I).

The limiting YM capacity ratio for Scenario III is 1.7, showing that removal of the high-heat-release isotopes of cesium and strontium has only a small effect on increasing repository capacity. In this case the long-term (300-yr) heat release is dominated by the TRU elements that for this scenario remain in the reprocessed waste.

For plutonium separation alone (Scenario V) or for TRU separation (Scenario VI), only minor benefits of 10-30% repository capacity increase are projected. The short-term heat release from cesium and strontium remaining in the reprocessed fuel keeps the VHLW centerline temperature and, almost equally, the 40-yr integrated heat release near the limits of the un-reprocessed SNF (Scenario I).

Even Scenario IV, where cesium, strontium, and plutonium are removed from the waste, offers only a modest factor of 2.5 increase in waste packing density (or repository capacity). The minor actinides americium and curium still limit the long-term (300 yr) heat release.

Removal of Cs, Sr, and all actinides (Scenario VII), however, projects a repository capacity increase by a factor of 10, with this factor increase limited only by the waste fraction permitted in vitrified waste. Considering only the thermal constraints, the capacity increase would increase to 27-fold. Although a number of schemes can be envisioned to shift the constraint from weight fraction of waste in the VHLW back to a thermal constraint and, therefore, increase the repository capacity further (for example, decreasing the drift spacing or packing two or more waste packages in close proximity, or increasing the WP diameter and hence capacity), all of these options have disadvantages. A 10-fold increase in repository capacity, however, would still effectively preclude the need for additional repositories for hundreds of years and, therefore, deserves serious consideration.

Reprocessing of waste from the “Extended-LWR” and the “MOX-fueled-LWR” fuel/burn-up cases (Table 6-II) provides similar benefits compared to direct disposal of (un-reprocessed) SNF. These capacity-increase ratios are listed in Appendix N, but are omitted here for brevity. The isotopic distributions from both these cases, however, include substantially higher MA and higher cesium and strontium (plus other fission products, which is a result of the higher burn-up), so the total heat release is greater. The repository capacity for these un-reprocessed fuels, therefore, is reduced by factors of 0.57 (Extended-LWR) to 0.24 (MOX-Fueled-LWR) compared to the un-reprocessed “Standard-LWR-SNF” case. The thermal benefits of reprocessing, therefore, are effectively greater for these advanced-fuel forms, so a solution to the limiting waste-fraction constraint (*i.e.*, shifting back to the limiting thermal constraint) would provide much greater benefits compared to the Standard-LWR-SNF case.

6.5 Handling of Separated Wastes

As is indicated in Table 6-I, any of the SNF “pre-conditioning” scenarios considered in this study creates a number of new waste forms/streams. The following is a brief description of how the additional waste streams could be handled.

- *Uranium*: All the reprocessing schemes considered herein include separation of uranium to reduce the waste mass and, therefore, to lead to a significant reduction in the VHLW mass, and possibly volume. The separated uranium would be Class C waste and could be disposed of in shallow landfills, or stored for use in future fast-spectrum reactors.
- *Volatile Wastes*: Of the volatile wastes, only the iodine isotope ¹²⁹I constitutes a long-term radiological hazard. This material could be packaged as a salt and placed in the geological repository, or with some difficulty (and cost) it could be transmuted.

- *Cesium and Strontium*: These high-heat-release (HHR) radionuclides have short half-lives (~ 30 yr) and so disposal in “engineered” storage rather than “geologic” repositories might be a possibility. Considerable experience with handling these species has developed from reprocessing of the Hanford tank wastes (Jackson, 1977), where the encapsulated wastes are stored under water at the Waste Encapsulation Storage Facility to control the heat release. Because YM will remain open for ~100 yr after waste emplacement starts, the cesium and strontium could be contained in retrievable storage for up to three half-lives before being emplaced; this surface holdup would decrease the heat load by a factor of ~8. Alternately, these two fission products could be emplaced in a special low-cost, “sacrificeable” portion of the repository at very high loadings (Forsberg, 2000). Although the high temperatures generated by the high thermal loading repository could damage the surrounding rock, this would have little consequence because the radionuclides will decay away before they can migrate from the repository; the thermal limits imposed in YM are to prevent the rapid dissemination of long-lived isotopes from the waste packages. The small (5-cm outer diameter) waste packages could be emplaced in inexpensive small-bore horizontal or vertical boreholes, rather than expensive large-diameter (5-m) horizontal emplacement drifts, and could be placed in a shallow layer above the main repository. Also, “beneficial” large-scale uses for these radioisotopes can be identified, including food irradiation.
- *Transuranic Materials (Pu + MA)*: Removing these TRU elements yields significant benefits to the repository, including reducing the risk of nuclear proliferation by eliminating the “plutonium-mine” scenario, completely eliminating the possibility of criticality events, and eliminating some of the most radiotoxic species (e.g., ²³⁷Np). These advantages, however, are only realized if these elements are eliminated by transmutation in fast-spectrum reactors or accelerator-driven systems (OECD, 2002). These species, therefore, must be stored in retrievable storage until the technology can be developed to convert them to fission products and useful energy.

6.6 Economics of Increasing Repository Capacity

The cost of a geologic repository includes the cost of licensing; waste emplacement including tunneling, packaging, drip shields, *etc.*; ventilation; monitoring; and closure/decommissioning. A large percentage of the YM Project Total System Life Cycle Cost (TSLCC) relates to expenditures incurred for transportation, waste packaging, and drip shields. Given that transportation costs are not expected to decrease under any of the scenarios considered Table 6-I), the primary cost savings anticipated for the sending reduced-mass and/or reduced-heat-load waste product to YM will be in the waste packaging and drip shields, and if the latter prove unneeded, then savings in waste packaging should represent the area of largest cost reduction.

The solutions suggested in this study to increase the repository capacity by nominally 10-fold, however, require separate (but perhaps co-located) facilities including a reprocessing plant with waste encapsulation capacity (vitrification plus separate waste streams for uranium, for cesium and strontium, for activated cladding and structural material, and for volatile fission-product wastes); temporary retrievable storage for actinides and for cesium/strontium; and a fast-

spectrum waste-transmutation system for consuming the actinides. The actinides, including the recovered reactor-exposed uranium, project a future economic value that reflects potential energy content, although the present market value for these materials may be near zero or indeed negative until either waste transmutation and/or breeding electrical-generation technologies are developed and deployed. It is unlikely that the cost of the added reprocessing plant (much less the waste transmutation capability) can be justified by the savings anticipated by a more efficiently deployed and operated Yucca Mountain repository alone, where Yucca Mountain is defined as a repository for *70,000 tonneSNF*. Given that the TSLCC of this *70,000 tonneSNF* YM is nominally *60 B\$*, a 10-fold increase in repository capacity translates into the “creation” of a $\sim 9 \times 60 = 540 \text{ B\$}$ “asset” that is available for allocation towards the above-described technologies required to achieve this 10-fold increase in the ability to deal with an equivalent increase in SNF handling capability. Given that roughly half of this “asset” must be expended for activities that are independent of the repository “front-end” or pre-processing activities, in actuality perhaps only $\sim 300 \text{ B\$}$ would be available to apply towards processes that lead to the 10-fold increase in repository capacity. How this translates into a *per-kg* cost for such repository front-end processes (*e.g.*, reprocessing, component storage, transmutation, *etc.*) is addressed below.

At the present US capacity of $\sim 100 \text{ GWe}$ and an SNF generation rate of $\sim 30 \text{ tonneSNF/GWe/yr}$, the lifetime of the YM repository would be increased by $\sim 210 \text{ years}$. Given that a $\sim 300 \text{ B\$}$ “budget” is available to apply to the $9 \times 70,000 \text{ tonneSNF}$ avoided being sent for direct disposal, the aggregated unit cost of all processes required to achieve this 10-fold increase amounts to $430 \text{ \$/kgSNF}$, which in addition to reprocessing costs includes all storage and disposition cost of the new waste streams created, as well as the cost of transmutation technologies not covered by revenues attendant the generation of net-electricity. In addition to ignoring any scheduling and related present-valuing procedures, this simple analysis ignores the increases in effective SNF generation if utilities switch to Extended-LWR and then to MOX-fueled-LWR fuel cycles that generate thermally “hotter” waste. Lastly, the value of the fissile actinides recovered in principle should be added to the above “asset” to push the economic-breakeven aggregated unit cost available to pay for reprocessing/storage/new disposal (if plutonium is valued the same as fissile uranium in LEU derived from $30 \text{ \$/kgU}$ natural uranium, a unit cost of fissile plutonium of $\sim 3,000 \text{ \$/kgPu}$ results, which translates into total value in the repository-avoided SNF of $\sim 180 \text{ B\$}$, but this plutonium must fuel transmuters that produce electricity at $\sim 10\text{-}30\%$ increased energy cost (OECD, 2002; Krakowski, 2002), depending on the technology employed and the extent to which that technology impacts the commercial generation capacity (*e.g.*, support ratio of client-to-customer electricity generation). Generally, these “top-level” results are within a factor of 2-3 of economic “break-even” compared to unit costs for reprocessing, and further, more detailed investigations using more detailed cost models for the repository, reprocessing, and vitrification seem warranted.

Other simplified approaches to assessing the relative cost of repository direct disposal (DD) of SNF compared to some form of SNF “pre-conditioning” along the lines suggested by some of the Scenarios listed in Table 6-I can be envisaged. To that end, the following simple comparison based more on steady-state, equilibrium arguments was developed.

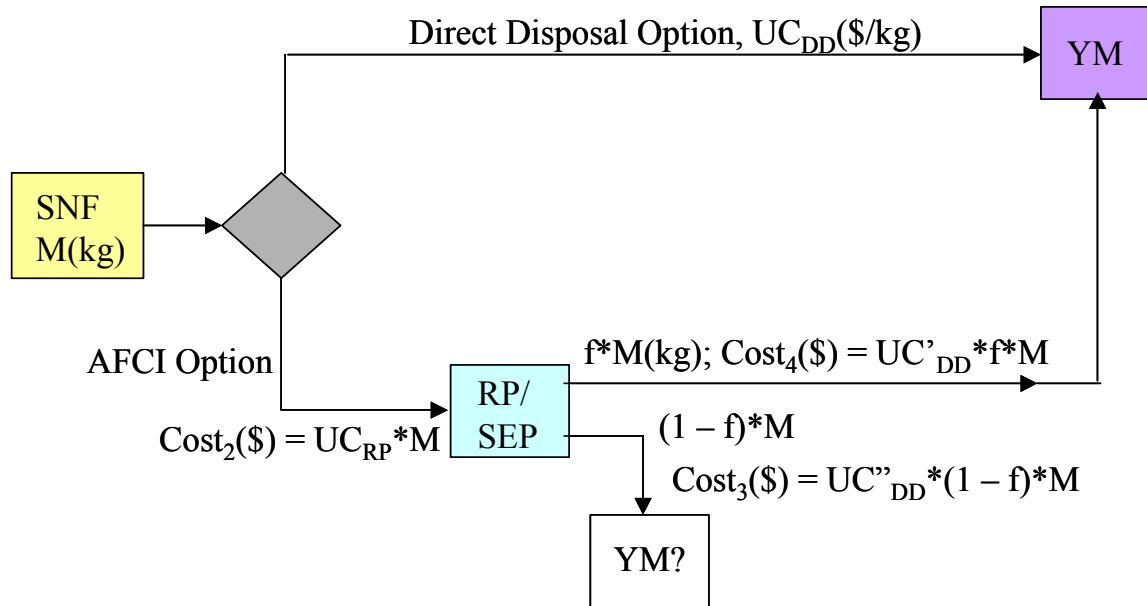


Figure 6-4. Comparison of a SNF direct-disposal (DD) option to a reprocessing-based SNF “pre-conditioning” option, showing key cost components expressed in terms of unit costs, $UC_i(\$/kg)$.

This model considers two options for dealing with a mass $M(kgSNF)$ of spent fuel; a) a direct-disposal option that costs $UC_{DD}(\$/kgSNF)$; and b) advanced fuel cycle initiative that reprocesses (RP) or separates (SEP) key SNF components (not specified, but along the lines and options reflected in Table 6-1) at a unit cost of $UC_{RP}(\$/kgSNF)$, while sending a (small) fraction f to the repository at a unit cost of $UC'_{DD}(\$/kgS)$ and dispositioning (other storage, transmutation, *etc.*) the remaining fraction, $1 - f$, at a cost of $UC''_{DD}(\$/kgNF)$, where the splits are not specified but $kgS + kgNF = kgSNF$.

If CR is defined as the cost of the APCI option relative to the DD option, it is easily shown, based on the mass flows depicted in Figure 6-4, that:

$$CR = \frac{UC_{RP}}{UC_{DD}} + (1 - f) \frac{UC''_{DD}}{UC_{DD}} + f \frac{UC'_{DD}}{UC_{DD}}. \quad (6-1)$$

Taking the first ratio of unit costs to be $UC_{RP}/UC_{DD} \sim 2-3$, $f \sim 0.1$, the second ratio of unit costs to be $(1 - f) * UC''_{DD}/UC_{DD} \sim 0.1$, and the last term to be $f UC'_{DD}/UC_{DD} \sim 1$, the cost ratio of the APCI option to that of the DD option is in the range $CR \sim 3-4$. Exception to such a high cost multiplier (CR) can be made when the total cost rather than just the YMP savings is considered; the ratio UC_{RP}/UC_{DD} may be too high and a number of benefits not reflected in this simple model can be identified for the APCI option, like increased (uranium) resource utilization, increased energy security, and other difficult-to-quantify attributes *etc.* In any case, the shortfall of CR in the range 2-4 accounting for missed benefits is not unlike that suggested by the “top-level” assessment made above using arguments based on the YM capacity ratio and the release of

“assets” to implement the technologies necessary to achieve the desired YM capacity ratios indicated in Fig. 6-3.

6.7 Conclusions

The capacity of a spent nuclear fuel geologic repository (*e.g.*, Yucca Mountain) can be increased 10-27-fold for Standard-LWR fuel by removing high-heat-release radionuclides, including the actinides plus cesium and strontium. The lower value (10-fold increase) is determined from mass-loading limitations of the VHLW waste package, which could be redesigned to approach the higher value (27-fold increase). The 10-fold increase in repository capacity would defer the need for a second repository for ~200 years at the present US nuclear energy generation rate, but less for a growth scenario. The cost of these alternative processing routes is uncertain, but the “assets” released through this 10-fold increase in repository capacity could be allocated to implement the technologies required to achieve the 10-fold increase at a unit cost of ~430 \$/kgSNF, or greater if an energy credit is attached to the contained fissile material. This rough estimate of economic “breakeven” remains a factor of 2-3 from current reprocessing estimates of unit processing costs, and this factor is not unlike the 2-4 range suggested by the equilibrium, steady-state model (Figure 6-4). Although these factors are significant, nonetheless further, more detailed mass-flow, repository-response; reactor/NFC-neutronics, and costing investigations are warranted.

7 SUMMARY AND FUTURE DIRECTIONS

This section summarizes FY02 developments, suggests an NFC modeling integration that incorporates those developments, and, based on the analysis/assessment “toolbox” that results, outlines directions for future work. The focus of this future work will be the time-dependent analysis of the set of condensed scenarios depicted in Figs. 2-4 and 2-5. The recent emergence of Generation-IV reactor concepts and the associated crosscutting NFC technologies (USDOE, 2002b) establishes a second future goal of the FY03 NFC Systems Analysis task. For the integration and common comparison to these newer, futuristic ideas, the steady-state (equilibrium) DELTA model will be adopted and implemented, and analyses similar to those leading to the scenario condensation depicted in Figs. 2-4 and 2-5 (Krakowski, 2002) will result for the Generation-IV recommendations, as an aid to roadmapping those ideas.

7.1 Model Integration

This fiscal year saw the development and application of a range of nuclear fuel cycle (NFC) models based on arrangement of approaches: a) the DELTA model for scoping analyses of a range of steady-state (equilibrium) scenarios [Sec. 2, (Krakowski, 2002)]; b) the FCOPT optimization model that searches for NFC technology combinations that minimize either cost or proliferation risk over the 100-year time horizon in the US using exogenous demand assumptions (Sec. 3); c) the NFCSim detailed simulation model applied over a variable (~100-year) time frame in the US; d) a top-level scoping model of the impacts on the carrying capacity of a Yucca Mountain (YM) like repository of varying the waste forms being emplaced through the application of a range of separations or reprocessing technologies, as well as related scaled-cost implications of better use of costs sunk into that project. These four modeling activities vary in detail of development and application, but all have been supported by a substantial and valuable neutronics effort in the form of the code Monteburns (Trellue, 1998; Poston, 1999), which performs system-dependent burn-up calculations. Neutronics calculations primarily focused on developing one two-tiered scenarios to burn all actinides from legacy SNF, that resulted in the optimal use of LWRs burning plutonium as MOX fuel with three recycles and two license extensions over the course of 48 years and about thirty 840-MWt ADS to burn the remaining material over 60 years of operation. Neutronics calculations also provided a basis for a range of core concepts development that in turn was picked up by the aforementioned NFC modeling activities. One proposal under consideration is to use part of the output (*e.g.*, collapsed cross-section sets) from Monteburns to run ORIGEN2.1 within the NFCSim simulation model to give a capability of real-time depletion and decay calculations. Combined with a means to project actual nuclear-energy demand that might describe a future in which this technology competes with other electrical-generation and liquid-fuel technologies [*e.g.*, MARKAL (Fishbone, 1982)] leads to an integrated NFC modeling capability of the kind suggested in Fig. 7-1.

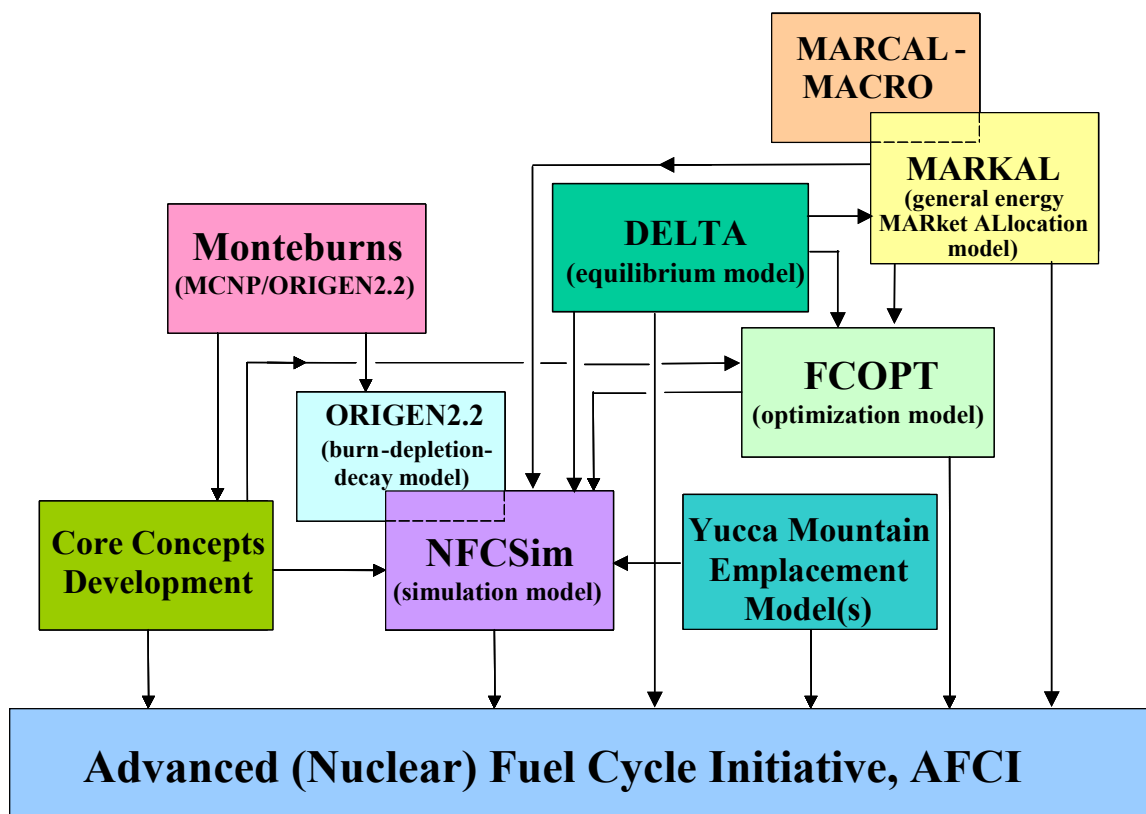


Figure 7-1. An integrated modeling approach for nuclear fuel cycle assessments.

The integrated view summarized on Figure 7-1 is a goal that has been approached through the largely developmental efforts of FY02, as elaborated in the previous sections of this report. Scenarios suggested by the DELTA model have been condensed into an array of options (Sec. 2.2) that are being subjected to time-dependent simulation by the recently completed NFCSim model (Sec. 4). The latter will be benchmarked with a comparable model of the French nuclear economy, COSI (Grouiller, 1991), once a comparison case is settled. The FCOPT optimization model (Sec. 3) requires further exploration before its main role as the “optimization eyes” for NFCSim is fulfilled; this goal will be achieved once a second benchmarking is made between the NFCSim simulation and the FCOPT optimization models, which is expected to be accomplished within the first few months of FY03. Only very preliminary, scaled indications have so far been reported by the Yucca Mountain Emplacement model (Sec. 6), which requires considerable quantitative development, that in turn will benefit from ongoing work just now initiated through a joint effort headed by Sandia National Laboratory (Baker, 2002). Lastly, while preparatory work has been initiated in FY02 in acquiring the needed MARKAL-MACRO software and a recent version of the MARKAL-US model, implementation of a realistic NFC into that model remains an important FY03 activity before the context-broadening connections reflected in Figure 7-1 can be completed. As is indicated on this integrating view, the NFCSim simulation model rests at the centrum of this modeling effort, with the FCOPT, MARKAL, neutronics, and Yucca Mountain Emplacement models playing important support and extension roles.

Generally, while the majority of FY02 was devoted to individual model development, the FY03 effort will focus on completing the integration suggested in Figure 7-1 and the early focusing onto specific questions and issues raised in conjunction with the Advanced Fuel Cycle Initiative (USDOE, 2002a) and the implementation of both near-term (Baker, 2002) and farther-term (Generation IV, 2002) elements of that initiative. To achieve this significant goal, the future directions for each of the key modeling activities comprising the integrated view given on Figure 7-1 must be completed, as is indicated in the following subsection.

7.2 Future Directions

The general process of integrating the various elements of this NFC assessment has been indicated above. Given in the following subsections are summaries of technical activities in each of the modeling elements needed to achieve the level of integration described in Sec. 7.1. In addition to the specific model-related activities described in the following subsections, a number of activities that apply to two or more of the modeling activities are identified, including:

- Provide costing and integrating (including neutronics) systems analyses of GEN-IV concepts, and systems support for related NFC facility designs, to establish a quantitative basis for comparison, road-mapping, and eventual down-section;
- Using the suite of models available, do a final evaluation of the ADS approach, as applied to the the most promising scenario wherein advanced plutonium-burning LWRs or HTGRs fulfill a low-to-moderate nuclear-energy growth, and the ADS functions primarily as minor-actinide burner (e.g., the ADSC scenario in Figure 2-1, or the upper future vision depicted in Fig. 2-4);
- Elaborate on non-proliferation metrics set for multi-criteria NFC analyses for eventual applications to NFCSim and FCOPT. Initiate definition of (nuclear) safeguards requirements for reprocessing, separations and fuel fabrication facilities for eventual applications to NFCSim and FCOPT and conceptual design of AFCI demonstration facilities;
- Initiate a range of advanced modeling tools/methods, including the development and application of Multi-Criterion Decision Analysis (MCDA) tools/methodology to aid in NFC down-selection process, as well as the development of technology demonstration performance requirements. Initiate model uncertainty methodology development and predictive model enhancement capabilities. Also, develop and apply methods whereby the impacts of Exogenous Technological Learning (ETL) and coupling with R&D resource allocation can be assessed, with particular application to the NFC optimization modeling activities.

7.2.1 DELTA Equilibrium Model

The DELTA model has fulfilled the original aim of providing “top-level” metrics for economic, proliferation-risk, waste-mitigation, and resource-utilization performances for a wide range of NFC operated under conditions of steady-state mass and energy balances. For that portion of ongoing work that focuses on an assessment of a condensed set of NFC scenarios under realistic time-dependent conditions, further advances of the DELTA model other than enhancing the steady-state mass and energy balances used, under possibly improved neutronic and costing data bases, is not warranted at this time. However, for the remaining part of the Systems Analysis task focused on the longer-term objectives espoused by the half-dozen concepts being suggested by the Generation IV activity (USDOE, 2002b), the DELTA model is ideally suited to integrate and assess these ideas into a self-consistent, albeit steady-state, cost-based comparative framework. For some of the Generation IV concepts, supporting neutronics computations will be needed to provide the DELTA model with needed mass-flow and composition input data.

7.2.2 FCOPT Optimization Model

The FCOPT model described in Sec. 3 is a good start in the direction of NFC optimizations, but a number of necessary improvements, advancements, and clarifications need to be addressed; these set the agenda for future work in advancing FCOPT as a tool to guide the simulation studies to be made by NFCSim, and includes:

- Improve the technical fidelity of the fairly simple description of the reactor technologies presently included in FCOPT, particularly as related to the neutronics database and detail of each generation technology;
- Incorporate more precise mass-balance constraints at the elemental, if not isotopic, level, while assuring that the fuel-consuming technologies cannot expand beyond the level of resource available without incurring appropriate penalties associated with the use of so-called “backstop” resources.
- Include non-linear (economy-of-scale, EOS) scalings in the cost estimating relationships (CERs) used to estimate annual charges, and eventually the present value of total costs used in the cost-based objective function, OBJ_{COST} ; inclusion of resource depletion costing for uranium heads the top of the list for improvements in this area, which is followed closely by capacity scaling of both generation, reprocessing, and disposal technologies.
- Develop costing algorithms that respond to the under-utilization of certain capital stocks (e.g., reprocessing plants that in earlier periods may have provided larger output) with appropriate cost penalties.
- Develop and implement a realistic, but simplified (e.g., primarily LWR-based technologies) benchmark between FCOPT and NFCSim. As part of this benchmarking/comparison activity, the use of a “simpler” model that tracks only LWRs

and ADSs might be useful to explore, whether the same optimized scenarios result, and to determine in more detail the conditions under which to implement an ADS, particularly with respect to the impacts of overall nuclear-energy demand and waste-control constraints.

7.2.3 NFCSim Simulation Model

The detailed NFC simulation serves as a focus of the AFCI Systems Analysis effort at Los Alamos, and the FY03 program will continue the development of this model as well as its early use to address key AFCI issues. Key elements of this task includes:

- Integrate/normalize NFCSim and FCOPT models using a relatively simple, LWR-based NFC scenario.
- Benchmark NFCSim with the CEAs COSI simulation model, once a benchmark case is identified that covers both the NFCSim model scope (US nuclear economy) and the COSI model scope (French nuclear economy).
- Benchmark NFCSim model with other NFC models currently being developed, such as the OECD dynamic simulation NFC model presently under development (Bertel, 2002) and/or the MIT model (Golay, 2002).
- Incorporate into NFCSim and apply a Yucca Mountain “Business” model based on the work proposed in Sec. 7.2.5.
- Incorporate into NFCSim and apply a proliferation model based on the extensive body of past work to evaluate the NFC *versus* NFF approaches.
- Develop a capability to analyze in a complete NFC context the most promising reactor concepts produced by the Generation IV roadmapping efforts.
- Extensively analyze one or more NFCs scenarios within timeframes and using technologies that are more representative of likely paths forward over the next 100 years.

7.2.4 MARKAL General-Energy Optimization Model

The primary aim of the use of MARKAL and MARKAL-MACRO is to generate insights into the role and effectiveness of key elements of the AFCI program in determining the market competitiveness of nuclear energy in the context of a general energy market that includes both electricity generation and liquid fuels. To this end, a NFC model comparable to that presently implemented in FCOPT, but not as detailed as that tracked by the NFCSim model, will be formulated and installed in MARKAL. The general market conditions under which the exogenous demands for nuclear energy used in both the FCOPT and NFCSim models will then be elucidated.

7.2.5 Yucca Mountain Emplacement Model

Like the neutronics task, the development of a Yucca Mountain Emplacement model is crucial to the credibility of any of the AFCI Systems Analysis tasks that form the integrated approach depicted in Figure 7-1. The present state-of-the-art in thermal/hydrological modeling is still not able to establish a sufficient basis for specifying the thermal requirements for the repository design (Bechtel, 2002). Therefore, the scaling of the (reduced) thermal load for reprocessed waste compared to direct-disposal SNF will continue to be used to evaluate a potential increase in repository capacity, using the Yucca Mountain Viability Assessment (USDOE, 1988) thermal loading as a “strawman” for comparison with different fuel types and reprocessing schemes. To that end, the start along these lines based on a spreadsheet model of heat-load scaling will be expanded to include:

- Investigate analytic or numerical means to connect more quantitatively to detailed time-dependent, three-dimensional finite-element thermal calculations of the Yucca Mountain repository: a) to quantify better the impacts SNF disposal when subjected to various reprocessing schemes (Table 6-I),; b) to make direct comparison with similar thermal calculations for direct disposal of SNF, and c) to establish a firmer basis for the semi-quantitative calculations described in Sec. 6.
- Expand the database of burn-up compositions of all US-generated SNF for the NFCSim simulation model to include repository heat load for existing SNF subject to different reprocessing schemes;
- Couple MonteBurns/ORIGEN2.2 neutronics calculations of SNF decay heat with NFCSim for tabulating repository heat loads for alternative fuels and reactors, including those used for waste transmutation;
- Include numerically the effects of incomplete separations on the decay heat generated in components extracted from reprocessed SNF;
- Investigate temporary retrievable storage options for the additional product streams recovered during SNF reprocessing operations, particularly plutonium and minor actinides destined for transmutation, and cesium and strontium that could be used to maintain “SNF standard” (NAS, 1994) in fuel forms for transmutation (Sec. 5.2.2) or alternately maintained in engineered storage before eventual repository emplacement.

7.2.6 Neutronics Support and Core Concepts Development

Activities under the neutronics task will continue in the dual role indicated on Figure 7-1: direct support of all systems analyses tasks, with an emphasis placed on the NFCSim model; and the development of advance core concepts needed to advance further the aims of AFCI. To these ends, the following directions will be pursued in FY03:

- Couple MonteBurns-calibrated real-time (ORIGEN2.2) neutronics calculations with NFCSim.
- Conclude the compilation of the database of burn-up compositions of all US SNF for NFCSim.
- Facilitate all neutronics aspects of high burn-up, high-recycle LWRs, and/or other new reactor designs, as applied in scenarios that emphasize advanced Tier-1 technologies 1 and/or Generation-IV technologies.
- Analyze the results of the Tier-1 neutronic calculations to determine what the actual benefit to the repository would be (*i.e.*, heat load, volume reduction, *etc.*) if Tier-2 were not implemented. The ingestion radiotoxicity would not be decreased significantly, but other aspects of repository performance may be positively impacted.
- Examine feasibility of increasing nonproliferation protection for MOX fuel by adding neptunium, all minor actinides, and/or yet-to-be-determined levels of ^{90}Sr and ^{137}Cs content to maintain “SNF standard” in fuel forms being proposed by various separations/reprocessing schemes.

This page is intentionally left blank.

REFERENCES

- BAETSLE, L.H., and Ch. De Raedt (1997), "Limitations of Actinide Recycle and Fuel Cycle Consequences: A Global Analysis; Part 2: Recycle of Actinides in Thermal Reactors: Impact of High Burn Up LWR-UO₂ Fuel Irradiation and Multiple Recycle of LWR-MOX Fuel on the Radiotoxic Inventory," Nuclear Engineering and Design **168**, 203-210. (1997).
- BAKER, A. (2002), private communication, Yucca Mountain Project Modeling Meeting, Sandia National Laboratory, Albuquerque, NM (September 30, 2002)
- BARBRAULT, P.; J. Vergnes, G. Manent, A. Harislur, M.Delpech, (1996) "Fuel Management Systems with Plutonium and U235 Enriched Uranium MOX Assemblies: Multirecycling Plutonium on Depleted or Enriched Uranium Support," Electricite de France report number EDF-96-NB-00153; DE97632829 (1996).
- BECHTEL (2002), "White Paper: Thermal Operating Modes", Bechtel SAIC Company LLC, February 2002. Prepared under DOE Contract DE-AC08-01RW12101. Unofficial copy located at <http://www.ypm.gov/documents/thermal/index.htm>
- BERNNAT, W., M. Soldevila, S. Cathalau, G. Schlosser, E. Sartori, K. Hesketh, and D. Lutz (1995), "PWR Benchmarks from OECD Working Party on Physics of Plutonium Recycle," Proc. Int. Conf. on Evaluation of Emerging Nuclear Fuel Cycle Systems, GLOBAL'95, **I**, 627 Versailles, France, (September 11–14, 1995).
- BERTEL, E. (2002), private communication, Organization for Economic Cooperation and Development (July 2002).
- BISHOP, J. M., (1998) **Java Gently**, Addison Wesley Longman Limited, Harlow, England (1998).
- BOWMAN, C. (1998) "Once-Through Thermal-Spectrum Accelerator-Driven System for LWR Waste Destruction without Reprocessing: Tier-1 Description," ADNA Corporation report ADNA/98-04 (1998).
- BRIESMEISTER, J. F. (ed), (1997), "MCNP – A General Monte Carlo N-particle Transport Code – Version 4B," Los Alamos National Laboratory, LA-12625-M Version 4B (1997). (also known as RSICC code number C00701).
- BROGLI, R. and R. A. Krakowski (2001), "Proliferation and the Civilian Nuclear Fuel Cycle: Towards a Simplified Recipe to Measure Proliferation Risk," Paul Scherrer Institute document PSI Bericht Nr. 01-10 (August 2001).
- BROOKE, A., D. Kendrick, A. Meeraus, and R. Raman (1998) "GAMS: A User's Guide," GAMS Development Corporation, 1217 Potomac Street, NW, Washington, DC 20007, USA (December 1998).

CARLSSON, J (1998), "Nuclear Waste Management in Sweden", Radwaste Magazine, **5**, 25 (1998).

CHARLTON, W. S., R. .F. LeBouf, and C. Beard, "Proliferation Resistance Assessment Methodology for Accelerator Transmutation of Waste," personal communication, University of Texas at Austin (July 2002).

CARTER, J, "Nuclear Non-Proliferation," Presidential Decision Directive 8 (March 24, 1977).

CROFF, A. G. (1980) "A User's Manual for ORIGEN2 Computer Code," ORNL/TM-7175, Oak Ridge National Laboratory (July 1980). (Also known as RSICC code number C00371).

CROFF, A.G. (1994), "A Concept for Increasing the Effective Capacity of a Unit Area of a Geologic Repository", Radioactive Waste Management and Environmental Restoration, **18**, 155-180 (1994).

DOZOL, J.F. et al (1997), "New Calix[4]arene Crown for the Selective Extraction of Caesium", International Conference on Future Nuclear Systems, Global'97, Vol. 2, pp. 1517 (1997).

EDMONDS, J. (1985) and J. M. Reilly, **Global Energy: Assessing the Future**, Oxford University Press, New York, NY (1985).

ENDFB-6 (2002), "Index of /ukrndc/doc/databases/ENDFB-6",
<http://kinr.kiev.ua/ukrndc/doc/databases/ENDFB-6/>.

EXTEND (2002), "Extend: Professional Simulation Tools," Imagine That Inc., San Jose, CA (2002) (<http://www.imagethatinc.com>).

FLANAGAN, D. (1997), **Java in a Nutshell, Second Edition**, O'Reilly & Associates, Inc., Sebastopol, CA (1997).

FISHBONE L. G. (1981) and H. Abilock, " MARKAL, A Linear-Programming Model for Energy Systems Analysis: Technical Description of the BNL Version," Energy Research 5, 353-375 (1981) [for more recent versions and application, please refer to the Energy Technology Systems Analysis Program at www.ecn.nl/unit_bs/etsap/].

FORSBERG, C.W. (2000), "Rethinking High-Level Waste Disposal: Separate Disposal of High-Heat Radionuclides (^{90}Sr and ^{137}Cs). Nuclear Technology, Volume 131, pps. 252-268, (2000).

GOLAY, M (2002), private communication, Massachusetts Institute of Technology (September 2002).

GROUILLER, J.-P., G. Flamenbaum, B. Sicard, M. Mus, J. Martin, J. G. Devezeaux de Lavergne, and O. Comellini, "COSI, A Simulation Software for a Pool of Reactors and Fuel Cycle Plants: Application to the Study of the Deployment of Fast Breeder Reactors," International

Conference on Fast Reactor Systems and Fuel Cycles, October 27-November 1, 1991, Kyoto, Japan (1991).

HERMANN, O. W. *et al.*, (1995) "Validation of the SCALE System for PWR Spent Fuel Isotopic Composition Analyses," Oak Ridge National Laboratory report ORNL/TM-12667 (March 1995).

HERMANN, O.W. (2000), "Benchmark of SCALE (SAS2H) Isotopic Predictions of Depletion Analyses for San Onofre PWR MOX Fuel," Oak Ridge National Laboratory report ORNL/TM-1999/326 (February 2000).

HIRSHCHBERG, S., G. Spiekerman, R. Dones, (1998) "Severe Accidents in the Energy Sector," Paul Scherrer Institut report PSI 98-16 (November 1998).

HORWITZ, E.P. *et al.* (1991), "SREX: A New Process for the Extraction and Recovery of Strontium from Acidic Nuclear Waste Streams", Solvent Extr. Ion Exch., vol. 9, pp. 1-25 (1991).

IAEA (1999), International Atomic Energy Agency, "The Physical Protection of Nuclear Material and Nuclear Facilities," International Atomic Energy Agency document INFCIRC/225/Rev. 4 (June 1999).

ICRP (1979), "Age-dependent Doses to Members of the Public from Intake of Radionuclides: Part 5 Compilation of Ingestion and Inhalation Dose Coefficients," International Commission on Radiation Protection Publication 72, Annals of the ICRP, **26**(1), Pergamon Press, Oxford UK (1979).

ICRP (1991), "1990 Recommendations of the International Commission on Radiological Protection," ICRP Publication 60, Annals of the International Commission on Radiation Protection, **21**, (1-3), Pergamon Press, Oxford, UK (1991).

ICRP (1996), "The ICRP Database of Dose Coefficients: Workers and Members of the Public," Task Force on Dose Calculations of Committee 2 of the International Commission on Radiological Protection, ISBN 0 08 042 7510 (1996).

KAWAI, K., A. Endo, and N. Hiroshi. (2002), "Dose coefficients for Radionuclides Produced in High Energy Proton Accelerator Facilities: Coefficients for Radionuclides not Listed in ICRP Publications," Japan Atomic Energy Research Institute report Data/Code 2002-013 (May 2002).

ILOG (1999), "CPLEX 6.5 User's Manual," ILOG, France (March 1999).

JACKSON, R. R. (1977), "Hanford Waste Encapsulation: Strontium and Cesium", Nuclear Technology, **32**, 10-15, (1977).

KRAKOWSKI, R. A. (1998), "Description of ERB (Edmonds, Reilly, Barns) Global E (Energy, Economics, Environment) Model," Los Alamos National Laboratory document LA-UR-98-1364 (April 1, 1998).

KRAKOWSKI, R. A. (1999a), "Los Alamos Contribution to the IAEA Overall Comparative Assessment of Different Energy Systems and Their Potential Role in Long-Term Sustainable Energy Mixes," Los Alamos National Laboratory document LA-UR-99-627 (February 3, 1999).

KRAKOWSKI, R. A. (1999b), "A. Multi-Attribute Approach to Generating Proliferation Risk Metrics," Los Alamos National Laboratory document LA-UR-96-3602 (Rev.) (March 25, 1999).

KRAKOWSKI, R. (2001), "Review of Approaches for Quantitative Assessment of the Risks of and Resistance to Nuclear Proliferation from the Civilian Nuclear Fuel Cycle Los Alamos," National Laboratory document LA-UR-01-169 (January 12, 2001).

KRAKOWSKI, R. A. and C. G. Bathke (2002), "Method for Quantitative Assessment of Cost and Proliferation Risks Associated with the Civilian Nuclear Fuel Cycle as Applied to the Advanced Accelerator Applications (AAA) Program," Los Alamos National Laboratory document LA-UR-02-2369 (April 26, 2002).

KYPREOS, S. (1996), "The MARKAL-MACRO Model and the Climate Change," Paul Scherrer Institute document PSI Bericht Nr. 96-14 (July 1996).

MacFARLANE, R.E. and D.W. Muir, (1994). "The NJOY Nuclear Data Processing System Version 91," Los Alamos National Laboratory report LA-12740-M (October 1994).

MANNE, A. S. and C.-O. Wene 1992), "MARKAL-MACRO: A Linked Model for Energy-Economy Analysis," Brookhaven National Laboratory document BNL-47161 (February 1992).

NAS (1994), **Management and Disposition of Excess Weapons Plutonium**, Report of the National Academy of Sciences (NAS), Committee on International Security and Arms Control (CISAC), W. K. H. Panofsky (Chair) (1994).

NRC (1991), "Annual Limits on Intake (ALIs) and Derived Air Concentrations (DACs) of Radionuclides for Occupational Exposure; Effluent Concentrations; Concentrations for Release to Sewage," Code of Federal Regulations, 10 CFR 20, Appendix B, Washington DC (May 21, 1991).

OECD (1995), Organization for Economic Co-operation and Development / Nuclear Energy Agency, OECD/NEA report "Physics of Plutonium Recycling," **2** and **3**, (1995).

OECD (2002), "Accelerator-driven Systems (ADS) and Fast Reactors (FR) in Advanced Nuclear Fuel Cycles: A Comparative Study," Organization for Economic Co-operation and Development / Nuclear Energy Agency report (2002).

ORNL (1999), "ORIGEN2.1, Isotope Generation and Depletion Code Matrix Exponential Method," Oak Ridge National Laboratory, Radiation Safety Information Computational Center (RSICC) Computer Code Collection report CCC-371 (May 1999).

PANKRATOV, D. V. *et al.* (1999), "Radiological Properties of Heavy Liquid Metal Targets of Accelerator-Driven Systems," Materials Research Society Symposium Proceedings, **556**, 1215–1221 (1999).

PAPAZAGLOU, A., E. P. Gyftopoulos, M. M. Miller, N. C. Rasmussen, and A. Raiffa, (1978) "A Methodology for the Assessment of the Proliferation Resistance of Nuclear Power Systems," Massachusetts Institute of Technology report MIT-El 78-02/022 (September 1978).

PAVELESCU, M. and I. Ursu (1982), "A Decision Problem Under Uncertainty for Nuclear Power System Development," Energy Research, **6**, 47 (1982).

POSTON, D. I. and H.R. Trellue, (1999) "User's Manual, Version 2.0, for MONTEBURNS, Version 1.0," LA-UR-99-4999, Los Alamos National Laboratory (September 1999). Also known as RSICC code number P00455.

SALVATORES, M., and P. Finck (2002), personal communication, Argonne National Laboratory (Cadarache, France; July 2002).

SCHULZ W.W. and E. P. Horwitz, (1988). "The TRUEX Process and the Management of Liquid TRU Waste", Separation Science and Technology, **23**, 1191-1210 (1988).

STANKOVSKY, A., *et al.*, (2001), "Accumulation and Transmutation of Spallation Products in the Target of Accelerator-Driven System," Journal of Nuclear Science and Technology, **38**(7), 503–510 (July 2001).

TRELLUE, H.R. (1998), "Development of Monteburns: A Code That Links MCNP and ORIGEN2 in an Automated Fashion for Burnup Calculations," Los Alamos National Laboratory report LA-13514-T (December 1998).

TRELLUE, H. R. and J.W. Davidson (2001), "Feasibility of Using Light Water Reactors to Transmute SNF," Los Alamos National Laboratory document LA-UR-01-5692 (October 2001).

TRELLUE, H.R. (2002), "The Answer Is No: Does Transmutation of Spent Nuclear Fuel Produce More Hazardous Material Than It Destroys?", *Radwaste Solutions*, American Nuclear Society, Chicago, Illinois, , pp. 40-43, (July/August 2002).

TRW-ESS (1999), "Design Feature Evaluation #26: Higher Thermal Loading", TRW Environmental Safety Systems Inc. (April 1999). (prepared under DOE Contract DE-AC08-91RW00134; unofficial copy located at http://www.ymp.gov/documents/rpa451m3_u/index.htm).

TURNER, J. E (1992), **Atoms, Radiation, and Radiation Protection**, p. 282, McGraw-Hill Publishing Company, New York, NY (1992).

URSU, I., M. Pavelescu, and M. Tutarici (1986), "A Deterministic Approach in the Optimization of a Nuclear Power System from Fuel Resource Point of View," Energy Research, **10**, 11 (1986).

URSU, I., M. Pavelescu, and G. Mociornita (1990), “Conditioned Minimization of Fuel Feed Rate for a CANDU-600 MWe Reactor,” *Energy Research*, **14**, 275 (1990).

USDOE (1998), “Viability Assessment of a Repository at Yucca Mountain”, U.S. Department of Energy report DOE/RW-0508 (December 1998).

USDOE (1999), “Manual for Control and Accountability of Nuclear Materials,” United States Department of Energy document DOE M 474.1-1 (August 11, 1999).

USDOE (2002a), “Report to Congress on the Advanced Accelerator Applications Program”, U.S. Department of Energy, Office of Nuclear Energy, Science, and Technology (in preparation, September 1, 2002).

USDOE (2002b), “A Technology Roadmap for Generation IV Nuclear Energy Systems: Technical Roadmap Report,” Nuclear Energy Research Advisory Committee report (August 2002).

USDOE (2002c), “Yucca Mountain Science and Engineering Report: Technical Information Supporting Site Recommendation Consideration”, Revision 1, DOE/RW-0539-1. (February 2002.) Unofficial copy located at http://www.ymp.gov/documents/ser_b/index.htm

USDOE (2002d) “Annual Spent Fuel Discharges and Burnup, 1968-1998” revised February 25, 2002. Located at http://www.eiadee.gov/cnearf/nuclear/spent_fuel/table2.html

USNWTRB (1999), “Moving Beyond Yucca Mountain: A Report to the U.S. Congress and the Secretary of Energy,” U.S. Nuclear Waste Technical Review Board (April 1999).

VAN TUYLE, G. J. (2001), “Candidate Approaches for an Integrated Nuclear Waste Management Strategy – Scoping Evaluation,” Los Alamos National Laboratory document LA-UR-01-5572 (November 2001).

VENNERI, F., A. Baxter, *et al.* (2001), “Deep-Burn Transmutation - A Practical Approach to the Destruction of Nuclear Waste in the Context of Nuclear Power Sustainability,” DOE Report FDO-E00-N-TRT-X-000132 (December 19, 2001).

WATERS, L. S. (ed.) (1999), “MCNPXTM User’s Manual, Version 2.1.5,” Los Alamos National Laboratory document LA-UR 99-6058 (November 15, 1999).

WHC (1990), “CURE: Clean Use of Reactor Energy”, Westinghouse Hanford Company, Document WHC-EP-0268. Prepared under DOE contract DE-AC-87RL10930 (May 1990).

WIESE, H.W. (1993), “Investigation of the Nuclear Inventories of High-Exposure PWR Mixed-Oxide Fuels with Multiple Recycling of Self-Generated Plutonium,” *Nuclear Technology*, **102**, 68-80 (April 1993).

WILSON, W. B. *et al.* (1998), "Recent Development of the CINDER'90 Transmutation Code and Data Library for Actinide Transmutation Studies," Proc. Int. Conf. on Evaluation of Emerging Nuclear Fuel Cycle Systems, GLOBAL'95, Versailles, France, September 11–14, 1995, p. 848 (1995).

BARON, R, M., D. Barns, H. M. Pitcher, J. A. Edmonds, M. A. Wise, (1992) "The Second Generation Model of Greenhouse Gas Emissions: Background and Initial Development," Coping with the Energy Future: Market and Regulations, **2**, 15th Annual Conference of the International Associations for Energy Economics on Coping with the Energy Future: Market and Regulations (18-20 May 1992).

YANG, W.S., and Khalil, H.S. (2000), "Reduction of Burnup Reactivity Loss in Accelerator Driven Transmutation Systems," Proceedings of the Fourth International Topical Meeting on Nuclear Applications of Accelerator Technology, Washington D.C., pp. 75-80, (November 12-15, 2000).

YOUINOU, G. (1999a) *et al.*, "Heterogeneous Assembly for Plutonium Multirecycling in PWRs: The Corail Concept," Proceedings International Conference on Future Nuclear Systems: GLOBAL '99, Jackson Hole, Wyoming (August 1999).

YOUINOU, G., M. Delpech, J.L. Guillet, A. Puill, and S. Aniel. (1999b), "Plutonium Management and Multirecycling in LWRs Using the Enriched Uranium Support," Proceedings International Conference on Future Nuclear Systems: GLOBAL '99, Jackson Hole, Wyoming (August 1999).

This page is intentionally left blank.

NOMENCLATURE^(a)

AAA	Advanced Accelerator Applications (Program)
AC _{xx} (M\$/yr)	Annual Charges for account xx (ACC, ROP, FF, PR, <i>etc.</i>)
ACC	Accelerator
ACT	Actinide
ADS	Accelerator Driven System
ADS0	Accelerator Driven System with no Tier-1 LWR
ADS1	Accelerator Driven System with one Tier-1 LWR MOX re-cycle
ADS2	Accelerator Driven System with two Tier-1 LWR MOX re-cycles
ADSC	Accelerator Driven System with CORAIL Tier-1, no Tier-0 LWR
AFCI	Advanced Fuel Cycle Initiative (USDOE, 2002a)
AL	Attractiveness Level (USDOE, 1999)
<AL>	System averaged AL
AL(m,p)	Attractiveness Level associated with a given material m in process p
ALI	Annual Limitation Intake
ALWR	Advanced LWR
AP	Actinide Product
ATW	Accelerator Transmutation of (nuclear) Waste
AUX	auxiliary power systems
a(m,p)	Matrix coefficient in LP constraint for material m and process p in FCOPT model
adsma	MA-burning ADS
adstr	TRU-burning ADS
<BU>(MWtd/kgIHM)	Average burn-up in (MOX or NNF/IMF) mixed LWR cores
B	Burn-up fraction, also BU _f , also Billions
BAU	Business As Usual (scenario)
BL	Blending of weapons-released HEU to make LEU
BLK	Blanket (FBR, FR, or ADS)
BR	FBR breeding ratio
BU(MWd/kgIHM)	Fissile fuel burn-up
BU _f	<i>per</i> -pass burn-up fraction
b(t)	Constraint variable in LP constraint for material m and process p in FCOPT model
CANDU	CANadian Deuterium Uranium reactor
CAT-I,III,III	Category of protection (IAEA, 1999; USDOE, 1999)
CDB(i)Cost Data Base	(i = lo, nm, hi, ch)
CEA	Commissariat Energie Atomique
CER	Cost Estimating Relationship
CFR	Coded Federal Regulations
COE(mill/kWeh)	Cost of Electricity
<COE>(mill/kWeh)	System-wide Cost of Electricity
CPU	Central Processing Unit
CR	FR conversion ratio
CS	Cooling Storage of spent nuclear fuel
CV, CV'	Conversion of U ₂ O ₃ to UF ₆ , or the reverse

DA	Decision Analysis
D&D	Decommissioning and Decontamination
DD	Direct Disposal (repository)
DR(1/yr)	Discount Rate
DU	Depleted Uranium
DUS	Depleted Uranium Storage
dpy(d/yr)	days <i>per</i> year
$E_F(\text{MeV/fission})$	fission energy yield
E^3	Energy-Economic-Environmental (models)
EF	Feed fraction of ^{235}U to ER
ELC	electricity- generating option for ADS
EOL	End-of-Life
EOS	Economy Of Scale
EPE	Electric Plant Equipment account
ER	Uranium isotopic enrichment
ERB	Edmonds-Reilly-Barns E^3 model (Baron, 1992)
ET	Tailings fraction
ETL	Endogenous Technological Learning
expospu	plutonium “exposure” or vulnerability at time t (kg yr);
exposual	AL-weighted plutonium exposure or vulnerability at time t (kg yr);
FBR	Fast Breeder Reactor
FCOPT	Fuel Cycle OPTimization model for NFC analyses
FCR(1/yr)	Fixed Charge Rate
$\text{FCR}^*(1/\text{yr})$	Modified Fixed Charge Rate, $\text{FCR}^*(1 + f_{\text{DD}}) + f_{\text{OM}}$
FE	Fuel Element
F	Fresh (fuel)
FF	Fuel Fabrication of enriched uranium fuel, or fresh fuel
FFSTR	Storage of Fabricated Fuel
FM	Fissile Material
FP	Fission Products
FPS	Fission Products Storage
FR	Fast (spectrum) Reactor
FR0	Tier-2 Fast (spectrum) Reactor with no Tier-1 LWR
FR2	Tier-2 Fast (spectrum) Reactor with two-recycle Tier-1 LWR
FSB	Fast-Spectrum Burner (FR, IFR, ADS, ATW)
FY0x	Fiscal Year 200x
f_{Lj}	Process (material) loss fraction for material j
f	Final condition, state
f_{ACC}	Re-circulating power fraction for accelerator
f_{AUX}	Re-circulation power to auxiliary (non-acceleratory) systems
f_{B}	Fraction of beam energy captured in (fission) thermal cycle
f_{brmet}	FBR using metal fuel (IFR)
f_{CAP}	Fraction of total capacity provided by technology nrx
f_{DD}	Fractional increase in FCR to accommodate D&D escrowing
f_{GEN}	Fraction of total generation provide by technology nrx
f_{GEN2}	Fraction of total generation supplied by tier-two technology

$f_{L,j}$	per-pass loss fraction (for species j)
f_M	COE disadvantage factor for lower-fidelity electrical power
f_{Minf}	f_M asymptote
f_{M1}	f_M value for $\rho = 1$
f_{MOX}	MOX core fraction
$f_{OM}(1/yr)$	Annual O&M charge as fraction of capital costs
freq	Specific theft/diversion frequency to accumulate a plutonium SQ
GAMS	General Arithmetic Modeling System (Brooke, 1998)
GCR	Gas-Cooled Reactor
GDP(\$/yr)	Gross Domestic Product
GHG	GreenHouse Gas
gen(nrx)	Annual electric generation (MW _{yr}) of technology nrx
HEU	Highly Enriched Uranium
HEUS	Highly Enriched Uranium Storage
HLW	High Level Waste
HLWSTR	Storage of HLW
HN	Heavy Nuclide
HM	Heavy Metal (U, Pu)
HTGR	High-Temperature Gas-cooled Reactor
HTOM	High Thermal Load Operating Mode
hg	high-growth nuclear energy scenario
hr	high recycle
hpy(h/y)	Hours <i>per</i> year
IAEA	International Atomic Energy Agency
IAM	Integrated Assessment Model
IHM(kg)	Initial heavy metal (in fresh fuel loading)
IMF	Inert Matrix Fuel
LCC	Life-Cycle Cost
$I_F(kg)$	fissile inventory in blanket
ID	Identification
IFR	Integral Fast Reactor
IHM	Initial Heavy Metal (U,Pu)
IHX	Intermediate Heat Exchanger
INFCE	International Nuclear Fuel-Cycle Evaluation
IS	Interim Storage of spent nuclear fuel
IAEA	International Atomic Energy Agency
i	Designates initial or input condition
JAERI	Japan Atomic Energy Research Institute
k_{eff}	Reactor core reactivity
L&LR	Land and Land Rights account
LANL	Los Alamos National Laboratory
LBE	Lead-Bismuth Eutectic
LCA	Life Cycle Assessment/Analysis
LCC	Life-Cycle Cost
LDRD	Laboratory Directed Research and Development
LEU	Low Enriched Uranium

LEUF	Fresh LEU
LEUS	Low Enriched Uranium Storage, or spent LEU
LLFP	Long-Lived Fission Products
LLW	Low Level Waste
LP	Linear Programming (model)
LTOM	Low Thermal Load Operating Mode
LWR	Light Water Reactor
lg	low growth nuclear energy scenario
lr	low recycle
lwrmx	MOX recycling LWR
lwrf	NFF/IMF recycling in LWR
lwrot	Once-Through LWR
MA	Minor Actinides (Np, Am, Cm)
MAS	Minor Actinides (Np, Am, Cm) Storage
MACRO	MACROeconomic
MARKAL	MARKet Allocation general energy optimization model
MAUA	Multi-Attribute Utility Analysis
MC(M\$/kgTRU)	Marginal Cost
MCA	Multi-Criteria Analysis
MCD	Multi-Criteria Decision Analysis
MCNP	Monte Carlo Neutron Photon transport code (MCNP, 1997)
MET	Metal (fuel)
MIT	Massachusetts Institute of Technology
MH	Material Handling (FF + PR)
MHRS	Main Heat Rejection System account
MM	Mining and Milling (of uranium fuel)
MOX, MX	Mixed (plutonium/uranium) Oxide fuel
MOXF	Fresh MOX fuel
MOXS	Spent MOX fuel
MPD(MWt/kg)	blanket Mass Power Density
MPE	Miscellaneous Plant Equipment account
MR(kg/yr)	Mass Rate at (nsc, nsc, npr)
MRS	Monitored Retrievable Storage of spent nuclear fuel
MTHM	Metric Tonnes Heavy Metal
MTIHM	Metric Tonnes Initial Heavy Metal
MVA	Material Vulnerability Analyses (for a proliferation metric)
m	Material index for FCOPT (Table 3-1, material entries generally not listed in this Nomenclature)
NASAP	Non-proliferation Alternative Systems Assessment Program
NEA	Nuclear Energy Agency (of the OECD)
NCYCLE -1	Number of plutonium recycles in thermal-spectrum technology
NF	Non-Fertile material
NF0	Non-Fertile fueled LWR with no recycle
NFC	Nuclear Fuel Cycle
NFCSim	NFC simulation model
NFF	Non-Fertile Fuel

NLP	Non-Linear Programming (model)
NPP	Nuclear Power Plant
NRC	Nuclear Regulatory Commission
NU	Natural Uranium
NUF	Fresh NU fuel.
NUS	Spent NU Fuel or NU storage
NW	Nuclear Weapon
NWA	Nuclear Weapons Aspiration level of Proliferation Agent.
nm	Nominal CDB
npr	NFC process index
nrx	Reactor technology index (RX + FF + CS + PR)
nsc	Scenario index
nucl	Reactor technology index, set used in FCOPT, same as nrx
OBJ _k (\$, kgPuyr)	Objective function for FCOPT optimization model, where k = COST or PROLiferation.
OECD	Organization for Economic Co-operation and Development
OT	Once-Through (LWR)
o	initial or original
P _{ET} (MWe)	Total electric power
P _E (MWe)	Net electric power
P _F (MW)	fission power
P _{TH} (MWt)	Thermal power
P&T	Partitioning and Transmutation
PE	Primary Energy
POD	Point-Of-Departure case
PR	Processing
PRSTR	Storage of Processed Material
PRA	Probabilistic Risk Analysis DA
PRI	Proliferation Risk Index
PSA	Parametric Systems Analysis
PSI	Paul Scherrer Institute
PUREX	Plutonium/Uranium Extraction
PUS	Separated plutonium storage
PYRO	Pyro-chemical separation
p	Process index for FCOPT (Table 3-2, process entries generally not listed in this Nomenclature)
p _f	Plant or capacity factor
pro	Cost-proliferation connectivity parameter [Eq. (3-4)]
pri	Instantaneous proliferation risk index or average Attractiveness Level, designated also as <AL>;
prii	Integrated proliferation risk index or average Attractiveness Level, also designated as <ALI>;
puinv	Plutonium inventory at time <i>t</i> .
puinval	AL-weighted inventory at time <i>t</i> ;
R/CA	Risk/Consequence Analysis DA
RCOST	Scenario energy cost relative to the base case

R&D	Research and Development
RD&D	Research, Development, and Demonstration
RDB	Repository Data Base
RFOM	Relative Figure-Of-Merit
RLOSS	TRU loss to repository relative to base case
ROP	Rest of Plant (all systems except accelerator and material handling)
RP	Repository (DD), reprocessing
RPE	Reactor Plant Equipment account
RPAL	Proliferation Attractiveness Level relative to the base case
RS	Run Series used in FCOPT parametric evaluations
RTC	Report to Congress (USDOE, 2002a)
RU	Recycled Uranium
RX	Reactor
r, dr(1/yr)	Discount rate
rcoe	Relative COE used in FCOPT
rp	reprocessing or lg scenario with LWR replacement
rpri	Relative PRI used in FCOPT
S	Spent (fuel)
SE	Structural Element
SEP	Separations (reprocessing for FSB technologies)
SFR	Swedish Final Repository
SM	Source Material (containing NW-usable material)
SNF	Spent Nuclear Fuel
SNFSTR	Storage of SNF
SNM	Special Nuclear Material
SQ(kgx)	Significant Quantity (8 kg for x = Pu, 25 kg for x = HEU)
SR	Support Ratio, $\sim 1/f_{\text{GEN2}}$
SREX	Strontium Extraction
SSM	Supply Side Management
SW	Separative Work
SWC(\$)	Separative Work Costs
SWU	Separative Work Unit
Sv	Sievert radiation dose unit
so	hg scenario with “shoot out” between fbr and htgr technologies
SPI	Specific plutonium inventory ($\text{kg}/\text{MW}_{\text{e}}\text{yr}/\text{yr}$);
TCONT(yr)	Plant construction time
THM	Non-electricity-generating (thermal) option for ADS
TLIFE(yr)	Plant (financial) life
TR	Transportation
TRU	Transuranics (Pu + MA)
TSB	Thermal Spectrum Burner
TSLCC(\$)	Total System Life Cycle Cost
$t_j(\text{yr})$	Process or hold-up ($j = \text{h}$) or residence ($j = \text{res}$) or maximum ($j = \text{max}$) times
UC(m,p)(\$/xxx)	Unit cost of material m and/or process p in FCOPT model, where xxx = kg, We, kg/yr, etc.

$UC_{ACC}(\$/Wb)$	Unit cost of accelerator (same as UCACC)
$UC_{FF}(\$/kg)$	Unit cost of fuel fabrication
$UC_{ROP}(\$/We)$	Unit cost of everything but accelerator (same as UC_{TRA})
$UC_{PR}(\$/kg)$	Unit cost of processing
$UC_{RP}(\$/kg)$	Unit cost of repository
$UC_{STR}(\$/kg/yr)$	Unit cost of storage
$UC_{SWU}(\$/SWU)$	Unit cost of separative work unit
$UC_{TR}(\$/kg)$	Unit cost of transportation
$UC_{TRA}(\$/We)$	Unit cost of "transmuter" (<i>e.g.</i> , everything but accelerator)
$UC_{TRU}(M\$/kgTRU)$	Unit cost of TRU destroyed by fission in transmuter system
$UCRPSNF(\$/kgSNF)$	Unit cost of SNF disposal in repository
UK	United Kingdom
UOX	Uranium Dioxide
UREX	Uranium Extraction process
US	United States
USD(\$)	US Dollars
USDOE	United States Department of Energy
UTC(\$/We)	Unit Total (capital) Cost (of electric-generating plant)
UTCACC(\$/Wb)	Unit Total (capital) Cost for accelerator of beam power Wb(watt)
UTCTH(\$/Wt)	Unit Total (capital) Cost (of non-electric-generating plant)
VA	YM Viability Assessment document
VHLW	Vitrified High-Level Waste, Very High-Level Waste
Vol	Volatiles
Wb(watt)	Accelerator beam power
WP	Waste Package
x	Variable
$x(m,p,t)(kg, kg/yr)$	FCOPT vector of material m, process p, time t
xx	Process or NFC component designator (MM, ER, RX, <i>etc.</i>)
x_f	^{235}U mass fraction in ER feed
x_p	^{235}U mass fraction in ER product (UOX)
x_t	^{235}U mass fraction in ER tailings
YM	Yucca Mountain
YMBM	Yucca Mountain Business Model
YMP	Yucca Mountain Project
$y_j^{i,f}$	Initial (i) and final (f) mass fraction of species j = Pu, MA, RU
ypu	Effective plutonium concentration in material <i>m</i> and process <i>p</i>
<hr/>	
$\alpha[MWtyr/kg(\text{fission})]$	Energy <i>per</i> kilogram fissioned
Δk_{eff}	Reactivity change
ε	Re-circulating power fraction
η_A	Accelerator "wall-plug" efficiency
η_{TH}	Thermal-to-electric conversion efficiency
$\Phi(x)$	Enrichment potential, $(2x - 1)\log[x/(1 - x)]$

$\tau_h(\text{yr})$
 ν

Process (npr, p) hold-up time^(a)
Average neutrons released *per* fission

^(a) This nomenclature list does not include most of the material and process notation used in the FCOPT model; please consult Table A-I and Table A-II.

Appendix A: Summary of Material (*m*) and Process (*p*) Definitions Used in the FCOPT Optimization Model

Table A-I. Summary of Materials Followed by the FCOPT Optimization Model.

Set{ <i>m</i> }	Definition
nu	Natural uranium
ru	Reactor-exposed uranium
du	Depleted uranium
lnu	Low-enriched uranium made from nu
lru	Low-enriched uranium made from ru
lwu	Low-enriched uranium made from heu
wpu	Weapons-grade/released plutonium
heu	Highly-enriched uranium released from weapons
rpu	Reactor-grade plutonium
mox	Mixed uranium-plutonium oxide
met	Metal-alloy (<i>e.g.</i> , plutonium-zirconium) fuel
rmet	Reactor-exposed/released met; spent fuel from {rifr,atw}
ru _x	Reactor-exposed/released {lnu,lru,lwu}; spent fuel from rxot
rm _x	Reactor-exposed/released mox; spent fuel from {rxmx,rxfb,rxhg}
bm _x	Mixed uranium-plutonium released from rxfb blanket
fp	Fission products
lfp	Long-lived fission products
ma	Minor actinides (Np, Am,Cm)
rfbr	Spent fuel from rxfb
rhtg	Spent fuel from rxhg

Table A-II. Summary of Processes Described by the FCOPT Optimization Model.

Set {<i>p</i>}	Definition
cv	$\text{U}_3\text{O}_8 \rightarrow \text{UF}_6$ conversion
erdif	^{235}U diffusion enrichment
ercen	^{235}U centrifugal enrichment
eravls	^{235}U laser enrichment
er	^{235}U enrichment {erdif,ercen,eravls}
ffux	Fuel fabrication of UO_2
ffmxrp	Fuel fabrication of mox from reprocessed spent fuel {rux rmx}
ffmxps	Fuel fabrication of mox from plutonium storage, pus
ffmxwp	Fuel fabrication of mox from weapons-released plutonium, wpu
ffmtrp	Fuel fabrication of met from reprocessed material {rux rmx} directly from reprocessing {rpcs, rpis}
ffmtsp	Fuel fabrication of met from reprocessed material derived from sep
ffmtps	Fuel fabrication of met from plutonium storage, pus
ffmtwp	Fuel fabrication of met from weapons-released plutonium (wpu) storage, wps
ffmtms	Fuel fabrication of met from minor actinides (ma) storage, mas
ff	Fuel-fabrication technologies {ffux,ffmxrp,ffmxps,ffmxwp}
ffsux	Low-enriched uranium {lnu, lru, lwu} fresh-fuel storage
ffsmx	Mixed U-Pu oxide (mox) fresh-fuel storage
ffsmt	Metal-fuel (met) fresh-fuel storage
bl	Blending of heu with nu, du, and/or ru
fes	Front-end storage technologies {dus,rus,bks,pus}
rxot	Once-through LWR reactor
rxmx	MOX-burning LWR reactor (full or partial core, as specified by fmox)
rxhg	MOX-burning high-temperature gas-cooled reactor (HTGR)
rxfb	MOX-burning fast-breeder reactor (FBR)
rifr	Integral fast reactor (IFR) critical transmuter/burner
atw	ADS sub-critical, accelerator-driven transmuter/burner
nucl	Full generation technology set {rxot,rxmx,rxhg,rxfb,rifr,atw}
rx	Reactor set {rxot,rxmx,rxhg,rxfb}
rlwr	LWR reactor set {rxot,rxmx}
fsb	Transmuter/burner set {rifr,atw}
fbbk	FBR (rxfb) breeding blanket
cs	Cooling storage (reactor-side) for either rux or rmx from all user/producer reactors
isu	Interim storage of spent UOX fuel (rux)
isp	Interim storage of spent MOX fuel (rmx)
is	Interim storage of spent UOX or MOX fuel {isu,isp}
dus	Depleted uranium storage
bks	FBR blanket MOX (bmx) storage
pus	Separated-plutonium (rpu) storage
mas	Separated minor-actinide (ma) storage

Table A-II. Summary of Processes Described by the FCOPT Optimization Model (continued).

Set {p}	Definition
sfs	Spent-fuel storage (cooling + interim) for fsb = {rifr,atw} and rxfb
fps	Separated fission-product storage (aggregated for all producers)
wps	Weapons-released plutonium (wpu) storage
wus	Weapons-released uranium (heu) storage
rpcs	Reprocessing with feed from cooling storage (cs), applies to rx technologies
rpis	Reprocessing with feed from interim storage (is), applies to rx technologies
rp	Reprocessing {rpcs,rpis,rpbks}
sepcs	Separation with feed from cooling storage (cs), applies to fsb technologies
sepis	Separation with feed from interim storage (is), applies to fsb technologies
sep	Separations {sepcs,sepis}
rpbks	Reprocessing with feed from rxfb blanket storage (bks)
ddcs	Direct (repository) disposal of spent fuel from cooling storage (cs)
ddis	Direct (repository) disposal of spent fuel from interim storage (is)
dd	Direct (repository) disposal of spent fuel {ddcs,ddis}
pudrp	Direct (repository) disposal of separated plutonium from reprocessing (rp)
pudpus	Direct (repository) disposal of separated plutonium from separated-plutonium storage (pus)
pud	Direct (repository) disposal of separated plutonium {pudrp,pudpus}
fpdfps	Separated fission-product disposal from reprocessing (rp)
fpdfsb	Separated fission-product disposal from fast-spectrum burners (fsb)
fpd	Separated fission-product disposal {fpdfps,fpdfsb}
mad	Separated minor-actinide disposal (actually, sent to fpd)
rep	All repository technologies: {ddcs, ddis, pudrp,pudpus,fpdfp,refpd,sefpd,fpd,fpdfps,fpdfsb}
fpdifr	Separated fission-product discharge from rifr (note: INACTIVE)
fpdatw	Separated fission-product discharge from atw (note: INACTIVE)
refpd	Separated fission-product disposal from rp (note: INACTIVE)
refps	Storage of fp material (including ma) from rp (note: INACTIVE)
sefpd	Separated fission-product disposal from sep (note: INACTIVE)
sefps	storage of fp material from sep (note: INACTIVE)
bes	Back-end disposal technologies { dd,pud,fpd}

This page is intentionally left blank.

Appendix B: Key Input Parameters Used in Evaluating the FCOPT Optimization Model

Table B-I. Key Input Parameters Used in Evaluating the FCOPT Optimization Model.

PARAMETER DEFINITION	Symbol	Unit	Value
CAPACITIES/LIMITS/BOUNDS			
Number of core loads in interim storage	bnisrx(nucl)	----	
o Once-through LWR (rxot)	bnisrx(rxot)	----	10
o MOX-fueled LWR (rxmx)	bnisrx(rxmx)	----	10
o MOX-fueled HTGR (rxhg)	bnisrx(rxhg)	----	10
o MOX-fueled FBR (rxfb)	bnisrx(rxfb)	----	10
o Metal-fueled IFR-based transmuter (rifr)	bnisrx(rifr)	----	10
o Metal-fueled ADS-based transmuter (atw)	bnisrx(atw)	----	10
Final repository capacity	ddcapf	kg(SNFeq)	7.0E(+07)
Reprocessing deployment-rate limit	rpratelim		2
Reprocessing capacity limit			
o Initial capacity	rpcapi	kg/yr	0
o Final capacity	rpcapf	kg/yr	1.0E(+08)
o Initial time	trpi	----	11
o Final time	trpf	----	21
o Exponent	exprp	----	1
Separated-plutonium storage capacity limit	bnpus	kg(Pu)	1.0E(+06)
Separated minor-actinide storage capacity limit	bnmas	kg(Pu)	1.0E(+06)
Unit Costs			
Mined and milled natural uranium	ucmm	\$/kg(NU)	30
Relative process cost for ru versus nu	frusnu	----	2
Conversion unit cost	uccv	\$/kgU	5
Enrichment unit cost	ucer	\$/kgSWU	90
Nominal transportation cost	uctr	\$/kg(HM)	50
Fuel Fabrication			
o Uranium oxide	ucffux	\$/kg(UOX)	250
o Uranium-plutonium mixed oxide	ucffmx	\$/kg(MOX)	3000
o Uranium-plutonium-zirconium metal	ucffmt	\$/kg(HM)	3000
Fresh-fuel annual storage cost			
o Uranium oxide	ucffsux	\$/kg(HM)/yr	100
o Mixed Pu-U oxide	ucffsmx	\$/kg(HM)/yr	100
o Metallic fuel	ucffmt	\$/kg(HM)/yr	100
Storage			
o Depleted uranium	ucdus	\$/kg(HM)/yr	10
o Blanket (rxfb)	ucbks	\$/kg(HM)/yr	60
o Cooling storage	uccs	\$/kg(HM)/yr	60
o Interim storage for rux	ucisu	\$/kg(HM)/yr	60
o Interim storage for rmx	ucisp	\$/kg(HM)/yr	60
o Reactor uranium storage	ucrus	\$/kg(HM)/yr	15
o Separated-plutonium storage	ucpus	\$/kg(HM)/yr	300
o Separated minor-actinide storage	ucmas	\$/kg(HM)/yr	300
o Separated fission-product storage	ucfps	\$/kg(FPP)/yr	100
o Weapons-released HEU	ucwus	\$/kg(HM)/yr	500
o Weapons-released plutonium	ucwps	\$/kg(HM)/yr	500
HEU blending unit cost	ucbl	\$/kg(U)	100

Table B-I. Key Input Parameters Used in Evaluating the FCOPT Optimization Model (continued).

PARAMETER DEFINITION	Symbol	Unit	Value
CAPACITIES/LIMITS/BOUNDS			
Installed unit total capital costs for generation	uct(nucl)		
o Once-through LWR (rxot)	utc(rxot)	\$/We	1.7
o MOX-fueled LWR (rxmx)	utc(rxmx)	\$/We	1.7
o MOX-fueled HTGR (rxhg)	utc(rxhg)	\$/We	2.3
o MOX-fueled FBR (rxfb)	utc(rxfb)	\$/We	2.6
o Metal-fueled IFR-based transmuter (rifr)	utc(rifr)	\$/We	2.6
o Metal-fueled ADS-based transmuter (atw)	utc(atw)	\$/We	3.0
Reprocessing and Separations			
o Reprocessing of UOX (rux)	ucrpx	\$/kg(HM)	1500
o Reprocessing of MOX (rmx)	ucrpmx	\$/kg(HM)	1500
o Reprocessing of FBR blanket materials (bm)	ucrbmx	\$/kg(HM)	1500
o Reprocessing of FSB materials (separations)	ucsep	\$/kg(HM)	4000
Repository Disposal			
o Repository SNF direct disposal	ucddf	\$/kg(SNF)	500
o Repository separated-plutonium direct disposal	ucpud	\$/kg(HM)	500
o Repository minor-actinide direct disposal	ucmad	\$/kg(HM)	500
o Repository fission-product direct disposal	ucfpd	\$/kg(FPP)	500
Generation Growth Constraints			
$dcap(nucl,t) < cap(nucl,t-1)*fgrow(nucl,t) + fseed(nucl)*gent(t)$			
$fgrow(nucl,t) = fgrowrx(nucl)*fgrowmx(t); fgriwnx = eps(t)$			
fgrowrx(nucl)			
o Once-through LWR (rxot)			2
o MOX-fueled LWR (rxmx)			2
o MOX-fueled HTGR (rxhg)			2
o MOX-fueled FBR (rxfb)			2
o Metal-fueled IFR-based transmuter (rifr)			2
o Metal-fueled ADS-based transmuter (atw)			2
fseed(nucl)			----
o Once-through LWR (rxot)			0.01
o MOX-fueled LWR (rxmx)			0.01
o MOX-fueled HTGR (rxhg)			0.01
o MOX-fueled FBR (rxfb)			0.01
o Metal-fueled IFR-based transmuter (rifr)			0.01
o Metal-fueled ADS-based transmuter (atw)			0.01
Proliferation Metric			
Object function	prolif		0
Multi-criteria unit cost	pro	\$/kg(AI)/yr	0
Top-Level Results			
Cost of electricity	coe	mill/kWeh	46.11
Fraction once-through LWR generation	fGEN(rxot)	---	0.8791
Proliferation metric	pri	kgPu/yr	4.85E+10
PC total cost	pvtot	\$	8.83E+11
Cost/proliferation metric	pvtot/pri	\$/kgPu/yr	18.2043

Appendix C: Description of Cost- and Proliferation-Based Objective Functions

C.1 Cost-Based Objective Function

The cost-based objective function, $OBJ_{COST}(\$)$, is the sum of the discounted annual charges incurred in the course of operating each of the key NFC process $\{p\}$ over the time frame of the optimization (typically, for the period 2000 \rightarrow 2100). This sum over key costing accounts evaluated at a given time t is comprised of 18 contributions ranging over the entire fuel cycle depicted in Figure 3-1. Listed below are the component annual charges that are then discounted to the reference year (2000) using a discount rate of r in the discounting term $pdr(t) = 1/(1 + r)^t$; Table A-I and Table A-II (Appendix A) should be consulted for material and process identifications, Table B-I (Appendix B) gives definitions for key unit costs, and the Nomenclature describes remaining variables:

Mining and Milling (mm):

$$ucmm(t)*x(nu,bl,t) + ucmm(t)*x(nu,cv,t) + ucmm(t)*x(nu,ffmxrp,t) \\ + ucmm(t)*x(nu,ffmxps,t) + ucmm(t)*x(nu,ffmxwp,t)$$

Conversion (cv):

$$+ uccv*x(nu,cv,t) + fruvsn*uccv*x(ru,cv,t)$$

Enrichment (er):

$$+ ucs*sof*nu*x(nu,er,t) + fruvsn*ucs*sof*ru*x(ru,er,t)$$

Front-End Storage (fes):

$$+ ucdus*x(du,dus,t) + ucrus*x(ru,rus,t) + ucwus*x(heu,wus,t) \\ + ucwps*x(wpu,wps,t)$$

Blending of (weapons-released) heu (bl):

$$+ fruvsn*ucbl*x(ru,bl,t) + ucbl*x(du,bl,t) + ucbl*x(nu,bl,t) \\ + ucbl*x(heu,bl,t)$$

Fuel Fabrication (ff):

$$+ ucffux*x(lnu,ffux,t) + fruvsn*ucffux*x(lru,ffux,t) + ucffux*x(lwu,ffux,t) \\ + ucffmx*x(nu,ffmxrp,t) + ucffmx*x(ru,ffmxrp,t) + ucffmx*x(du,ffmxrp,t) \\ + ucffmx*x(nu,ffmxps,t) + ucffmx*x(ru,ffmxps,t) + ucffmx*x(du,ffmxps,t) \\ + ucffmx*x(ru,ffmxwp,t) + ucffmx*x(ru,ffmxwp,t) + ucffmx*x(du,ffmxwp,t) \\ + ucffmx*x(rpu,ffmxrp,t) + ucffmx*x(rpu,ffmxps,t) + ucffmx*x(wpu,ffmxwp,t) \\ + ucffmt*x(rpu,ffmtsp,t) + ucffmt*x(rpu,ffmtsp,t) + ucffmt*x(rpu,ffmtsp,t) \\ + ucffmt*x(wpu,ffmtwp,t) + ucffmt*x(ma,ffmtms,t)$$

Fresh-Fuel Storage (ffs):

$$+ ucffsux*x(lnu,ffsux,t) + ucffsux*x(lru,ffsux,t) + ucffsux*x(lwu,ffsux,t) \\ + ucffsmt*x(mox,ffsmt,t) + ucffsmt*x(met,ffsmt,t)$$

Plutonium Tariff (pu)^(a):

$$+ ucpurp * x(rpu, fmxrp, t) + ucpups * x(rpu, fmxps, t) + ucpuwp * x(wpu, fmxwp, t)$$

Capital and O&M Charges for all Reactor Technologies $nucl$ (cap)^(b):

O&M plus capital charges if $fcr > 0$:

$$+ SUM(nucl, (\\ (fcr(nucl) + fom(nucl)) * utc(nucl) * gen(nucl, t) * 1000000 / avail(nucl) / (1 - epsilon(nucl)) \\) \\)$$

IDC plus capital charges if $fcr = 0$:

$$+ SUM(nucl, \$ (fcr(nucl) LE 0), (\\ SUM(tt1 \$ (ORD(tt1) GE ORD(t) AND ((ORD(tt1) LE MIN(CARD(t), ORD(t) + tlife(nucl))))), \\ SUM(tt1 \$ (ORD(tt1) GE ORD(t) AND ((ORD(tt1) LE (ORD(t) + tlife(nucl))))), \\ SUM(tt1 \$ (ORD(tt1) GE ORD(t) AND ((ORD(tt1) LE (CARD(t))))), \\ icost(nucl, t) / (1 + dr) ** (ORD(tt1) - ORD(t)) \\) \\) \\)$$

Unaccounted capital charges for residual generation installed prior to 2000:

$$+ SUM(nucl, (\\ (fcrresid(nucl) + fom(nucl)) * utc(nucl) * resid(nucl, t) * 1000000 / avail(nucl) / (1 - epsilon(nucl)) \\) \\)$$

SNF Cooling Storage (cs):

$$+ uccs * x(rux, cs, t) + uccs * x(rmx, cs, t) + uccs * x(rfbr, cs, t) + uccs * x(rhtg, cs, t)$$

SNF Interim Storage (is):

$$+ ucisu * x(rux, isu, t) + ucisp * x(rmx, isp, t) + ucisp * x(rfbr, isp, t) + ucisp * x(rhtg, isp, t)$$

Irradiated (FBR) Blanket Storage (bks):

$$+ ucbks * x(bmx, bks, t)$$

Separated Plutonium Storage (pus):

$$+ ucpus * x(rpu, pus, t)$$

Minor Actinide Storage (mas):

$$+ ucmas * x(ma, mas, t)$$

Fission Product Storage (fps):

$$+ ucfps * x(fp, fps, t)$$

Reprocessing for $rx = \{rxot, rxmx, rxhg, rxfb\}$ (rp):

$$+ ucrpux*x(rux, rpcs, t) + ucrpux*x(rux, rpis, t) + ucrpmx*x(rmx, rpcs, t) + ucrpmx*x(rmx, rpis, t) \\ + ucrpmx*x(rhtg, rpcs, t) + ucrpmx*x(rhtg, rpis, t) + ucrpmx*x(rfbr, rpcs, t) + \\ ucrpmx*x(rfbr, rpis, t) + ucrpbmx*x(bmx, pbks, t)$$

Separations for $fsb = \{rifr, atw\}$ (sep):

$$+ ucsep*x(rux, sepcs, t) + ucsep*x(rux, sepis, t) + ucsep*x(rmx, epcs, t) + ucsep*x(rmx, sepis, t) \\ + ucsep*x(rhtg, sep, t) + ucsep*x(rfbr, sep, t) + ucsep*x(rmet, sep, t)$$

Repository Disposal (dd):

$$+ ucdd*x(rux, dd, t) + ucdd*x(rmx, dd, t) + ucput*x(rpu, pud, t) + ucdd*x(rhtg, dd, t) \\ + ucdd*x(rfbr, dd, t) + ucfpd*x(fp, dd, t) + ucmad*x(ma, dd, t) \\ - ucdd*x(rux, dd, t-1) - ucdd*x(rmx, dd, t-1) - ucput*x(rpu, pud, t-1) - ucdd*x(rhtg, dd, t-1) \\ - ucdd*x(rfbr, dd, t-1) - ucfpd*x(fp, fpd, t-1) - ucmad*x(ma, dd, t-1)$$

^(a)Charges imposed to control the use of “free” plutonium; if need be.

^(b)Annual capital charges incurred for all generation technologies $nucl = \{rxot, rxmx, rxhg, rxhg, rifr, atw\}$; when the fixed charge rate is not used ($fcr = 0$), then the first of these three expressions computes only annual operating and maintenance (O&M) charges as a fraction $fom(1/yr)$ of capital investment. In these expressions the compact nomenclature of GAMS (Brooke, 1998) is retained, where $ORD(t)$ is the ordinal of the element t in the set of all times $\{2000, 2001, \dots, t, \dots, 2100\}$ and $CARD(t)$ is the cardinal (last) value of the set $\{t\}$. The total investment cost, $icost(nucl, t)$, is the capital cost of the capacity increment $dcap(nucl, t)$ of generation technology $nucl$ added at time t , and accounts for all payments discounted to the time of deployment, including interest charges incurred during the construction time $tconst(nucl)$ of a plant with operational lifetime $tlife(nucl)$. The computation of $icost(nucl, t)$ is describe by the following expression, given again in GAMS notation:

$$icost(nucl, t) = dcap(nucl, t) * 1000000 * (utc(nucl) * SUM(l \$(ORD(l) LE tconst(nucl)), \\ (1/tconst(nucl) * ((1 + dr)**ORD(l)))) * (dr * (1 + dr)**tlife(nucl)) / ((1 + dr)**tlife(nucl) - 1) \\)$$

Finally, the total installed capacity for technology $nucl$ at time t is given by:

$$cap(nucl, t) = resid(nucl, t) + \\ SUM(t1 \$((ORD(t1) LE ORD(t)) AND (ORD(t1) GE MAX(ORD(t) - tlife(nucl) + 1, ts))), \\ dcap(nucl, t1))$$

Appendix F gives a further explanation of this capital costing procedure; as for all other terms in this costing objective function, $OBJ_{COST}(\$)$, these are discounted to the reference year (2000) using the discount rate dr and summed over the optimization period (2000,2100).

C.2 Proliferation Risk Objective Function

Numerous studies have been performed regarding how best to estimate quantitatively the proliferation risk of a certain fuel-cycle process, including Expert Delphi Group, Comparative Value Measures, Multi-Attribute Utility Analysis (MAUA), Risk/Consequence or Probabilistic Risk Analysis, and a range of Multi-Criteria Optimization techniques; these have all recently been reviewed (Krakowski, 2001). A highly subjective MAUA method for generating relative proliferation risk indices (*pri*) was applied to the E³ model (Krakowski, 1999a,b) that generates the exogenous demands can be used to drive FCOPT, and this model was coded as a post processor to FCOPT. This proliferation risk model is a hybrid of earlier work in this area (Silvennoinen, 1982; Papazoglou, 1978). Figure C-1 illustrates and partially explains the level of detail and assumption required for the evaluation of an MAUA-based *pri* at each point within the NFC where source material (SM) for a nuclear weapon might reside; details can be found in (Krakowski, 1999b), including the first three levels of sub-utility functions and the respective (highly subjective) weighting functions needed to aggregate the resulting estimate into a single metric. Although this MAUA proliferation model was incorporated into FCOPT as a post-processing operation performed during the cost optimization, resources were insufficient to find a way for the resulting proliferation-risk index to be incorporated linearly into a proliferation-risk objective function. The required development, the strong likelihood of an NLP problem resulting, and the incomplete understanding of FCOPT responses, even for linear problems, led to the adoption of a simpler, heuristic approach to proliferation-risk optimization (minimization) in FCOPT. Nonetheless, future efforts along this MAUA line using the approach illustrated in Figure C-1, or more recent reincarnations (Charlton, 2002) thereof, will be pursued in the future.

One approach to developing a simpler approach to proliferation-risk optimization (minimization) examined (Brogli, 2001) a simplified and transparent “recipe” that might be used by nuclear utilities to classify related source materials [SMs, *e.g.*, fresh (F) and spent (S) nuclear fuels]. Comparisons of the results of these computations are made with spent and fresh fuels based on LEU, mixed (U, Pu) oxide fuel (MOX), and natural uranium [NU, as used in the Canadian deuterium-uranium reactors (CANDUs)]; highly enriched uranium (HEU) as used in some research reactors is also included as part of the comparison ensemble (Brogli, 2001). One approach evolved from this effort, wherein the basic Attractiveness Level (*AL*) metric suggested by the USDOE (1999) was applied in setting protection Categories for various forms of SM. While the quantitative *AL* designations ranged from A through E, as described below, assignments of a numerical ranking and then assigning such a ranking to SM at particular locations in the NFC (Figure 3-1) gives a measure of importance with respect to proliferation potential/propensity/risk/*etc.* The use of *AL* values as weights that reflect the importance of fissile material in a given form at a given node in the NFC is described and applied in FCOPT as a proliferation objective function, *OBJ_{PROL}*, to be minimized. As with the MAUA methodology, only a relative (to a point-of-departure or POD case) proliferation metric results, which nonetheless is useful in assessing tradeoffs with economic or costing parameters, capacity limitations, technology deployment rates, *etc.* (Sec. 3.2.2.5). First, the approach behind these *AL* assignments is summarized below before describing the algebra of its application through FCOPT to the problem at hand. First, however, the concept of Attractiveness Level, as viewed from both USDOE (1999) and IAES (1999) perspectives, is elaborated.

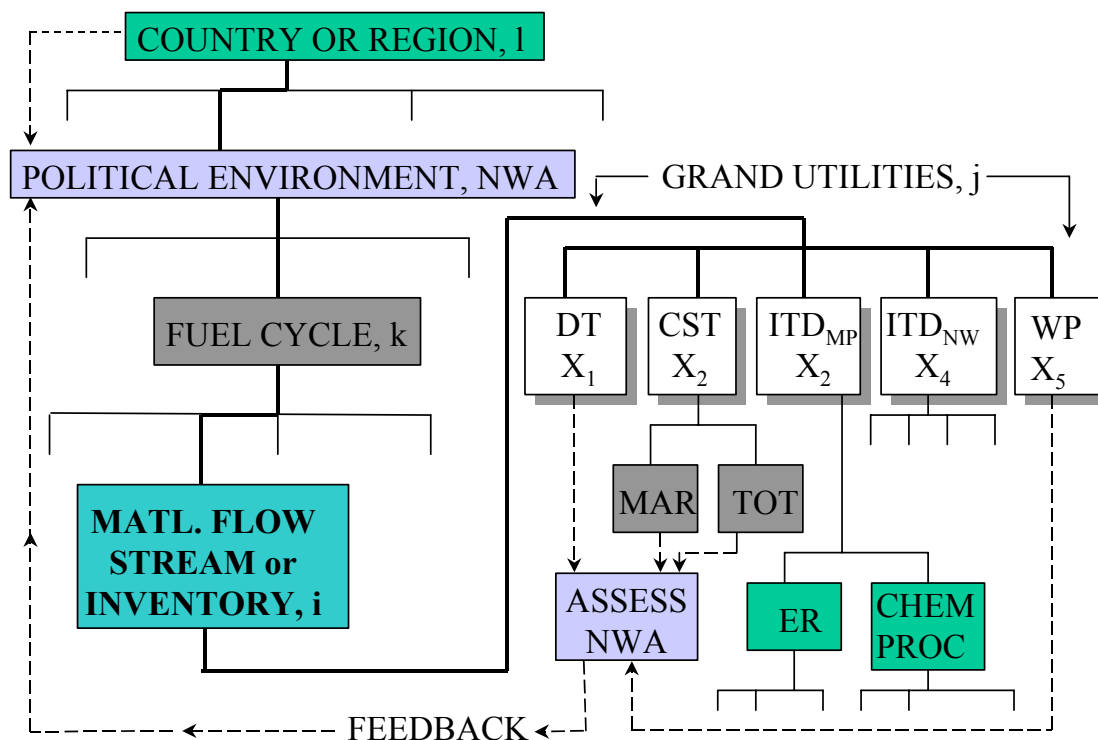


Figure C-1. Schematic logic flow diagram of the application of MAUA at stream i in fuel cycle k in country I having Nuclear Weapons Aspiration Level (demands, need, scope) NWA. Five "grand" utility functions must be evaluated to reflect the value attributed to the proliferator through such attributes as Development Time (DT), Cost (CST), Inherent Technical Difficult related to Material Processing (ITD_{MP}), Inherent Technical Difficult related to Nuclear Weapon fabrication (ITD_{NW}), and discovery or Warning Period (WP).

The International Atomic Energy Agency (IAEA) has also recommended a set of criteria for the level of protection needed to assure fissile materials ^{233}U , ^{235}U , and plutonium isotopes are safe from illicit use through diversion or theft for the construction of nuclear explosive devices (IAEA, 1999). The above-described USDOE guidance represents more elaborated and extended recommendations in the form of quantitative *AL* assignments (A \rightarrow E) and offers a more graded and hopefully useful/usable set of criteria. Both sets of protection categories are based on kind [^{233}U , ^{235}U , and Pu (all isotopes)], concentration (as in the case of ^{235}U), and mass of fissile material. A summary description of the USDOE recommended *AL* values, along with comparable, but less-detailed (graded) groupings suggested by the IAEA, is given in Table C-I.

Each of the *AL* values associated with the USDOE guidelines and the "subclasses" for the comparable IAEA guidelines for a given mass of the respective weapons-usable material has associated with it a protection Category I, II, or III. The highest level of protection requires three barriers and corresponds to Category I. The lowest level of protection, Level III, corresponds to an unfenced, unbarred building. Although not duplicating the IAEA protection guidelines, the USDOE regulations offer a greater category and material gradation. Figure C-2 and Figure C-3

depict graphically the mass-*AL*-category “phase space” for the graded DOE regulations. Side-by-side comparisons with the IAEA guidelines for both ^{235}U and for $^{233}\text{U}/\text{Pu}$ (all isotopes) also are given. Also shown on the figures are estimates of masses of weapons-usable materials for SM derived from fresh (F) and spent (S) fuels going to or taken from a CANDU reactor (NUF and NUS, with NU = natural uranium); an LWR reactor (LEUF and LEUS, with LEU low-enriched uranium); an LWR operated on mixed (U, Pu) oxide fuel (MOXF and MOXS, with MOX = Mixed OXide); and a research reactor (10 MWt) operated on highly enriched uranium (HEUF and HEUS) (Brogli, 2001).

Table C-I. Descriptions of USDOE (1999) and IAEA (1999) Fissile Material Attractiveness Levels Related to the Assignment of Protection Categories (Figures C-1 and C-2).

USDOE ALs or Grades (USDOE, 1999):

- Grade A (weapons): assembled weapons and test devices;
- Grade B (pure products): pits, major components, button ingots, recastable metal, directly convertible materials;
- Grade C (high-grade materials): carbides, oxides, nitrate solutions ($>25\text{ g/l}$), fuel elements and assemblies, alloys and mixtures, UF_4 or UF_6 ($>50\%$ enriched), etc.;
- Grade D (low-grade materials): solutions ($1\text{--}25\text{ g/l}$), process residues requiring extensive reprocessing, moderately irradiated material, ^{238}Pu (except waste), UF_4 or UF_6 ($>20\%$ but $<50\%$ enriched); and
- Grade E (other materials): highly irradiated forms, solutions ($<1\text{ g/l}$), uranium containing $<20\%\ ^{235}\text{U}$ (any form, any quantity).

IAEA INFCIRC/225/Rev. 4 Designations (IAEA, 1999):

- Refers to un-irradiated material; irradiated material moves to the next category;
 - Uranium subclasses:
 - (a): Uranium enriched to $\geq 20\%\ ^{235}\text{U}$;
 - (b): Uranium enriched to $\geq 10\%\ ^{235}\text{U}$, but $< 20\%\ ^{235}\text{U}$;
 - (c): uranium enriched above natural levels (0.711%), but $< 10\%\ ^{235}\text{U}$.
-

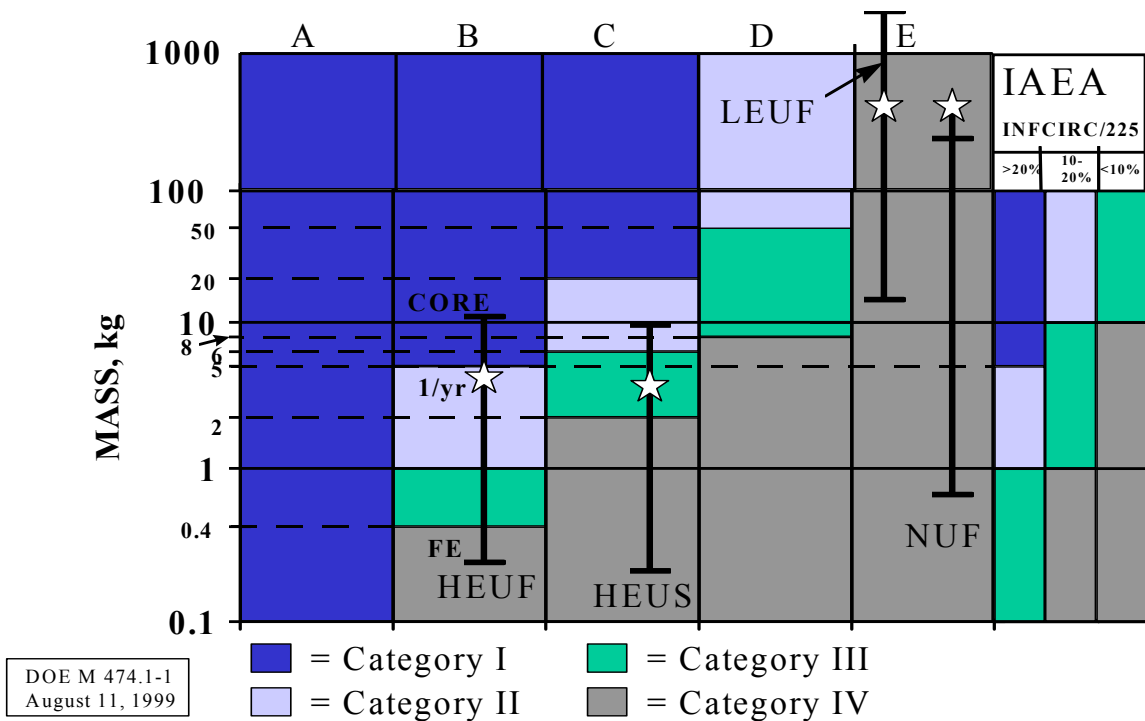


Figure C-2. Comparison of USDOE (1999) regulations and IAEA (1999) guidelines for protection categories versus material mass and DOE-graded Attractiveness Levels (AL) and IAEA subclasses for ^{235}U .

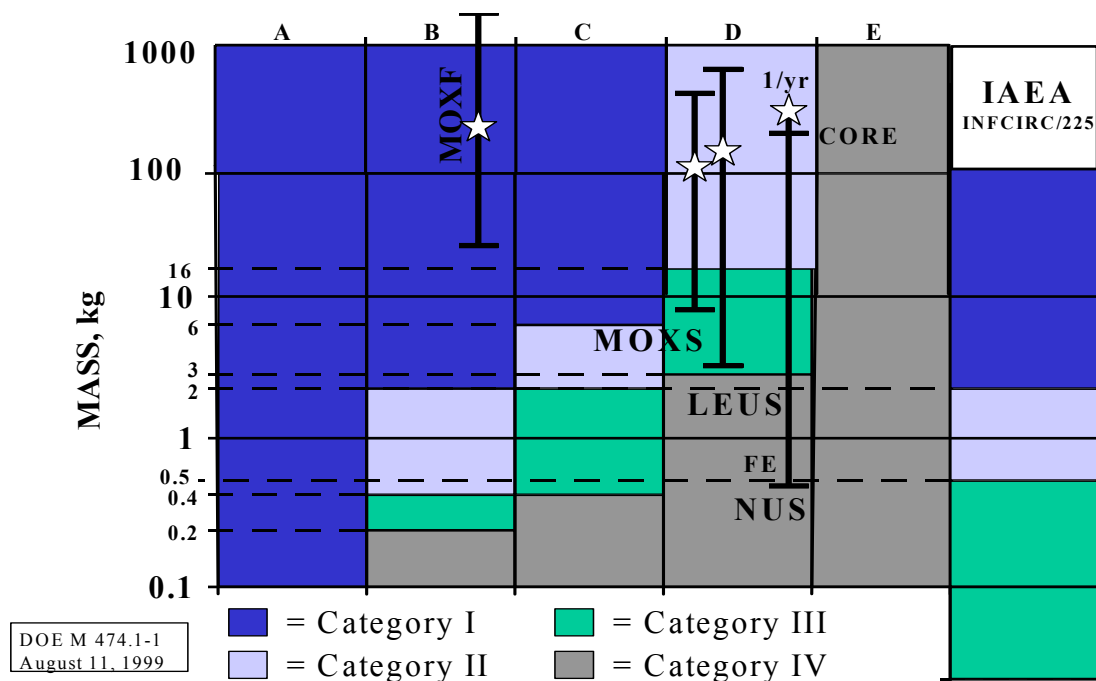


Figure C-3. Comparison of USDOE (1999) regulations and IAEA (1999) guidelines for protection categories versus material mass and DOE-graded Attractiveness Levels (AL) (no IAEA subclasses) for $^{233}\text{U}/\text{Pu}$ (all isotopes).

The CANDU and LWR fuel forms used to generate the ranges depicted on Figure C-2 and Figure C-3 used reactors in the *1000-MWe* class. The length of the vertical line designating each entry is determined by: a) the mass (*kg*) of weapons-usable material *per* fuel element at the bottom; b) the mass (*kg*) of weapons-usable material per core loading at the top; and c) the mass of weapons-usable material transferred out of the respective cores each year (*kg/yr*) and designated by the star-like shape.

Along with the assignment of decadal numerical values to the $A \rightarrow B$ *AL* categories (10,000 \rightarrow 1, respectively), the application of this simple *AL* concept to model proliferation propensity quantitatively in the FCOPT model is made through the use of the following definitions:

$AL(m,p)$:	attractiveness level of the material m in the given process p , as defined in Table C-I (USDOE, 1999) and assigned numerical values above on the scale of $1 \rightarrow 10,000$, as described above;
$tres(m,p)$:	effective time constraints for plutonium-bearing material m in process p , for those process characterized by mass flow through (<i>e.g.</i> , not inventories); in the case where the vector $x(m,p,t)$ describes an inventory, $tres = 1 \text{ yr}$;
$ypu(m,p)$	effective plutonium concentration in material m and process p ;
$puinv$	plutonium inventory at time t .
$x(m,p,t)$	inventory (<i>kg</i>) or flow rate (<i>kg/yr</i>) of material m in process p at time t ;
$puinval$	<i>AL</i> -weighted plutonium inventory at time t ;
$expospu$	plutonium “exposure” or vulnerability at time t (<i>kg yr</i>);
$expospual$	<i>AL</i> -weighted plutonium exposure or vulnerability (<i>kg yr</i>) at time t ;
pri	instantaneous proliferation risk index or average Attractiveness Level, designated also as $\langle AL \rangle$;
$prii$	integrated proliferation risk index or average Attractiveness Level; in some cases is also designated as $\langle ALI \rangle$;
SPI	specific plutonium inventory (<i>kg/MW_{eyr}/yr</i>);
$freq$	specific theft/diversion (no distinction is made at this level of analysis) for one Significant Quantity ($SQ = 8 \text{ kgPu}$) to be stolen/diverted (<i>1/yr/MW_{eyr}/yr</i>); this quantity is similar to the frequency for a major core disruption used to assess this aspect of risk attendant to the large-scale application of commercial nuclear power.

Expressions for each of these definitions, as evaluated by FCOPT, are given below. Plutonium inventory, where mpu and ppu are subsets of the material set m and process set p that contain plutonium in some form, $puinv(t)$:

$$puinv(t) = \sum_{mpu} \sum_{ppu} ypu(mpu, ppu) * tres(ppu) * x(mpu, ppu, t) \quad (C-1)$$

AL -weighted plutonium inventory, $puinval(t)$:

$$puinval(t) = \sum_{mpu} \sum_{ppu} AL(mpu, ppu) * ypu(mpu, ppu) * tres(ppu) * x(mpu, ppu, t) \quad (C-2)$$

Plutonium direct exposure or vulnerability to theft/diversion, $xpospu(t)$:

$$xpospu(t) = \int_0^t puinv(t) dt \quad (C-3)$$

Plutonium AL -weighted exposure or vulnerability to theft/diversion, $xpospual(t)$:

$$xpospual(t) = \int_0^t puinval(t) dt \quad (C-4)$$

Instant average AL Proliferation Risk Index, PRI :

$$pri(t) = \frac{puinval(t)}{puinv(t)} \equiv < AL > (t) \quad (C-5)$$

Integral average AL Proliferation Risk Index, $PRII$:

$$prii(t) = \frac{xpospual(t)}{xpospu(t)} \equiv < ALI > (t) \quad (C-6)$$

Specific (system-wide) Plutonium Inventory, $SPI(kgPu/MW_{yr}/yr)$:

$$spi(t) = \frac{puinv(t)}{gent(t)} \quad (C-7)$$

Allowed diversion frequency needed to accumulate one ‘‘Significant Quantity’’ of plutonium ($SQ = 8 \text{ kgPu}$), $freq(1/yr/MW_{yr}/yr)$:

$$freq(t) = \frac{SQ}{(xpospual(t)/10000) * (gent(t)/1000)} \quad (C-8)$$

In computing these parameters, the Attractiveness Level, $AL(m,p)$, of each material analyzed was (estimated) input, as suggested in Table C-II; other key parameters needed for the evaluation of these parameters are given in Table C-III (effective residence times in process p , which if unity is actually one year or is applied to a storage facility); and Table C-IV (mass fraction of plutonium in material m contained in process p). When used as an objective function in place of discounted total energy costs, the parameter $xpospual(t_{MAX})$ is minimized, where t_{MAX} is the last year of the optimization period (2100). Once computed and a feasible optimum is found and returned by the CPLEX optimizer (ILOG, 1999) that is operated under GAMS (Brook, 1998), the NFC system average $\langle AL \rangle$ given by Eq. (C-5) provides a global Attractiveness Level measured against the "quantified" USDOE scale of (A,E) \Rightarrow (10000,1). When expressed as a specific (e.g., *per GWeyr/yr*), the theft/diversion frequency $freq(t)$ given by Eq. (C-8) is normalized by the upper level of AL ($A = 10,000$).

When applying this AL -based "methodology", not only must the subjectivity of the user in assigning AL values to a particular nuclear-weapons source-material form be recognized, but also differences among the purporting institutions (e.g., USDOE and, less directly, the IAEA) must be appreciated. For the purposes of this study, only shifts in proliferation propensity with changing economic and operational/policy variable (e.g., storage or repository capacities, technology deployment rates, *etc.*) and the (plutonium) AL -weighted exposure/vulnerability at the end of the optimization, $xpospual(tend)$, is monitored relative to values reported for a point-of departure or base case. Along with the cost of electricity, $COE(\text{mill/kWeh})$, derived from the discounted present value of total cost that results when OBJ_{COST} , OBJ_{PROL} , or a combination of OBJ_{COST} and OBJ_{PROL} [e.g., Eq. (3-4)] objective functions are optimized; these relative COE and $xpospual$ values are designated as $rpri$ and $rcoe$, respectively.

Table C-II. Attractiveness Levels (AL) Assigned for Various Material-Process Combinations.

Proc.\Matl.	wpu	rpu	rux	rmx	rfbr	rhtg	bmh	mox	met	rmet
pus	0	1000	0	0	0	0	0	0	0	0
bks	0	1000	0	0	0	0	100	0	0	0
wps	1000	0	0	0	0	0	0	0	0	0
ffmxrp	0	100	0	0	0	0	0	0	0	0
ffmxps	0	100	0	0	0	0	0	0	0	0
ffmxwp	100	0	0	0	0	0	0	0	0	0
ffmtrp	0	0	0	0	0	0	0	0	1000	0
ffmtsp	0	0	0	0	0	0	0	0	1000	0
ffmtps	0	0	0	0	0	0	0	0	1000	0
ffmtwp	0	0	0	0	0	0	0	0	1000	0
ffmtms	0	0	0	0	0	0	0	0	1000	0
cs	0	0	10	10	10	10	0	0	0	0
isu	0	0	10	0	0	0	0	0	0	0
isp	0	0	0	10	10	10	0	0	0	0
rpes	0	0	1000	1000	1000	1000	0	0	0	0
rpis	0	0	1000	1000	1000	1000	0	0	0	0
rpbks	0	0	0	0	0	0	1000	0	0	0
sep	0	0	10	10	10	10	0	0	0	1000
rxot	0	0	100	0	0	0	0	0	0	0
rxmx	0	0	0	0	0	0	0	100	0	0
rxhg	0	0	0	0	0	0	0	100	0	0
rxfb	0	0	0	0	0	0	0	100	0	0
rifr	100	100	100	100	100	100	0	0	100	100

Table C-III. Effective Time Constraints for Plutonium-Bearing Materials in Different Processes Throughout the NFC.

Proc.\Matl.	wpu	rpu	rux	rmx	rfbr	rhtg	bmh	mox	met	rmet
pus	1	1	1	1	1	1	1	1	1	1
bks	1	1	1	1	1	1	1	1	1	1
wps	1	1	1	1	1	1	1	1	1	1
ffmxrp	1	1	1	1	1	1	1	1	1	1
ffmxps	1	1	1	1	1	1	1	1	1	1
ffmxwp	1	1	1	1	1	1	1	1	1	1
ffmtrp	1	1	1	1	1	1	1	1	1	1
ffmtsp	1	1	1	1	1	1	1	1	1	1
ffmtps	1	1	1	1	1	1	1	1	1	1
ffmtwp	1	1	1	1	1	1	1	1	1	1
ffmtms	1	1	1	1	1	1	1	1	1	1
cs	1	1	1	1	1	1	1	1	1	1
isu	1	1	1	1	1	1	1	1	1	1
isp	1	1	1	1	1	1	1	1	1	1
rpes	1	1	2	2	2	2	1	1	1	1
rpis	1	1	2	2	1	1	1	1	1	1
rpbks	1	1	1	1	1	1	2	1	1	1
sep	1	1	2	2	2	2	1	1	1	1
rxot	1	1	3	1	1	1	1	1	1	1
rxmx	1	1	3	1	1	1	1	3	1	1
rxhg	1	1	1	1	1	1	1	3	1	1
rxfb	1	1	1	1	1	1	4	3	1	1
rifr	1	1	1	1	1	1	1	1	1	1
atw	1	1	1	1	1	1	1	1	1	1
dd	1	1	1	1	1	1	1	1	1	1

Table C-IV. Effective Plutonium Concentration for Various Material-Process Combinations Throughout the NFC.

Proc.\Matl.	wpu	rpu	rux	rmx	rfbr	rhtg	bmh	mox	met	rmet
pus	0	1	0	0	0	0	0	0	0	0
bks	0	0	0	0	0	0	0.07	0	0	0
wps	1	0	0	0	0	0	0	0	0	0
ffmxrp	0	1	0	0	0	0	0	0	0	0
ffmxps	0	1	0	0	0	0	0	0	0	0
ffmxwp	1	0	0	0	0	0	0	0	0	0
ffmtrp	0	0	0	0	0	0	0	0	0	0
ffmtsp	0	0	0	0	0	0	0	0	0	0
ffmtps	0	0	0	0	0	0	0	0	0	0
ffmtwp	0	0	0	0	0	0	0	0	0	0
ffmtms	0	0	0	0	0	0	0	0	0	0
cs	0	0	0.01	0.05	0.05	0.04	0	0	0	0
isu	0	0	0.01	0	0	0	0	0	0	0
isp	0	0	0	0.05	0.05	0.04	0	0	0	0
rpes	0	0	0.01	0.05	0.05	0.04	0	0	0	0
rpis	0	0	0.01	0.05	0.05	0.04	0	0	0	0
rpbks	0	0	0	0	0	0	0.1	0	0	0
sep	0	0	0.01	0.05	0.05	0.04	0	0	0	0
rxot	0	0	0.01	0	0	0	0	0	0	0
rxmx	0	0	0	0	0	0	0	0.07	0	0
rxhg	0	0	0	0	0	0	0	0.08	0	0
rxfb	0	0	0	0	0	0	0	0.1	0	0
rifr	0	0	0	0	0	0	0	0	0.2	0.05
atw	0	0	0	0	0	0	0	0	0.9	0.1
dd	0	0	0.01	0.05	0.05	0.04	0	0	0	0

Appendix D: Qualitative Description of Key FCOPT Constraints

D.1 Mining and Milling (*mm*)

This constraint determines the cumulated inventory of natural uranium (*nu*) that has been used up to a given time *t*, and in this sense differs from all other inventories considered. At any time *t*, $x(nu, mm, t)$ is equal to the previous inventory at time *t* - 1 plus the natural uranium (*nu*) sent to conversion, (weapons HEU) blending, and fabrication of MOX fuel from any of the three plutonium sources (directly from reprocessing, separated plutonium storage, and weapons-released material).

D.2 Conversion (*cv*)

The $U_2O_3 \rightarrow UF_6$ conversion constraints determine how much natural and recycled uranium (*nu* and *ru*, respectively) from the conversion process go to enrichment as UF_6 . The loss of material from conversion is noted here by the parameter $1 - ycv$, where *ycv* is the efficiency of conversion. The amount of this lost material is small but is not yet taken into account in this model.

D.3 Enrichment (*er*)

The enrichment constraints relate the amount of natural and (reactor) recycled uranium, respectively, sent to fuel fabrication to the amount leaving enrichment. The term *yernu* represents how much *nu* is needed to achieve the desired *lnu* enrichment, *yerru* is the efficiency for *ru* enrichment, and $1 - yer$ is the fraction of material lost during the enrichment process. The residence time of material in the enrichment facility is *ter*.

D.4 Fuel Fabrication (*ffxxx*; *xx* = *ux*, *mx*, *mt*)

The fuel-fabrication constraints divide according to the kind of fuel being fabricated (e.g., UOX, MOX, metallic, etc.). The time dependencies of all fuel-fabrication constraints are expressed in terms of lengths of time, *tffux*, *tffmx*, or *tffmt* (in years) required to fabricate the respective fuels. The fraction of material lost in fabrication is taken as $1 - \{yffux, yffmx, yffmt\}$, respectively; these loss fractions are generally small and in the present version of FCOPT are not accounted. It is specified that a fraction $1 - fmox$ of *rxmx*-recycle LWR cores are fueled with UOX, with the remainder of the core fueled with MOX. Enriched uranium is needed for the UOX portion of the core, as well as in the full core of an *rxot* technology. The amount of enriched natural, recycled, and weapons-blended uranium all must be accounted separately by each fabricated-fuel balance. A separate fuel-fabrication constraint specifically enforces uranium and plutonium balances within all MOX fuels with the inclusion of the respective initial plutonium loading, *ypui(nucl)*. These constraints generally take the form of balances made on the amount of uranium versus plutonium contained in the respective MOX fuel made from different plutonium sources [e.g.,

reprocessed plutonium, rpu , derived from both reprocessing and storage ($p = rpis$ or $rpcs$ and pus , respectively), and weapons plutonium, wpu] that derive from separate plutonium sources.

D.5 Blending (bl)

The blending constraints specify the amount of weapons-released enriched uranium, heu , must be blended with nu , du , or ru to produce a specific, final blended stream of UOX fuel, lwu . The concentration (weight fraction) of the feed material m , $yuox(m)$, must be specified for each material stream, as listed in Appendix E. The amount of blended LEU leaving this blending process is determined by two constraints; one that balances the total mass of uranium entering and leaving the blending operation (nu , ru , du , and heu) and one that enforces a strict (^{235}U) isotopic balance. The holdup time for the blending process is tbl .

D.6 Depleted Uranium Storage (dus)

The dus constraint is based on a balance of the du inventory in storage. This balance requires the du inventory at the time t equal that at time $t - 1$ plus mass flow of du from the enrichment process minus the du stream directed to all MOX fuel-fabrication processes.

D.7 Weapons Uranium Storage (wus)

This constraint describes a balance wherein the heu inventory at time t equals the inventory at time $t - 1$ plus any heu released (exogenously) from the weapons programs into the commercial fuel cycle minus the heu flowing to the blending process; $gheu(t)$ is the exogenous rate of heu release from the weapons program. The amount of weapons-grade uranium released in any given year is determined by a combination of weapons- and uranium-market-control policy issues; the rate $gheu$ will impact both uranium unit costs and proliferation. The inventory of heu tracked in FCOPT is only that which has entered the commercial reactor stream and does not include heu stored at weapons facilities; the process wus is a commercial storage for weapons-released HEU. Hence, the expression that describes the rate $gheu(\text{kg/yr})$ parametrically is constrained by estimates of the total amount of heu available for release to commercial use.

D.8 Weapons Plutonium Storage (wps)

As with heu storage, an exogenous and time-dependent release rate, $gwpu(\text{kg/yr})$, to this commercial storage facility, wps , is specified, so that only a controlled quantity can be introduced into MOX fuel-fabrication stream at a given time. Similar to the case for heu , policy issues dictate the release rate of wpu . This constraint reflects a current wps inventory of weapons plutonium that is equal to the amount contained during the previous time interval plus $gwpu$ minus the amount of wpu directed either to the various fuel-fabrication facilities.

D.9 Separations (*sep*)

Separations technology involves the partitioning of spent fuel into uranium (which goes to uranium storage, *rus*), other actinides, *ma*, either for consumption in *fsb* = {*rifr*, *atw*} technologies or disposition in a repository, *dd*, and fission products, *fp* or *lfp*. The latter long-lived fission products are possibly directed to an *fsb* technology, or to storage and/or disposal; a minor-actinide storage, *mas*, and the attendant material balance are specified. A distinction was made between “separations”, *sep*, and “reprocessing”, *rp* = *rpcs* or *rpis* depending on whether the reprocessing stream derives from cooling storage (*cs*) or interim storage (*is*), because minor actinides from the *sep* process are classified and used as fuel and are not (necessarily) a source of waste that is sent to disposal. The material balances that are attendant to the *sep* process are made around streams directed to the metal fuel-fabrication process, *ffmtsp*, that feeds the *fsb* technologies. The separations-related mass balances are made over the attendant material streams: *ma*, *rpu*, and uranium {*du*, *ru*, *nu*}, with the latter only of relevance to the *rifr* transmuting technology. Material sent to *sep* is derived either from cooling storage, *sepcs*, or from interim storage, *sepis*.

D.10 Electricity Generation [*gen(nucl,t)*]

The generation mix, *gen(nucl,t)*, is at the center of the set of constraints that comprise the FCOPT model. At one hand is the need to satisfy the exogenous demand, *gent(t)*, and on the other hand all front-end and back-end mass flows and storage requirements are driven by *gen(nucl,t)* in a combination that minimizes the objective function, *OBJ* [Eq. (3-4)]. The central constraint requires that the total amount of electrical energy generated annually by all *nucl* technologies must meet the exogenous demand must equal the total amount of electrical energy generated each year by all reactor types. The total, exogenously specified demand, *gent(MWyr/yr)*, for nuclear energy can be determined for a range of global energy scenarios, (Krakowski, 1999, 2002) or specified in terms of an annual growth rate as follows for $t > t_0$:

$$gent(t) = gent(t_0) * (1 + dgrowth)^{t-t_0} . \quad (D-1)$$

The amount of fuel needed to power a given reactor technology (*kgIHM/MWyr*) is equal to the annual energy generation for that reactor divided by the term *alf(MWyr/kgIHM)*, where,

$$alf(rx,t) = \eta_{th} (1 - \varepsilon) BU / (dpy) , \quad (D-2)$$

and η_{th} is the thermal conversion efficiency, ε is the re-circulating power fraction (the fraction of power needed to operate the reactor and, therefore, is not sent to the commercial electrical grid for sale), *BU*(*MWtd/kgIHM*), is the fuel burn-up, and *dpy* = 365 *d/yr*. Hence, for each reactor technology the ratio *gen(nucl,t)/alf(nucl)* must equal the sum of all fresh fuel directed thereto, $x(\{leu, mox, met\}, nucl, t)$, where *leu* = {*lnu*, *lru*, *lwu*}. These balances require that fuel is exposed in a given reactor for a certain period of time (the irradiation period, *trx*); only the amount of fuel needed to replenish the reactor after a given exposure or burn-up is transferred. It is then assumed that the SNF outflow from this replenishment moves to cooling storage (*cs*) after

irradiation, for a specified time before being transferred directly to a repository (*ddcs*), to a reprocessing facility (*rpcs*), or to an interim storage (*is*). These comments apply primarily to the commercial power-generating technologies, $rx = \{rxot, rxmx, rxhg, rxfb\}$; the fast-spectrum burners or transmuters, $fsb = \{rifr, atw\}$ are assumed to operate with an intrinsically combined cooling plus interim storage that is lumped together for monitoring purposes into a process identified as *sfs* (spent-fuel storage that applies for the generally high-recycle technologies constrained in the *fsb* generation technology set). The *fsb* technologies are expected to be high-recycle systems that, depending on the uranium loading, will generate intrinsic amounts of actinides that are presented as added fuel. The *per-pass* material loss, *floss*, incurred in the separations process, the quantity *alf(fsb)* used to connect power generation with material flows is modified as follows:

$$alf1(fsb,t) = alf(fsb,t)/[floss/buf(fsb,t) + (1 - floss)*(1 - cr(fsb))], \quad (D-3)$$

where the conversion ratio is $cr(fsb)$ (~ 0.6 for *rifr*, ~ 0.0 for *atw*), and the *per-pass* burn-up fraction is *BUf*, as is given below:

$$BUf(nucl,t) = BU(nucl)/dpy/(N_A * e * Q / (A/1000) / spy). \quad (D-4)$$

The physical constants are N_A = Avogadro's number ($6.022 * 10^{23}$ atoms/mole), Q = energy *per* fission (200 MeV/fission), e = electric charge ($1.602 * 10^{-19}$ J/eV), A = average mass of actinides in burner (assume 239 kg/kmole), and $spy = 3.15(10)^7$ s/yr.

In an attempt to include the vintaging of generation capital, a variable, *dcap(nucl,t)*, is introduced that reflects the yearly addition to existing capital stock of generating technologies. The variable *dcap* is then limited in the rate at which the annual deployment of that technology can occur. This annual addition of generating capacity is represented in the *gen(nucl,t)*-related constraints, as is the inventory associated with a certain generation capacity that has the units of capacity (*MWe*). The capacity $cap(nucl,t) = gen(nucl,t)/avail(nucl,t)$, where *avail(nucl,t)* is the exogenous availability of technology *nucl* at time *t* [coupling of *avail* to the magnitude of the existing stock, *cap*, allows endogenous technical learning (ETL) to be implemented, but the LP problem then becomes an NLP problem; this important element will be introduced in future versions of FCOPT]. At any given time, *cap(nucl,t)* is equal to the sum of the annual additions, *dcap*, over the past $t - tlife$ years, where *tlife(nucl)* is the lifetime of the reactor. Also, to a more realistic (correct) LP initiation, a residual inventory of generation stock, *resid(nucl,t)* deployed in the years prior to the start of the optimization is exogenously specified. The parameter *resid(nucl,t)* diminishes to zero over the first 10 to 15 years of the optimization period, unless the technology under consideration was nonexistent previously and the residual inventories remain zero for all time steps until the minimization of the objective function requires its deployment. Under these conditions, the capacity of technology *nucl* at time *t* is given by

$$cap(nucl,t) = resid(nucl,t) + \sum_{t'=t-tlife+1}^t dcap(nucl,t'). \quad (D-5)$$

The formulary given under (*cap*) in Sec. C elaborates on this computation procedure in the language of GAMS (Brooke, 1998).

In addition to these general constraints imposed on deployment and attempts to deal with pre-optimization-timeframe “end effects”, additional constraints are imposed on the conversion rate of *rxot* to MOX-fueled *rxmx* technologies, as well as the fraction of total generation, *gent(t)*, that is allowed to be supplied by technologies included in the set *fsb*. Within the *rxmx* technologies, the fraction of the core loaded with MOX, *fmox(t)*, can be exogenously prescribed.

Finally, the amount of energy produced by each technology *nucl* at a given time is limited to be no more than a factor times the amount generated in the previous time interval, thereby limiting the deployment rate of the advanced technologies; time is required to develop new technologies, to conduct a safety analyses, to implement a new fuel types, *etc.* This somewhat artificial constraint is a surrogate for a constraint that must be imposed by a more realistic capital vintaging constraint that remains to be developed and implemented. Each of the generation technologies considered is subject to this constraint, which is given as follows:

$$dcap(nucl,t) < cap(nucl,t-1)*fgrow(nucl,t) + fseed(nucl)*gent(t), \quad (D-6)$$

where the parameter *fgrow(nucl,t)* is equal to some factor *fgrowrx(nucl)* times the growth rate, *epsrx(t)*, of overall nuclear energy demand, *gent(t)*. The small fraction *fseed(nucl)* is included to allow a “seed” from which previously unused advanced technologies can grow into the overall generation mix, should economics allow [*vis-à-vis OBJ_{COST}*, in the case of a cost-based optimization, Eq. (3-2)]. A related constraint on the rate of de-deployment is also included as a separate constraint to disallow the sudden “disappearance” of previously viable generation technologies, albeit if the optimization includes related economic penalties for pre-mature (*e.g.*, before end-of-life) removal from the generation market, such a constraint should be unnecessary/redundant/nonbinding.

D.11 FBR Blanket Replenishment (*bks*)

The MOX-fueled FBR technology, *rxfb*, is only superficially modeled in terms of neutronics input and breeding potential. Fuel-fabrication, SNF cooling and interim storage, and SNF (*rmx*) plus exposed breeding-blanket material (*bmx*) reprocessing share the respective processes with the other MOX-burning options (*rxmx*, *rxhg*). As is indicated, the UOX fed to the blanket and the MOX retrieved therefrom are tracked as separate materials because of the unique properties of this material, particularly for the exposed blanket-generated MOX (*e.g.*, potentially high proliferation propensity because of high fissile-plutonium and low fission-product content). Hence, material stored in the post-blanket storage, *bks*, is tracked separately. As soon as the blanket for the *rxbr* completes a yet-to-be-specified breeding cycle (only breeding ratio, *br*, is specified), it must be replenished with more *du* to re-constitute a new blanket. The amount of *du* needed is equal to the rate of fissile-core consumption times the breeding ratio, *gen(rxbr,t)*br/alf(rxbr,t)*, where *gen(rxbr,t)* is the annual electricity generation and *alf(rxbr,t)* is given by Eq. (D-2).

D.12 Cooling Storage (*cs*)

These constraints express material balances for cooling storage, which in FCOPT receives both spent UO₂ fuel (*ru_x*) and spent MOX fuel from $gen = rm_x, rxhg$, and $rxfb$ (e.g., $m = rm_x, rhtg$, and $rfbr$). For the purpose of this model, it is assumed that material going into cooling storage after irradiation in each reactor being considered for a time $trx(nucl)$ must be cooled for a fixed amount of time, $tcs(yr)$, before being transferred to interim storage (*is*), or to reprocessing (*rpis*); an option also is included for direct repository disposal from cooling storage, *ddcs*. All SNF can go from *is* to direct disposal (*ddis*), to reprocessing (*rpis*), or to separations (*sepcs*) for *rpu* and *ma* extraction and subsequent burning in *fsb* technologies. This SNF balance over the interim storage for both *ru_x* and *rm_x* specifies that the amount of material that is actually transferred from *rx* to *is* at time *t* must equal (greater than) the material that came into the reactor at time *t* – $trx(nucl) - tcs$.

Generally, inventory of SNF $\{ru_x, rm_x, rhtg, rfbr\}$ in cooling storage at time *t* is equal to the inventory at *t* – 1, minus what was removed to interim storage (*isp* or *isu*, where $is = isp + isu$; a distinction is made between *ru_x* and SNF that began life as MOX, $\{rm_x, rhtg, rfbr\}$), plus material added from reactor discharges at time *t*, minus any material removed to direct disposal (*ddcs*), reprocessing (*rpis*), or separations (*sepcs*). The latter transfers are options that generally are not exercised in generating the results presented herein; such transfers to *dd*, *rp*, or *sep* are typically restricted to take place from interim storage, *is*. The above balances apply to all plutonium-bearing SNF forms generated from the four $rx = \{rxot, rxmx, rxhg, rxfb\}$ generation technologies, but such MOX materials created in the FBR blanket (*bmx*) are sent to a special irradiated blanket storage, *bks*.

A unique initial condition must be applied to the SNF storage situation presently existing in the US; little or no formal interim storage exists in the US, and all SNF technically is classified initially as residing in cooling storage, in spite of the fact that much of this SNF inventory has fulfilled the *tcs* residency time that qualifies a transfer to interim SNF storage if such interim storage facilities were available. To accommodate an artificial $cs \rightarrow is$ transfer starting at the beginning of the optimization (year 2000), a linear transfer over the time $trxc_s(nucl)$ is forced to “prime start” the *is* inventories; typically, these transfers are assumed to occur over a period of ~6-10 years. In addition, a limiting *cs* capacity is applied as a constraint that specifies a limit of *bn_{cs}(kg)*; because of the residence time constraint, this global capacity constraint is typically not binding in most optimally feasible solutions yielded by FCOPT.

D.13 Interim Storage (*is*)

Unlike the cooling storage, a differentiation is made in the interim storage depending on whether the SNF is transferred from *cs* originated as UOX (*lnu, lru, lwu*) or MOX (*mox*); the former is placed in *isu* and the later in *isp*, with interim storage in general being $is = isu + isp$. Again, only SNF generated from the *rx* generation technologies are delivered to *is*, with SNF from the *fsb* technologies going to a separate and aggregated storage system that is designated as *sfs*. The material balances made on interim storage (one each for *ru_x*, *rm_x*, *rhtg*, and *rfbr*) requires that the SNF inventory in interim storage equal the amount that was previously stored, plus whatever material leaves cooling storage, minus the material that leaves for either direct disposal (*ddis*),

reprocessing (*rpis*), or separations (*sepcs*). Capacity limits, again expressed in *kg* units, are also applied to the integrated interim storage in terms of a factor $bnisrx(nucl,t)$ equal to the number of active core inventories. In addition to requiring an “input – output = accumulation” mass balance of the kind described above, some assurances are required that backflow from *is* to *cs* does not occur; an approximation of this constraint for spent fuel *rux* (SNF from generation technology *rxot*) takes the following form:

$$x(rux, rpis, t) + x(rux, ddis, t) + x(rux, sepis, t) + x(rux, isu, t) - x(rux, isu, t-1) > 0.0 \quad .(D-7)$$

D.14 Reprocessing

As noted above, reprocessing of SNF applies only to the $rx = \{rxot, rxmx, rxhg, rxfb\}$ generation technologies; the “reprocessing” that is required for the high-recycle $fsb = \{rifr, atw\}$ technologies occurs in the “separations” process, *sep*, which receives material from both *is* and *cs*, as well as from *sfs* (associated only with the storage of SNF generated during the operation of the highly recycling *fsb* technologies). The amount of material that can be delivered to reprocessing at present is restricted by a capacity limit, $rpcap(t)$ in units of *kgHM/yr*, that initially is zero (for the US) up to some time *trpi* and increases to a final limit, $rpcapf(kg/yr)$, at some time *trpf*, where the increase is described by a power function in time using a exponent *exprp* (including linearity, where *exprp* = 1). Other capacity constraints were also explored, including one that requires the total reprocessing capacity available at any given time be less than a specified fraction of the total power generated from various reactors. This constraint was considered on the basis that time is required to develop reprocessing technology initially as well as to increase reprocessing capabilities to meet significant future needs; the required reprocessing capacity cannot be increased rapidly by large increments at once, so it was assumed that the reprocessing capacity (*kgHM/yr*) = $pnxyyy * cap(rx)(t - trx(rx))$, where $yyy = rux, mx, bmx$, $rx = \{rxot, rxmx, rxhg, rxfb\}$, and $cap(rx, t) = gen(rx, t) / alf(rx)$.

D.15 MOX Recycle Limits

The amount of MOX fuel that can be recycled is constrained to be less than the amount of MOX fuel currently in a user reactor $\{rxmx, rxhg, rxfb\}$ times a fraction representing the total number of times the fuel can be recycled, *ncyc*. This constraint limits the amount of fuel that can be sent for reprocessing and, therefore, determines how many times recycled fuel can be reprocessed. For the MOX/LWR technology *rxmx*, this takes the form:

$$\begin{aligned} x(rmx, rpccs, t) + x(rmx, rpmcs, t) + x(rmx, rpcis, t) + x(rmx, rpmis, t) < \\ x(mox, rxmx, t - trx(inmx)) * (1 - 1/ncyc). \end{aligned} \quad (D-8)$$

D.16 Other Material Storages (*rus*, *pus*, *wps*, *mas*, *fps*)

The four key storage technologies other than SNF cooling storage and interim storages (*cs*, *is*), as well as storage of SNF associated with the *fsb* technologies (*sfs*), are provided for separated

product [uranium (*ru*), plutonium (*rpu*, *wpu*), minor actinide (*mas*), and fission products (*fp*, *lfp*)]. While the individual mass balances leading to the attendant constraints can contain a large number of terms (Appendix E), the general form of these balances is straightforward: inventory at time t minus the respective inventory at time $t - 1$ equals input at time t from various far-ranging parts of the NFC minus output to other receiving components of the NFC. Each balance must also reflect the respective mass fractions of the input and output streams, as well as material loss fractions. For example, in the case of (separated) reactor plutonium, *rpu*, the amount of material that goes to (separated) plutonium storage at time t , *pus*, is equal to that which was in plutonium storage at the previous time $t - 1$; minus the *rpu* that is sent to MOX fuel fabrication, *ffmxps*, to metal-fuel fabrication (for *fsb* technologies), *ffmtps*, and direct disposal, *pudpus*; plus any *rpu* that is added through reprocessing at the previous time $t - 1$, *trp*, as well as from separations at time $t - 1$, *tsep*. Again, the plutonium mass fractions in each of these respective streams must enter appropriately into the overall balance. It is noted that for each of the separated materials, more than a single, aggregated storage facility is envisaged; this level of disaggregation into less communal facilities must be done in more advanced optimization models, or, more appropriately, in more detailed, technology-rich simulation models, like NFCSim (Sec. 4).

D.17 Direct Disposal in Repository (*dd*)

The following materials are vectored to the direct-disposal (*dd*) repository: $\{rux, rmx, rhtg, rfbr, fp, ma, rpu\}$. Early formulation of FCOPT considered a range of three direct-disposal repository options, but the level of detail ascribed to the back-end of the NFC, as well as the postponement of a development and evaluation of repository-related environmental metric, suggested model simplification, particularly in view of the complexity (“richness”) of results (Sec. 3.2) generated by an already simplified NFC model (Appendix E). Like the constraints imposed on the SNF and separated-product storage constraints, the repository constraints represent a set of simple mass-balance equations that increment mainly heavy-metal (HM) inventories by an assemblage of input streams from around the far reaches of the NFC being optimized. Similar to the interim storage (*is*), reprocessing ($rp = rpcs, rpis$), and separations processes ($sep = specs, sepis$), direct-disposal repositories that can accept material do not exist in the US. Hence, a startup algorithm ramps the repository capacity from $ddcapi = 0$ at time $tddi$ to $ddcapf$ at time $tddf$, after which this capacity is held constant for the remainder of the optimization period. These repository constraints are similar to those describe above for the various storage facilities, except that planned output material streams are zero. It is noted that a direct-disposal stream for separated reactor plutonium, *rpu*, is included in the mass-balance constraints, although this kind of intentional disposal is unlikely, but given the development of an appropriate driver function, such a stream and the cumulating end point could be used to model diversion impacts.

Appendix E: Summary and Synopsis of Key Constraints (Mass and Energy Balances, Capacity Limits, *etc.*)

Approximately 95 constraints, along with the cost- or proliferation-risk- based objective function define the NFC problem described by the FCOPT Linear-Programming (LP) model. Of these 95 constraints, 19 are exploratory and inactive. Table B-I defines and lists values used to evaluate the coefficients used in each of the constraint equations described below. These constraint equations give the relationships between the vector $x(m,p,t)$, which represents either an inventory (kg) of material m in process p at time t or a mass flow rate (kg/yr); no differentiation is made between mass inventory or rate, which is determined within the context of a given equation. Table A-I and Table A-II identify the species m and process p used throughout the FCOPT model. A one-year time interval is adopted for all cases reported herein.

Each constraint equation is given a name of the form $nc_xxx(t)$ as well as a number (N); the former follows the convention used in the GAMS (Brooke, 1996) programming language used to evaluate the LP model, where the constraint is applied for all times greater than a fixed value [e.g., ts , where ts is the starting time corresponding to the year 2000, with times less than ts being considered to generate a historical record of events leading to the start of a given optimization. In the GAMS context, this condition is specified by $\$(ORD(t) \geq ts)$, where $ORD(t)$ is the ordinal of the time set $t = \{1990, 1991, \dots, 2100\}$, and the optimization commences at time $ts = 2000$; the period (1900,1999) defines a history of key inventories and rates.].

(1) Mining and Milling (accumulated use) for process $p = mm$ (mining and milling) and material $m = nu$ (natural uranium); this constraint is unique in that it tracks accumulated use of the uranium resource, which is needed to determine resource depletion and attendant natural-uranium cost increase. In addition to supplying requirements of the $U_3O_8 \rightarrow UF_6$ conversion ($p = cv$), natural uranium can be used in the range of MOX fuel fabrication processes ($ffmx$) that operate on plutonium derived from reprocessing (rp), storage (pus), released weapons materials (wp) released for burn-down in commercial reactors. Material nm is also used in the process $p = bl$ that blends highly enriched weapons uranium released from nuclear weapons.

$nc_mm(t)\$(ORD(t) \geq ts)$:

$$x(nu,mm,t) - x(nu,mm,t-1) - x(nu,cv,t) - x(nu,bl,t) - x(nu,ffmxrp,t) - x(nu,ffmxps,t) - x(nu,ffmxwp,t) = 0.0;$$

(2) Conversion of material $m = nu$ (natural uranium) and reactor-recycled (e.g., containing ^{236}U) uranium ($m = ru$) with an efficiency of conversion equal to ycv and a processes time $tcv(yr)$.

$nc_cvnu(t)\$(ORD(t) \geq ts)$:

$$x(nu,er,t) - x(nu,cv,t-tcv)*ycv = 0.0;$$

(3) Conversion of material $m = ru$ (reactor uranium, containing ^{236}U) with an efficiency of conversion equal to ycv and a processes time $tcv(\text{yr})$.

nc_cvru(t)\$(ORD(t) GE ts):

$$x(ru, er, t) - x(ru, cv, t - tcv) * ycv = 0.0;$$

(4) Enrichment of natural uranium in process $p = er$ using materials $m = nu$ to form low-enrichment uranium designated as lnu , lru , or lwu , where the latter is made from blending weapons highly enriched uranium, $m = heu$, as is passed through process $p = bl$ instead of $p = er$. The isotopic mass balance over process $p = er$ yields the following coefficients used in this constraint:

$$\begin{aligned} yernu &= (xf(nu) - xt)/(xp(nu) - xt) = \text{ratio of product to feed stream for } m = nu \\ yerru &= (xf(ru) - xt)/(xp(ru) - xt) = \text{ratio of product to feed stream for } m = ru, \end{aligned}$$

where:

$$\begin{aligned} xf(nu) &= \text{weight fraction of } ^{235}\text{U} \text{ in nu feed (0.00711);} \\ xp(nu) &= \text{weight fraction of } ^{235}\text{U} \text{ in enriched uranium made from nu (~0.035)} \\ xf(ru) &= \text{weight fraction of } ^{235}\text{U} \text{ in ru feed (~0.01);} \\ xp(ru) &= \text{weight fraction of } ^{235}\text{U} \text{ in enriched uranium made from nu (~0.040);} \\ xt(nu, ru) &= \text{tails assay (~0.003, depends on xp, xf, ucmm($/kgNU), and} \\ &\quad \text{ucer($/SWU));} \end{aligned}$$

The mass efficiency (one minus the loss fraction) is given by yer , and the delay time in process $p = er$ is designated by $ter(\text{yr})$.

nc_ernu(t)\$(ORD(t) GE ts):

$$- x(nu, er, t - ter) * yer * yernu + x(lnu, fflux, t) = 0.0;$$

(5) Enrichment of reactor-exposed uranium in process $p = er$ using materials $m = ru$; rest of the discussion given in constraint (4) applies here, except that the value for $xp(ru)$ is somewhat higher than for $xp(nu)$ because of the ^{236}U contained in the former.

nc_erru(t)\$(ORD(t) GE ts):

$$- x(ru, er, t - ter) * yer * yerru + x(lru, fflux, t) = 0.0;$$

(6-13) Fuel Fabrication (ff) process using a range of feed materials for enriched uranium ($p = lnu$, lru , lwu) or plutonium (depending on source of plutonium: rp = direct from reprocessing; ps = direct from separated plutonium storage; wp = direct from weapons-released material). These processes are designated as $p = \{fflux, fflux\}$, with the latter further defined as $p = ffluxrp, ffluxps, ffluxwp$. Materials used are $m = lru$, lnu , lwu (for UOX fabrication); $m = ru$, du , or nu for unenriched uranium plus rpu and wpu plutonium for MOX fabrication. The flow of $m = \{lru$,

l_{nu} , l_{wu} into the fuel fabrication facility at time $t - t_{ffux}$, where t_{ffux} is the time required for UOX fuel fabrication, is required to equal the mass flow of $m = l_{ru} + l_{nu} + l_{wu}$ to the user reactors, $nucl = \{rxot, rxmx, rxhg\}$ at time t ; the material loss fraction is y_{ffux} in the UOX fuel-fabrication facility. The following constraints enforce the coupling of reactors, $p = nucl$, and the various fuel-fabrication plants, $\{p = ffux, ffmux\}$, with $m = \{l_{nu}, l_{ru}, l_{wu}, mox, rpu, wpu, nu, ru, du\}$ representing the primary material of concern. First, the UOX part of the LWR cores must be equal to the same amount of material that was fabricated at time $t - t_{ffux}$, reduced by the mass-loss efficiency, y_{ffux} . The materials $m = \{l_{nu}, l_{ru}, l_{wu}\}$ must be appropriately separated into the following constraints (6-7):

(6) Balance of $m = l_{nu}$ from $p = ffux$ going to reactors $nucl = \{rxot, rxmx\}$.

nc_ffl_{nu}(t)\$(ORD(t) GE ts):

$$- x(l_{nu}, ffux, t - t_{ffux}) * y_{ffux} + x(l_{nu}, rxot, t) + x(l_{nu}, rxmx, t) < 0.0;$$

(7) Balance of $m = l_{ru}$ from $p = ffux$ going to reactors $nucl = \{rxot, rxmx\}$, where the nominal fuel-fabrication time is t_{ffux} .

nc_ffl_{ru}(t)\$(ORD(t) GE ts):

$$- x(l_{ru}, ffux, t - t_{ffux}) * y_{ffux} + x(l_{ru}, rxot, t) + x(l_{ru}, rxmx, t) = 0.0;$$

(8) Balance of $m = l_{wu}$ from $p = ffux$ going to reactors $nucl = \{rxot, rxmx\}$.

nc_ffl_{wu}(t)\$(ORD(t) GE ts):

$$- x(l_{wu}, ffux, t - t_{ffux}) * y_{ffux} + x(l_{wu}, rxot, t) + x(l_{wu}, rxmx, t) = 0.0;$$

(9) Uranium balance for $m = \{nu, ru, du\}$ going to the MOX fuel fabrication, $p = ffmux$, for the MOX-user reactors $nucl = \{rxmx, rxhg, rxfb\}$. In this constraint the material loss fraction in process $p = ffmux$ is $1 - y_{ffmux}$, the nominal fuel-fabrication time is t_{ffmux} , and the initial plutonium loading in these respective reactors are $y_{pui}(nucl)$, as given in Table B-I.

nc_fr_{mxu}(t)\$(ORD(t) GE ts):

$$\begin{aligned} & - x(nu, ffmuxrp, t - t_{ffmux}) * y_{ffmux} - x(nu, ffmuxps, t - t_{ffmux}) * y_{ffmux} \\ & - x(nu, ffmuxwp, t - t_{ffmux}) * y_{ffmux} - x(ru, ffmuxrp, t - t_{ffmux}) * y_{ffmux} \\ & - x(ru, ffmuxps, t - t_{ffmux}) * y_{ffmux} - x(ru, ffmuxwp, t - t_{ffmux}) * y_{ffmux} \\ & - x(du, ffmuxrp, t - t_{ffmux}) * y_{ffmux} - x(du, ffmuxps, t - t_{ffmux}) * y_{ffmux} \\ & - x(du, ffmuxwp, t - t_{ffmux}) * y_{ffmux} \\ & + x(mox, rxfb, t) * (1 - y_{pui}(rxfb)) + x(mox, rxhg, t) * (1 - y_{pui}(rxhg)) \\ & + x(mox, rxmx, t) * (1 - y_{pui}(rxmx)) = 0.0; \end{aligned}$$

(10) Uranium balance for $p = \{nu, ru, du\}$ directed to the metal-fuel reactors (mainly $nucl = rifr$, but to a lesser extent including $nucl = atw$). In this constraint the material loss fraction in

process $p = \text{ffmt}$ (metal-fuel fabrication facility) is $1 - \text{yffmt}$, the nominal fuel-fabrication time is tffmt , and the initial plutonium loadings in these respective reactors are $\text{ypui}(\text{nucl})$, as given in Table B-I.

$\text{nc_frxmtu}(t) \$ (\text{ORD}(t) \text{ GE ts})$:

$$\begin{aligned} & -x(\text{nu}, \text{ffmtrp}, t - \text{tffmt}) * \text{yffmt} - x(\text{nu}, \text{ffmtps}, t - \text{tffmt}) * \text{yffmt} \\ & -x(\text{nu}, \text{ffmtwp}, t - \text{tffmt}) * \text{yffmt} - x(\text{nu}, \text{ffmtsp}, t - \text{tffmt}) * \text{yffmt} \\ & -x(\text{ru}, \text{ffmtrp}, t - \text{tffmt}) * \text{yffmt} - x(\text{ru}, \text{ffmtps}, t - \text{tffmt}) * \text{yffmt} \\ & -x(\text{ru}, \text{ffmtwp}, t - \text{tffmt}) * \text{yffmt} - x(\text{ru}, \text{ffmtsp}, t - \text{tffmt}) * \text{yffmt} \\ & -x(\text{du}, \text{ffmtrp}, t - \text{tffmt}) * \text{yffmt} - x(\text{du}, \text{ffmtps}, t - \text{tffmt}) * \text{yffmt} \\ & -x(\text{du}, \text{ffmtwp}, t - \text{tffmt}) * \text{yffmt} - x(\text{du}, \text{ffmtsp}, t - \text{tffmt}) * \text{yffmt} \\ & + x(\text{met}, \text{rifr}, t) * (1 - \text{ypui}(\text{rifr}) - \text{ymai}(\text{rifr})) \\ & + x(\text{met}, \text{atw}, t) * (1 - \text{ypui}(\text{atw}) - \text{ymai}(\text{atw})) = 0.0; \end{aligned}$$

(11) Plutonium balance on MOX fuel in all user reactors, $\text{nucl} = \{\text{rxmx}, \text{rxhg}, \text{rxfb}\}$. The plutonium directed to the respective fuel-fabrication plants is of the form $m = \{\text{rpu}, \text{wpu}\}$, with $m = \text{rpu}$ derived directly from reprocessing, $p = \text{rp}$, or from separated-plutonium storage, $p = \text{pus}$. In this constraint the material loss fraction in process $p = \text{ffmx}$ (oxide-fuel fabrication facility) is $1 - \text{yffmx}$, the nominal fuel-fabrication time is tffmx , and the initial plutonium loadings in these respective reactors are $\text{ypui}(\text{nucl})$, as given in Table B-I.

$\text{nc_frxmxpu}(t) \$ (\text{ORD}(t) \text{ GE ts})$:

$$\begin{aligned} & -x(\text{rpu}, \text{ffmxrp}, t - \text{tffmx}) * \text{yffmx} - x(\text{rpu}, \text{ffmxps}, t - \text{tffmx}) * \text{yffmx} \\ & -x(\text{wpu}, \text{ffmxwp}, t - \text{tffmx}) * \text{yffmx} + x(\text{mox}, \text{rxmx}, t) * \text{ypui}(\text{rxmx}) \\ & + x(\text{mox}, \text{rxfb}, t) * \text{ypui}(\text{rxfb}) + x(\text{mox}, \text{rxhg}, t) * \text{ypui}(\text{rxhg}) = 0.0; \end{aligned}$$

(12) Plutonium balance on metallic fuel for all user reactors, $\text{nucl} = \{\text{rifr}, \text{atw}\}$. Forms of plutonium are $m = \{\text{rpu}, \text{wpu}\}$ and $m = \text{rpu}$ derives directly from processes $p = \{\text{rp}, \text{sep}, \text{pus}\}$, where a distinction is made between reprocessing ($p = \text{rp}$) associated with non-transmuting technologies, $\text{nucl} = \{\text{rxot}, \text{rxmx}, \text{rxhg}, \text{rxgb}\}$ and “separations” associated with transmuting technologies, $\text{nucl} = \{\text{rifr}, \text{atw}\}$. In this constraint the material loss fraction in process $p = \text{ffmt}$ (metal-fuel fabrication facility) is $1 - \text{yffmt}$, the nominal fuel-fabrication time is tffmt , and the initial plutonium loadings in these respective reactors are $\text{ypui}(\text{nucl})$, as given in Table B-I.

$\text{nc_frxmtpu}(t) \$ (\text{ORD}(t) \text{ GE ts})$:

$$\begin{aligned} & -x(\text{rpu}, \text{ffmtrp}, t - \text{tffmt}) * \text{yffmt} - x(\text{rpu}, \text{ffmtsp}, t - \text{tffmt}) * \text{yffmt} \\ & -x(\text{rpu}, \text{ffmtps}, t - \text{tffmt}) * \text{yffmt} - x(\text{wpu}, \text{ffmtwp}, t - \text{tffmt}) * \text{yffmt} \\ & + x(\text{met}, \text{rifr}, t) * \text{ypui}(\text{rifr}) + x(\text{met}, \text{atw}, t) * \text{ypui}(\text{atw}) = 0.0; \end{aligned}$$

(13) Minor-actinide balance for metal-fuel systems applied to all user reactors, $\text{nucl} = \{\text{rifr}, \text{atw}\}$. The minor actinides derive directly from $p = \{\text{rp}, \text{sep}, \text{mas}\}$. In this constraint the material loss fraction in process $p = \text{ffmt}$ (metal-fuel fabrication facility) is $1 - \text{yffmt}$, the nominal fuel-

fabrication time is t_{ffmt} , and the initial minor-actinide loadings in these respective reactors are $y_{mai}(nucl)$, as given in Table B-I.

nc_frxtmtma(t)\$(ORD(t) GE ts):

$$\begin{aligned} & -x(ma,ffmtrp,t-t_{ffmt}) * y_{ffmt} - x(ma,ffmtsp,t-t_{ffmt}) * y_{ffmt} \\ & -x(ma,ffmtms,t-t_{ffmt}) * y_{ffmt} - x(wpu,ffmtwp,t-t_{ffmt}) * y_{ffmx} \\ & + x(ma,rifr,t) * y_{mai}(rifr) + x(ma,atw,t) * y_{mai}(atw) = 0.0; \end{aligned}$$

(14,15) Weapons-released highly enriched uranium, $m = heu$ is blended to reactor specification is process $p = bl$. The materials directed to this process are $m = \{heu, du, ru, nu\}$, with $yuox(i = heu, lnu, lru, du)$ being the ^{235}U mass fractions in UOX made from the respective materials; the hold-up time in the blending process is $t_{bl}(yr)$.

(14) Total uranium balance in blending process $p = bl$.

nc_bl(t)\$(ORD(t) GE ts):

$$\begin{aligned} & x(heu,bl,t-t_{bl}) + x(nu,bl,t-t_{bl}) + x(ru,bl,t-t_{bl}) + x(du,bl,t-t_{bl}) \\ & - x(lwu,ffux,t) = 0.0; \end{aligned}$$

(15) ^{235}U balance in blending process $p = bl$, where $yuox(uxxx)$ is the ^{235}U concentration in the respective fuels, and the hold-up time in the blending process is $t_{bl}(yr)$.

nc_bl2(t)\$(ORD(t) GE ts):

$$\begin{aligned} & x(lwu,ffux,t) * yuox(ulnu) - x(heu,bl,t-t_{bl}) * yuox(uheu) \\ & - x(ru,bl,t-t_{bl}) * yuox(uru) - x(du,bl,t-t_{bl}) * yuox(udu) = 0.0; \end{aligned}$$

(16) Depleted uranium storage, $p = dus$, balance, with the materials entering into this balance being $m = \{nu, ru, du\}$. As for many of these kinds of balances, the amount of du in storage at time t equals that in storage at $t - 1$ plus the uranium tails generated from enrichment minus the du used in MOX fabrication and minus du directed to the blanket used in the $nucl = rxfb$ technology. In this constraint, ter is the holdup time in enrichment, and t_{ffux} and t_{ffmx} are the holdup times for the UOX and MOX fuel-fabrication facilities, with t_{bl} being the holdup time in the weapons HEU blending operation and t_{bl} being the holdup time in the FBR ($rxfb$) blanket.

nc_dus(t)\$(ORD(t) GE ts):

$$\begin{aligned} & x(du,dus,t) - x(du,dus,t-1) \\ & - x(nu,er,t-ter) * (1 - y_{ernu}) * y_{er} - x(ru,er,t-ter) * (1 - y_{erru}) * y_{er} \\ & + x(du,ffmxrp,t) + x(du,ffmxps,t) + x(du,ffmxwp,t) \\ & + x(du,fbbk,t) + x(du,bl,t) = 0.0; \end{aligned}$$

(17) Weapons-released uranium storage, $p = wus$. The material is $m = heu$, and the exogenous release rate is $gheu(kgHEU/yr)$.

nc_wus(t)\$(ORD(t) GE ts):

$$x(heu, wus, t) + x(heu, bl, t) - x(heu, wus, t-1) = gheu(t);$$

(18) Weapons-released plutonium storage, $p = wps$ balance has interfaces (mainly MOX and metallic-fuel fabrication) through which the material $m = wpu$ is sent and is released to storage at an exogenous release rate, $gwpu(kgWPU/yr)$.

nc_wps(t)\$(ORD(t) GE ts):

$$x(wpu, wps, t) - x(wpu, wps, t-1) + x(wpu, ffmtwp, t) + x(wpu, fmxwp, t) = gwpu(t);$$

(19-23) Exogenous electricity demand (19) and mass-energy correspondences (20-23) are made for the set nucl of six power-generating technologies: $rxot = OT/LWR$; $rxmx = MOX/LWR$; $rxhg = HTGR$; $rxfb = FBR$; $rifr = IFR$ -based FSB; $atw = ADS$ -based FSB. In formulating these central constraints, the following variables are introduced:

- $gen(nucl, t)$ = annual generation ($Mwey/yr$) by reactor $nucl$ in year t ;
- $nucl$ = set of all reactors, $rx = \{rxot, rxmx, rxhg, rxfb\}$ a subset of commercial power – generating technologies, and $fsb = \{rifr, atw\}$ a subset of transmuting technologies;
- $load(rx, t) = gen(rx, t)/alf(rx, t)$ = fuel requirement ($kgHM/yr$);
- $alf(rx, t) = etath(rx, t) * (1 - epsilon(rx)) * BU(rx, t)/dpy$, with $alf(fsb, t) = etath(rxfb, t) * (1 - epsilon(fsb)) * pna * elq * ef / (aave/1000) / spy$;
- $alf1(fsb, t) = alf(fsb, t) / (floss/BUf(fsb, t) + (1 - floss) * (1 - cr(fsb)))$; $alf1$ is a correction for internal material recycle and intrinsic breeding in fsb systems;
- $load(fsb, t) = x(wpu, fsb, t) + x(rpu, fsb, t) + x(ma, fsb, t)$.

(19) Satisfy total exogenous generation demand, $gent(t) MWey/y$.

nc_gent(t)\$(ORD(t) GE ts):

$$gen(rxot, t) + gen(rxmx, t) + gen(rxhg, t) + gen(rxfb, t) + gen(rifr, t) + gen(atw, t) = gent(t);$$

(20) Loading-to-generation constraint for $rx = rxot$.

nc_rxot(t)\$(ORD(t) GE ts):

$$x(lwu, rxot, t) + x(lnu, rxot, t) + x(lru, rxot, t) - gen(rxot, t)/alf(rxot, t) = 0.0;$$

(21) Loading-to-generation constraint for $rx = rmx$.

nc_rmx(t)\$(ORD(t) GE ts):

$$x(lwu,rxmx,t) + x(lnu,rxmx,t) + x(lru,rxmx,t) + x(mox,rxmx,t) - gen(rmx,t)/alf(rmx,t) = 0.0;$$

(22) Loading-to-generation constraint for (MOX-fueled) $rx = rxhg$.

nc_rxhg(t)\$(ORD(t) GE ts):

$$x(mox,rxhg,t) - gen(rxhg,t)/alf(rxhg,t) = 0.0;$$

(23) Loading-to-generation constraint for (MOX-fueled) $rx = rxfb$.

nc_rxfb(t)\$(ORD(t) GE ts):

$$x(mox,rxfb,t) - gen(rxfb,t)/alf(rxfb,t) = 0.0;$$

(24) Blanket and loading-to-generation constraint for (MOX-fueled) $rx = rxfb$; blanket plutonium output is assumed to be proportional to $rxfb$ power generation; the core (and blanket) residence time is $trx(rxfb)$, and the breeding ratio is br (Table B-I).

nc_rxbk(t)\$(ORD(t) GE ts):

$$x(bmx,bks,t) + x(bmx,rpbks,t) - x(bmx,bks,t-1) - gen(rxfb,t-trx(rxfb))*br/alf(rxfb,t-1) = 0.0;$$

(25) Loading-to-generation constraint for $rx = rifr$, where $ypui$ and $ymai$ are initial plutonium and minor-actinide loadings for these fsb technologies.

nc_rxifr(t)\$(ORD(t) GE ts):

$$x(met,rifr,t)*(ypui(rifr) + ymai(rifr)) - gen(rifr,t)/alf1(rifr,t) = 0.0;$$

(26) Loading-to-generation constraint for $rx = atw$, where $ypui$ and $ymai$ are initial plutonium and minor-actinide loadings for these fsb technologies.

nc_rxatw(t)\$(ORD(t) GE ts):

$$x(met,atw,t)*(ypui(atw) + ymai(atw)) - gen(atw,t)/alf1(atw,t) = 0.0 ;$$

(27) Overall plutonium fuel-fabrication mass balance for *fsb* metal-fuel-fabrication facility, where *tffmt* is the holdup time in the metal-fuel fabrication facility.

nc_ffpufsb(t)\$(ORD(t) GE ts):

$$\begin{aligned} & x(\text{met}, \text{atw}, t) * \text{ypui}(\text{atw}) + x(\text{met}, \text{rifr}, t) * \text{ypui}(\text{rifr}) \\ & - x(\text{rpu}, \text{ffmtrp}, t - t\text{ffmt}) - x(\text{rpu}, \text{ffmtsp}, t - t\text{ffmt}) \\ & - x(\text{rpu}, \text{ffmtps}, t - t\text{ffmt}) - x(\text{rpu}, \text{ffmtwp}, t - t\text{ffmt}) = 0.0; \end{aligned}$$

(28) Overall minor-actinide fuel-fabrication mass balance for *fsb* metal-fuel-fabrication facility, where *tffmt* is the holdup time in the metal-fuel fabrication facility.

nc_ffmafsb(t)\$(ORD(t) GE ts):

$$\begin{aligned} & x(\text{met}, \text{atw}, t) * \text{ymai}(\text{atw}) + x(\text{met}, \text{rifr}, t) * \text{ymai}(\text{rifr}) \\ & - x(\text{ma}, \text{ffmtms}, t - t\text{ffmt}) = 0.0; \end{aligned}$$

(29-31) Balance on discharge from *fsb* ($m = \{ma, fp, lfp\}$), where: (Note: INACTIVE).

- *fbdma* is *fsb* generation of $m = ma$ for disposal;
- *fbdfp* is *fsb* generation of $m = fp$ for disposal ;
- *fbdlfp* is *fsb* generation of $m = lfp$ for disposal.

(29) Discharge of $m = ma$ from $rx = rifr$ to $p = fpdifr$ fission-product disposal.

nc_fbdifma(t)\$(ORD(t) GE ts):

$$\begin{aligned} & x(\text{ma}, \text{fpdifr}, t) - \text{fbdma} * x(\text{wpu}, \text{rifr}, t - \text{trx}(\text{rifr})) \\ & - \text{fbdma} * x(\text{rpu}, \text{rifr}, t - \text{trx}(\text{rifr})) - \text{fbdma} * x(\text{ma}, \text{rifr}, t - \text{trx}(\text{rifr})) \\ & - \text{fbdma} * x(\text{rux}, \text{rifr}, t - \text{trx}(\text{rifr})) - \text{fbdma} * x(\text{rmx}, \text{rifr}, t - \text{trx}(\text{rifr})) \\ & - \text{fbdma} * x(\text{rhtg}, \text{rifr}, t - \text{trx}(\text{rifr})) - \text{fbdma} * x(\text{rfbr}, \text{rifr}, t - \text{trx}(\text{rifr})) = 0.0; \end{aligned}$$

(30) Discharge of $m = fp$ from $rx = rifr$ to *fpdifr* fission product disposal.

nc_fbdiffp(t)\$(ORD(t) GE ts):

$$\begin{aligned} & x(\text{fp}, \text{fpdifr}, t) - \text{fbdfp} * x(\text{wpu}, \text{rifr}, t - \text{trx}(\text{rifr})) \\ & - \text{fbdfp} * x(\text{rpu}, \text{rifr}, t - \text{trx}(\text{rifr})) - \text{fbdfp} * x(\text{ma}, \text{rifr}, t - \text{trx}(\text{rifr})) \\ & - \text{fbdfp} * x(\text{rux}, \text{rifr}, t - \text{trx}(\text{rifr})) - \text{fbdfp} * x(\text{rmx}, \text{rifr}, t - \text{trx}(\text{rifr})) \\ & - \text{fbdfp} * x(\text{rhtg}, \text{rifr}, t - \text{trx}(\text{rifr})) - \text{fbdfp} * x(\text{rfbr}, \text{rifr}, t - \text{trx}(\text{rifr})) = 0.0; \end{aligned}$$

(31) Discharge of $m = \text{lfp}$ from $rx = \text{rifr}$ to fpdifr fission-product disposal.

$\text{nc_fbdiflp}(t) \$ (\text{ORD}(t) \text{ GE ts})$:

$$\begin{aligned} & x(\text{fp}, \text{fpdifr}, t) - \text{fbdlfp} * x(\text{wpu}, \text{rifr}, t - \text{trx}(\text{rifr})) \\ & - \text{fbdlfp} * x(\text{rpu}, \text{rifr}, t - \text{trx}(\text{rifr})) - \text{fbdlfp} * x(\text{ma}, \text{rifr}, t - \text{trx}(\text{rifr})) \\ & - \text{fbdlfp} * x(\text{rux}, \text{rifr}, t - \text{trx}(\text{rifr})) - \text{fbdlfp} * x(\text{rmx}, \text{rifr}, t - \text{trx}(\text{rifr})) \\ & - \text{fbdlfp} * x(\text{rhtg}, \text{rifr}, t - \text{trx}(\text{rifr})) - \text{fbdlfp} * x(\text{rfbr}, \text{rifr}, t - \text{trx}(\text{rifr})) = 0.0; \end{aligned}$$

(32-34) Discharge from atw ($m = \{\text{ma}, \text{fp}, \text{lfp}\}$) (Note: INACTIVE).

(32) Discharge of $p = \text{ma}$ from $rx = \text{atw}$ to fpdatw fission-product disposal.

$\text{nc_fbdatma}(t) \$ (\text{ORD}(t) \text{ GE ts})$:

$$\begin{aligned} & x(\text{ma}, \text{fpdatw}, t) - \text{fbdma} * x(\text{wpu}, \text{atw}, t - \text{trx}(\text{atw})) \\ & - \text{fbdma} * x(\text{ma}, \text{atw}, t - \text{trx}(\text{atw})) \\ & - \text{fbdma} * x(\text{rux}, \text{atw}, t - \text{trx}(\text{atw})) - \text{fbdma} * x(\text{rmx}, \text{atw}, t - \text{trx}(\text{atw})) \\ & - \text{fbdma} * x(\text{rhtg}, \text{atw}, t - \text{trx}(\text{atw})) - \text{fbdma} * x(\text{rfbr}, \text{atw}, t - \text{trx}(\text{atw})) = 0.0; \end{aligned}$$

(33) Discharge of $m = \text{fp}$ from $rx = \text{atw}$ to fpdatw fission-product disposal.

$\text{nc_fbdatfp}(t) \$ (\text{ORD}(t) \text{ GE ts})$:

$$\begin{aligned} & x(\text{fp}, \text{fpdatw}, t) - \text{fbdfp} * x(\text{wpu}, \text{atw}, t - \text{trx}(\text{atw})) \\ & - \text{fbdfp} * x(\text{rpu}, \text{atw}, t - \text{trx}(\text{atw})) - \text{fbdfp} * x(\text{ma}, \text{atw}, t - \text{trx}(\text{atw})) \\ & - \text{fbdfp} * x(\text{rmx}, \text{atw}, t - \text{trx}(\text{atw})) \\ & - \text{fbdfp} * x(\text{rhtg}, \text{atw}, t - \text{trx}(\text{atw})) - \text{fbdfp} * x(\text{rfbr}, \text{atw}, t - \text{trx}(\text{atw})) = 0.0; \end{aligned}$$

(34) Discharge of $m = \text{lfp}$ from $rx = \text{atw}$ to fpdatw fission-product disposal.

$\text{nc_fbdatlp}(t) \$ (\text{ORD}(t) \text{ GE ts})$:

$$\begin{aligned} & x(\text{lfp}, \text{fpdatw}, t) - \text{fbdlfp} * x(\text{wpu}, \text{atw}, t - \text{trx}(\text{atw})) \\ & - \text{fbdlfp} * x(\text{rpu}, \text{atw}, t - \text{trx}(\text{atw})) - \text{fbdlfp} * x(\text{ma}, \text{rifr}, t - \text{trx}(\text{atw})) \\ & - \text{fbdlfp} * x(\text{rmx}, \text{atw}, t - \text{trx}(\text{atw})) \\ & - \text{fbdlfp} * x(\text{rhtg}, \text{atw}, t - \text{trx}(\text{atw})) - \text{fbdlfp} * x(\text{rfbr}, \text{atw}, t - \text{trx}(\text{atw})) = 0.0; \end{aligned}$$

(35) Maximum fraction of LWRs allowed to operate with MOX cores (fmx).

$\text{nc_fm}(t) \$ (\text{ORD}(t) \text{ GE ts})$:

$$\text{gen}(\text{rxot}, t) / \text{alf}(\text{rxot}, t) - \text{gen}(\text{rxmx}, t) / \text{alf}(\text{rxmx}, t) * (1 - \text{fm}) / \text{fm} > 0.0;$$

(36) Maximum MOX core fraction allowed in LWR technologies (*f_{mox}*).

nc_fmoxmax(t)\$(ORD(t) GE ts):

$$gen(rmx, t) / alf(rmx, t) * f_{mox}(t) - x(mox, rxmx, t) = 0.0;$$

(37) Minimum MOX core fraction allowed in LWR technologies (*f_{moxmin}*).

nc_fmoxmin(t)\$(ORD(t) GE ts):

$$gen(rmx, t) / alf(rmx, t) * f_{moxmin} - x(mox, rxmx, t) < 0.0;$$

(38) Limit on grid contribution allowed by FSB technologies (*ffsb*).

nc_fsbmax(t)\$(ORD(t) GE ts):

$$gen(rifr, t) + gen(atw, t) < f_{fsb} * gent(t);$$

(39) Upper limit on rate of *gen(nucl, t)* introduction with respect to the overall growth rate of nuclear generation, *gent(t)*.

nc_grow(nucl, t)\$(ORD(t) GE ts):

$$d_{cap}(nucl, t) < cap(nucl, t-1) * f_{grow}(nucl, t) + f_{seed}(nucl) * gent(t);$$

(40) Limit on rates of decommissioning of generation technologies (Note: INACTIVE)

nc_dec(nucl, t)\$(ORD(t) GE ts):

$$d_{cap}(nucl, t) < f_{decrx}(nucl) * cap(nucl, t);$$

(41) Balance on *m = du* for *rxfb* blanket; i.e., a constraint on the rate of *rxfb* blanket refurbishment with fresh *du*.

nc_dubk(t)\$(ORD(t) GE ts):

$$x(du, fbbk, t) - gen(rxfb, t) * br / alf(rxfb, t) < 0.0;$$

(42-46) Balances on cooling storage, *p = cs*, for both *m = rux* and *rmx*, which are tracked separately; the following definitions and algorithms are used (refer to Table B-I for more details); *p = rpcs* is the feed rate of spent fuel (*rux* or *rmx*) to reprocessing directly from the cooling storage; *p = rpis* is the corresponding feed rate from interim storage, *is*. The materials of concern include *m = {rux, lru, lnu, lwu, rmx, mox}*. Note that *p = {rpcs, rpis}* deal only with SNF from *rx = {rxot, rxmx, rxhg, rxfb}* technologies.

(42) Cooling storage ($p = cs$) balance for $rxot$ and $rxmx$ technologies; SNF from both is sent to cs together. The (linear) function $frxcs(nucl,t)$ “eases” SNF from cs to is at the beginning of the optimization, since at the start (year 2000) all SNF is technically in cs , although technically much of this inventory can be classified as “cooled” and ready for interim storage status, albeit such facilities do not exist at present.

nc_csru(t)\$(ORD(t) GE ts):

$$\begin{aligned} & x(rux,cs,t) - x(rux,cs,t-1) - x(lnu,rxot,t-trx(rxot)) \\ & - x(lru,rxot,t-trx(rxot)) - x(lwu,rxot,t-trx(rxot)) \\ & - x(lnu,rxmx,t-trx(rxmx)) - x(lru,rxmx,t-trx(rxmx)) \\ & - x(lwu,rxmx,t-trx(rxmx)) + x(rux,cs,t-trxcs(rxot))*frxcs(rxot,t) \\ & + x(rux,cs,t)/(trxcs(rxot) + tinc)*(1. - frxcs(rxot,t)) \\ & + x(rux,rpcs,t) + x(rux,sepcs,t) + x(rux,ddcs,t) > 0.0 ; \end{aligned}$$

(43) Minimum cooling-storage inventory constraint.

nc_csrumin(t)\$(ORD(t) GE ts):

$$\begin{aligned} & x(rux,cs,t) > x(lnu,rxot,t-trx(rxot)) + x(lru,rxot,t-trx(rxot)) \\ & + x(lwu,rxot,t-trx(rxot)) + x(lnu,rxmx,t-trx(rxmx)) \\ & + x(lru,rxmx,t-trx(rxmx)) + x(lwu,rxmx,t-trx(rxmx)); \end{aligned}$$

(44) MOX cs balance for $rxmx$ generation technology; the function $frxcs(nucl,t)$ is an exogenous means to make the transition from cs to is at the beginning of the optimization.

nc_csmx(t)\$(ORD(t) GE ts):

$$\begin{aligned} & x(rmx,cs,t) - x(rmx,cs,t-1) - x(mox,rxmx,t-trx(rxmx)) \\ & + x(rmx,cs,t-trxcs(rxmx))*frxcs(rxmx,t) \\ & + x(rmx,rpcs,t) + x(rmx,sepcs,t) + x(rmx,ddcs,t) = 0.0; \end{aligned}$$

(45) Balance on SNF from $p = rxhg$ (HTGR) deliveries; $m = rhtg$ is SNF from MOX-fueled $rxhg$ technology; the function $frxcs(nucl,t)$ is an exogenous means to make the transition from cs to is at the beginning of the optimization.

nc_cshtg(t)\$(ORD(t) GE ts):

$$\begin{aligned} & x(rhtg,cs,t) - x(rhtg,cs,t-1) - x(rhtg,rxmx,t-trx(rxhg)) \\ & + x(rhtg,cs,t-trxcs(rxhg))*frxcs(rxhg,t) \\ & + x(rhtg,rpcs,t) + x(rhtg,sepcs,t) + x(rhtg,ddcs,t) = 0.0; \end{aligned}$$

(46) Cooling-storage balance for $rxfb$ SNF deliveries; $rfbr$ is SNF from MOX-fueled $rxfr$; the function $frxcs(nucl,t)$ is an exogenous means to make the transition from cs to is at the beginning of the optimization.

nc_csfrbr(t)\$(ORD(t) GE ts):

$$\begin{aligned} & x(rfbr,cs,t) - x(rfbr,cs,t-1) - x(rfbr,rxmx,t-trx(rxfb)) \\ & + x(rfbr,cs,t-trxcs(rxfb))*frxcs(rxfb,t) \\ & + x(rfbr,rpcs,t) + x(rfbr,sepcs,t) + x(rfbr,ddcs,t) = 0.0; \end{aligned}$$

(47-50) Minimum-time constraint for SNF in cooling storage (Note: INACTIVE).

(47) Minimum time in cs for $m = rux$ (spent UOX).

nc_tcsru(t)\$(ORD(t) GE ts):

$$\begin{aligned} & x(rux,cs,t) - x(lnu,rxot,t-trx(rxot)) - x(lru,rxot,t-trx(rxot)) \\ & - x(lwu,rxot,t-trx(rxot)) - x(lnu,rxmx,t-trx(rxmx)) \\ & - x(lru,rxmx,t-trx(rxmx)) - x(lwu,rxmx,t-trx(rxmx)) > 0.0; \end{aligned}$$

(48) Minimum time in cs for $m = rmx$ (spent MOX).

nc_tcsrmx(t)\$(ORD(t) GE ts):

$$x(rmx,cs,t) - x(mox,rxmx,t-trx(rxmx)) > 0.0;$$

(49) Minimum time in cs for $m = rhtg$ (SNF from $rxhg$).

nc_tcsrht(t)\$(ORD(t) GE ts):

$$x(rhtg,cs,t) - x(mox,rxhg,t-trx(rxhg)) > 0.0;$$

(50) Minimum time in cs for $m = rfbr$ (SNF from $rxfb$).

nc_tcsrfbr(t)\$(ORD(t) GE ts):

$$x(rfbr,cs,t) - x(mox,rxfb,t-trx(rxfb)) > 0.0;$$

(51) Constraint imposed on cs capacity limit, $bncs(kg)$. One option relates $bncs$ to the total amount of core loadings, as follows:

$$bncs = \sum_{t=trx}^{t-trx-ncs} \sum_{rx} gen(rx,t) / alf(rx,t);$$

The other option is simply to specify the value of $bncs$, which is the option taken here.

nc_cscap(t)\$(ORD(t) GE ts):

$$x(rux,cs,t) + x(rmx,cs,t) + x(rhtg,cs,t) + x(rfbr,cs,t) < bncs;$$

(52-60) Interim storage (is) mass balances for rux and rmx tracked separately, where: $p = ddis$ is spent fuel to dd (direct disposal repository) from is and $ddcs$ is spent fuel to dd from cs . The stream $p = sepi$ is material sent to separations ($p = sep$) in preparation for exposure to $fsb = \{rifr, atw\}$. Interim storage of spent UOX ($m = rux$) is designated as $p = isu$, and that for spent MOX ($m = rmx$) is $p = isp$.

(52) Interim storage balance for $m = rux$.

nc_isrux(t)\$(ORD(t) GT ts):

$$\begin{aligned} & x(rux, isu, t) - x(rux, isu, t-1) + x(rux, ddis, t) + x(rux, rpis, t) \\ & + x(rux, sepi, t) - x(rux, cs, t - trxc(rxt)) * frxc(rxt, t) \\ & - x(rux, cs, t) / (trxc(rxt) + tinc) * (1 - frxc(rxt, t)) = 0.0; \end{aligned}$$

(53) Interim storage balance for $m = rmx$.

nc_isrux(t)\$(ORD(t) GE ts):

$$\begin{aligned} & x(rmx, isp, t) - x(rmx, isp, t-1) + x(rmx, ddis, t) + x(rmx, rpis, t) \\ & + x(rmx, sepi, t) - x(rmx, cs, t - trxc(rmx)) = 0.0; \end{aligned}$$

(54) Interim storage (is) balance for rxhg-originated SNF (mainly $m = rhtg$ or $mox \rightarrow rmx$)

nc_ishtgr(t)\$(ORD(t) GE ts):

$$\begin{aligned} & x(rhtg, isp, t) - x(rhtg, isp, t-1) + x(rhtg, ddis, t) + x(rhtg, rpis, t) \\ & + x(rhtg, sepi, t) - x(rhtg, cs, t - trxc(rxhg)) = 0.0; \end{aligned}$$

(55) Interim storage (is) balance for rxfb-originated SNF (mainly $m = rfbr$ or $mox \rightarrow rmx$)

nc_isfbr(t)\$(ORD(t) GE ts):

$$\begin{aligned} & x(rfbr, isp, t) - x(rfbr, isp, t-1) + x(rfbr, ddis, t) + x(rfbr, rpis, t) \\ & + x(rfbr, sepi, t) - x(rfbr, cs, t - trxc(rxfb)) = 0.0; \end{aligned}$$

(56) Interim storage (is) capacity limits set as a number $bnisrx(nucl)$ core loadings.

nc_iscap(t)\$(ORD(t) GE ts):

$$\begin{aligned} & x(rux, isu, t) + x(rmx, isp, t) + x(rhtg, isp, t) + x(rfbr, isp, t) \\ & - bnisrx(rxot) * gen(rxot, t) / alf(rxot, t) \\ & - bnisrx(rxmx) * gen(rxmx, t) / alf(rxmx, t) \\ & - bnisrx(rxhg) * gen(rxhg, t) / alf(rxhg, t) - bnisrx(rxfb) * gen(rxfb, t) / alf(rxfb, t) < 0.0; \end{aligned}$$

(57) Interim storage (is) overall balance and backflow constraint imposed on $m = rux$.

nc_bfisrux(t)\$(ORD(t) GE ts10):

$$\begin{aligned} & x(rux, rpis, t) + x(rux, ddis, t) + x(rux, sepis, t) + x(rux, isu, t) \\ & - x(rux, isu, t-1) > 0.0; \end{aligned}$$

(58) Interim storage(is) overall balance and backflow constraint imposed on $m = rmx$.

nc_bfisrmx(t)\$(ORD(t) GE ts):

$$\begin{aligned} & x(rmx, rpis, t) + x(rmx, ddis, t) + x(rmx, sepis, t) \\ & + x(rux, isp, t) - x(rux, isp, t-1) > 0.0; \end{aligned}$$

(59) Interim storage (is) overall balance and backflow constraint on $rxhg$ -originated SNF.

nc_bfisrhtg(t)\$(ORD(t) GE ts):

$$\begin{aligned} & x(rhtg, rpis, t) + x(rhtg, ddis, t) + x(rhtg, sepcs, t) \\ & + x(rhtg, isp, t) - x(rhtg, isp, t-1) > 0.0 ; \end{aligned}$$

(60) Interim storage (is) overall balance and backflow constraint for $rxfb$ -originated SNF.

nc_bfisrfbr(t)\$(ORD(t) GE ts):

$$\begin{aligned} & x(rfbr, rpis, t) + x(rfbr, ddis, t) + x(rfbr, sepis, t) \\ & + x(rfbr, isp, t) - x(rfbr, isp, t-1) > 0.0; \end{aligned}$$

(61) Lower capacity limits for reprocessing plant, $p = rpxx$, where: (Note: INACTIVE)

- $rpcs$ = feed spent fuel to rp from cs ;
- $rpis$ = feed spent fuel to rp from is ;
- $rpbks$ = feed spent fuel to rp from bks ;
- $pn = pnrux*(1 - fmox(t-1)) + pnrmx*fmox(t-1)$;
- $pnruxdn$ = lower capacity factor;
- $pnurxup$ = upper capacity factor;

$nc_rpcapdn(t)$(ORD(t) GE trpf):$

$$\begin{aligned}
 & x(rux, rpcs, t-trp) + x(rux, rpis, t-trp) \\
 & + x(rmx, rpcs, t-trp) + x(rmx, rpis, t-trp) \\
 & + x(rhtg, rpcs, t-trp) + x(rhtg, rpis, t-trp) \\
 & + x(rfbr, rpcs, t-trp) + x(rfbr, rpis, t-trp) \\
 & + x(bmx, rpbks, t-trp) \\
 & - pnruxdn * gen(rxot, t) / alf(rxot, t) \\
 & - pnruxdn * fmox(t) * gen(rmx, t) / alf(rmx, t) \\
 & - pnruxdn * gen(rhcg, t) / alf(rhcg, t) \\
 & - pnbmxdn * gen(rxfb, t) / alf(rxfb, t) > 0.0;
 \end{aligned}$$

(62) Upper capacity limits for reprocessing plant, $rp = rpxx$: (Note: INACTIVE)

$nc_rpcapup(t)$(ORD(t) GE trpf):$

$$\begin{aligned}
 & x(rux, rpcs, t-trp) + x(rux, rpis, t-trp) \\
 & + x(rmx, rpcs, t-trp) + x(rmx, rpis, t-trp) \\
 & + x(rhtg, rpcs, t-trp) + x(rhtg, rpis, t-trp) \\
 & + x(rfbr, rpcs, t-trp) + x(rfbr, rpis, t-trp) \\
 & + x(bmx, rpbks, t-trp) \\
 & - pnruxup * gen(rxot, t) / alf(rxot, t) \\
 & - pnruxup * fmox(t) * gen(rmx, t) / alf(rmx, t) \\
 & - pnruxup * gen(rhcg, t) / alf(rhcg, t) \\
 & - pnbmxup * gen(rxfb, t) / alf(rxfb, t) < 0.0;
 \end{aligned}$$

(63) Deployment rate limit for reprocessing plant, $rp = rpxx$ (Note: INACTIVE).

$nc_rprate(t)$(ORD(t) GE trpf):$

$$\begin{aligned}
 & x(rux, rpcs, t) + x(rux, rpis, t) + x(rmx, rpcs, t) + x(rmx, rpis, t) \\
 & + x(rhtg, rpcs, t) + x(rhtg, rpis, t) + x(rfbr, rpcs, t) + x(rfbr, rpis, t) \\
 & + x(bmx, rpbk, t) \\
 & - rpratelim * (x(rux, rpcs, t-1) + x(rux, rpis, t-1) \\
 & + x(rmx, rpcs, t-1) + x(rmx, rpis, t-1) + x(rhtg, rpcs, t-1) \\
 & + x(rhtg, rpis, t-1) \\
 & + x(rfbr, rpcs, t-1) + x(rfbr, rpis, t-1) + x(bmx, rpbks, t-1)) < 0.0;
 \end{aligned}$$

(64) Capacity limit for reprocessing plant, $p = rpxx$, where $rpcap(t)$ is exogenous input.

nc_rpcap(t)\$(ORD(t) GE ts):

$$\begin{aligned} & x(rux, rpcs, t) + x(rux, rpis, t) + x(rmx, rpcs, t) + x(rmx, rpis, t) \\ & + x(rhtg, rpcs, t) + x(rhtg, rpis, t) + x(rfbr, rpcs, t) + x(rfbr, rpis, t) \\ & + x(bmx, rpbks, t) < rpcap(t); \end{aligned}$$

(65) Constraint to assure $(isu + isp) \rightarrow rpis$ flow (Note: INACTIVE).

nc_isrp(t)\$(ORD(t) GE ts1)

$$\begin{aligned} & x(rux, isu, t-1) + x(rmx, isp, t-1) + x(rhtg, isp, t-1) + x(rfbr, isp, t-1) \\ & - x(rux, rpis, t) - x(rmx, rpis, t) - x(rhtg, rpis, t) - x(rfbr, rpis, t) > 0.0; \end{aligned}$$

(66) Plutonium balance on reprocessing plant, $p = rpxx$, where $pudrp$ = direct disposal of separated plutonium from $p = rp$; $pudpus$ = direct disposal of separated plutonium from $p = pus$; and pud = direct disposal of separated plutonium = $pudrp + pudpus$ (Note: INACTIVE).

nc_purp(t)\$(ORD(t) GE ts):

$$\begin{aligned} & x(rpu, ffmxrp, t) + x(rpu, ffmtrp, t) + x(rpu, pudrp, t) \\ & + x(rpu, pus, t) - x(rpu, pus, t-1) \\ & - x(rux, rpis, t-trp) * ypuf(rxot) * yrp - x(rux, rpcs, t-trp) * ypuf(rxot) * yrp \\ & - x(rmx, rpis, t-trp) * ypuf(rmxmx) * yrp - x(rmx, rpcs, t-trp) * ypuf(rmxmx) * yrp \\ & - x(rhtg, rpis, t-trp) * ypuf(rxhg) * yrp - x(rhtg, rpcs, t-trp) * ypuf(rxhg) * yrp \\ & - x(rfbr, rpis, t-trp) * ypuf(rxfb) * yrp - x(rfbr, rpcs, t-trp) * ypuf(rxfb) * yrp \\ & - x(bmx, rpb, t-trp) * ybpu > 0.0; \end{aligned}$$

(67) MOX recycle limit in $rxot$, where $ncyc$ = number of recycles and $incyc = 1/ncyc$.

nc_ncyclwr(t)\$(ORD(t) GE ts):

$$\begin{aligned} & x(rmx, rpcs, t) + x(rmx, rpis, t) \\ & - x(mox, rxmx, t-trx(rxmx)) * (1 - incyc) < 0.0; \end{aligned}$$

(68) MOX recycle limit in $rxhg$.

nc_ncychtg(t)\$(ORD(t) GE ts):

$$\begin{aligned} & x(rhtg, rpcs, t) + x(rhtg, rpis, t) \\ & - x(mox, rxhg, t-trx(rxhg)) * (1 - incyc) < 0.0; \end{aligned}$$

(69) MOX recycle limit in *rxfb*.

nc_ncycfbr(t)\$(ORD(t) GE ts):

$$x(rfbr, rpcs, t) + x(rfbr, rpis, t) - x(mox, rxfb, t - trx(rxfb)) * (1 - incyc) < 0.0;$$

(70) Material balance on reactor-exposed uranium storage, $p = rus$, where ybp_u = fraction plutonium in *rxfb* blanket; and $rpbks$ = feed spent fuel sent to rp from *rxfb* blanket storage, $p = bks$.

nc_rus(t)\$(ORD(t) GE ts):

$$\begin{aligned} & x(ru, rus, t) + x(ru, bl, t) + x(ru, cv, t) + x(ru, ffmxps, t) \\ & + x(ru, ffmxrp, t) + x(ru, ffmxwp, t) - x(ru, rus, t-1) \\ & - x(bmx, rpbkst-trp) * (1 - ybp_u) * yrp \\ & - x(rmx, rpcs, t-trp) * (1 - ypuf(rmx) - ymaf(rmx)) * yrp \\ & - x(rmx, rpis, t-trp) * (1 - ypuf(rmx) - ymaf(rmx)) * yrp \\ & - x(rhtg, rpcs, t-trp) * (1 - ypuf(rxhg) - ymaf(rxhg)) * yrp \\ & - x(rhtg, rpis, t-trp) * (1 - ypuf(rxhg) - ymaf(rxhg)) * yrp \\ & - x(rfbr, rpcs, t-trp) * (1 - ypuf(rxfb) - ymaf(rxfb)) * yrp \\ & - x(rfbr, rpis, t-trp) * (1 - ypuf(rxfb) - ymaf(rxfb)) * yrp \\ & - x(rux, rpcs, t-trp) * (1 - ypuf(rxot) - ymaf(rxot)) * yrp \\ & - x(rux, rpis, t-trp) * (1 - ypuf(rxot) - ymaf(rxot)) * yrp \\ & - x(rmet, sep, t-tsep) * (1 - ypuf(rifr) - ymaf(rifr)) * ysep = 0.0; \end{aligned}$$

(71) Plutonium balance on separated plutonium storage, $p = pus$.

nc_pus(t)\$(ORD(t) GE ts):

$$\begin{aligned} & x(rpu, pus, t) - x(rpu, pus, t-1) + x(rpu, ffmxps, t) + x(rpu, ffmtps, t) \\ & + x(rpu, ffmxrp, t) + x(rpu, ffmtrp, t) + x(rpu, ffmtsp, t) \\ & + x(rpu, ffmxwp, t) + x(rpu, ffmtwp, t) + x(rpu, pudrp, t) \\ & + x(rpu, pudpus, t) \\ & - x(rux, rpis, t-trp) * ypuf(rxot) * yrp - x(rux, rpcs, t-trp) * ypuf(rxot) * yrp \\ & - x(rmx, rpis, t-trp) * ypuf(rmx) * yrp - x(rmx, rpcs, t-trp) * ypuf(rmx) * yrp \\ & - x(rhtg, rpis, t-trp) * ypuf(rxhg) * yrp - x(rhtg, rpcs, t-trp) * ypuf(rxhg) * yrp \\ & - x(rfbr, rpis, t-trp) * ypuf(rxfb) * yrp - x(rfbr, rpcs, t-trp) * ypuf(rxfb) * yrp \\ & - x(bmx, rpbks, t-trp) * ybp_u \\ & - x(rmet, sep, t-tsep) * (ypuf(rifr) + ypuf(atw)) * ysep = 0.0; \end{aligned}$$

(72) Separated reactor-grade plutonium (*rpu*) storage capacity limit.

nc_puscap(t)\$(ORD(t) GE ts)

$$x(rpu, pus, t) < bnpus;$$

(73) Separated plutonium storage ($p = pus$) forced depletion rate (Note: INACTIVE).

nc_pusdepl(t)\$(ORD(t) GE ts10):

$$x(rpu,ffmtps,t) > (bnpus - x(rpu,pus,t))/tpus;$$

or

$$\begin{aligned} & gen(atw,t)/alf1(atw,t) + gen(rifr,t)/alf1(rifr,t) \\ & > (bnpus - x(rpu,pus,t))/tpus; \end{aligned}$$

or

$$\begin{aligned} & x(met,atw,t)*ymai(atw) + x(met,rifr,t)*ymai(rifr) \\ & > (bnpus - x(rpu,pus,t))/tpus; \end{aligned}$$

(74) Minor-actinide ($m = ma$) balance, where $ybma$ = fraction of ma in bmx , and $ymaf(rxxx)$ = final ma content in respective SNF.

nc_mas(t)\$(ORD(t) GE ts):

$$\begin{aligned} & x(ma,mas,t) - x(ma,mas,t-1) + x(ma,ffmtms,t) + x(ma,mad,t) \\ & - x(rux,rpcs,t-trp)*ymaf(rxot) - x(rux,rpis,t-trp)*ymaf(rxot) \\ & - x(rmx,rpcs,t-trp)*ymaf(rmxmx) - x(rmx,rpis,t-trp)*ymaf(rmxmx) \\ & - x(rhtg,rpcs,t-trp)*ymaf(rxhg) - x(rhtg,rpis,t-trp)*ymaf(rxhg) \\ & - x(rfbr,rpcs,t-trp)*ymaf(rxfb) - x(rfbr,rpis,t-trp)*ymaf(rxfb) \\ & - x(rmet,sep,t-tsep)*ymaf(rifr) - x(rmet,sep,t-tsep)*ymaf(atw) \\ & - x(bmx,rpbks,t-trp)*ybma = 0.0; \end{aligned}$$

(75) Separated reactor-grade plutonium (rpu) storage (pus) capacity limit.

nc_mascap(t)\$(ORD(t) GE ts):

$$x(ma,mas,t) < bnmas;$$

(76) Separated reactor-grade plutonium (rpu) storage (pus) forced depletion constraint (Note: INACTIVE).

nc_masdepl(t)\$(ORD(t) GE ts10):

$$x(ma,ffmtms,t) > (bnmas - x(ma,mas,t))/tmas;$$

(77) Mass balance on spent fuel storage for *fsb* technologies.

nc_sfs(t)\$(ORD(t) GE ts):

$$x(rmet,sfs,t) - x(rmet,sf,t-1) - x(met,atw,t-trx(atw)) \\ - x(met,rifr,t-trx(rifr)) + x(rmet,sep,t) = 0.0;$$

(78) Enforce connection of $p = sep$ with $p = ffmtsp$ (metal-fuel fabrication from materials derived from $p = sep$).

nc_sfsff(t)\$(ORD(t) GE ts)

$$x(rmet,sep,t-tsep) - x(met,ffmtsp,t) = 0.0 ;$$

(79) Fission-products balance over combined reprocessing ($p = rpxx$) and separations ($p = sep$) systems, where $ybfp$ = fraction fp in bmx and the materials of consideration are $m = \{fp, ru, rmx, bmx, rhtg, rfbr, rmet\}$

nc_fprp(t)\$(ORD(t) GE ts):

$$x(fp,fp,t) - x(fp,fp,t-1) + x(fp,fpd,t) \\ - x(rux,rpcs,t-trp)*yfp(rxot) - x(rux,rpis,t-trp)*yfp(rxot) \\ - x(rmx,rpcs,t-trp)*yfp(rmxmx) - x(rmx,rpis,t-trp)*yfp(rmxmx) \\ - x(rhtg,rpcs,t-trp)*yfp(rxhg) - x(rhtg,rpis,t-trp)*yfp(rxhg) \\ - x(rfbr,rpcs,t-trp)*yfp(rxfb) - x(rfbr,rpis,t-trp)*yfp(rxfb) \\ - x(bmx,rpbks,t-trp)*ybfp \\ - x(rux,sepcs,t-tsep)*yfp(rxot) - x(rux,sepis,t-tsep)*yfp(rxot) \\ - x(rmx,sepcs,t-tsep)*yfp(rmxmx) - x(rmx,sepis,t-tsep)*yfp(rmxmx) \\ - x(rhtg,sepcs,t-tsep)*yfp(rxhg) - x(rhtg,sepis,t-tsep)*yfp(rxhg) \\ - x(rfbr,sepcs,t-tsep)*yfp(rxfb) - x(rfbr,sepis,t-tsep)*yfp(rxfb) \\ - x(rmet,sep,t-tsep)*yfp(rifr) - x(rmet,sep,t-tsep)*yfp(atw) = 0.0;$$

(80) Capacity constraint imposed on separations, $p = sep$, where $pnsepup$ is an upper capacity factor in terms of *fsb* core loadings.

nc_sepcap(t)\$(ORD(t) GE ts):

$$x(rux,sepcs,t-tsep) + x(rux,sepis,t-tsep) \\ + x(rmx,sepcs,t-tsep) + x(rmx,sepis,t-tsep) \\ + x(rhtg,sepcs,t-tsep) + x(rhtg,sepis,t-tsep) \\ + x(rfbr,sepcs,t-tsep) + x(rfbr,sepis,t-tsep) \\ + x(rmet,sep,t-tsep) \\ - pnsepup*gen(atw,t)/alf1(atw,t) \\ - pnsepup*gen(rifr,t)/alf1(rifr,t) < 0.0;$$

(81) Balance over fission-product disposal, $p = fpd$.

nc_fpd(t)\$(ORD(t) GE ts)

$$x(fp,dd,t) - x(fp,dd,t-1) - x(fp,fpd,t) = 0.0;$$

(82) Balance over minor-actinide disposal, $p = mad$.

nc_mad(t)\$(ORD(t) GE ts):

$$x(ma,dd,t) - x(ma,dd,t-1) - x(ma,mad,t) = 0.0;$$

(83) Balance over separated plutonium “disposal”, $p = pud$, where $pudrp$ represents the stream of plutonium sent to pud from rp ; $pudps$ represents plutonium sent to pud from separated plutonium storage, $p = pus$.

nc_pud(t)\$(ORD(t) GE ts):

$$x(rpu,pud,t) - x(rpu,pudrp,t) - x(rpu,pudpus,t) - x(rpu,pud,t-1) = 0.0;$$

(84) "Disposed"/residual plutonium capacity constraint, $pudcap(t)$.

nc_pdcap(t)\$(ORD(t) GE ts).

$$x(rpu,pud,t) < pudcap(t);$$

(85) Mass balance for $m = rux$ over the repository, $p = dd$.

nc_ddru(t)\$(ORD(t) GE ts):

$$x(rux,dd,t) - x(rux,dd,t-1) - x(rux,ddcs,t) - x(rux,ddis,t) = 0.0;$$

or alternatively, either of the following two constraints can be used/explored:

$$- x(rux,ddcs,t)$(ORD(t) GE ts10)$$

and

$$- x(rux,ddis,t)$(ORD(t) GE ts10) = 0.0;$$

or

$$- x(rux,ddcs,t)*frxcs(rxot,t) - x(rux,ddis,t)*frxcs(rxot,t) = 0.0;$$

where $ts10 = ts + 10$.

(86) Mass balance over $m = rmx$ at the repository, $p = dd$.

nc_ddmx(t)\$(ORD(t) GE ts):

$$x(rmx,dd,t) - x(rmx,dd,t-1) - x(rmx,ddcs,t) - x(rmx,ddis,t) = 0.0;$$

or alternatively, either of the following two constraints can be used/explored:

- $x(rmx,ddcs,t)$(ORD(t) GE ts10)$

and

- $x(rmx,ddis,t)$(ORD(t) GE ts10) = 0.0;$

or

- $x(rmx,ddcs,t)*frxs(rmx,t) - x(rmx,ddis,t)*frxs(rmx,t) = 0.0$;

(87) Mass balance over $m = rhtgr$ at the repository, $p = dd$.

nc_ddhtgr(t)\$(ORD(t) GE ts):

$$x(rhtg,dd,t) - x(rhtg,dd,t-1) - x(rhtg,ddcs,t) - x(rhtg,ddis,t) = 0.0;$$

(88) Mass balance over $m = rfbr$ at the repository, $p = dd$.

nc_ddfbr(t)\$(ORD(t) GE ts):

$$x(rfbr,dd,t) - x(rfbr,dd,t-1) - x(rfbr,ddc,t) - x(rfbr,ddis,t) = 0.0;$$

(89) Backflow constraint applied to the repository, $p = dd$.

nc_ddbf(t)\$(ORD(t) GE ts):

$$x(rux,dd,t) + x(rmx,dd,t) + x(rhtg,dd,t) + x(rfbr,dd,t) + x(fp,dd,t) \\ - x(rux,dd,t-1) - x(rmx,dd,t-1) - x(rhtg,dd,t-1) - x(rfbr,dd,t-1) - x(fp,dd,t-1) > 0.0;$$

(90) Constraint on repository fill-rate, where $pndd$ is a fill-rate factor, and $ddcap(t)$ is an exogenous time-dependent capacity (kg). (Note: INACTIVE).

nc_ddrate(t)\$(ORD(t) GE ts1):

$$x(rux,dd,t) + x(rmx,dd,t) + x(rhtg,dd,t) + x(rfbr,dd,t) + x(fp,dd,t) \\ + x(ma,dd,t) - x(rux,dd,t-1) - x(rmx,dd,t-1) - x(rhtg,dd,t-1) \\ - x(rfbr,dd,t-1) - x(fp,dd,t-1) - x(ma,dd,t-1) \\ - pndd*gen(rxot,t)/alf(rxot,t) - pndd*gen(rmx,t)/alf(rmx,t) \\ - pndd*gen(rxhg,t)/alf(rxhg,t) - pndd*gen(rxfb,t)/alf(rxfb,t) \\ < ddcap(t);$$

or, alternatively, the following three constraints have also been explored:

$$x(rux,dd,t) - x(rux,dd,t-1) - pndd*gen(rxot,t)/alf(rxot,t) < 0.0;$$

$$x(rux,ddcs,t) + x(rux,ddis,t) - pndd*gen(rxot,t)/alf(rxot,t) < 0.0;$$

$$\begin{aligned} & x(rux,ddcs,t) + x(rux,ddis,t) + x(rmx,ddcs,t) + x(rmx,ddis,t) \\ & + x(rhtg,ddcs,t) + x(rhtg,ddis,t) + x(rfbr,ddcs,t) + x(rfbr,ddis,t) \\ & - pndd*gen(rxot,t)/alf(rxot,t) - pndd*gen(xmx,t)/alf(xmx,t) \\ & - pndd*gen(rxhg,t)/alf(rxhg,t) - pndd*gen(rxfb,t)/alf(rxfb,t) \\ & < ddcap(t); \end{aligned}$$

(91) Constraint on $p = dd$ fill rate for first $ts10$ (10) years after start of optimization ($ts = 2000$) (Note: INACTIVE).

nc_ddratei(t)\$((ORD(t) GE ts) AND (ORD(t) LE ts10)):

$$\begin{aligned} & x(rux,dd,t) + x(rmx,dd,t) + x(rhtg,dd,t) + x(rfbr,dd,t) \\ & + x(fp,dd,t) + x(ma,dd,t) \\ & - x(rux,dd,t-1) - x(rmx,dd,t-1) - x(rhtg,dd,t-1) - x(rfbr,dd,t-1) \\ & - x(fp,dd,t-1) - x(ma,dd,t-1) \\ & < gen(rxot,t)/alf(rxot,t); \end{aligned}$$

or

$$< x(rux,cs,1999)/100;$$

or

$$< ddcap(t)/10;$$

or

$$= 0.0;$$

or the alternative constraint was explored:

$$\begin{aligned} & x(rux,ddcs,t) + x(rux,ddis,t) + x(rmx,ddcs,t) + x(rmx,ddis,t) \\ & + x(rhtg,ddcs,t) + x(rhtg,ddis,t) + x(rfbr,ddcs,t) + x(rfbr,ddis,t) \\ & < ddcap(t); \end{aligned}$$

(92) Repository SNF capacity constraint, $ddcap(t)$.

nc_ddcap(t)\$ (ORD(t) GE ts):

$$\begin{aligned} & x(rux,dd,t) + x(rmx,dd,t) + x(rhtg,dd,t) \\ & + x(fbr,dd,t) + x(fp,dd,t) + x(ma,dd,t) < ddcap(t); \end{aligned}$$

(93) Mass balance for fuel-fabrication ($p = \text{ffxxx}$) and reactor ($p = \text{nucl}$) for UOX.

nc_ffrxux(t)\$(ORD(t) GE ts):

$$\begin{aligned} & x(\text{lru}, \text{rxot}, t) + x(\text{lru}, \text{rxmx}, t) + x(\text{lwu}, \text{rxot}, t) \\ & + x(\text{lru}, \text{rxmx}, t) + x(\text{lru}, \text{rxmx}, t) + x(\text{lwu}, \text{rxmx}, t) \\ & - x(\text{lru}, \text{ffux}, t - \text{tffux}) - x(\text{lru}, \text{ffux}, t - \text{tffux}) - x(\text{lwu}, \text{ffux}, t - \text{tffux}) < 0.0; \end{aligned}$$

(94) Mass balance for fuel-fabrication ($p = \text{ffxxx}$) and reactor ($p = \text{rx}$) for MOX.

nc_ffrxmx(t)\$(ORD(t) GE ts):

$$\begin{aligned} & x(\text{mox}, \text{rxmx}, t) * \text{ypui}(\text{rxmx}) + x(\text{mox}, \text{rxhg}, t) * \text{ypui}(\text{rxhg}) + x(\text{mox}, \text{rxfb}, t) * \text{ypui}(\text{rxfb}) \\ & - x(\text{rpu}, \text{ffmxrp}, t - \text{tffmx}) - x(\text{rpu}, \text{fmxps}, t - \text{tffmx}) \\ & - x(\text{wpu}, \text{ffmxwp}, t - \text{tffmx}) < 0.0; \end{aligned}$$

(95) Mass balance for fuel-fabricaton ($p = \text{ffxxx}$) and reactor ($p = \text{fsb}$) for metallic fuel, $p = \text{met}$.

nc_ffrxmt(t)\$(ORD(t) GE ts):

$$\begin{aligned} & x(\text{met}, \text{rifr}, t) * \text{ypui}(\text{rifr}) + x(\text{met}, \text{atw}, t) * \text{ypui}(\text{atw}) \\ & + x(\text{met}, \text{rifr}, t) * \text{ymai}(\text{rifr}) + x(\text{met}, \text{atw}, t) * \text{ymai}(\text{atw}) \\ & - x(\text{rpu}, \text{ffmtrp}, t - \text{tffmt}) - x(\text{rpu}, \text{ffmtps}, t - \text{tffmt}) - x(\text{wpu}, \text{ffmtwp}, t - \text{tffmt}) \\ & - x(\text{ma}, \text{ffmtms}, t - \text{tffmt}) < 0.0; \end{aligned}$$

This page is intentionally left blank.

Appendix F: Elaboration of Vintaging and Discounting for the Cost-Based Objective Function

A limitation of the earlier version of the FCOPT model was the lack of a cost penalty incurred when one reactor technology became slightly more costly and was subsequently replaced by a technology that is slightly cheaper. Vintaging attempts to dull this “knife-edge” effect of in- and out-swapping of technologies that is generally inherent in most LP models. A cost penalty for a system that becomes cheaper is added in the form of the cost of future investment. In this way, a given reactor technology cannot be easily turned on and off, but is required to operate for a given lifetime, and it becomes more costly to implement a second type of reactor. The algorithms used to implement vintaging are described below.

Through the cost-based objective function, OBJ_{COST} , a cost is attached to each of the variables that describe the fuel-cycle flow and storage, $x(m,p,t)$. For most of these variables a cost per unit of material stored or processed is imposed through the use of an appropriated unit cost (\$/kg or \$/kg/yr, depending on whether that variable describes an inventory or an process-flow rate. By multiplying the variable with the unit cost, and summing, an overall annual charge for that part of the fuel cycle is obtained. By discounting each annual charge to a base year and summing over the optimization period, the CPLEX optimizer searches for a combination of variables, $x(m,p,t)$ that minimizes this discounted life-cycle cost. Most unit costs are input as constants, but instead of using a fixed charge rate, fc_r , to determine the annual charge for capital incurred for each generation technology, as was done in an earlier version of FCOPT, the vintaging procedure described below was implemented.

That part of the objective function that reflects the capital cost of the generation technology $nucl$ reactors is represented as follows:

$$\sum_{rx=1}^{nrx} \sum_{t=1}^{nt} \frac{icap(nucl,t)}{(1+dr)^{t-1}} \quad , \quad (F-1)$$

where

- nrx = the number of reactors,
- nt = the number of timesteps over which optimization occurs,
- $icap(rx,t)$ = the capital expended for reactor $nucl$ in time t , including interest
- dr = during construction, and
= a discount rate.

The total capital investment for generation technology $nucl$, $icap(nucl,t)$ at time t is determined by first estimating the annualized investment for adding the incremental capacity $dcap(nucl,t)$ of generation technology $nucl$, including interest during construction (IDC); the investment cost, $icost(rx,t)$, of bringing on line the new capacity, $dcap(nucl,t)$, having a construction time, $tconst(nucl,t)$ and a lifetime, $tlife(nucl,t)$, is given by the following expression:

$$icost(nucl,t) = dcap(nucl,t) * utc(nucl) * idc(nucl) * crf(nucl), \quad (F-2)$$

where the unit total capital cost is $utc(\$/We)$, the capital recovery factor, $crf(1/yr)$, or payback or revenue generation rate in equal increments needed to return all capital expense attendant to the implementation of new generation capacity $dcap(nucl,t)$ at time t , and is given by,

$$crf(nucl) = \frac{dr * (1 + dr)^{life(nucl)}}{(1 + dr)^{life(nucl)} - 1}, \quad (F-3)$$

and the interest incurred during the construction of $tconst(yr)$ is given by.

$$idc(nucl) = \sum_{i=1}^{tconst(nucl)} \frac{(1 + dr)^i}{tconst(nucl)}. \quad (F-4)$$

The capital cost $icap(nucl,t)$ needed to compute the capital component of the cost-based objective function described in Sec. C.1 (Appendix C) derives from $icost(nucl,t)$ by discounting all charges back to the time t , as given in the following expression:

$$icap(nucl,t) = \sum_{i=t}^{\max(t+life(nucl),nt)} \frac{icost(nucl,t)}{(1 + dr)^{i-t}}. \quad (F-5)$$

The cost of capital incurred for generation technology $nucl$ at time t , $icap(nucl,t)$, is added to all other charges incurred from other parts of the NFC and discounted back to the reference year to give the total costs incurred over the optimization period, $OBJ_{COST}(\$)$. The ratio of $OBJ_{COST}(\$)$ to the discounted total electrical generation over the optimization period (2000,2100) is used as the primary economic metric, which is expressed as $coe(mill/kWeh)$, as is described by Eq. 3-11).

Appendix G: Correspondence Map of Material(*m*)/Process(*p*) Combinations

The following matrix illustrates the material and process combinations modeled in FCOPT and, if they are valid, whether they are analyzed as a flow rate (F) or an inventory (I), with (C) indicating an inventory of cumulative use.

M/P	MM(1)	CV(2)	ER(3)	FF(5)						
				FFUX(4)	FFMX(6)			FFMT(10)		
					FFRP(7)	FFPS(8)	FFWP(9)	FFRP(11)	FFPS(12)	FFWP(13)
NU(1)	C	F	F		F	F	F	F (rxif)	F (rxif)	F (rxif)
RU(2)		F	F		F	F	F	F (rxif)	F (rxif)	F (rxif)
DU(3)					F	F	F	F (rxif)	F (rxif)	F (rxif)
LNU(4)				F						
LRU(5)				F						
LWU(6)				F						
RUX(7)										
WPU(8)							F			F
HEU(9)										
RPU(10)					F	F		F	F	
MOX(11)										
RMX(12)										
RHTG(13)										
RFBR(14)										
BMX(15)										
MET(16)										
RMET(17)										
FP(18)										
LFP(19)								F	F	F
MA(20)								F	F	F

M/P	BL	RX(14)					
		RXOT(15)	RXMX(16)	RXHG(17)	RXBR(18)	IFR(19)	ATW(20)
NU(1)	F						
RU(2)	F						
DU(3)	F						
LNU(4)	F	F	F				
LRU(5)	F	F	F				
LWU(6)	F	F	F				
RUX(7)		F					
WPU(8)							
HEU(9)	F						
RPU(10)							
MOX(11)			F	F	F		
RMX(12)							
RHTG(13)			F				
RFBR(14)				F			
BMX(15)				F			
MET(16)						F	F
RMET(17)						F	F
FP(18)							
LFP(19)						F	F
MA(20)						F	F

M/P	BK(21)	CS(22)	IS(23)		DUS(26)	RUS(27)	BKS(28)	PUS(29)	FPS(30)	MAS(31)	SFS(32)
			ISU(24)	ISP(25)							
NU(1)	F										
RU(2)	F					I					
DU(3)	F				I						
LNU(4)											
LRU(5)											
LWU(6)											
RUX(7)		I	I								
WPU(8)								I			
HEU(9)											
RPU(10)								I			
MOX(11)											
RMX(12)		I		I							
RHTG(13)		I		I							
RFBR(14)		I		I							
BMX(15)	F						I				
MET(16)											
RMET(17)											
FP(18)									I	I	I
LFP(19)									I		
MA(20)										I	

M/P	REFPS(33)	SEFPS(34)	WPS(35)	WUS(36)	RP(37)			SEP(41)		
					CS(38)	IS(39)	BKS(40)	CS(42)	IS(43)	SFS(44)
NU(1)										
RU(2)										
DU(3)										
LNU(4)										
LRU(5)										
LWU(6)										
RUX(7)										
WPU(8)			I		F	F				
HEU(9)				I						
RPU(10)										
MOX(11)										
RMX(12)					F	F		F	F	
RHTG(13)					F	F		F	F	
RFBR(14)					F	F		F	F	
BMX(15)							F			
MET(16)										
RMET(17)										F
FP(18)	I	I								
LFP(19)	I	I								
MA(20)	I									

M/P	DD(45)		PUD(48)		FPD(51)	
	CS(46)	IS(47)	RP(49)	PUS(50)	REFPS(52)	SEFPS(53)
NU(1)						
RU(2)						
DU(3)						
LNU(4)						
LRU(5)						
LWU(6)						
RUX(7)	F, I					
WPU(8)						
HEU(9)						
RPU(10)			F, I	F,I		
MOX(11)						
RMX(12)	F, I	F, I				
RHTG(13)	F, I	F, I				
RFBR(14)	F, I	F, I				
BMX(15)						
MET(16)						
RMET(17)						
FP(18)					F,I	F,I
LFP(19)					F,I	F,I
MA(20)					F,I	

This page is intentionally left blank.

Appendix H: Summary of FCOPT Input Data (Supplement to Table B-I)

Parameter\Generation Technology (nucl)	rxot	rxmx	rxhg	rxfb	rifr	atw
Thermal-conversion Efficiency, etath	0.3420	0.3420	0.4000	0.3810	0.3810	0.3702
Plant availability or capacity factor, avail	0.855	0.8550	0.8550	0.8550	0.8550	0.8000
Re-circulation power fraction, epsilon	0.02	0.02	0.02	0.02	0.02	0.15
Nominal fuel burn-up, bu(MWtd/kgIHM)	55	49	140	140	140	140
Nominal fuel residence time, trx(yr)	4	4	4	2	1	1
Fuel cooling-storage time, trxc(yr)	6	6	6	6	3	3
Fissile plutonium fraction, fpuf	0.6	0.5	0.6	0.7	0.7	0.7
Upper limit growth factor, fgrowth	2	2	2	2	2	2
Negative-growth limit factor, fdecrx	0.01	0.01	0.01	0.01	0.01	0.01
Technology introduction "seeding" factor, fseed	0.01	0.01	0.01	0.01	0.01	0.01
Conversion ratio, cr					0.60	0.00
Number of core throughputs allowed in is per reactor, bnrx	10	10	10	10	10	10
Fissile loadings (weight fractions)						
o Initial plutonium loading, ypui	0.0000	0.0700	0.0800	0.1000	0.2000	0.9000
o Initial minor-actinide loading, ymai	0.0000	0.0000	0.0000	0.0000	0.0500	0.1000
o Final plutonium loading, ypuf	0.0100	0.0500	0.0400	0.0500	0.2000	0.9000
o Final minor-actinide loading, ymaf	0.0010	0.0030	0.0050	0.0005	0.0500	0.1000
o Final fission-product loading, yfp	0.0400	0.0400	0.1000	0.0600	0.1000	0.1000
o Final long-lived fission-product loading, yllfp	0.0040	0.0040	0.0100	0.0060	0.0100	0.0100
Costing Parameters						
o Unit total cost (\$/We), utc	1.7	1.7	2.3	2.6	2.6	3.0
o Fixed charge rate, fcr(1/yr) ^(c)	0.0	0.0	0.0	0.0	0.0	0.0
o Fixed charge rate (1/yr) for residual capacity, fcrresid	0.08	0.08	0.08	0.08	0.08	0.08
o Annual O&M charges as fraction of capital cost (1/yr), fom	0.03	0.03	0.03	0.03	0.03	0.03
o Construction time (yr), tconst	6	6	8	8	8	10
o Plant life time (yr), tlife	40	40	40	40	40	40
o Time remaining for technology nucl at ts (yr), teol	40	40	40	40	40	40

Technology Parameter	Value
Parameters for exogenous introduction LWR/MOX ^(a) , fmox(t)	
o Minimum fmox, fmoxmin	0.1
o Initial fmox, fmoxo	0
o Final fmox, fmoxf	1
o Time constant for fmox(t), taumox(yr)	10
Process residence times, (yr)	
o Conversion, tcv	0
o Enrichment, ter	0
o UOX fuel fabrication, tffux	1
o MOX fuel fabrication, tffmx	1
o MET fuel fabrication, tffmt	1
o Weapons HEU blending time, tffmt	4
o Cooling storage time, tcs	4
o Interim storage time, tis	10
o Reprocessing, trp	2
o Separations, tsep	1
Number of MOX recycles plus one, ncyc	1
Maximum fraction total generation by fsb technologies, ffsb	1
Cooling storage capacity in numbr of cores, ncs	10
Interim storage capacity in numbr of cores, nis	20

Technology Parameter (continued-1)	Value
Reprocessing capacity limits ^(b)	
o UOX rp lower capacity factor, pnruxdn	0
o MOX rp lower capacity factor, pnrmtxdn	0
o BMX rp lower capacity factor, pnbmtxdn	0
o RMET sep lower capacity factor, pnsepdn	1
o UOX rp upper capacity factor, pnruxup	100
o MOX rp upper capacity factor, pnrmtxup	1
o BMX rp upper capacity factor, pnbmtxup	1
o RMET sep upper capacity factor, pnsepup	10
o reprocessing deployment limit, rpratelim	2
Process efficiencies (1 - loss fraction)	
o Ore => U ₃ O ₈ conversion, ymm	0.96
o U ₃ O ₈ => UF ₆ conversion, ycv	0.98
o Enrichment uranium losses, yer	0.98
o UOX fuel-fabrication losses, yffux	0.98
o MOX fuel fabrication losses, yffmx	0.98
o MET fuel fabrication losses, yffmt	0.98
o Reprocessing plant losses, yrp	0.98
o Generic separations efficiency, ysep	0.99
Waste-product generation fractions by fsb technologies for dd	
o Minor actinides, fbdma	0.0050
o Fission products, fbdfp	0.0030
o Long-lived fission products, fbdlfp	0.0020
Uranium enrichment parameters (²³⁵ U concentrations)	
o NU feed, xfnu	0.0071
o RU feed, xfru	0.0100
o Product for nu feed, xpnu	0.0350
o Product for ru feed, xpru	0.0400
o Tailings for nu feed, xtnu	0.0030
o Tailings for ru feed, xtru	0.0030
o Weapons-released uranium, xheu	0.9500

Technology Parameter (continued-2)	Value
²³⁵ U concentrations in various fuels, yuox	
o Natural uranium	0.0071
o LEU made from nu	0.0350
o Reactor-exposed UOX	0.0100
o LEU made from ru	0.0400
o Depleted uranium, du	0.0010
o LEU made from du	0.0350
o Highly enriched uranium, heu	0.9500
FBR blanket discharge	
o Plutonium mass fraction, ybpu	0.0600
o Minor -actinide discharge, ybma	0.0010
o Breeding ratio, br	1.2000
Repository deployment parameters	
o Final dd capacity (kgHM), ddcapf	7.00E+07
o Initial dd capacity (kgHM), ddcap i	0.00E+00
o Ordinal of start of dd capacity ramp, tddi	21
o Ordinal of end of dd capacity ramp, tddf	61
Reprocessing deployment parameters	
o Final rp capacity (kgHM per yr), rpcapf	1.00E+08
o Initial rp capacity (kgHM per yr), rpcapi	0.00E+00
o Ordinal of start of rp capacity ramp, trpi	11
o Ordinal of end of rp capacity ramp	31
o exponent for rpcapi -> rpcapf, exrp	1

Technology Parameter (continued-3)	Value
Unit Costs of Front- and Back-End Processes	
Unit cost of conversion (\$/kgU), uccv	5
Unit cost of separative work (\$/kgU-SWU), ucsu	90
Cost of heu blending (\$/kgU), ucbl	1000
Fuel fabrication	
o UOX fabrication (\$/kgHM, ucffux	250
o MOX fabrication (\$/kgHM), ucffmx	3000
o Metal-fuel fabrication (\$/kgHM), ucffmt	3000
Cost of fresh-fuel storage (\$/kgHM/yr)	
o UOX fresh-fuel annual storage cost, ucffsux	100
o MOX fresh-fuel annual storage cost, ucffsmx	100
o Metal-fuel fresh-fuel annual storage cost, ucffsmt	100
Unit cost of sf transport (\$/kgHM) , uctr	50
Factor increase in cv er and ff charges for ru vs nu, fruvsn	2.0
Unit costs of storage (\$/kg(HM,FPP)/yr):	
o du storage, ucdus	10
o bks storage, ucbks	60
o cs storage, uccs	60
o is storage (rux), ucisu	60
o is storage (rmx), ucisp	60
o ru storage, ucru	15
o rpu storage, ucrpu	300
o ma storage, ucma	300
o fp storage, ucfp	100
o heu storage, ucwu	500
o wpu storage, ucwps	500
Costs of disposal (\$/kgHM,kgFPP):	
o Direct disposal for snf, ucdd	500
o Separated plutonium dd, ucpld	500
o Fission product dd, ucfpd	500
o Minor actinide dd, ucma	500
Costs of reprocessing (\$/kgU):	
o Once-through uox, ucrpu	1500
o Recycled mox, ucrpmx	1500
o FBR (rxfb) blanket, ucrpbmx	1500
o Separations (rux rmx rhtg rfbr and rmet), ucsep	4000
Storage capacity limits	
o Cooling storage capacity (kgSNF), bncc	1.00E+09
o Interim storage capacity (kgSNF), bnis	1.00E+09
o Separated-plutonium storage capacity (kgPu), bnps	1.00E+07
o Separated-plutonium storage depletion time (yr), tpus	1
o Minor-actinide storage capacity (kgMA), bnma	1.00E+06
o Minor-actinide storage depletion time (yr), tmas	10

^(a) $f_{\text{mox}}(t) = (f_{\text{moxf}} - f_{\text{moxo}})(1 - \exp(-t/\tau_{\text{mox}})) + f_{\text{moxo}}$

^(b) $r_{\text{pyy}}(\text{kgHM/yr}, t - \text{trx}) > p_{\text{nyyy}} * \text{loadrx}(t)$; where yyy = rux,rmx; rx = ot, mx

^(c) If zero, the vintaging procedure described in Appendix B is used.

Appendix I: Benchmarking of Neutronics Methods (Monteburns Code)

A previous benchmarking study for Monteburns compared calculated results to experimental data for a PWR burning UO₂ fuel in the United States (Trellue, 1998). This benchmarking used an infinite PWR assembly, and error was calculated using Eq. (I-1). Results are compared in Table I-I. It also included results for the sample problem using a generic 1/8-core model that did not yield any more accuracy or errors than an infinitely reflected assembly (it is better for some isotopes and worse for others), thereby indicating that either one will be sufficient for additional calculations.

$$\text{Percent Error} = (\text{Calculated/Measured} - 1) * 100. \quad (\text{I-1})$$

Table I-I. Benchmark of Monteburns to Experimental Data for PWR Burn-up Calculations (Burn-up ~28.5 GWd/tonneIHM).

Isotope	Published	One Assembly w/ORIGEN2	% error	1/8 Core
U235	0.00618	0.00603	-2.44	0.00603
U236	0.00282	0.00285	1.24	0.00280
U238	0.834	0.838	0.54	0.841
Pu238	1.14E-04	1.06E-04	-7.01	8.511e-5
Pu239	0.00439	0.00431	-1.77	0.00407
Pu240	0.00197	0.00199	1.14	0.00182
Pu241	6.81E-04	6.49E-04	-4.72	6.74e-4
Np237	3.04E-04	3.11E-04	2.45	2.70-4

A limited amount of experimental data is available on MOX irradiation; therefore, the Europeans developed a set of benchmark problems involving reactor physics that simulate irradiation calculations for multiple recycles of MOX fuel (OECD, 1995). The purpose of the OECD exercise was to compare results obtained by many well-known neutronics/burn-up codes for MOX fuel in both PWRs and fast reactors using different isotopic compositions of plutonium (corresponding to different recycles). The results obtained from the different codes were not as similar as desired, but these investigations proved that existing codes and nuclear data could indeed be used for multiple recycles of plutonium in the future (Bernnat, 1995). By simulating these problems in Monteburns, benchmarking of the code for MOX fuel calculations can be done. Although these problems do not directly compare Monteburns results to experimental data, they represent a valid test of the data and techniques used by Monteburns for problems involving the multi-recycling of MOX. Three different problems in these exercises applicable to PWRs are encountered: a cell problem with poor quality plutonium (recycled five times or “fifth generation” plutonium), one with good quality (plutonium obtained directly from spent nuclear fuel or “first generation” plutonium), and an exercise to calculate void reactivity effects. Results from the first and last benchmark using the code Monteburns are presented here.

The first problem explored involved the use of poor quality plutonium in an infinitely reflected pin of MOX fuel irradiated to a burn-up of 50 GWtd/tonneHM. Results are compared to the range of values calculated by other codes are given in Table I-II. The k_{∞} for the final burn-up step was not actually in the range of values calculated by other codes, but it was not too far off, and it was within the published range for all other burn-up steps. Although not listed here, results with a better quality of plutonium were all well within the range of published values.

Table I-II. Results of k_{∞} Calculations as a Function of Burn-up in the Monteburns Code as Compared to Other Codes.

Burn-up (GWtd/tonneHM)	Published k_{∞} range	k_{∞} using Monteburns
0	1.1043 to 1.1396	1.13250
10	1.0398 to 1.0777	1.07249
33	0.9645 to 1.0081	1.00465
42	0.9405 to 0.9833	0.98209
50	0.9208 to 0.9641	0.96754

The other problem addressed the issue of calculating void reactivity coefficients for safety calculations for MOX fuel. The void reactivity coefficient represents the change in reactivity with a decrease in the amount of water (moderator) in the system. The two geometries proposed for the void coefficient problems analyzed here are that of an infinitely reflected pin-cell (consisting of a fuel rod surrounded by water) and that of a macro-cell that consisted of an outer zone of UO_2 fuel and an inner zone with either UO_2 or MOX fuel with one of three different plutonium compositions (corresponding to H, M, and L, which is a high, medium and low plutonium enrichment, respectively, within the MOX). The cases were each analyzed both fully moderated and voided in the inner region and the difference in k_{∞} between the moderated and voided cases using MCNP were compared to the results calculated by other codes in Table I-III (Monteburns was not used here because there was no burn-up involved). Two different cross section sets were used [ENDFB-V and ENDFB-VI(ENDFB-6, 2002)], and results often fell within the range of values calculated by other codes for one or both data sets, meaning that overall, Monteburns was comparable to other burn-up codes used for MOX fuel calculations.

Table I-III. Reactivity Change δk_{∞} Between Moderated and Voided Cases.

Fuel Type	Pincell (published)	Pincell (calculated) ENDF-V	Pincell (calculated) ENDF-VI
UO ₂	-0.7246 to -0.7436	-0.7610	-0.7315
H-MOX	0.0500 to 0.0768	0.0562	0.0809
M-MOX	-0.1233 to -0.1901	-0.1489	-0.1197
L-MOX	-0.3709 to -0.4456	-0.3978	-0.3702
Fuel Type	Macrocell (published)	Macrocell (calculated) ENDF-V	Macrocell (calculated) ENDF-VI
UO ₂	-0.0138 to -0.0164	-0.0145	-0.01455
H-MOX	0.0004 to 0.0067	0.0042	0.00627
M-MOX	-0.0005 to 0.0057	0.0042	0.00568
L-MOX	-0.0043 to 0.0026	0.0017	0.0002

One set of experimental data for the measured isotopic compositions of MOX fuel rods does, however, exist. These data are for the San Onofre PWR, which burned MOX fuel samples in the 1970s (Hermann, 2000). Data for one assembly are given in the reference, and, using an infinitely reflected assembly model, the burn-up of the sample was calculated using Monteburns. The resulting isotopic compositions were decayed for the appropriate cooling time to be comparable to the measured results. The differences in composition between the measured and calculated data (using Monteburns) for sample 079 are given in Table I-IV. The percent error seen for most of the isotopes was less than 5%, but for ²³⁸Pu was much greater (*i.e.*, almost 70%). Since that large of an error is not seen in Monteburns for other analyses, it is assumed that the measured, not the calculated, data was incorrect.

Table I-IV. Benchmark of Compositions from Monteburns to Experimental MOX Data.

Isotope	Measured	Calculated	Percent Error
U235	4.400	4.550	3.40
U236	0.489	0.482	-1.32
U238	943.2	941.5	-0.18
Pu238	0.282	0.087	-69.32
Pu239	16.49	17.31	4.97
Pu240	7.677	7.661	-0.21
Pu241	3.656	3.865	5.73
Pu242	0.897	0.854	-4.79
Nd148	0.227	0.234	3.04

No experimental data for ADSs yet exists; therefore, benchmarking for ADS system was not performed, although Monteburns results were compared to those calculated by Argonne National Laboratory in FY01 (Van Tuyle, 2001).

This page is intentionally left blank.

Appendix J: Calculation of Neutronic Safety Parameters

Showing that the LWR comprised of MOX fuel could indeed perform the proposed irradiations within the neutronic safety limitations currently seen with UO₂ fuel for each pass was a major component of this research. The most significant parameters in neutronic safety calculations include the Doppler fuel temperature coefficient, the moderator temperature coefficient, soluble boron efficiency, void reactivity coefficient, and control/shutdown rod worth. The Doppler fuel temperature coefficient is the change in the reactivity of the system (k_{eff}) caused by changes in the fuel temperature. The Doppler coefficient should be negative, which means that the reactivity decreases when the fuel temperature increases. This negativity is beneficial for accident scenarios in which the core overheats and the fuel temperature rises; it is advantageous for the system k_{eff} to decrease instead of increase and potentially go supercritical (*i.e.*, when k_{eff} is greater than 1.0). The reason it is termed “Doppler” coefficient instead of just “fuel” temperature coefficient is that broadening of the resonances with temperature is called the Doppler effect and is seen primarily in the fuel (particularly for the actinides) of a reactor system.

The moderator temperature coefficient is similar to the Doppler fuel temperature coefficient in that it represents how the reactivity of the system changes as the temperature of the moderator increases. Both the change in density, and in the cross section of the material must be accounted for when studying the moderator temperature coefficient of a system. The other reactivity coefficient that is often measured is the void reactivity coefficient (see benchmark in Appendix I). This reactivity coefficient represents the effect that a decrease in the water/moderator (such as a loss of coolant accident) has on the reactivity of the system. A decrease of 25% percent of the water in the system was considered for this study. All reactivity coefficients were measured in terms of change in reactivity ($1 \text{ pcm} = 10^{-5} \Delta k_{\text{eff}}$) *per* degree change in temperature. Temperature changes are modeled by changing the cross section of the fuel or moderator material in MCNP. For those cross sections that do not exist in MCNP, temperature-dependent cross sections can be developed for numerous isotopes using the NJOY code (MacFarlane, 1994). An identifier is then placed in the files used by MCNP and MonteBurns. Any number of cross sections can be generated in this fashion. For this research, a small FORTRAN code was written to change the cross sections of interest in the MCNP input file and run MCNP to get new values of k_{eff} from which reactivity coefficients were calculated.

One of the ways that reactivity is controlled as a function of irradiation in a PWR is by adding soluble boron to the water. The parameters that are typically measured include the critical boron concentration and the soluble boron efficiency. Critical boron concentration is the amount of boron that is necessary to keep the system exactly critical at the beginning of a cycle. It is typically measured in units of parts per million (ppm), which is milligrams of boron per kilograms of water. The concentration of boron in the water is adjusted up to several times daily during reactor operation to keep the reactor exactly critical and typically decreases significantly during an irradiation cycle. It is not practical to model each of these changes explicitly, so in this research, only two different concentrations are tracked each cycle, the second being exactly half of the first and implemented about halfway through each irradiation cycle.. The value of k_{eff} at the beginning of each cycle was about 1.035, and at the end of each cycle was approximately

unity to represent a critical reactor. It is assumed that an increased boron concentration and/or control rod insertion would keep the system critical at the beginning of each cycle. Critical boron concentration should not be greater than 2,500 ppm because it could lead to re-crystallization, and it is usually less than 1,500 ppm (Youinou, 1999a). Soluble boron efficiency represents how well insertions of boron decrease the reactivity of the reactor. Boron efficiency is calculated in terms of the change in reactivity (pcm) per ppm boron added or removed from the water. It should be at least 4 pcm/ppm to assure adequate control measures in the reactor. For this research, the boron concentration was adjusted (using a short FORTRAN 77 program) so that it both increased and decreased by 100 ppm per case, and the resulting reactivity changes were calculated.

The last measure is that of the worth of the control and shutdown rods. In a reactor, control rods are used to help keep the system critical throughout a cycle (*i.e.*, with a k_{eff} of 1.035 at the beginning of each cycle, control rods may be used to reduce it to 1.0). Shutdown rods are used to make the reactor sub-critical (shutdown) either at the end of a cycle or in case of an emergency. In this research, control rods were assumed to be silver, cadmium, and indium. Shutdown rods were made of boron carbide (B_4C), which is an even stronger neutron absorber. Both control and shutdown rods are located in clusters, which in this case are comprised of nine rods each and occupy the guide tube locations of certain assemblies. The assemblies that have control or shutdown rod clusters in the design being studied are given in Figure J-1. Such a design was developed so that the total worth of control and shutdown rods was more than 5,000 pcm (for UO_2 fuel) and the worth should be similar in all MOX fuel cases designed in this research.

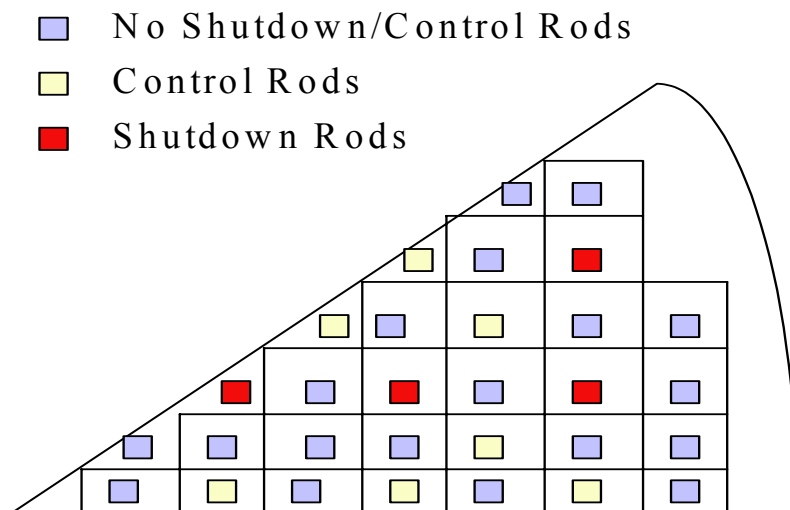


Figure J-1. Location of control/shutdown rods in core.

The first step in performing safety calculations for multi-recycling with a full core of MOX fuel was to make sure that Monteburns/MCNP was calculating values similar to those seen in literature. The way these calculations were performed is to set up a 1/8-core model in MCNP with assemblies of UO_2 or MOX fuel. Again, these assemblies are grouped into three different

regions depending on the number of cycles through which they have been irradiated in the reactor (see Figure 5-1). The burn-up calculations were performed using MonteBurns, which saves the MCNP input file at the beginning and end of each step. The MCNP input file for the beginning and end of an average equilibrium step was then modified using a FORTRAN77 program to provide the Doppler reactivity coefficient, moderator temperature coefficient, boron efficiency, void reactivity coefficient, control and shutdown rod worth. The Doppler coefficient was calculated using Eq. F-1 and the effective multiplication factors (k_{eff}) obtained by running two of the new MCNP input files that use cross sections corresponding to fuel temperatures 100 degrees above and 100 degrees below that of the default (base) case. The moderator temperature coefficient was calculated similarly, but the change in temperature was only 50 degrees K and the density of the water changed slightly (-/+ 0.002 g/cc with every degree up or down in temperature respectively).

$$100000 \text{ pcm}/\Delta k^* \{((k_{\text{highT}} - k_{\text{default}}) + (k_{\text{default}} - k_{\text{lowT}}))/2\} / \Delta(\text{Temp (K) or ppm B}). \quad (\text{J-1})$$

The boron efficiency was calculated by changing the boron concentration to be 100 ppm less than and 100 ppm greater than the default case in two different MCNP files respectively, and then using Eq. (J-1) to get the necessary results. The void reactivity coefficient was calculated by obtaining the k_{eff} from a case in which the density of the water was decreased by 25% and subtracting it from the k_{eff} of the basecase. The control and shutdown rod worth were obtained by calculating the k_{eff} when control and/or shutdown rod clusters were inserted into the reactor (*i.e.*, into the guide tube holes of the assemblies that contain them) and subtracting it from the value of k_{eff} of the base case. The total rod worth was that which occurred when both control and shutdown rods were inserted. Initial boron concentrations were also calculated for the beginning of cycle cases to make sure they did not exceed 2,500 ppm.

The most is known about uranium oxide fuels, thus safety calculations were performed for standard and extended burn-ups of enriched UO_2 fuel in a LWR. The standard burn-up cycle was considered to be a burn-up of about 38 GWtd/tonneIHM with an enrichment of 3.2 w% uranium, which is common for the H.B. Robinson PWR assembly design (Heremann, 1995) used in this research. The extended burn-up cycle was considered to be a burn-up of about 60 GWtd/tonneIHM with an enrichment of 4.2 w% uranium. A sample case for a full core of MOX fuel case was subsequently explored with a plutonium concentration of 8.3 w% heavy metal. The results for these three cases both at the beginning and end of a representative cycle (BOC and EOC, respectively) appear in Table J-I.

Table J-1. Basic Neutronic Safety Results.

	Standard BOC	Standard EOC	Extended BOC	Extended EOC	MOX BOC	MOX EOC
Doppler coefficient	-1.885	-2.195	-2.15	-2.64	-3.155	-2.94
Moderator coeffic.	-49.66	-62.71	-47.83	-43.66	-47.13	-51.99
Boron efficiency	7.59	9.24	5.4	7.01	1.3	2.4
Void coefficient	-222.56	-266.36	-209.56	-205.32	-198.72	-216.64
Control rod worth	4,566	3,631	3,780	2,837	2,275	2,305
Shutdown rod worth	2,616	2,011	2,281	2,320	1,905	1,843
Total rod worth	7,640	5,315	5,454	5,214	4,111	4,064
Modified rod worth	-	-	-	-	5,092	5,083
Critical Boron Concentration	1,600	-	1,260	-	1,733	-

These basic safety calculations confirm the results reported in literature, which means that they are being done correctly. The absolute values of the Doppler and moderator coefficients are larger, and the void coefficient is smaller, for MOX fuel than for traditional UO₂ fuel, although all three are still negative. The larger Doppler and moderator coefficients lead to smaller control and shutdown rod worth for MOX fuel, which is seen in Table J-I as well. In fact, the total rod worth is less than 5,000 pcm for a full core of MOX fuel, which is a major safety concern. The other noticeable safety problem for MOX fuel is that efficiency of the soluble boron decreases significantly from traditional UO₂ cases. This boron efficiency should be greater than 4 pcm/ppm to provide adequate safety in a system. The standard UO₂ case has sufficiently high boron efficiencies, the extended LWR case has boron efficiencies that almost reach the limit but are still sufficient, but the MOX case does not meet the designated safety criteria for boron efficiency either at the beginning or the end of a cycle. Therefore, to implement a full core of MOX fuel, both the control/shutdown rod worth and the boron efficiency must be increased.

It was discovered that with 8.3 % plutonium content in heavy metal, a slight ¹⁰B enrichment (to 25%) was needed to get a boron efficiency of 4 pcm/ppm both at the beginning and end of cycle. Replacing 12 fuel rods with water holes (an over-moderated assembly) and using boron carbide control rods also increased the total rod worth above 5,000 pcm. Therefore, a baseline case was made for further MOX fuel calculations using 12 water holes instead of fuel rods, control and shutdown rods made of B₄C, and slightly enriched boron in both the control/shutdown rods and soluble water. The boron enrichment can always be increased if higher boron efficiency is desired. As it is now stands, the baseline case meets all neutronic safety parameters seen for extended burn-up of UO₂ fuel.

Appendix K: Spallation Product Radioactivity

One issue addressed in designing ADSs involves the maximization of spallation neutron production and effectiveness. This maximization depends on both the target material and the placement of the target with respect to the blanket. It is assumed for the studies presented here that the target is cylindrical and that the blanket surrounds it in the form of hexagonal assemblies with the beam entering from the top, although the beam can also enter the target from the bottom or side. When bombarded with a 1-GeV proton beam, the target creates about 20 to 30 spallation neutrons per proton. Some of these neutrons are captured in the actinides or other materials (*i.e.*, long-lived fission products) in the system; others go on to cause fissions at a rate of about 400 fissions per source proton with a $k_{\text{eff}} \approx 0.97$ (Bowman, 1998).

To determine the biological hazard that a particular material represents to humans, a measure must be developed to quantify the risk. Radiotoxicity is a widely accepted measure for this hazard because it gives the probability that a material will cause harm if ingested or inhaled. The International Commission on Radiological Protection (ICRP) represents radiotoxicity in terms of the estimated number of cancer deaths that might result following the ingestion or inhalation of a set of radionuclides, or effective dose (ICRP, 1991). Effective dose is calculated by obtaining the weighted sum of committed dose equivalents multiplied by appropriate weighting factors for relevant organs and tissues. The ICRP reports fractional absorption and the summed effective dose for many radionuclides (ICRP, 1979). For ingestion, it is assumed that the radionuclides are incorporated either into the food or water a person is eating or drinking and are readily absorbed from the gastrointestinal (GI) tract. Inhalation radiotoxicity calculations include retention of deposited activity in various respiratory tract regions with clearance from the regions by breathing out, movement of the particles to the GI tract and lymph nodes, and absorption into body fluids. Values are reported for fast, moderate, and slow absorption, but the highest of the three is used by default here. Effective dose is given separately for ingestion and inhalation in units of dose per activity (Sieverts per Becquerel (Sv/Bq)) for the isotope of interest (ICRP, 1996). Effective doses are reported for ages ranging from three months (to represent an infant) to an adult, but it is the adult values that are used in this study.

The more recent version of the Code of Federal Regulations (CFR) published by the Nuclear Regulatory Commission (NRC) expresses radiotoxicity in units of annual limit on intake (ALI). The ALI is defined as the greatest value for annual intake (represented by I and usually in terms of μCi) that satisfies the two conditions below [where $H_{50,T}$ is the committed dose equivalent per unit activity of intake (Sv/Bq) in tissue T from the radionuclide and w_T is the weighting fraction for that tissue] (Turner, 1992):

$$I \sum w_T \hat{H}_{50,T} \leq 0.05 \text{ Sv},$$
$$I \hat{H}_{50,T} \leq 0.5 \text{ Sv}.$$
(K-1)

The committed dose equivalent is the dose equivalent resulting from the intake of a radionuclide over a subsequent 50-year period. The inhalation ALIs reported in the CFR represent an aerosol

with an activity median aerodynamic diameter of 1 micron for retention periods of days (for half-lives less than 10 days), weeks (for half-lives between 10 and 100 days), and years (for half-lives greater than 100 days) in the pulmonary region of the lung. Other ALIs for airborne and liquid effluents and discharges to sanitary sewer systems (i.e. from ingestion) are also reported (NRC, 1991).

However, neither the ICRP nor the CFR report values for all radionuclides of interest. For this reason, the Japanese developed their own set of radiotoxicity data for about 300 radionuclides not listed in the ICRP (Kawai, 2002). The data include radiotoxicities for the alpha-emitting rare earth isotopes ^{150}Gd and ^{154}Dy that are important in spallation targets.

Numerous studies have been performed on the long-term radiotoxicity of transuranic materials (TRU) and fission products, both within SNF and those generated from the transmutation process. However, because the concept of using an ADS is relatively new, little research has been done on the radiotoxicity of the radionuclides generated during the spallation process (spallation products, SPs). Most of the common radioactive fission products are emitters of beta radiation, but some of the radionuclides generated during spallation are alpha emitters. Thus, both ingestion and inhalation radiotoxicity of the spallation products that are generated could be significant. In a repository, ingestion toxicity may be considered to be more important than inhalation radiotoxicity because the potential biological hazard to humans occurs when the isotope is absorbed in nearby ground water or brine and transported from the repository to potential human drinking water. Inhalation radiotoxicity is important to analyze in case of a breach of containment inside the accelerator facility and/or for short-term (*i.e.*, above-ground) storage concerns.

The radiotoxicity of several different targets and proton beam energies are examined in this paper. Previous studies involving heavy liquid-metal spallation targets have shown that important contributors to the radiotoxicity of an LBE-cooled target can result in higher radiotoxicities than fission products (Pankratov, 1999). Isotopes of concern for the LBE target (or any LBE-cooled target) include ^{208}Po , ^{210}Po , ^{202}Pb , ^{207}Bi , and ^{193}Pt and, for both the LBE and tungsten targets, rare earth isotopes such as ^{146}Sm , ^{148}Gd , ^{150}Gd , and ^{154}Dy (Stankovsky, 2001).

For this research, studies were done using the code MCNPX to calculate spallation product yields in three different spallation targets (LBE, lead, and tungsten) and Monteburns with the CINDER90 option to calculate the depletion and decay of radioisotopes (Waters, 1999; Wilson, 1995). Bertini was the default module in MCNPX that was used to calculate spallation product yields, but the calculation hopefully will be performed again in the near future with a more accurate module called CEM2K. The results presented here show that spallation product inventories are initially more significant than fission products, but over the course of 300 years these isotopes decay to radiotoxicity levels greater than that of natural uranium ore.

The results from spallation product generation are normalized per metric ton of heavy metal input for the ADS. In other words, the initial inventory of actinides in the sample ADS examined is about 1,500 kg, and about 0.840 kg/day is added in a 840-MWt system. Over the course of 60 years (the assumed operational period), about 20 tonne of actinides can be burned in one such ADS. The radiotoxicities curves presented in this section assume the use of 1 tonne of actinides

derived from SNF [which is compared to 5 tonne of natural uranium ore (0.72 wt % * 5 = 3.6 wt %, a common enrichment of low-enriched uranium fuel)], so the results for the spallation product inventories in one ADS were divided by 20 for more appropriate comparison. Figures K-1 and K-2 compare the ingestion and inhalation radiotoxicities, respectively, for a proton beam energy of 1 GeV for the three different targets. LBE was assumed to be the coolant for all targets (constituting about 30 vol % of lead and tungsten)); therefore, all of the results are composed of some LBE spallation products. Figure K-2 shows that the ingestion radiotoxicities of spallation products (especially LBE) are greater than that of fission products from transmutation for the first year, but not thereafter. The ingestion radiotoxicities of the SPs decrease to less than ten times that of natural uranium ore within ten years and less than that of natural uranium ore within a few hundred years, as do fission products. Lead and LBE SPs pose a greater inhalation hazard than fission products in the first six months but decay quickly, whereas the inhalation radiotoxicity from tungsten SPs is greater than that of fission products for several hundred years, at which point the radiotoxicities of all fission and spallation products decay below that of natural uranium ore. Hence, the results show that spallation products do not pose a significant long-term radiotoxicity hazard but can be important in short-term storage facilities.

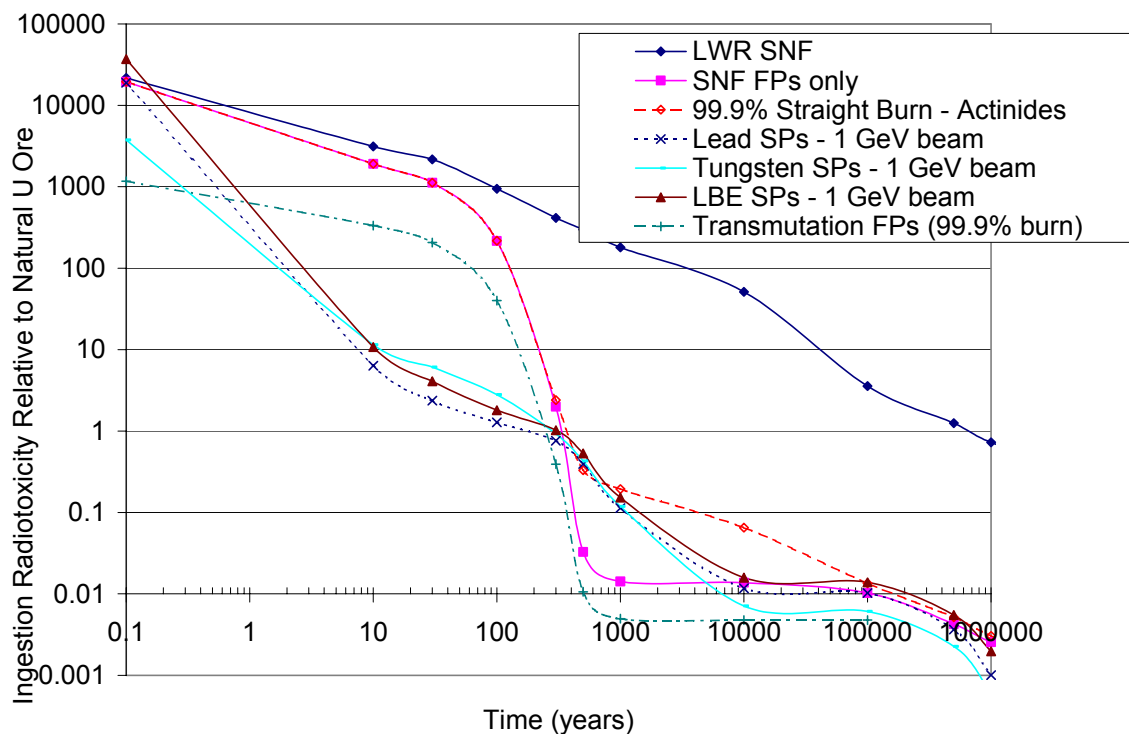


Figure K-1. Ingestion radiotoxicity of spallation products compared to SNF.

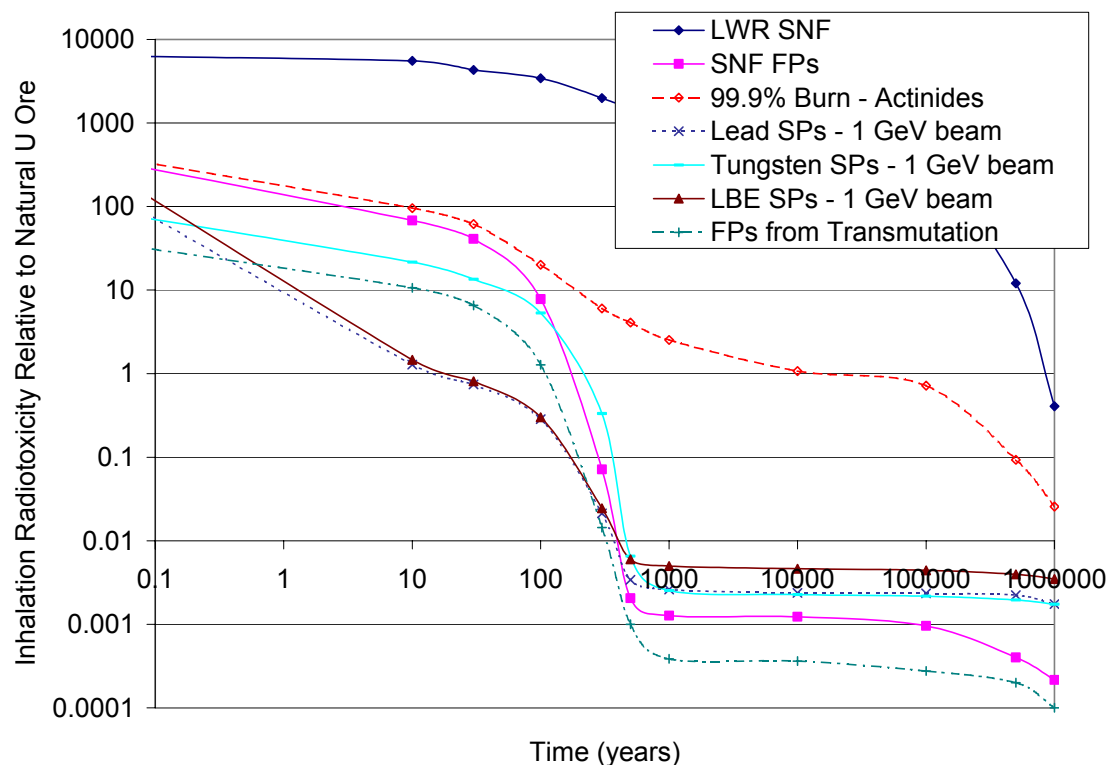


Figure K-2. Inhalation radiotoxicity of spallation products compared to SNF.

The radiotoxicity increases approximately linearly with proton beam energy. At a proton-beam energy of 1.6 GeV, therefore, both the ingestion and inhalation radiotoxicities are about twice that created for a 800-MeV beam. To decrease the radiotoxicity risk, the proton beam energy must be adjusted accordingly (but certainly, the greater the energy, the more efficient the spallation process). The isotope ^{210}Po plays the strongest role for ingestion and inhalation radiotoxicity initially because all targets are LBE cooled. The tungsten target also has approximately a 10% contribution from isotopes with atomic numbers around that of tungsten. However, after ten years, a different isotopic breakdown appears. The isotopes making the greatest contribution to each target material for both ingestion and inhalation radiotoxicity after ten years are given in Figures K-3 and K-4, respectively. The isotopes ^{207}Bi and ^{194}Hg contribute a majority of the ingestion radiotoxicity for the lead and lead-bismuth targets, whereas ^{148}Gd definitely plays the greatest role for ingestion in the tungsten target and for inhalation radiotoxicity in all of the targets.

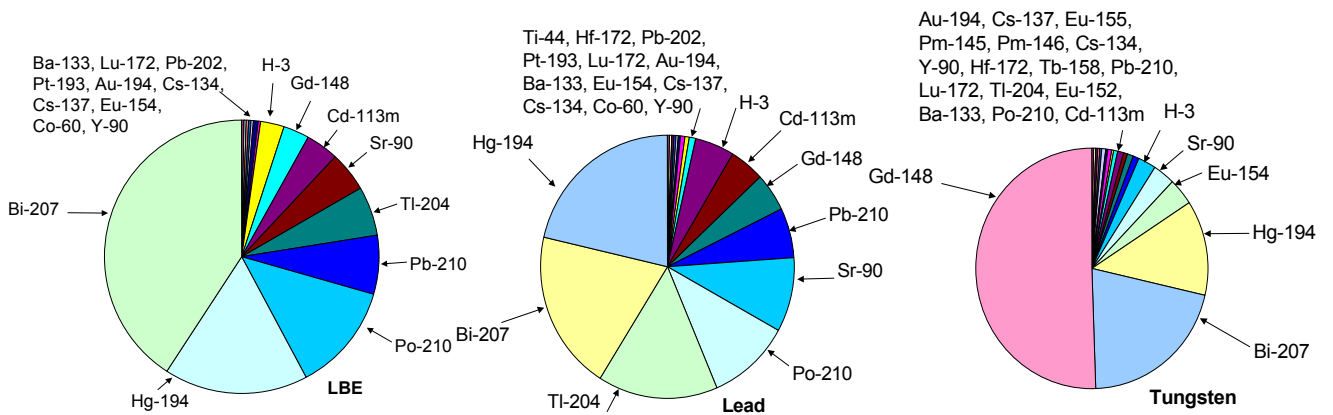


Figure K-3. Ingestion radiotoxicity for each target by isotope.

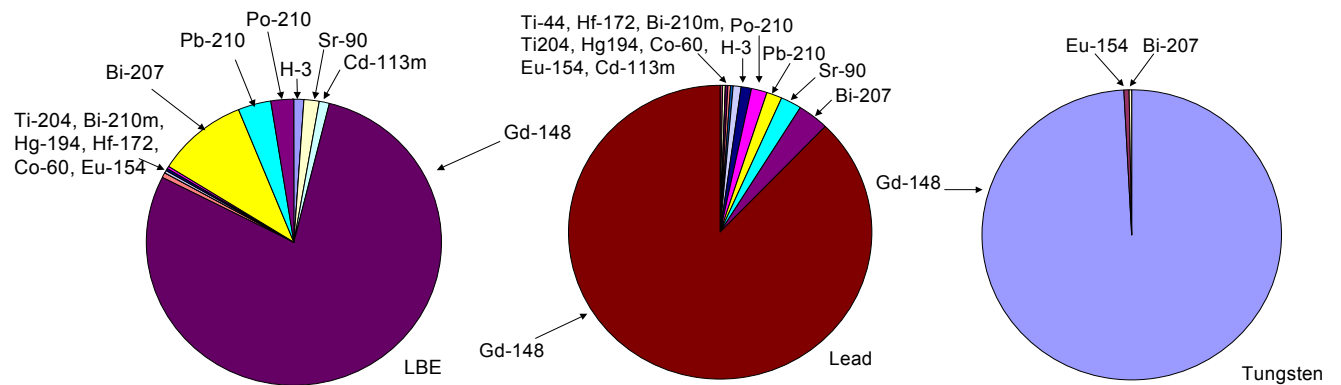


Figure K-4. Inhalation radiotoxicity for each target by isotope.

This page is left blank intentionally.

Appendix L: Sample OREGIN2.1 Input for Use in NFCSim Nuclear Fuel Cycle Simulation Model.

```

-1
-1
-1
TIT      ORIGIN2 input file for NFCSim
LIP      0 0 0
RDA ***  Libs 204,205,206 = PWRU
LIB      0 1 2 3 204 205 206 9 3 0 3 0
RDA
RDA      Read initial comps into vector 1 from below in grams
INP      1 1 0 -1 4 4
MOV      1 3 0 1.0
RDA ***
RDA ***  Set output options (print in grams)
HED      1  INITIAL
CUT      5  1.0-5  -1
OPTA     4*8 7 8 7 8 7 19*8
OPTL     4*8 7 8 7 8 7 19*8
OPTF     4*8 7 8 7 8 7 19*8
RDA ***
RDA      Begin burn
BUP
HED      2  IRRADIATED FUEL
DOL      1  79
IRP      12.4 3200.0 1 2 4 1
MOV      2 1 0 1.0
CON      1
IRP      12.4 3200.0 1 2 4 1
MOV      3 1 0 1.0
BUP
RDA      Begin Decay
DEC      1.0 2 3 5 1
HED      3  1 YR DECAY
DEC      1.0 3 4 5 1
HED      4  2 YR DECAY
DEC      3.0 4 5 5 1
HED      5  5 YR DECAY
DEC      5.0 5 6 5 1
HED      6  10 YR DECAY
DEC      10.0 6 7 5 1
HED      7  20 YR DECAY
DEC      10.0 7 8 5 1
HED      8  30 YR DECAY
DEC      10.0 8 9 5 1
HED      9  40 YR DECAY
DEC      10.0 9 10 5 1
HED     10  50 YR DECAY
DEC      25.0 10 11 5 1
HED     11  75 YR DECAY
DEC      25.0 11 12 5 1
HED     12  100 YR DECAY
OUT      12 1 1 0
RDA

```

END

```

2  922350  2561000.0  922380  97403000.0  0 0  0 0
2  922340   23029.0  922360   13160.0  0 0
0 0 0 0 0 0 0 0 0 0 0 0

```

The final isotopic mix reported above corresponds to 100 tonneHM input (oxygen in the oxide is ignored in this case because it is only the isotopic content from fission expressed in heavy metal that is of interest here). The ORIGEN2.1 libraries that must be modified to run the cases indicated in bold, as are the fluxes and time frames that define each burn-up and must be changed for each case. The total irradiation time is divided into 80 different internal ORIGEN2.1 burn-up steps to generate more accurate results. The isotopic results calculated using the Monteburns code compared the results obtained from only to running ORIGEN2.1 with average cross section libraries generated by Monteburns are given in Table L-I. The results derived using only ORIGEN2.1 appear to be sufficiently accurate for the purposes of NFCSim.

Table L-I. Comparison of ORIGEN2.1 Results with NFCSim Technique *versus* Those Obtained by Monteburns (Weight Fraction of Each Isotope Used).

	UO ₂ - Low Burn-up		UO ₂ - High Burn-up		MOX – 1st Pass		MOX – 2nd Pass	
Ending isotopics	Monteburns	ORIGEN	Monteburns	ORIGEN	Monteburns	ORIGEN	Monteburns	ORIGEN
U235	6.17E-03	5.86E-03	5.69E-03	5.54E-03	3.58E-03	3.38E-03	1.01E-02	9.68E-03
U236	3.33E-03	3.35E-03	6.02E-03	5.96E-03	7.33E-04	7.26E-04	1.90E-03	1.94E-03
U238	0.97953	0.98098	0.97289	0.97368	0.92767	0.92741	0.91509	0.91522
Pu239	4.85E-03	4.80E-03	5.90E-03	6.36E-03	2.19E-02	2.21E-02	2.00E-02	2.12E-02
Pu240	2.17E-03	1.87E-03	3.07E-03	2.50E-03	1.92E-02	1.83E-02	2.01E-02	1.94E-02
Pu241	1.32E-03	1.53E-03	1.95E-03	2.37E-03	1.05E-02	1.08E-02	1.10E-02	1.11E-02
Pu242	5.56E-04	6.20E-04	1.21E-03	1.27E-03	9.25E-03	9.21E-03	1.24E-02	1.21E-02
%actinides burned	3.12	3.26	5.95	6.17	4.79	5.11	4.79	5.12

Appendix M: Design Parameters of the Yucca Mountain Repository.

The design of the Yucca Mountain nuclear waste repository is still in flux. In large part, this uncertainty reflects conflicting views of the effect of geologic, hydrological, and thermal processes on the fate of the waste packages (WPs) containing spent nuclear fuel (SNF). One school of thought feels that it would be desirable to maintain a relatively high temperature ($> 97\text{ C}$) for a long time (thousands of years), to prevent contact of liquid water with the WPs; metal corrosion rates are known to be enhanced by contact with liquid water. Another school of thought prefers to maintain a low temperature, both because corrosion is slower at low temperature, and because it is thought that uncertainties in predicting geological and hydrological behavior are smaller if the temperature excursions are reduced (USNWTRB, 1999). The dispute is exacerbated by the realization that the capacity of the YM site is greatly affected by the chosen operating mode; “Low Thermal Loading” operating modes in general require substantially more repository area for a given quantity of SNF than do “High Thermal Loading” operating modes. Because the repository area at the YM site is limited, and because the economic and political costs are high for choosing a second repository site, this matter is far from settled.

In Sec. 6 we discussed a method to increase greatly (factor of 10-27) the capacity of a geologic repository by removing from the SNF certain elements, *i.e.*, the high-heat release fission products cesium and strontium and the long-lived actinides plutonium, americium, and curium. In this Appendix we provide background information important to understanding the “strawman” used for comparison; this is the design specified in the Yucca Mountain Viability Assessment (USDOE 1998). We also provide information on both low thermal load and high thermal load operating modes that have been considered, on higher density emplacement methods that have been recommended as suitable for low heat release radionuclides that the suggested reprocessing schemes will generate, and on the extended cooling periods for existing spent nuclear fuel relative to the 10-year cooling period used in the present (and in many other) thermal calculations. The following is only a summary of the information available in the referenced documents, which should be consulted for details and explanation.

M.1 Details of the Yucca Mountain “Viability Assessment” Design

The capacity of the YM repository is undefined, although there is a statutory limit (Nuclear Waste Policy Act of 1982) that no more than 70,000 metric tonnes of heavy metal (MTHM) of waste will be emplaced prior to a second repository being brought into operation. The 70,000 MTHM is further specified as consisting of 63,000 MTHM of commercial SNF, 2,333 MTHM of DOE spent nuclear fuel, and 4,667 MTHM (equivalent) of high-level radioactive waste. Considering only the commercial SNF, the VA plan is to emplace it at 85 MTHM/acre covering an area of 741 acres. This is a substantial fraction of the approximately 1550 - 2000 acres available at the YM site (USDOE, 1988).

Waste will be emplaced over ~ 24 years at a rate of ~ 3000 MTHM/yr after a ramp-up period; hotter and cooler waste packages will be interspersed to achieve an average linear thermal

loading of ~ 1.45 kW/meter and no WP shall exceed 11.8 kW. The waste will be emplaced in 5.5-meter diameter emplacement drifts, in double-walled (Alloy 22 and stainless steel) waste packages supported off the drift floor. The emplacement drifts will be ventilated and monitored for ~ 100 years, then covered with titanium drip shields and the repository closed and decommissioned. The emplacement drifts may or may not be backfilled prior to closure (USDOE 1988, BECHTEL 2002).

M.2 Low and High Thermal Load Operating Modes

A number of low thermal load operating modes (LTOM) have been considered (see, for example, BECHTEL 2002). The LTOM are achieved by a combination of lowering areal loadings by increasing drift spacing or reducing linear loadings within the drift, increased ventilation periods, and aging the waste in a surface site to permit some of the decay heat to dissipate into the air.

High thermal load operating modes (HTOM) generally are achieved by increasing the areal density of waste. Increases up to ~ 170 MTHM/acre have been considered (TRW-ESS 1999). Nonuniform loadings are also considered, with higher loadings around the perimeter of the emplacement area to counteract the greater effective cooling in the regions with no neighboring heat loads.

M.3 Higher Density Emplacement Methods for Low Heat Release Radionuclides

Fosberg (Fosberg, 1999) has noted that the very low heat release (VLHR) waste resulting from removal of the cesium, strontium, and actinides (*i.e.*, Scenario VII of Sec. 6), could be disposed of in underground “silos” of perhaps 10,000 MTHM capacity, at extremely low cost compared to the YM concept. Indeed, Sweden has implemented such silos, e.g. the Swedish Final Repository for Radioactive Operational Waste, (SFR), for disposal of waste with similar heat releases (Carlsson, 1998). The SFR is 50 meters high and 25 meters diameter, and surrounded by a layer of bentonite clay to prevent diffusion of radionuclides out of the storage area.

This high-volume, low surface area emplacement concept would also be ideal for disposal of high-volume, low heat release waste such as SNF clads and hulls, and low-volume, low-heat release volatile wastes such as carbon-14, iodine-129, *etc.* that are released in the reprocessing step.

M.4 Extended Cooling Periods for Existing Spent Nuclear Fuel

Commercial SNF has been discharged at least since 1968. The existing records (for example, USDOE 2002d) may not be complete as to burn-up and quantity. However, clearly the fuel cooling period averages considerably longer than the 10 years cooling assumed in Sec. 6, and inspection of the data indicates that burn-up has increased steadily from very low values (a few *GWd/MTHM*) to values close to those in Sec. 6, “Standard LWR” burn-up of 38 *GWd/MTHM*.

Because the decay heat of SNF decreases with cooling time, it is interesting to calculate the actual age of SNF consigned to a geologic repository assuming that the oldest waste is emplaced first (this ensures the lowest thermal load at any given time). From the records of SNF production (USDOE 2002d), and assuming that the existing SNF is emplaced at 3,000 MTHM/yr (USDOE 1998) with no ramp-up, starting in 2010, the cooling period for the SNF may be calculated directly. The result is shown in Figure M-1, where both the oldest and youngest fuel (black diamonds and red circles, respectively) consigned in a given year are shown; the data points are calculated at 5-year intervals.

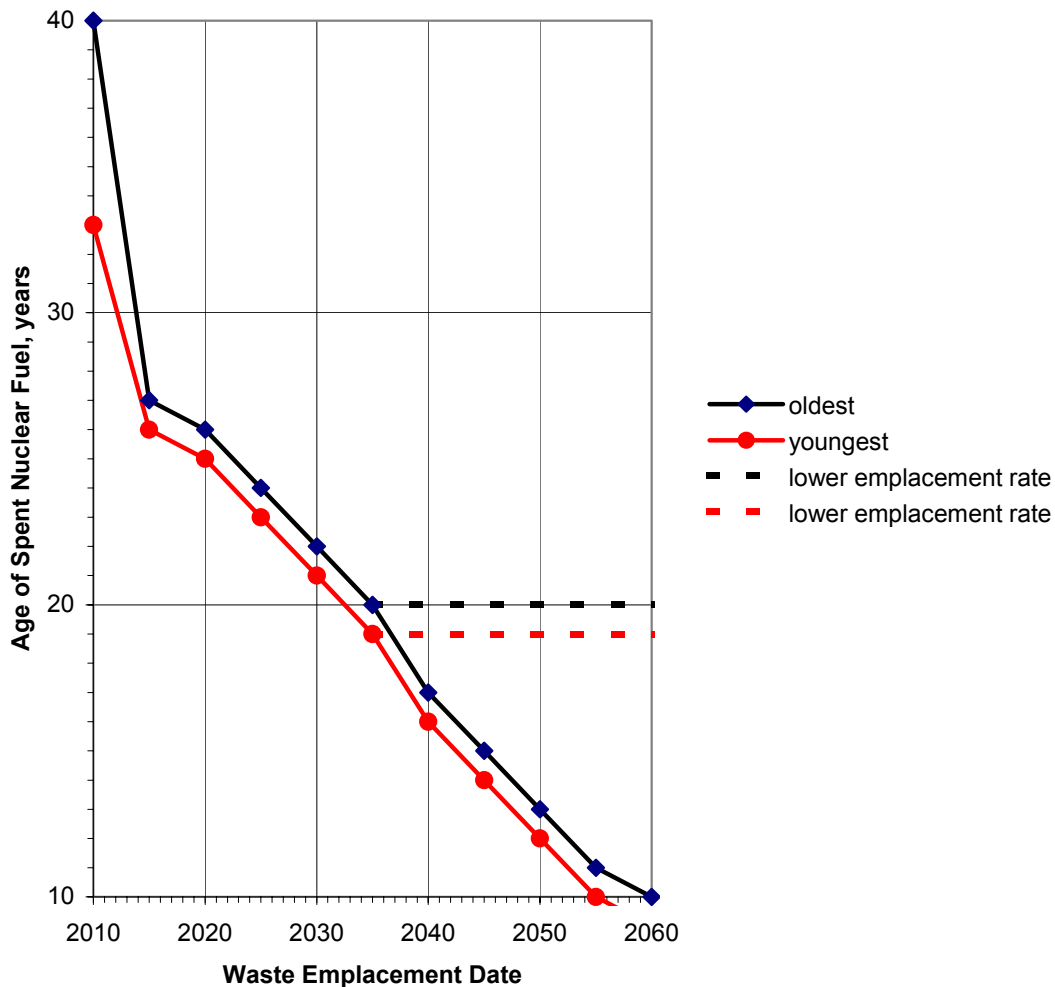


Figure M-1. Projected Age at Emplacement of Commercial SNF.

Note that the age decreases rapidly at the start of emplacement, reflecting the much larger emplacement rate (constant 3,000 MTHM/yr starting in 2010) compared to the small SNF production rate during the early years of commercial nuclear power. Indeed, when the YM repository is “filled” with the allotted 63,000 MTHM of commercial SNF in ~ 2031, the production rate for “fresh” SNF is still projected to be lower than the emplacement rate, ~2500

MTHM/yr, while the average age at emplacement has dropped only to ~ 21 years. Figure M-1 shows two projections for periods after 2035, one in which the emplacement rate (in a putative second repository, *e.g.*, YM2) continues at 3000 MTHM/yr (solid curves), and one in which a lower emplacement rate of 2500 MTHM/yr matches the projected production rate (dashed curves). Note that the age of emplaced SNF can be maintained at ~20 years in the steady-state, but at the higher emplacement rate the age decreases to the nominal value of 10 years only after ~2055.

Thus, future calculations for age of SNF at emplacement in a geological repository should probably be based on a more realistic value of 20 years or greater cooling time, rather than the “standard” assumption of 10 years used to date.

Further analyses will include the reduced heat loads expected from the longer cooling periods and also the reduced fuel burn-up from the existing SNF.

Appendix N: Details of Thermal Heat Load Calculations for Section 6

In this Appendix we present some of the details of the calculations that are described in Sec. 6. As described, the program Monteburns is used to determine the “initial” (end of irradiation period, start of cooling period) isotopic distribution of three types of SNF (Standard LWR irradiated to 38 GWd/MTHM burn-up, Extended LWR irradiated to 60 GWd/MTHM , and MOX-fueled LWR irradiated to 49 GWd/MTHM). The program ORIGEN2.1 was then used to determine the decay heat and composition (plus other quantities not reported herein) of the three types of SNF as a function of time. The contributions from various components (Table N-I) of the SNF were separately summed to permit calculation of the effects on the decay heat and mass of SNF subjected to different degrees of cleanup (as listed in Sec. 6, Table 6-I).

Table N-I. Elements of SNF used for calculations of Scenarios II-VII.

Brief Description	Extended Description	Used in Mass Calculations	Used in Thermal Calculations
Structure	All structural portions of the initial fuel (hulls, clad, etc.) except uranium oxide or mixed oxide	Monteburns tabulates structural elements separately	Monteburns tabulates structural elements separately
Volatile FPs	Fission Products released from SNF during the dissolution step, which can be trapped by a number of physical and/or chemical means	Hydrogen, Carbon (volatilizes as monoxide or dioxide), Krypton, Xenon, Bromine, Iodine	Hydrogen, Carbon (volatilizes as monoxide or dioxide), Krypton, Xenon, Bromine, Iodine
Uranium	Uranium, all isotopes	Uranium	Uranium
Plutonium	Plutonium, all isotopes	Plutonium	Plutonium
Minor Actinides	Actinides excluding uranium and plutonium	Actinides plus their daughters, excluding uranium and plutonium	Actinides plus their daughters, excluding uranium and plutonium
High-Heat-Release FPs	Short-lived, high heat release fission products cesium and strontium	Cesium, Strontium	Cesium, Strontium and their short-lived decay products (certain isotopes of Barium and Yttrium)

Although Monteburns and ORIGEN2.2 both follow individual isotopes, our calculations sum over isotopes to reflect the fact that the separation procedures are element-specific, not isotope-specific (*i.e.*, all isotopes of a given element are separated simultaneously). Because the “summed over isotopes” data is considerably more compact than the full data set, we report only the summed data herein. Note that the mass calculations include long-lived and stable isotopes even though these contribute little or nothing to the decay heat.

Note also that a slightly different summation is used in the mass and thermal calculations for “high heat release FPs”. When the separation is performed (at a nominal 10-yr cooling time) only the cesium and strontium are separated from the remaining waste, and so their masses are subtracted from that of the other FPs. However, the majority of the decay heat arising from these elements is actually released by their short-lived decay products (^{137}Ba is the daughter of ^{137}Cs , and ^{90}Y is the daughter of ^{90}Sr), so in the thermal calculations these elements are included in the “cesium plus strontium” category.

The remainder of this appendix consists of tables and figures that summarize the mass and heat load calculations. For each of three fuels (Standard LWR, Extended LWR, and MOX-fueled LWR) we present the following:

- The mass of each element as a function of time, summed over isotopes. The ORIGEN2.2 output is presented for time periods up to 300 yr. The masses reported represent 1/24 of a full reactor core, i.e. they are not normalized to initial metric tonnes of heavy metal.
- The decay heat as a function of time, summed over isotopes for each element. The ORIGEN2.q output is presented for time periods up to 300 yr. The decay heat represents the contribution of 1/24 of a full reactor core, i.e. they are not normalized to initial metric tonnes of heavy metal.
- The decay heat as a function of time for the different fractions separated as described in Section 6, Table 6-I, Scenarios I-VII. Normalized to initial metric tonnes of heavy metal.
- The integrated decay heat as a function of time for the components separated as described in Sec. 6, Table 6-I, Scenarios I-VII. Normalized to initial metric tonnes of heavy metal.
- The capacity benefit ratios calculated for Standard LWR fuel, for Enhanced LWR fuel, and for MOX-fueled LWR fuel are all presented in Table N-XIV.

Note that these tables are intentionally kept as brief as possible; the figures presented in the text extend to 10,000 yr (and the calculations were followed through 1,000,000 yr). However, as described in Sec. 6 only the data through 300 yr are used in calculations that rank the different separation schemes, so only that data is presented herein.

N.1 Standard LWR

Table N-II presents the masses of each element in 1/24 of a full reactor core using “Standard LWR” fuel. The calculations assume an initial UOX fuel enriched to 3.2wt% ^{235}U , irradiated to a burn-up of 38 GWd/MTM . Structural elements (hulls, clads, etc.) constitute 11.85% of the initial mass.

Table N-II. Mass (*grams*) of Each Element for Standard LWR Fuel (1/24 Reactor).

ACTINIDES AND DAUGHTERS													
	INITIAL	1.0YR	3.0YR	5.0YR	10.0YR	15.0YR	20.0YR	25.0YR	30.0YR	40.0YR	50.0YR	100.0YR	300.0YR
He	1.312E+00	2.244E+00	2.873E+00	3.333E+00	4.475E+00	5.628E+00	6.784E+00	7.935E+00	9.077E+00	1.132E+01	1.351E+01	2.346E+01	5.279E+01
Th	3.877E-03	5.549E-03	8.946E-03	1.239E-02	2.121E-02	3.031E-02	3.970E-02	4.939E-02	5.935E-02	8.009E-02	1.018E-01	2.232E-01	8.238E-01
Pa	7.635E-04	7.899E-04	8.373E-04	8.846E-04	1.003E-03	1.122E-03	1.240E-03	1.359E-03	1.478E-03	1.716E-03	1.954E-03	3.144E-03	7.900E-03
U	3.360E+06	3.360E+06	3.360E+06	3.360E+06	3.360E+06	3.360E+06	3.360E+06	3.360E+06	3.360E+06	3.360E+06	3.360E+06	3.361E+06	3.361E+06
Np	1.854E+03	1.575E+03	1.577E+03	1.581E+03	1.594E+03	1.612E+03	1.635E+03	1.662E+03	1.691E+03	1.755E+03	1.823E+03	2.180E+03	3.398E+03
Pu	3.373E+04	3.385E+04	3.343E+04	3.304E+04	3.219E+04	3.153E+04	3.100E+04	3.058E+04	3.025E+04	2.977E+04	2.945E+04	2.886E+04	2.832E+04
Am	6.707E+02	9.036E+02	1.336E+03	1.726E+03	2.547E+03	3.184E+03	3.676E+03	4.054E+03	4.343E+03	4.725E+03	4.931E+03	4.972E+03	3.764E+03
Cm	2.347E+02	1.855E+02	1.623E+02	1.506E+02	1.260E+02	1.057E+02	8.898E+01	7.514E+01	6.371E+01	4.646E+01	3.469E+01	1.307E+01	9.120E+00
SUBTOTAL	3.397E+06	3.397E+06	3.397E+06	3.397E+06	3.397E+06	3.397E+06	3.397E+06	3.397E+06	3.397E+06	3.397E+06	3.397E+06	3.397E+06	3.397E+06
STRUCTURE	4.749E+05	4.749E+05	4.749E+05	4.749E+05	4.749E+05	4.749E+05	4.749E+05	4.749E+05	4.749E+05	4.749E+05	4.749E+05	4.749E+05	4.749E+05
ACT+FP	3.397E+06	3.397E+06	3.397E+06	3.397E+06	3.397E+06	3.397E+06	3.397E+06	3.397E+06	3.397E+06	3.397E+06	3.397E+06	3.397E+06	3.397E+06
SUBTOTAL	3.872E+06	3.872E+06	3.872E+06	3.872E+06	3.872E+06	3.872E+06	3.872E+06	3.872E+06	3.872E+06	3.872E+06	3.872E+06	3.872E+06	3.872E+06
FISSION PRODUCTS													
	INITIAL	1.0YR	3.0YR	5.0YR	10.0YR	15.0YR	20.0YR	25.0YR	30.0YR	40.0YR	50.0YR	100.0YR	300.0YR
H	2.293E-01	2.168E-01	1.937E-01	1.732E-01	1.308E-01	9.879E-02	7.461E-02	5.635E-02	4.256E-02	2.428E-02	1.385E-02	8.379E-04	1.116E-08
Li	7.389E-04	7.389E-04	7.389E-04	7.389E-04	7.389E-04	7.389E-04	7.389E-04	7.389E-04	7.389E-04	7.389E-04	7.389E-04	7.389E-04	7.389E-04
Be	5.940E-04	5.940E-04	5.940E-04	5.940E-04	5.940E-04	5.940E-04	5.940E-04	5.940E-04	5.940E-04	5.940E-04	5.940E-04	5.940E-04	5.939E-04
C	1.045E-04	1.044E-04	1.044E-04	1.044E-04	1.043E-04	1.043E-04	1.042E-04	1.041E-04	1.041E-04	1.040E-04	1.038E-04	1.032E-04	1.007E-04
Zn	2.657E-04	1.581E-07	1.581E-07	1.581E-07	1.581E-07	1.581E-07	1.581E-07	1.581E-07	1.581E-07	1.581E-07	1.581E-07	1.581E-07	1.581E-07
Ga	1.449E-04	3.803E-06	3.803E-06	3.803E-06	3.803E-06	3.803E-06	3.803E-06	3.803E-06	3.803E-06	3.803E-06	3.803E-06	3.803E-06	3.803E-06
Ge	2.688E+00	2.687E+00	2.687E+00	2.687E+00	2.687E+00	2.687E+00	2.687E+00	2.687E+00	2.687E+00	2.687E+00	2.687E+00	2.687E+00	2.687E+00
As	8.226E-01	8.136E-01	8.136E-01	8.136E-01	8.136E-01	8.136E-01	8.136E-01	8.136E-01	8.136E-01	8.136E-01	8.136E-01	8.136E-01	8.136E-01
Se	2.207E+02	2.207E+02	2.207E+02	2.207E+02	2.207E+02	2.207E+02	2.207E+02	2.207E+02	2.207E+02	2.207E+02	2.207E+02	2.207E+02	2.206E+02
Br	8.422E+01	8.417E+01	8.417E+01	8.417E+01	8.417E+01	8.417E+01	8.417E+01	8.418E+01	8.418E+01	8.418E+01	8.418E+01	8.419E+01	8.424E+01
Kr	1.427E+03	1.421E+03	1.411E+03	1.402E+03	1.383E+03	1.370E+03	1.361E+03	1.354E+03	1.349E+03	1.342E+03	1.339E+03	1.336E+03	1.336E+03
Rb	1.315E+03	1.320E+03	1.331E+03	1.340E+03	1.358E+03	1.371E+03	1.381E+03	1.388E+03	1.393E+03	1.399E+03	1.402E+03	1.406E+03	1.406E+03

Table N-II. Mass (*grams*) of Each Element for Standard LWR Fuel (1/24 Reactor) (continued).

	INITIAL	1.0YR	3.0YR	5.0YR	10.0YR	15.0YR	20.0YR	25.0YR	30.0YR	40.0YR	50.0YR	100.0YR	300.0YR
Sr	3.478E+03	3.343E+03	3.162E+03	2.958E+03	2.777E+03	2.617E+03	2.475E+03	2.348E+03	2.236E+03	2.136E+03	1.969E+03	1.537E+03	1.350E+03
Y	1.804E+03	1.754E+03	1.753E+03	1.753E+03	1.753E+03	1.753E+03	1.753E+03	1.753E+03	1.753E+03	1.753E+03	1.753E+03	1.753E+03	1.753E+03
Zr	1.377E+04	1.373E+04	1.382E+04	1.391E+04	1.411E+04	1.430E+04	1.446E+04	1.460E+04	1.472E+04	1.494E+04	1.510E+04	1.554E+04	1.572E+04
Nb	1.189E+02	5.316E+00	1.092E-02	1.154E-02	1.786E-02	2.419E-02	3.052E-02	3.685E-02	4.318E-02	5.583E-02	6.849E-02	1.318E-01	3.849E-01
Mo	1.291E+04	1.323E+04	1.324E+04	1.324E+04	1.324E+04	1.324E+04	1.324E+04	1.324E+04	1.324E+04	1.324E+04	1.324E+04	1.324E+04	1.324E+04
Tc	3.132E+03	3.144E+03	3.144E+03	3.144E+03	3.144E+03	3.144E+03	3.144E+03	3.144E+03	3.144E+03	3.144E+03	3.144E+03	3.143E+03	3.141E+03
Ru	9.646E+03	9.164E+03	8.923E+03	8.863E+03	8.843E+03	8.842E+03	8.842E+03	8.842E+03	8.842E+03	8.843E+03	8.843E+03	8.843E+03	8.845E+03
Rh	1.635E+03	1.794E+03	1.794E+03	1.794E+03	1.794E+03	1.794E+03	1.794E+03	1.794E+03	1.794E+03	1.794E+03	1.794E+03	1.794E+03	1.794E+03
Pd	5.310E+03	5.633E+03	5.873E+03	5.934E+03	5.954E+03	5.954E+03	5.954E+03	5.954E+03	5.954E+03	5.954E+03	5.954E+03	5.954E+03	5.954E+03
Ag	3.395E+02	3.361E+02	3.350E+02	3.349E+02	3.349E+02	3.349E+02	3.349E+02	3.349E+02	3.349E+02	3.349E+02	3.349E+02	3.349E+02	3.349E+02
Cd	4.737E+02	4.773E+02	4.783E+02	4.783E+02	4.782E+02	4.780E+02	4.779E+02	4.778E+02	4.777E+02	4.776E+02	4.775E+02	4.775E+02	4.774E+02
In	8.847E+00	9.279E+00	9.381E+00	9.473E+00	9.669E+00	9.823E+00	9.944E+00	1.004E+01	1.012E+01	1.022E+01	1.029E+01	1.039E+01	1.040E+01
Sn	3.844E+02	3.826E+02	3.824E+02	3.824E+02	3.824E+02	3.824E+02	3.824E+02	3.824E+02	3.824E+02	3.824E+02	3.823E+02	3.823E+02	3.821E+02
Sb	1.337E+02	1.208E+02	1.036E+02	9.300E+01	8.140E+01	7.808E+01	7.713E+01	7.686E+01	7.678E+01	7.675E+01	7.675E+01	7.675E+01	7.676E+01
Te	1.938E+03	1.925E+03	1.942E+03	1.953E+03	1.964E+03	1.968E+03	1.968E+03	1.969E+03	1.969E+03	1.969E+03	1.969E+03	1.969E+03	1.969E+03
I	1.003E+03	9.797E+02	9.802E+02	9.802E+02	9.802E+02	9.802E+02	9.802E+02	9.802E+02	9.802E+02	9.802E+02	9.802E+02	9.802E+02	9.802E+02
Xe	2.127E+04	2.128E+04	2.128E+04	2.128E+04	2.128E+04	2.128E+04	2.128E+04	2.128E+04	2.128E+04	2.128E+04	2.128E+04	2.128E+04	2.128E+04
Cs	1.073E+04	1.053E+04	1.016E+04	9.873E+03	9.341E+03	8.917E+03	8.549E+03	8.223E+03	7.933E+03	7.445E+03	7.057E+03	6.035E+03	5.570E+03
Ba	5.526E+03	5.696E+03	6.070E+03	6.354E+03	6.886E+03	7.310E+03	7.678E+03	8.004E+03	8.294E+03	8.782E+03	9.170E+03	1.019E+04	1.066E+04
La	4.819E+03	4.808E+03	4.808E+03	4.808E+03	4.808E+03	4.808E+03	4.808E+03	4.808E+03	4.808E+03	4.808E+03	4.808E+03	4.808E+03	4.808E+03
Ce	1.059E+04	9.746E+03	9.317E+03	9.245E+03	9.230E+03	9.230E+03	9.230E+03	9.230E+03	9.230E+03	9.230E+03	9.230E+03	9.230E+03	9.230E+03
Pr	4.318E+03	4.428E+03	4.428E+03	4.428E+03	4.428E+03	4.428E+03	4.428E+03	4.428E+03	4.428E+03	4.428E+03	4.428E+03	4.428E+03	4.428E+03
Nd	1.454E+04	1.533E+04	1.576E+04	1.583E+04	1.585E+04	1.585E+04	1.585E+04	1.585E+04	1.585E+04	1.585E+04	1.585E+04	1.585E+04	1.585E+04
Pm	7.181E+02	5.613E+02	3.309E+02	1.951E+02	5.206E+01	1.390E+01	3.710E+00	9.907E-01	2.648E-01	1.903E-02	1.404E-03	1.231E-07	1.364E-18
Sm	2.648E+03	2.827E+03	3.057E+03	3.192E+03	3.334E+03	3.370E+03	3.379E+03	3.380E+03	3.380E+03	3.378E+03	3.375E+03	3.366E+03	3.350E+03
Eu	6.187E+02	5.944E+02	5.767E+02	5.622E+02	5.363E+02	5.205E+02	5.109E+02	5.052E+02	5.019E+02	4.994E+02	4.996E+02	5.072E+02	5.228E+02
Gd	4.478E+02	4.763E+02	4.946E+02	5.097E+02	5.371E+02	5.544E+02	5.655E+02	5.726E+02	5.772E+02	5.822E+02	5.844E+02	5.861E+02	5.861E+02
Tb	1.189E+01	1.149E+01	1.148E+01	1.148E+01	1.148E+01	1.148E+01	1.148E+01	1.148E+01	1.148E+01	1.148E+01	1.148E+01	1.148E+01	1.148E+01
Dy	5.851E+00	6.269E+00	6.280E+00	6.280E+00	6.280E+00	6.280E+00	6.280E+00	6.280E+00	6.280E+00	6.280E+00	6.280E+00	6.280E+00	6.280E+00
Ho	6.925E-01	6.917E-01	6.917E-01	6.917E-01	6.917E-01	6.917E-01	6.916E-01	6.916E-01	6.916E-01	6.915E-01	6.915E-01	6.913E-01	6.905E-01
Er	2.831E-01	2.846E-01	2.847E-01	2.847E-01	2.847E-01	2.847E-01	2.847E-01	2.848E-01	2.848E-01	2.848E-01	2.849E-01	2.851E-01	2.859E-01
Tm	3.364E-04	3.123E-04	3.044E-04	3.035E-04	3.029E-04	3.028E-04	3.028E-04	3.028E-04	3.028E-04	3.028E-04	3.028E-04	3.028E-04	3.028E-04
Yb	6.401E-05	1.047E-04	1.126E-04	1.135E-04	1.141E-04	1.142E-04	1.142E-04	1.142E-04	1.142E-04	1.142E-04	1.142E-04	1.142E-04	1.142E-04
TOTAL FP	1.354E+05	1.354E+05	1.354E+05	1.354E+05	1.354E+05	1.354E+05	1.354E+05	1.354E+05	1.354E+05	1.354E+05	1.354E+05	1.354E+05	1.354E+05

Table N-II. Mass (*grams*) of Each Element for Standard LWR Fuel (1/24 Reactor) (continued).

	INITIAL	1.0YR	3.0YR	5.0YR	10.0YR	15.0YR	20.0YR	25.0YR	30.0YR	40.0YR	50.0YR	100.0YR	300.0YR
ACT+FP	3.532E+06	3.532E+06	3.532E+06	3.532E+06	3.532E+06	3.532E+06	3.532E+06	3.532E+06	3.532E+06	3.532E+06	3.532E+06	3.532E+06	3.532E+06
TOTAL	4.007E+06	4.007E+06	4.007E+06	4.007E+06	4.007E+06	4.007E+06	4.007E+06	4.007E+06	4.007E+06	4.007E+06	4.007E+06	4.007E+06	4.007E+06

Table N-III presents the decay heat of each element in 1/24 of a full reactor core using “Standard LWR” fuel. The calculations assume an initial UOX fuel enriched to 3.2wt% ²³⁵U, irradiated to a burn-up of 38 GWD/MTHM. Structural elements (hulls, clads, etc.) constitute 11.85% of the initial mass.

Table N-III. Decay Heat (*watts*) of Each Element for Standard LWR Fuel.

ACTINIDES AND DAUGHTERS													
	INITIAL	1.0YR	3.0YR	5.0YR	10.0YR	15.0YR	20.0YR	25.0YR	30.0YR	40.0YR	50.0YR	100.0YR	300.0YR
U	1.970E+05	1.600E-01	1.607E-01	1.611E-01	1.618E-01	1.627E-01	1.640E-01	1.656E-01	1.676E-01	1.719E-01	1.765E-01	1.984E-01	2.378E-01
Np	1.790E+05	2.768E-01	2.768E-01	2.768E-01	2.769E-01	2.772E-01	2.776E-01	2.780E-01	2.785E-01	2.796E-01	2.808E-01	2.872E-01	3.086E-01
Pu	2.354E+03	4.598E+02	4.591E+02	4.527E+02	4.367E+02	4.219E+02	4.079E+02	3.948E+02	3.824E+02	3.594E+02	3.386E+02	2.579E+02	1.263E+02
Am	2.310E+03	4.864E+01	9.793E+01	1.425E+02	2.362E+02	3.088E+02	3.650E+02	4.081E+02	4.411E+02	4.847E+02	5.083E+02	5.133E+02	3.767E+02
Cm	7.133E+03	1.884E+03	4.955E+02	4.029E+02	3.307E+02	2.734E+02	2.260E+02	1.869E+02	1.546E+02	1.058E+02	7.256E+01	1.148E+01	3.761E-01
SUBTOTAL	3.878E+05	2.393E+03	1.053E+03	9.986E+02	1.004E+03	1.005E+03	9.994E+02	9.903E+02	9.785E+02	9.504E+02	9.199E+02	7.832E+02	5.039E+02
STRUCTURE	6.485E+01	1.580E-07	1.579E-07	1.579E-07	1.578E-07	1.577E-07	1.576E-07	1.575E-07	1.574E-07	1.573E-07	1.571E-07	1.562E-07	1.527E-07
ACT+FP	3.878E+05	2.393E+03	1.053E+03	9.986E+02	1.004E+03	1.005E+03	9.994E+02	9.903E+02	9.785E+02	9.504E+02	9.199E+02	7.832E+02	5.039E+02
SUBTOTAL	3.879E+05	2.393E+03	1.053E+03	9.986E+02	1.004E+03	1.005E+03	9.994E+02	9.903E+02	9.785E+02	9.504E+02	9.199E+02	7.832E+02	5.039E+02
FISSION PRODUCTS													
	INITIAL	1.0YR	3.0YR	5.0YR	10.0YR	15.0YR	20.0YR	25.0YR	30.0YR	40.0YR	50.0YR	100.0YR	300.0YR
As	2.423E+04	0.000E+00	0.000E+00	0.000E+00	0.000E+00	0.000E+00	0.000E+00	0.000E+00	0.000E+00	0.000E+00	0.000E+00	0.000E+00	0.000E+00
Se	4.937E+04	4.036E-04	4.036E-04	4.036E-04	4.036E-04	4.035E-04	4.035E-04	4.035E-04	4.035E-04	4.034E-04	4.034E-04	4.032E-04	4.023E-04
Br	1.369E+05	0.000E+00	0.000E+00	0.000E+00	0.000E+00	0.000E+00	0.000E+00	0.000E+00	0.000E+00	0.000E+00	0.000E+00	0.000E+00	0.000E+00
Kr	1.856E+05	5.036E+01	4.425E+01	3.888E+01	2.814E+01	2.037E+01	1.474E+01	1.067E+01	7.722E+00	4.045E+00	2.119E+00	8.337E-02	2.020E-07
Rb	3.786E+05	4.299E-05	6.858E-08	6.858E-08	6.858E-08	6.858E-08	6.858E-08	6.858E-08	6.858E-08	6.858E-08	6.858E-08	6.858E-08	6.858E-08
Sr	3.482E+05	3.734E+02	3.013E+02	2.873E+02	2.550E+02	2.264E+02	2.010E+02	1.785E+02	1.584E+02	1.249E+02	9.842E+01	2.994E+01	2.564E-01
Y	5.661E+05	1.667E+03	1.439E+03	1.372E+03	1.218E+03	1.081E+03	9.601E+02	8.524E+02	7.567E+02	5.964E+02	4.701E+02	1.430E+02	1.225E+00
Zr	2.958E+05	4.678E+02	1.718E-01	8.784E-04	8.159E-04	8.159E-04	8.159E-04	8.159E-04	8.159E-04	8.159E-04	8.159E-04	8.158E-04	8.158E-04
Nb	6.386E+05	9.970E+02	3.602E-01	4.750E-04	5.334E-04	6.806E-04	7.948E-04	8.832E-04	9.518E-04	1.046E-03	1.103E-03	1.181E-03	1.188E-03
Mo	2.861E+05	0.000E+00	0.000E+00	0.000E+00	0.000E+00	0.000E+00	0.000E+00	0.000E+00	0.000E+00	0.000E+00	0.000E+00	0.000E+00	0.000E+00
Tc	4.124E+05	2.674E-02	2.674E-02	2.674E-02	2.674E-02	2.674E-02	2.674E-02	2.674E-02	2.674E-02	2.674E-02	2.674E-02	2.673E-02	2.672E-02
Ru	9.637E+04	9.197E+01	1.619E+01	4.093E+00	1.315E-01	4.223E-03	1.356E-04	4.357E-06	1.399E-07	1.447E-10	1.493E-13	0.000E+00	0.000E+00
Rh	1.196E+05	1.033E+04	2.612E+03	6.602E+02	2.121E+01	6.831E-01	2.247E-02	8.823E-04	7.691E-05	5.001E-06	4.560E-07	2.943E-12	5.106E-33
Pd	1.157E+04	2.874E-05	2.874E-05	2.874E-05	2.874E-05	2.874E-05	2.874E-05	2.874E-05	2.874E-05	2.874E-05	2.874E-05	2.874E-05	2.874E-05
Ag	1.649E+04	1.001E+02	1.320E+01	1.740E+00	1.098E+02	7.042E-05	1.566E-06	1.102E-06	1.069E-06	1.013E-06	9.588E-07	7.298E-07	2.450E-07
Cd	6.710E+03	4.911E-01	3.715E-01	3.379E-01	2.664E-01	2.101E-01	1.657E-01	1.306E-01	1.030E-01	6.406E-02	3.983E-02	3.703E-03	2.766E-07
In	2.731E+04	5.024E-04	1.811E-08	7.366E-13	8.179E-14	8.179E-14	8.179E-14	8.179E-14	8.179E-14	8.179E-14	8.179E-14	8.179E-14	8.179E-14
Sn	5.952E+04	5.619E+00	1.347E-01	1.045E-02	5.573E-03	5.456E-03	5.362E-03	5.273E-03	5.191E-03	5.042E-03	4.912E-03	4.477E-03	4.064E-03
Sb	2.324E+05	1.441E+02	8.666E+01	5.256E+01	1.507E+01	4.349E+00	1.280E+00	4.017E-01	1.504E-01	5.792E-02	5.035E-02	4.965E-02	4.958E-02

Table N-III. Decay Heat (*watts*) of Each Element for Standard LWR Fuel (continued).

	INITIAL	1.0YR	3.0YR	5.0YR	10.0YR	15.0YR	20.0YR	25.0YR	30.0YR	40.0YR	50.0YR	100.0YR	300.0YR
Te	2.406E+05	1.882E+01	5.771E+00	3.446E+00	9.856E-01	2.820E-01	8.071E-02	2.309E-02	6.609E-03	5.411E-04	4.431E-05	1.631E-10	1.296E-15
I	5.588E+05	6.088E-05	6.088E-05	6.088E-05	6.088E-05	6.088E-05	6.088E-05	6.088E-05	6.088E-05	6.088E-05	6.088E-05	6.088E-05	6.088E-05
Xe	2.639E+05	5.456E-07	4.405E-13	4.024E-19	3.210E-34	0.000E+00	0.000E+00	0.000E+00	0.000E+00	0.000E+00	0.000E+00	0.000E+00	0.000E+00
Cs	4.801E+05	4.898E+03	2.699E+03	1.567E+03	5.779E+02	3.626E+02	2.946E+02	2.572E+02	2.282E+02	1.809E+02	1.436E+02	4.522E+01	4.455E-01
Ba	2.818E+05	1.496E+03	1.428E+03	1.364E+03	1.215E+03	1.082E+03	9.643E+02	8.591E+02	7.653E+02	6.074E+02	4.821E+02	1.519E+02	1.495E+00
La	4.913E+05	2.674E-04	3.220E-12	3.220E-12	3.220E-12	3.220E-12	3.220E-12	3.220E-12	3.220E-12	3.220E-12	3.220E-12	3.220E-12	3.220E-12
Ce	1.182E+05	1.095E+03	1.840E+02	3.098E+01	3.607E-01	4.199E-03	4.888E-05	5.690E-07	6.625E-09	8.978E-13	1.217E-16	0.000E+00	0.000E+00
Pr	1.788E+05	1.211E+04	2.040E+03	3.435E+02	3.999E+00	4.656E-02	5.420E-04	6.310E-06	7.345E-08	9.954E-12	1.349E-15	0.000E+00	0.000E+00
Nd	2.516E+04	5.815E-07	7.624E-27	0.000E+00	0.000E+00	0.000E+00	0.000E+00	0.000E+00	0.000E+00	0.000E+00	0.000E+00	0.000E+00	0.000E+00
Pm	2.725E+04	1.890E+02	1.101E+02	6.493E+01	1.734E+01	4.633E+00	1.239E+00	3.325E-01	8.964E-02	6.773E-03	5.930E-04	2.717E-07	3.064E-18
Eu	1.166E+04	2.218E+02	1.881E+02	1.596E+02	1.060E+02	7.049E+01	4.695E+01	3.130E+01	2.088E+01	9.306E+00	4.154E+00	7.451E-02	4.724E-08
TOTAL FP	6.583E+06	3.426E+04	1.117E+04	5.950E+03	3.460E+03	2.854E+03	2.485E+03	2.190E+03	1.938E+03	1.523E+03	1.201E+03	3.703E+02	3.517E+00
AP+FP	6.583E+06	3.426E+04	1.117E+04	5.950E+03	3.460E+03	2.854E+03	2.485E+03	2.190E+03	1.938E+03	1.523E+03	1.201E+03	3.703E+02	3.517E+00
ACT+FP	6.971E+06	3.666E+04	1.222E+04	6.949E+03	4.464E+03	3.859E+03	3.484E+03	3.180E+03	2.916E+03	2.474E+03	2.121E+03	1.154E+03	5.075E+02
TOTAL	6.971E+06	3.666E+04	1.222E+04	6.949E+03	4.464E+03	3.859E+03	3.484E+03	3.180E+03	2.916E+03	2.474E+03	2.121E+03	1.154E+03	5.075E+02

Table N-IV presents the decay heat as a function of time separated into different fractions as described in Sec. 6, Table 6-I. The decay heat is normalized to initial metric tonnes of heavy metal.

Table N-IV. Decay Heat of Separated Fractions for Standard LWR fuel.

DECAY TIME, YR	DECAY HEAT, WATTS per INITIAL METRIC TONNE OF HEAVY METAL						
	SCENARIO						
	I	II	III	IV	V	VI	VII
INITIAL	1.974E+06	(a)	(a)	(a)	(a)	(a)	(a)
1	1.038E+04	(a)	(a)	(a)	(a)	(a)	(a)
3	3.460E+03	(a)	(a)	(a)	(a)	(a)	(a)
5	1.967E+03	(a)	(a)	(a)	(a)	(a)	(a)
10	1.264E+03	1.256E+03	3.312E+02	2.075E+02	1.132E+03	9.716E+02	4.697E+01
15	1.093E+03	1.087E+03	3.076E+02	1.881E+02	9.673E+02	8.024E+02	2.324E+01
20	9.864E+02	9.821E+02	2.970E+02	1.815E+02	8.667E+02	6.993E+02	1.413E+01
25	9.003E+02	8.972E+02	2.893E+02	1.776E+02	7.855E+02	6.169E+02	9.027E+00
30	8.256E+02	8.233E+02	2.830E+02	1.747E+02	7.151E+02	5.463E+02	5.983E+00
40	7.004E+02	6.992E+02	2.718E+02	1.701E+02	5.975E+02	4.302E+02	2.832E+00
50	6.005E+02	5.998E+02	2.617E+02	1.659E+02	5.040E+02	3.394E+02	1.343E+00
100	3.267E+02	3.266E+02	2.219E+02	1.488E+02	2.536E+02	1.050E+02	1.896E-01
300	1.437E+02	1.436E+02	1.426E+02	1.069E+02	1.079E+02	1.009E+00	4.013E-02
^(a) Scenarios II-VII follow reprocessing at 10 years							

Table N-V presents the integrated decay heat as a function of time separated into different fractions as described in Sec. 6, Table 6-I. The integrated decay heat is normalized to initial metric tonnes of heavy metal.

Table N-V. Integrated Decay Heat of Separated Fractions for Standard LWR Fuel.

TIME AFTER REPROCESSING YRS	INTEGRATED DECAY HEAT, JOULES <i>per</i> INITIAL METRIC TONNE OF HEAVY METAL						
	SCENARIO						
	I	II	III	IV	V	VI	VII
5	1.856E+11	1.845E+11	5.037E+10	3.119E+10	1.653E+11	1.395E+11	5.322E+09
10	3.494E+11	3.476E+11	9.806E+10	6.035E+10	3.098E+11	2.578E+11	8.211E+09
15	4.982E+11	4.957E+11	1.443E+11	8.868E+10	4.401E+11	3.615E+11	1.001E+10
20	6.342E+11	6.314E+11	1.895E+11	1.165E+11	5.583E+11	4.532E+11	1.118E+10
30	8.745E+11	8.711E+11	2.770E+11	1.709E+11	7.649E+11	6.065E+11	1.251E+10
40	1.079E+12	1.076E+12	3.612E+11	2.239E+11	9.383E+11	7.274E+11	1.313E+10
90	1.789E+12	1.785E+12	7.418E+11	4.719E+11	1.514E+12	1.043E+12	1.406E+10
290	3.195E+12	3.191E+12	1.874E+12	1.272E+12	2.589E+12	1.184E+12	1.467E+10

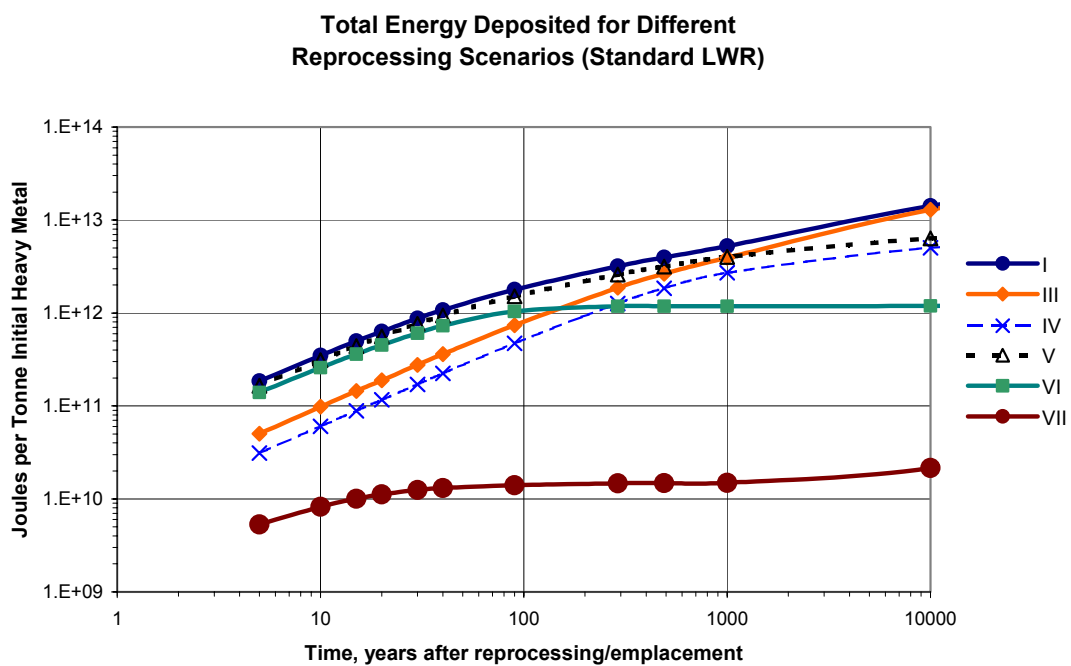


Figure N-1. Integrated decay heat of separated fractions for Standard LWR Fuel.

N.2 Extended LWR

Table N-VI presents the masses of each element in 1/24 of a full reactor core using “Extended LWR” fuel. The calculations assume an initial UOX fuel enriched to 4.2wt% ²³⁵U, irradiated to a burn-up of 60 *GWd/MTHM*. Structural elements (hulls, clads, etc.) constitute 11.85% of the initial mass.

Table N-VI. Mass (*grams*) of Each Element for Extended LWR Fuel (1/24 Reactor).

ACTINIDES+DAUGHTERS													
	INITIAL	1.0YR	3.0YR	5.0YR	10.0YR	15.0YR	20.0YR	25.0YR	30.0YR	40.0YR	50.0YR	100.0YR	300.0YR
He	5.922E+00	7.999E+00	9.687E+00	1.100E+01	1.409E+01	1.698E+01	1.971E+01	2.229E+01	2.473E+01	2.928E+01	3.344E+01	5.059E+01	9.468E+01
Th	2.085E-03	2.785E-03	4.302E-03	5.948E-03	1.058E-02	1.595E-02	2.208E-02	2.896E-02	3.656E-02	5.384E-02	7.370E-02	2.056E-01	1.028E+00
Pa	1.706E-04	1.879E-04	2.244E-04	2.610E-04	3.525E-04	4.442E-04	5.362E-04	6.283E-04	7.205E-04	9.052E-04	1.090E-03	2.014E-03	5.709E-03
U	3.271E+06	3.271E+06	3.271E+06	3.271E+06	3.271E+06	3.271E+06	3.271E+06	3.271E+06	3.272E+06	3.272E+06	3.272E+06	3.272E+06	3.273E+06
Np	2.913E+03	2.677E+03	2.680E+03	2.684E+03	2.702E+03	2.728E+03	2.760E+03	2.796E+03	2.835E+03	2.921E+03	3.014E+03	3.495E+03	5.136E+03
Pu	4.246E+04	4.252E+04	4.198E+04	4.148E+04	4.039E+04	3.954E+04	3.885E+04	3.831E+04	3.787E+04	3.723E+04	3.680E+04	3.590E+04	3.496E+04
Am	1.556E+03	1.865E+03	2.439E+03	2.958E+03	4.047E+03	4.892E+03	5.545E+03	6.046E+03	6.429E+03	6.934E+03	7.206E+03	7.251E+03	5.612E+03
Cm	8.458E+02	7.359E+02	6.657E+02	6.200E+02	5.220E+02	4.410E+02	3.741E+02	3.189E+02	2.733E+02	2.044E+02	1.574E+02	7.113E+01	5.509E+01
SUBTOTAL	3.319E+06	3.319E+06	3.319E+06	3.319E+06	3.319E+06	3.319E+06	3.319E+06	3.319E+06	3.319E+06	3.319E+06	3.319E+06	3.319E+06	3.319E+06
STRUCTURE	4.749E+05	4.749E+05	4.749E+05	4.749E+05	4.749E+05	4.749E+05	4.749E+05	4.749E+05	4.749E+05	4.749E+05	4.749E+05	4.749E+05	4.749E+05
ACT+FP	3.319E+06	3.319E+06	3.319E+06	3.319E+06	3.319E+06	3.319E+06	3.319E+06	3.319E+06	3.319E+06	3.319E+06	3.319E+06	3.319E+06	3.319E+06
SUBTOTAL	3.794E+06	3.794E+06	3.794E+06	3.794E+06	3.794E+06	3.794E+06	3.794E+06	3.794E+06	3.794E+06	3.794E+06	3.794E+06	3.794E+06	3.794E+06
FISSION PRODUCTS													
	INITIAL	1.0YR	3.0YR	5.0YR	10.0YR	15.0YR	20.0YR	25.0YR	30.0YR	40.0YR	50.0YR	100.0YR	300.0YR
H	3.463E-01	3.274E-01	2.926E-01	2.615E-01	1.975E-01	1.492E-01	1.127E-01	8.512E-02	6.429E-02	3.667E-02	2.092E-02	1.265E-03	1.685E-08
Li	7.823E-04	7.823E-04	7.823E-04	7.823E-04	7.823E-04	7.823E-04	7.823E-04	7.823E-04	7.823E-04	7.823E-04	7.823E-04	7.823E-04	7.823E-04
Be	9.330E-04	9.330E-04	9.329E-04	9.329E-04	9.329E-04	9.329E-04	9.329E-04	9.329E-04	9.329E-04	9.329E-04	9.329E-04	9.329E-04	9.328E-04
C	1.641E-04	1.640E-04	1.640E-04	1.640E-04	1.639E-04	1.638E-04	1.637E-04	1.636E-04	1.635E-04	1.633E-04	1.631E-04	1.621E-04	1.582E-04
Zn	2.289E-04	2.355E-07	2.355E-07	2.355E-07	2.355E-07	2.355E-07	2.355E-07	2.355E-07	2.355E-07	2.355E-07	2.355E-07	2.355E-07	2.355E-07
Ga	1.297E-04	5.982E-06	5.982E-06	5.982E-06	5.982E-06	5.982E-06	5.982E-06	5.982E-06	5.982E-06	5.982E-06	5.982E-06	5.982E-06	5.982E-06
Ge	4.187E+00	4.186E+00	4.186E+00	4.186E+00	4.186E+00	4.186E+00	4.186E+00	4.186E+00	4.186E+00	4.186E+00	4.186E+00	4.186E+00	4.186E+00
As	1.255E+00	1.248E+00	1.248E+00	1.248E+00	1.248E+00	1.248E+00	1.248E+00	1.248E+00	1.248E+00	1.248E+00	1.248E+00	1.248E+00	1.248E+00
Se	3.390E+02	3.390E+02	3.390E+02	3.390E+02	3.390E+02	3.390E+02	3.390E+02	3.390E+02	3.390E+02	3.390E+02	3.390E+02	3.389E+02	3.389E+02
Br	1.254E+02	1.254E+02	1.254E+02	1.254E+02	1.254E+02	1.254E+02	1.254E+02	1.254E+02	1.254E+02	1.254E+02	1.254E+02	1.254E+02	1.255E+02
Kr	2.160E+03	2.152E+03	2.137E+03	2.124E+03	2.099E+03	2.080E+03	2.067E+03	2.057E+03	2.050E+03	2.042E+03	2.037E+03	2.032E+03	2.032E+03
Rb	1.995E+03	2.002E+03	2.017E+03	2.030E+03	2.055E+03	2.074E+03	2.087E+03	2.097E+03	2.104E+03	2.113E+03	2.117E+03	2.122E+03	2.122E+03

Table N-VI. Mass (*grams*) of Each Element for Extended LWR Fuel (1/24 Reactor, continued).

	INITIAL	1.0YR	3.0YR	5.0YR	10.0YR	15.0YR	20.0YR	25.0YR	30.0YR	40.0YR	50.0YR	100.0YR	300.0YR
Sr	5.091E+03	4.955E+03	4.819E+03	4.690E+03	4.392E+03	4.128E+03	3.893E+03	3.684E+03	3.499E+03	3.189E+03	2.945E+03	2.312E+03	2.038E+03
Y	2.677E+03	2.638E+03	2.637E+03	2.637E+03	2.637E+03	2.637E+03	2.637E+03	2.637E+03	2.637E+03	2.637E+03	2.637E+03	2.637E+03	2.637E+03
Zr	2.114E+04	2.113E+04	2.126E+04	2.139E+04	2.169E+04	2.196E+04	2.219E+04	2.240E+04	2.258E+04	2.289E+04	2.314E+04	2.377E+04	2.405E+04
Nb	1.012E+02	4.418E+00	1.793E-02	2.019E-02	2.980E-02	3.942E-02	4.903E-02	5.865E-02	6.826E-02	8.749E-02	1.067E-01	2.029E-01	5.874E-01
Mo	2.040E+04	2.067E+04	2.068E+04	2.068E+04	2.068E+04	2.068E+04	2.068E+04	2.068E+04	2.068E+04	2.068E+04	2.068E+04	2.068E+04	2.068E+04
Tc	4.670E+03	4.680E+03	4.680E+03	4.680E+03	4.680E+03	4.680E+03	4.680E+03	4.680E+03	4.680E+03	4.680E+03	4.679E+03	4.679E+03	4.676E+03
Ru	1.533E+04	1.482E+04	1.455E+04	1.448E+04	1.446E+04	1.446E+04	1.446E+04	1.446E+04	1.446E+04	1.446E+04	1.446E+04	1.446E+04	1.446E+04
Rh	2.343E+03	2.484E+03	2.484E+03	2.484E+03	2.484E+03	2.484E+03	2.484E+03	2.484E+03	2.484E+03	2.484E+03	2.484E+03	2.484E+03	2.484E+03
Pd	9.762E+03	1.013E+04	1.040E+04	1.047E+04	1.049E+04	1.049E+04	1.049E+04	1.049E+04	1.049E+04	1.049E+04	1.049E+04	1.049E+04	1.049E+04
Ag	5.305E+02	5.257E+02	5.239E+02	5.237E+02	5.236E+02	5.236E+02	5.236E+02	5.236E+02	5.236E+02	5.236E+02	5.236E+02	5.236E+02	5.237E+02
Cd	9.385E+02	9.435E+02	9.451E+02	9.452E+02	9.448E+02	9.445E+02	9.443E+02	9.441E+02	9.440E+02	9.438E+02	9.437E+02	9.435E+02	9.435E+02
In	9.282E+00	9.732E+00	9.925E+00	1.010E+01	1.047E+01	1.076E+01	1.099E+01	1.117E+01	1.132E+01	1.152E+01	1.165E+01	1.183E+01	1.185E+01
Sn	6.278E+02	6.262E+02	6.260E+02	6.260E+02	6.260E+02	6.260E+02	6.260E+02	6.260E+02	6.260E+02	6.259E+02	6.259E+02	6.259E+02	6.256E+02
Sb	1.926E+02	1.759E+02	1.537E+02	1.401E+02	1.252E+02	1.209E+02	1.197E+02	1.194E+02	1.193E+02	1.192E+02	1.192E+02	1.192E+02	1.192E+02
Te	3.095E+03	3.090E+03	3.112E+03	3.125E+03	3.140E+03	3.144E+03	3.146E+03	3.146E+03	3.146E+03	3.146E+03	3.146E+03	3.146E+03	3.147E+03
I	1.556E+03	1.537E+03	1.538E+03	1.538E+03	1.538E+03	1.538E+03	1.538E+03	1.538E+03	1.538E+03	1.538E+03	1.538E+03	1.538E+03	1.538E+03
Xe	3.282E+04	3.283E+04	3.283E+04	3.283E+04	3.283E+04	3.283E+04	3.283E+04	3.283E+04	3.283E+04	3.283E+04	3.283E+04	3.283E+04	3.283E+04
Cs	1.707E+04	1.669E+04	1.607E+04	1.561E+04	1.477E+04	1.412E+04	1.355E+04	1.305E+04	1.261E+04	1.186E+04	1.126E+04	9.698E+03	8.984E+03
Ba	9.207E+03	9.560E+03	1.018E+04	1.064E+04	1.148E+04	1.213E+04	1.269E+04	1.319E+04	1.364E+04	1.439E+04	1.498E+04	1.655E+04	1.726E+04
La	7.460E+03	7.451E+03	7.451E+03	7.451E+03	7.451E+03	7.451E+03	7.451E+03	7.451E+03	7.451E+03	7.451E+03	7.451E+03	7.451E+03	7.451E+03
Ce	1.563E+04	1.491E+04	1.454E+04	1.448E+04	1.447E+04	1.447E+04	1.447E+04	1.447E+04	1.447E+04	1.447E+04	1.447E+04	1.447E+04	1.447E+04
Pr	6.757E+03	6.850E+03	6.850E+03	6.850E+03	6.850E+03	6.850E+03	6.850E+03	6.850E+03	6.850E+03	6.850E+03	6.850E+03	6.850E+03	6.850E+03
Nd	2.362E+04	2.430E+04	2.467E+04	2.473E+04	2.475E+04	2.475E+04	2.475E+04	2.475E+04	2.475E+04	2.475E+04	2.475E+04	2.475E+04	2.475E+04
Pm	7.433E+02	5.784E+02	3.410E+02	2.010E+02	5.365E+01	1.432E+01	3.825E+00	1.022E+00	2.735E-01	1.979E-02	1.498E-03	2.204E-07	2.464E-18
Sm	4.338E+03	4.520E+03	4.757E+03	4.896E+03	5.041E+03	5.079E+03	5.087E+03	5.088E+03	5.087E+03	5.084E+03	5.081E+03	5.068E+03	5.048E+03
Eu	9.804E+02	9.420E+02	9.103E+02	8.843E+02	8.375E+02	8.086E+02	7.907E+02	7.797E+02	7.731E+02	7.673E+02	7.665E+02	7.757E+02	7.963E+02
Gd	1.087E+03	1.130E+03	1.163E+03	1.189E+03	1.238E+03	1.269E+03	1.289E+03	1.302E+03	1.310E+03	1.319E+03	1.323E+03	1.326E+03	1.326E+03
Tb	2.144E+01	2.076E+01	2.074E+01	2.074E+01	2.074E+01	2.074E+01	2.074E+01	2.074E+01	2.074E+01	2.074E+01	2.074E+01	2.074E+01	2.074E+01
Dy	1.159E+01	1.230E+01	1.232E+01	1.232E+01	1.232E+01	1.232E+01	1.232E+01	1.232E+01	1.232E+01	1.232E+01	1.232E+01	1.232E+01	1.232E+01
Ho	1.852E+00	1.850E+00	1.850E+00	1.850E+00	1.850E+00	1.850E+00	1.850E+00	1.850E+00	1.850E+00	1.849E+00	1.849E+00	1.848E+00	1.845E+00
Er	8.874E-01	8.900E-01	8.901E-01	8.901E-01	8.902E-01	8.903E-01	8.904E-01	8.905E-01	8.906E-01	8.907E-01	8.909E-01	8.918E-01	8.950E-01
Tm	1.221E-03	1.106E-03	1.073E-03	1.068E-03	1.065E-03	1.064E-03	1.064E-03	1.064E-03	1.064E-03	1.064E-03	1.064E-03	1.064E-03	1.064E-03
Yb	4.410E-04	5.986E-04	6.313E-04	6.360E-04	6.394E-04	6.399E-04	6.400E-04	6.400E-04	6.400E-04	6.400E-04	6.400E-04	6.400E-04	6.400E-04

Table N-VI. Mass (*grams*) of Each Element for Extended LWR Fuel (1/24 Reactor, continued).

	INITIAL	1.0YR	3.0YR	5.0YR	10.0YR	15.0YR	20.0YR	25.0YR	30.0YR	40.0YR	50.0YR	100.0YR	300.0YR
TOTAL FP	2.128E+05	2.128E+05	2.128E+05	2.128E+05	2.128E+05	2.128E+05	2.128E+05	2.128E+05	2.128E+05	2.128E+05	2.128E+05	2.128E+05	2.128E+05
ACT+FP	3.532E+06	3.532E+06	3.532E+06	3.532E+06	3.532E+06	3.532E+06	3.532E+06	3.532E+06	3.532E+06	3.532E+06	3.532E+06	3.532E+06	3.532E+06
TOTAL	4.007E+06	4.007E+06	4.007E+06	4.007E+06	4.007E+06	4.007E+06	4.007E+06	4.007E+06	4.007E+06	4.007E+06	4.007E+06	4.007E+06	4.007E+06

Table N-VII presents the decay heat of each element in 1/24 of a full reactor core using “Extended LWR” fuel. The calculations assume an initial UOX fuel enriched to 4.2wt% ²³⁵U, irradiated to a burn-up of 60 GWD/MTHM. Structural elements (hulls, clads, etc.) constitute 11.85% of the initial mass.

Table N-VII. Decay Heat (*watts*) of Each Element for Extended LWR Fuel.

ACTINIDES+DAUGHTERS													
	INITIAL	1.0YR	3.0YR	5.0YR	10.0YR	15.0YR	20.0YR	25.0YR	30.0YR	40.0YR	50.0YR	100.0YR	300.0YR
U	1.705E+05	1.048E-01	1.087E-01	1.119E-01	1.186E-01	1.248E-01	1.312E-01	1.378E-01	1.446E-01	1.584E-01	1.720E-01	2.308E-01	3.321E-01
Np	1.575E+05	6.524E-01	6.523E-01	6.523E-01	6.524E-01	6.526E-01	6.529E-01	6.534E-01	6.539E-01	6.552E-01	6.565E-01	6.638E-01	6.875E-01
Pu	3.719E+03	1.040E+03	1.036E+03	1.021E+03	9.835E+02	9.481E+02	9.145E+02	8.825E+02	8.520E+02	7.950E+02	7.428E+02	5.377E+02	2.015E+02
Am	4.524E+03	7.950E+01	1.450E+02	2.042E+02	3.286E+02	4.250E+02	4.995E+02	5.568E+02	6.005E+02	6.583E+02	6.895E+02	6.953E+02	5.112E+02
Cm	1.501E+04	4.645E+03	1.847E+03	1.601E+03	1.318E+03	1.089E+03	9.002E+02	7.440E+02	6.150E+02	4.204E+02	2.876E+02	4.429E+01	1.013E+00
SUBTOTAL	3.512E+05	5.765E+03	3.029E+03	2.827E+03	2.631E+03	2.463E+03	2.315E+03	2.184E+03	2.068E+03	1.875E+03	1.721E+03	1.278E+03	7.147E+02
STRUCTURE	5.374E+01	5.681E-07	5.680E-07	5.678E-07	5.675E-07	5.671E-07	5.668E-07	5.665E-07	5.661E-07	5.654E-07	5.647E-07	5.613E-07	5.479E-07
ACT+FP	3.512E+05	5.765E+03	3.029E+03	2.827E+03	2.631E+03	2.463E+03	2.315E+03	2.184E+03	2.068E+03	1.875E+03	1.721E+03	1.278E+03	7.147E+02
SUBTOTAL	3.513E+05	5.765E+03	3.029E+03	2.827E+03	2.631E+03	2.463E+03	2.315E+03	2.184E+03	2.068E+03	1.875E+03	1.721E+03	1.278E+03	7.147E+02
FISSION PRODUCTS													
	INITIAL	1.0YR	3.0YR	5.0YR	10.0YR	15.0YR	20.0YR	25.0YR	30.0YR	40.0YR	50.0YR	100.0YR	300.0YR
As	1.836E+04	0.000E+00	0.000E+00	0.000E+00	0.000E+00	0.000E+00	0.000E+00	0.000E+00	0.000E+00	0.000E+00	0.000E+00	0.000E+00	0.000E+00
Se	3.709E+04	6.238E-04	6.238E-04	6.238E-04	6.237E-04	6.237E-04	6.237E-04	6.236E-04	6.236E-04	6.235E-04	6.235E-04	6.231E-04	6.218E-04
Br	1.009E+05	0.000E+00	0.000E+00	0.000E+00	0.000E+00	0.000E+00	0.000E+00	0.000E+00	0.000E+00	0.000E+00	0.000E+00	0.000E+00	0.000E+00
Kr	1.387E+05	7.035E+01	6.182E+01	5.432E+01	3.931E+01	2.845E+01	2.059E+01	1.490E+01	1.079E+01	5.651E+00	2.960E+00	1.174E-01	2.848E-07
Rb	2.871E+05	5.842E-05	1.035E-07	1.035E-07	1.035E-07	1.035E-07	1.035E-07	1.035E-07	1.035E-07	1.035E-07	1.035E-07	1.035E-07	1.035E-07
Sr	2.738E+05	5.062E+02	4.409E+02	4.204E+02	3.732E+02	3.313E+02	2.942E+02	2.611E+02	2.318E+02	1.827E+02	1.440E+02	4.381E+01	3.751E-01
Y	4.540E+05	2.330E+03	2.106E+03	2.008E+03	1.783E+03	1.583E+03	1.405E+03	1.247E+03	1.107E+03	8.728E+02	6.880E+02	2.093E+02	1.792E+00
Zr	2.444E+05	3.879E+02	1.431E-01	1.291E-03	1.240E-03	1.240E-03	1.240E-03	1.240E-03	1.240E-03	1.240E-03	1.240E-03	1.239E-03	1.239E-03
Nb	5.354E+05	8.271E+02	2.989E-01	7.089E-04	8.709E-04	1.081E-03	1.244E-03	1.370E-03	1.468E-03	1.603E-03	1.684E-03	1.796E-03	1.805E-03
Mo	2.492E+05	0.000E+00	0.000E+00	0.000E+00	0.000E+00	0.000E+00	0.000E+00	0.000E+00	0.000E+00	0.000E+00	0.000E+00	0.000E+00	0.000E+00
Tc	3.694E+05	3.981E-02	3.981E-02	3.981E-02	3.980E-02	3.980E-02	3.980E-02	3.980E-02	3.980E-02	3.980E-02	3.980E-02	3.979E-02	3.977E-02
Ru	8.763E+04	9.773E+01	1.839E+01	4.649E+00	1.493E-01	4.797E-03	1.541E-04	4.950E-06	1.590E-07	1.644E-10	1.685E-13	0.000E+00	0.000E+00
Rh	1.164E+05	1.174E+04	2.967E+03	7.501E+02	2.410E+01	7.776E-01	2.599E-02	1.142E-03	1.297E-04	9.558E-06	8.732E-07	5.636E-12	9.778E-33
Pd	1.083E+04	4.917E-05	4.917E-05	4.917E-05	4.917E-05	4.917E-05	4.917E-05	4.917E-05	4.917E-05	4.917E-05	4.917E-05	4.917E-05	4.917E-05
Ag	1.679E+04	1.691E+02	2.229E+01	2.938E+00	1.854E-02	1.192E-04	2.119E-06	2.119E-06	2.057E-06	1.948E-06	1.845E-06	1.404E-06	4.714E-07
Cd	5.821E+03	8.513E-01	7.043E-01	6.404E-01	5.050E-01	3.982E-01	3.140E-01	2.476E-01	1.953E-01	1.214E-01	7.550E-02	7.021E-03	5.244E-07
In	2.351E+04	1.477E-03	5.341E-08	2.017E-12	8.424E-14	8.424E-14	8.424E-14	8.424E-14	8.424E-14	8.424E-14	8.424E-14	8.424E-14	8.424E-14
Sn	4.987E+04	5.075E+00	1.293E-01	1.401E-02	8.986E-03	8.806E-03	8.653E-03	8.511E-03	8.378E-03	8.138E-03	7.930E-03	7.228E-03	6.563E-03
Sb	1.934E+05	1.856E+02	1.114E+02	6.759E+01	1.940E+01	5.608E+00	1.662E+00	5.329E-01	2.098E-01	9.083E-02	8.108E-02	8.019E-02	8.008E-02

Table N-VII. Decay Heat (*watts*) of Each Element for Extended LWR Fuel (continued).

	INITIAL	1.0YR	3.0YR	5.0YR	10.0YR	15.0YR	20.0YR	25.0YR	30.0YR	40.0YR	50.0YR	100.0YR	300.0YR
Te	1.971E+05	2.065E+01	7.388E+00	4.431E+00	1.267E+00	3.627E-01	1.038E-01	2.969E-02	8.497E-03	6.958E-04	5.697E-05	2.097E-10	3.826E-15
I	4.609E+05	9.572E-05	9.572E-05	9.572E-05	9.572E-05	9.572E-05	9.572E-05	9.572E-05	9.572E-05	9.572E-05	9.572E-05	9.572E-05	9.572E-05
Xe	2.170E+05	1.252E-06	1.095E-12	1.000E-18	7.980E-34	0.000E+00	0.000E+00	0.000E+00	0.000E+00	0.000E+00	0.000E+00	0.000E+00	0.000E+00
Cs	3.992E+05	8.753E+03	4.772E+03	2.726E+03	9.465E+02	5.672E+02	4.540E+02	3.949E+02	3.500E+02	2.774E+02	2.202E+02	6.935E+01	6.835E-01
Ba	2.298E+05	2.294E+03	2.190E+03	2.091E+03	1.863E+03	1.660E+03	1.479E+03	1.317E+03	1.174E+03	9.316E+02	7.394E+02	2.329E+02	2.292E+00
La	4.003E+05	2.180E-04	4.239E-12	4.239E-12	4.239E-12	4.239E-12	4.239E-12	4.239E-12	4.239E-12	4.239E-12	4.239E-12	4.239E-12	4.239E-12
Ce	9.707E+04	9.424E+02	1.583E+02	2.666E+01	3.104E-01	3.613E-03	4.206E-05	4.897E-07	5.701E-09	7.726E-13	1.047E-16	0.000E+00	0.000E+00
Pr	1.496E+05	1.042E+04	1.755E+03	2.956E+02	3.441E+00	4.006E-02	4.664E-04	5.430E-06	6.321E-08	8.567E-12	1.161E-15	0.000E+00	0.000E+00
Nd	2.169E+04	4.803E-07	6.297E-27	0.000E+00	0.000E+00	0.000E+00	0.000E+00	0.000E+00	0.000E+00	0.000E+00	0.000E+00	0.000E+00	0.000E+00
Pm	2.387E+04	1.946E+02	1.135E+02	6.693E+01	1.788E+01	4.783E+00	1.282E+00	3.453E-01	9.379E-02	7.383E-03	7.256E-04	4.901E-07	5.534E-18
Eu	1.534E+04	4.017E+02	3.408E+02	2.892E+02	1.922E+02	1.279E+02	8.519E+01	5.680E+01	3.790E+01	1.689E+01	7.541E+00	1.350E-01	7.761E-08
TOTAL FP	5.425E+06	3.935E+04	1.507E+04	8.809E+03	5.264E+03	4.309E+03	3.741E+03	3.294E+03	2.912E+03	2.287E+03	1.802E+03	5.558E+02	5.291E+00
AP+FP	5.436E+06	3.935E+04	1.507E+04	8.809E+03	5.264E+03	4.310E+03	3.741E+03	3.294E+03	2.912E+03	2.288E+03	1.802E+03	5.558E+02	5.291E+00
ACT+FP	5.787E+06	4.511E+04	1.810E+04	1.164E+04	7.895E+03	6.773E+03	6.056E+03	5.478E+03	4.981E+03	4.162E+03	3.523E+03	1.834E+03	7.200E+02
TOTAL	5.788E+06	4.511E+04	1.810E+04	1.164E+04	7.895E+03	6.773E+03	6.056E+03	5.478E+03	4.981E+03	4.162E+03	3.523E+03	1.834E+03	7.200E+02

Table N-VIII presents the decay heat as a function of time separated into different fractions as described in Sec. 6, Table 6-I. The decay heat is normalized to initial metric tonnes of heavy metal.

Table N-VIII. Decay Heat of Separated Fractions for Extended LWR Fuel.

DECAY TIME, YR	DECAY HEAT, WATTS per INITIAL METRIC TONNE OF HEAVY METAL						
	SCENARIO						
	I	II	III	IV	V	VI	VII
INITIAL	1.639E+06	(a)	(a)	(a)	(a)	(a)	(a)
1	1.277E+04	(a)	(a)	(a)	(a)	(a)	(a)
3	5.124E+03	(a)	(a)	(a)	(a)	(a)	(a)
5	3.295E+03	(a)	(a)	(a)	(a)	(a)	(a)
10	2.235E+03	2.224E+03	8.182E+02	5.397E+02	5.397E+02	1.479E+03	7.336E+01
15	1.918E+03	1.909E+03	7.369E+02	4.685E+02	4.685E+02	1.212E+03	3.968E+01
20	1.715E+03	1.709E+03	6.803E+02	4.214E+02	4.214E+02	1.053E+03	2.498E+01
25	1.551E+03	1.547E+03	6.350E+02	3.852E+02	3.852E+02	9.283E+02	1.671E+01
30	1.410E+03	1.407E+03	5.966E+02	3.554E+02	3.554E+02	8.216E+02	1.107E+01
40	1.178E+03	1.177E+03	5.356E+02	3.105E+02	3.105E+02	6.460E+02	4.908E+00
50	9.974E+02	9.965E+02	4.893E+02	2.790E+02	2.790E+02	5.094E+02	2.183E+00
100	5.192E+02	5.191E+02	3.619E+02	2.097E+02	2.097E+02	1.573E+02	8.464E-02
300	2.038E+02	2.037E+02	2.023E+02	1.452E+02	1.452E+02	1.486E+00	2.999E-02
(a) Scenarios II-VII follow reprocessing at 10 years							

Table N-IX presents the integrated decay heat as a function of time separated into different fractions as described in Sec. 6, Table 6-I. The integrated decay heat is normalized to initial metric tonnes of heavy metal.

Table N-IX. Integrated Decay Heat of Separated Fractions for Extended LWR Fuel.

TIME AFTER REPROCESSING YRS	INTEGRATED DECAY HEAT, JOULES per INITIAL METRIC TONNE OF HEAVY METAL						
	SCENARIO						
	I	II	III	IV	V	VI	VII
5	3.270E+11	3.255E+11	1.226E+11	7.941E+10	2.823E+11	2.116E+11	8.648E+09
10	6.132E+11	6.106E+11	2.343E+11	1.496E+11	5.258E+11	3.901E+11	1.366E+10
15	8.706E+11	8.672E+11	3.381E+11	2.131E+11	7.422E+11	5.462E+11	1.690E+10
20	1.104E+12	1.100E+12	4.352E+11	2.715E+11	9.364E+11	6.841E+11	1.907E+10
30	1.511E+12	1.507E+12	6.136E+11	3.764E+11	1.269E+12	9.145E+11	2.146E+10
40	1.854E+12	1.849E+12	7.752E+11	4.694E+11	1.543E+12	1.096E+12	2.252E+10
90	3.010E+12	3.004E+12	1.442E+12	8.523E+11	2.411E+12	1.569E+12	2.354E+10
290	5.138E+12	5.132E+12	3.174E+12	1.960E+12	3.927E+12	1.780E+12	2.387E+10

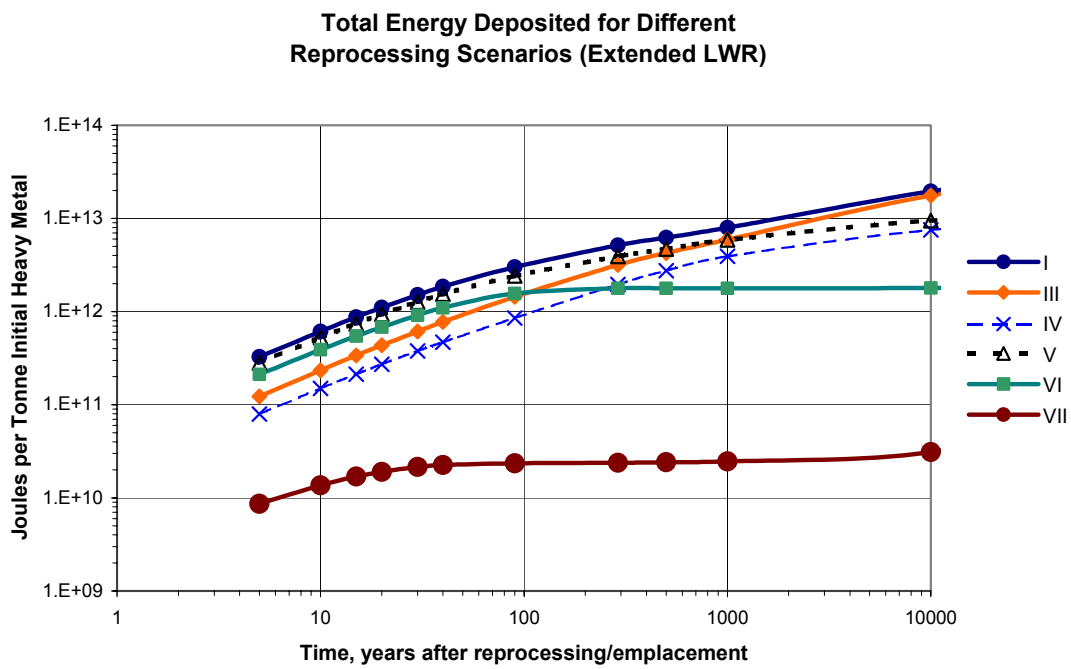


Figure N-2. Integrated decay heat of separated fractions for Extended LWR Fuel.

N.3 MOX-Fueled LWR

Table N-X presents the masses of each element in 1/24 of a full reactor core using “MOX-fueled LWR” fuel. The calculations assume an initial MOX fuel of 9.0wt% Pu irradiated to a burn-up of 49 *GWd/MTM*. Structural elements (hulls, clads, *etc.*) constitute 11.91% of the initial mass.

Table N-X. Mass (*grams*) of Each Element for MOX-Fueled LWR Fuel (1/24 Reactor).

ACTINIDES AND DAUGHTERS													
	INITIAL	1.0YR	3.0YR	5.0YR	10.0YR	15.0YR	20.0YR	25.0YR	30.0YR	40.0YR	50.0YR	100.0YR	300.0YR
He	3.584E+01	4.567E+01	5.457E+01	6.176E+01	7.873E+01	9.459E+01	1.095E+02	1.235E+02	1.368E+02	1.614E+02	1.838E+02	2.759E+02	5.108E+02
Pb	1.373E+05	2.853E+05	8.412E+05	1.723E+04	4.867E+04	8.586E+04	1.238E+03	1.609E+03	1.964E+03	2.626E+03	3.229E+03	5.742E+03	9.043E+03
Th	1.323E+03	2.111E+03	4.256E+03	7.139E+03	1.749E+02	3.222E+02	5.119E+02	7.424E+02	1.012E+01	1.664E+01	2.453E+01	8.171E+01	4.700E+00
Pa	2.298E-04	2.422E-04	2.650E-04	2.881E-04	3.469E-04	4.070E-04	4.681E-04	5.301E-04	5.927E-04	7.193E-04	8.471E-04	1.491E-03	4.058E-03
U	2.965E+06	2.965E+06	2.965E+06	2.966E+06	2.966E+06	2.966E+06	2.967E+06	2.967E+06	2.967E+06	2.968E+06	2.969E+06	2.971E+06	2.976E+06
Np	8.417E+02	6.857E+02	7.064E+02	7.358E+02	8.422E+02	9.870E+02	1.161E+03	1.359E+03	1.574E+03	2.040E+03	2.536E+03	5.109E+03	1.387E+04
Pu	2.021E+05	2.012E+05	1.984E+05	1.959E+05	1.904E+05	1.861E+05	1.826E+05	1.798E+05	1.776E+05	1.744E+05	1.722E+05	1.676E+05	1.626E+05
Am	1.026E+04	1.182E+04	1.473E+04	1.735E+04	2.287E+04	2.714E+04	3.044E+04	3.296E+04	3.489E+04	3.742E+04	3.878E+04	3.886E+04	3.009E+04
Cm	4.647E+03	4.139E+03	3.778E+03	3.527E+03	2.988E+03	2.542E+03	2.174E+03	1.869E+03	1.618E+03	1.239E+03	9.802E+02	5.049E+02	4.150E+02
Bk	4.227E-04	1.917E-04	3.939E-05	8.095E-06	1.550E-07	2.968E-09	5.684E-11	1.088E-12	2.084E-14	7.945E-18	3.068E-19	3.034E-19	3.010E-19
Cf	2.975E-04	5.193E-04	6.551E-04	6.731E-04	6.559E-04	6.374E-04	6.224E-04	6.097E-04	5.988E-04	5.806E-04	5.656E-04	5.094E-04	3.497E-04
SUBTOTAL	3.183E+06	3.183E+06	3.183E+06	3.183E+06	3.183E+06	3.183E+06	3.183E+06	3.183E+06	3.183E+06	3.183E+06	3.183E+06	3.183E+06	3.183E+06
STRUCTURE	4.518E+05	4.518E+05	4.518E+05	4.518E+05	4.518E+05	4.518E+05	4.518E+05	4.518E+05	4.518E+05	4.518E+05	4.518E+05	4.518E+05	4.518E+05
ACT+FP	3.183E+06	3.183E+06	3.183E+06	3.183E+06	3.183E+06	3.183E+06	3.183E+06	3.183E+06	3.183E+06	3.183E+06	3.183E+06	3.183E+06	3.183E+06
SUBTOTAL	3.635E+06	3.635E+06	3.635E+06	3.635E+06	3.635E+06	3.635E+06	3.635E+06	3.635E+06	3.635E+06	3.635E+06	3.635E+06	3.635E+06	3.635E+06
FISSION PRODUCTS													
	INITIAL	1.0YR	3.0YR	5.0YR	10.0YR	15.0YR	20.0YR	25.0YR	30.0YR	40.0YR	50.0YR	100.0YR	300.0YR
H	3.104E-01	2.935E-01	2.623E-01	2.345E-01	1.771E-01	1.338E-01	1.010E-01	7.630E-02	5.763E-02	3.288E-02	1.876E-02	1.134E-03	1.510E-08
Li	1.181E-03	1.181E-03	1.181E-03	1.181E-03	1.181E-03	1.181E-03	1.181E-03	1.181E-03	1.181E-03	1.181E-03	1.181E-03	1.181E-03	1.181E-03
Be	6.855E-04	6.855E-04	6.855E-04	6.855E-04	6.855E-04	6.855E-04	6.855E-04	6.855E-04	6.855E-04	6.854E-04	6.854E-04	6.854E-04	6.854E-04
C	1.205E-04	1.205E-04	1.205E-04	1.205E-04	1.204E-04	1.203E-04	1.202E-04	1.202E-04	1.201E-04	1.200E-04	1.198E-04	1.191E-04	1.162E-04
Zn	2.335E-04	1.006E-07	1.006E-07	1.006E-07	1.006E-07	1.006E-07	1.006E-07	1.006E-07	1.006E-07	1.006E-07	1.006E-07	1.006E-07	1.006E-07

Table N-X. Mass (*grams*) of Each Element for MOX-Fueled LWR Fuel (1/24 Reactor, continued).

	INITIAL	1.0YR	3.0YR	5.0YR	10.0YR	15.0YR	20.0YR	25.0YR	30.0YR	40.0YR	50.0YR	100.0YR	300.0YR
Ga	1.263E+04	6.448E-06	6.448E-06	6.448E-06	6.448E-06	6.448E-06	6.448E-06	6.448E-06	6.448E-06	6.448E-06	6.448E-06	6.448E-06	6.448E-06
Ge	2.808E+00	2.807E+00	2.807E+00	2.807E+00	2.807E+00	2.807E+00	2.807E+00	2.807E+00	2.807E+00	2.807E+00	2.807E+00	2.807E+00	2.807E+00
As	9.077E-01	9.021E-01	9.021E-01	9.021E-01	9.021E-01	9.021E-01	9.021E-01	9.021E-01	9.021E-01	9.021E-01	9.021E-01	9.021E-01	9.021E-01
Se	1.944E+02	1.944E+02	1.944E+02	1.944E+02	1.944E+02	1.944E+02	1.944E+02	1.944E+02	1.944E+02	1.944E+02	1.944E+02	1.944E+02	1.944E+02
Br	7.615E+01	7.613E+01	7.613E+01	7.613E+01	7.613E+01	7.613E+01	7.613E+01	7.613E+01	7.613E+01	7.614E+01	7.614E+01	7.615E+01	7.620E+01
Kr	1.017E+03	1.013E+03	1.006E+03	9.996E+02	9.871E+02	9.780E+02	9.715E+02	9.668E+02	9.634E+02	9.591E+02	9.568E+02	9.545E+02	9.544E+02
Rb	8.772E+02	8.812E+02	8.883E+02	8.945E+02	9.070E+02	9.160E+02	9.226E+02	9.273E+02	9.307E+02	9.350E+02	9.372E+02	9.396E+02	9.397E+02
Sr	2.161E+03	2.089E+03	2.031E+03	1.976E+03	1.851E+03	1.739E+03	1.640E+03	1.552E+03	1.474E+03	1.343E+03	1.240E+03	9.726E+02	8.569E+02
Y	1.112E+03	1.083E+03	1.083E+03	1.083E+03	1.083E+03	1.083E+03	1.083E+03	1.083E+03	1.083E+03	1.083E+03	1.083E+03	1.082E+03	1.082E+03
Zr	1.177E+04	1.172E+04	1.178E+04	1.183E+04	1.196E+04	1.207E+04	1.217E+04	1.226E+04	1.234E+04	1.247E+04	1.257E+04	1.284E+04	1.295E+04
Nb	8.051E+01	3.569E+00	1.354E-02	1.440E-02	1.976E-02	2.512E-02	3.048E-02	3.584E-02	4.120E-02	5.192E-02	6.264E-02	1.162E-01	3.306E-01
Mo	1.422E+04	1.444E+04	1.445E+04	1.445E+04	1.445E+04	1.445E+04	1.445E+04	1.445E+04	1.445E+04	1.445E+04	1.445E+04	1.445E+04	1.445E+04
Tc	3.690E+03	3.699E+03	3.699E+03	3.699E+03	3.699E+03	3.699E+03	3.699E+03	3.699E+03	3.699E+03	3.699E+03	3.699E+03	3.698E+03	3.696E+03
Ru	1.379E+04	1.317E+04	1.281E+04	1.272E+04	1.269E+04	1.269E+04	1.269E+04	1.269E+04	1.269E+04	1.269E+04	1.269E+04	1.269E+04	1.269E+04
Rh	2.775E+03	2.911E+03	2.912E+03	2.912E+03	2.912E+03	2.912E+03	2.912E+03	2.912E+03	2.912E+03	2.912E+03	2.912E+03	2.912E+03	2.912E+03
Pd	1.190E+04	1.238E+04	1.274E+04	1.283E+04	1.286E+04	1.286E+04	1.286E+04	1.286E+04	1.286E+04	1.286E+04	1.286E+04	1.286E+04	1.286E+04
Ag	8.372E+02	8.316E+02	8.295E+02	8.292E+02	8.292E+02	8.292E+02	8.292E+02	8.292E+02	8.292E+02	8.292E+02	8.292E+02	8.292E+02	8.292E+02
Cd	1.165E+03	1.171E+03	1.173E+03	1.173E+03	1.172E+03	1.172E+03	1.172E+03	1.172E+03	1.171E+03	1.171E+03	1.171E+03	1.171E+03	1.171E+03
In	1.407E+01	1.453E+01	1.473E+01	1.491E+01	1.529E+01	1.559E+01	1.583E+01	1.602E+01	1.617E+01	1.638E+01	1.651E+01	1.670E+01	1.672E+01
Sn	5.622E+02	5.607E+02	5.606E+02	5.606E+02	5.605E+02	5.605E+02	5.605E+02	5.605E+02	5.605E+02	5.605E+02	5.605E+02	5.604E+02	5.602E+02
Sb	1.798E+02	1.633E+02	1.412E+02	1.277E+02	1.129E+02	1.086E+02	1.074E+02	1.071E+02	1.070E+02	1.070E+02	1.069E+02	1.070E+02	1.070E+02
Te	2.666E+03	2.662E+03	2.684E+03	2.698E+03	2.712E+03	2.717E+03	2.718E+03	2.718E+03	2.718E+03	2.718E+03	2.718E+03	2.718E+03	2.719E+03
I	1.484E+03	1.467E+03	1.468E+03	1.468E+03	1.468E+03	1.468E+03	1.468E+03	1.468E+03	1.468E+03	1.468E+03	1.468E+03	1.468E+03	1.468E+03
Xe	2.341E+04	2.341E+04	2.341E+04	2.341E+04	2.341E+04	2.341E+04	2.341E+04	2.341E+04	2.341E+04	2.341E+04	2.341E+04	2.341E+04	2.341E+04
Cs	1.469E+04	1.446E+04	1.405E+04	1.374E+04	1.313E+04	1.263E+04	1.220E+04	1.182E+04	1.148E+04	1.091E+04	1.045E+04	9.254E+03	8.709E+03
Ba	6.272E+03	6.481E+03	6.888E+03	7.205E+03	7.815E+03	8.309E+03	8.740E+03	9.122E+03	9.462E+03	1.003E+04	1.049E+04	1.169E+04	1.223E+04
La	5.304E+03	5.296E+03	5.296E+03	5.296E+03	5.296E+03	5.296E+03	5.296E+03	5.296E+03	5.296E+03	5.296E+03	5.296E+03	5.296E+03	5.296E+03
Ce	1.085E+04	1.025E+04	9.940E+03	9.889E+03	9.878E+03	9.878E+03	9.878E+03	9.878E+03	9.878E+03	9.878E+03	9.878E+03	9.878E+03	9.878E+03
Pr	4.752E+03	4.832E+03	4.832E+03	4.832E+03	4.832E+03	4.832E+03	4.832E+03	4.832E+03	4.832E+03	4.832E+03	4.832E+03	4.832E+03	4.832E+03
Nd	1.562E+04	1.618E+04	1.648E+04	1.654E+04	1.655E+04	1.655E+04	1.655E+04	1.655E+04	1.655E+04	1.655E+04	1.655E+04	1.655E+04	1.655E+04
Pm	7.340E+02	5.696E+02	3.358E+02	1.980E+02	5.283E+01	1.410E+01	3.765E+00	1.006E+00	2.690E-01	1.939E-02	1.449E-03	1.689E-07	1.882E-18
Sm	3.637E+03	3.817E+03	4.048E+03	4.184E+03	4.324E+03	4.357E+03	4.361E+03	4.361E+03	4.357E+03	4.349E+03	4.341E+03	4.309E+03	4.256E+03
Eu	1.009E+03	9.792E+02	9.423E+02	9.120E+02	8.578E+02	8.248E+02	8.050E+02	7.937E+02	7.877E+02	7.847E+02	7.876E+02	8.154E+02	8.684E+02
Gd	6.909E+02	7.247E+02	7.637E+02	7.962E+02	8.557E+02	8.937E+02	9.183E+02	9.344E+02	9.449E+02	9.564E+02	9.614E+02	9.654E+02	9.655E+02
Tb	2.999E+01	2.923E+01	2.920E+01	2.920E+01	2.920E+01	2.920E+01	2.920E+01	2.920E+01	2.920E+01	2.920E+01	2.920E+01	2.920E+01	2.920E+01

Table N-X. Mass (*grams*) of Each Element for MOX-Fueled LWR Fuel (1/24 Reactor, continued).

	INITIAL	1.0YR	3.0YR	5.0YR	10.0YR	15.0YR	20.0YR	25.0YR	30.0YR	40.0YR	50.0YR	100.0YR	300.0YR
Dy	1.725E+01	1.804E+01	1.807E+01	1.807E+01	1.807E+01	1.807E+01	1.807E+01	1.807E+01	1.807E+01	1.807E+01	1.807E+01	1.807E+01	1.807E+01
Ho	1.689E+00	1.687E+00	1.687E+00	1.687E+00	1.687E+00	1.687E+00	1.687E+00	1.687E+00	1.687E+00	1.687E+00	1.687E+00	1.686E+00	1.684E+00
Er	7.466E-01	7.487E-01	7.487E-01	7.487E-01	7.488E-01	7.489E-01	7.489E-01	7.490E-01	7.490E-01	7.491E-01	7.492E-01	7.498E-01	7.518E-01
Tm	8.416E-04	7.879E-04	7.731E-04	7.715E-04	7.704E-04	7.702E-04	7.702E-04	7.702E-04	7.702E-04	7.702E-04	7.702E-04	7.702E-04	7.702E-04
Yb	2.168E-04	2.945E-04	3.093E-04	3.109E-04	3.120E-04	3.122E-04	3.122E-04	3.122E-04	3.122E-04	3.122E-04	3.122E-04	3.122E-04	3.122E-04
TOTAL FP	1.576E+05	1.576E+05	1.576E+05	1.576E+05	1.576E+05	1.576E+05	1.576E+05	1.576E+05	1.576E+05	1.576E+05	1.576E+05	1.576E+05	1.576E+05
ACT+FP	3.341E+06	3.341E+06	3.341E+06	3.341E+06	3.341E+06	3.341E+06	3.341E+06	3.341E+06	3.341E+06	3.341E+06	3.341E+06	3.341E+06	3.341E+06
TOTAL	3.793E+06	3.793E+06	3.793E+06	3.793E+06	3.793E+06	3.793E+06	3.793E+06	3.793E+06	3.793E+06	3.793E+06	3.793E+06	3.793E+06	3.793E+06

Table N-XI presents the decay heat of each element in 1/24 of a full reactor core using “MOX-fueled LWR” fuel. The calculations assume an initial MOX fuel of 9.0wt% Pu, irradiated to a burn-up of 49 *GWd/MTM*. Structural elements (hulls, clads, *etc.*) constitute 11.91% of the initial mass.

Table N-XI. Decay Heat (*watts*) of Each Element of MOX-Fueled LWR Fuel.

ACTINIDES AND DAUGHTERS													
	INITIAL	1.0YR	3.0YR	5.0YR	10.0YR	15.0YR	20.0YR	25.0YR	30.0YR	40.0YR	50.0YR	100.0YR	300.0YR
U	1.069E+05	2.370E-01	2.485E-01	2.605E-01	2.925E-01	3.274E-01	3.645E-01	4.030E-01	4.422E-01	5.213E-01	5.987E-01	9.295E-01	1.495E+00
Np	9.624E+04	3.256E+00	3.256E+00	3.256E+00	3.256E+00	3.257E+00	3.259E+00	3.262E+00	3.265E+00	3.271E+00	3.278E+00	3.316E+00	3.440E+00
Pu	1.216E+04	5.593E+03	5.561E+03	5.480E+03	5.279E+03	5.089E+03	4.908E+03	4.736E+03	4.572E+03	4.264E+03	3.983E+03	2.875E+03	1.056E+03
Am	1.486E+04	6.214E+02	9.529E+02	1.253E+03	1.882E+03	2.370E+03	2.746E+03	3.035E+03	3.255E+03	3.545E+03	3.700E+03	3.715E+03	2.730E+03
Cm	6.753E+04	2.236E+04	1.003E+04	8.814E+03	7.263E+03	6.003E+03	4.962E+03	4.102E+03	3.391E+03	2.320E+03	1.588E+03	2.476E+02	7.499E+00
SUBTOTAL	2.977E+05	2.858E+04	1.655E+04	1.555E+04	1.443E+04	1.347E+04	1.262E+04	1.188E+04	1.122E+04	1.013E+04	9.275E+03	6.841E+03	3.799E+03
STRUCTURE	3.771E+01	1.931E-07	1.930E-07	1.930E-07	1.929E-07	1.928E-07	1.927E-07	1.925E-07	1.924E-07	1.922E-07	1.920E-07	1.908E-07	1.862E-07
ACT+FP	2.977E+05	2.858E+04	1.655E+04	1.555E+04	1.443E+04	1.347E+04	1.262E+04	1.188E+04	1.122E+04	1.013E+04	9.275E+03	6.841E+03	3.799E+03
SUBTOTAL	2.977E+05	2.858E+04	1.655E+04	1.555E+04	1.443E+04	1.347E+04	1.262E+04	1.188E+04	1.122E+04	1.013E+04	9.275E+03	6.841E+03	3.799E+03
FISSION PRODUCTS													
	INITIAL	1.0YR	3.0YR	5.0YR	10.0YR	15.0YR	20.0YR	25.0YR	30.0YR	40.0YR	50.0YR	100.0YR	300.0YR
As	1.300E+04	0.000E+00	0.000E+00	0.000E+00	0.000E+00	0.000E+00	0.000E+00	0.000E+00	0.000E+00	0.000E+00	0.000E+00	0.000E+00	0.000E+00
Se	2.562E+04	3.986E-04	3.986E-04	3.986E-04	3.986E-04	3.985E-04	3.985E-04	3.985E-04	3.985E-04	3.984E-04	3.984E-04	3.982E-04	3.973E-04
Br	6.547E+04	0.000E+00	0.000E+00	0.000E+00	0.000E+00	0.000E+00	0.000E+00	0.000E+00	0.000E+00	0.000E+00	0.000E+00	0.000E+00	0.000E+00
Kr	9.477E+04	3.441E+01	3.024E+01	2.657E+01	1.923E+01	1.392E+01	1.007E+01	7.291E+00	5.277E+00	2.764E+00	1.448E+00	5.720E-02	1.389E-07
Rb	2.058E+05	1.969E-05	4.476E-08	4.476E-08	4.476E-08	4.476E-08	4.476E-08	4.476E-08	4.476E-08	4.476E-08	4.476E-08	4.476E-08	4.476E-08
Sr	2.165E+05	2.238E+02	1.861E+02	1.775E+02	1.575E+02	1.399E+02	1.242E+02	1.102E+02	9.787E+01	7.714E+01	6.080E+01	1.850E+01	1.584E-01
Y	3.761E+05	1.016E+03	8.890E+02	8.476E+02	7.525E+02	6.681E+02	5.931E+02	5.266E+02	4.675E+02	3.685E+02	2.904E+02	8.834E+01	7.564E-01
Zr	2.183E+05	3.135E+02	1.153E-01	7.331E-04	6.912E-04	6.912E-04	6.912E-04	6.912E-04	6.912E-04	6.912E-04	6.912E-04	6.912E-04	6.911E-04
Nb	4.956E+05	6.683E+02	2.415E-01	4.098E-04	4.773E-04	5.980E-04	6.915E-04	7.640E-04	8.202E-04	8.975E-04	9.439E-04	1.008E-03	1.014E-03
Mo	2.519E+05	0.000E+00	0.000E+00	0.000E+00	0.000E+00	0.000E+00	0.000E+00	0.000E+00	0.000E+00	0.000E+00	0.000E+00	0.000E+00	0.000E+00
Tc	3.802E+05	3.146E-02	3.146E-02	3.146E-02	3.146E-02	3.146E-02	3.146E-02	3.146E-02	3.146E-02	3.146E-02	3.146E-02	3.145E-02	3.143E-02
Ru	9.487E+04	1.199E+02	2.420E+01	6.118E+00	1.965E-01	6.312E-03	2.028E-04	6.513E-06	2.092E-07	2.157E-10	2.237E-13	0.000E+00	0.000E+00
Rh	1.270E+05	1.545E+04	3.905E+03	9.870E+02	3.171E+01	1.022E+00	3.391E-02	1.415E-03	1.440E-04	1.014E-05	9.256E-07	5.973E-12	1.036E-32

Table N-XI. Decay Heat (*watts*) of Each Element of MOX-Fueled LWR Fuel (continued).

Pd	1.160E+04	7.217E-05	7.217E-05	7.217E-05	7.217E-05	7.217E-05	7.217E-05	7.217E-05	7.217E-05	7.217E-05	7.217E-05	7.217E-05	7.217E-05	7.217E-05	7.217E-05
Ag	1.796E+04	1.989E+02	2.622E+01	3.456E+00	2.181E-02	1.404E-04	3.679E-06	2.741E-06	2.662E-06	2.520E-06	2.386E-06	1.816E-06	6.098E-07		
Cd	5.569E+03	8.800E-01	7.308E-01	6.646E-01	5.240E-01	4.132E-01	3.259E-01	2.570E-01	2.026E-01	1.260E-01	7.835E-02	7.283E-03	5.439E-07		
In	2.249E+04	9.755E-04	3.524E-08	1.402E-12	1.270E-13	1.270E-13	1.270E-13	1.270E-13	1.270E-13	1.270E-13	1.270E-13	1.270E-13	1.270E-13		
Sn	4.590E+04	4.746E+00	1.207E-01	1.357E-02	8.945E-03	8.740E-03	8.563E-03	8.398E-03	8.243E-03	7.965E-03	7.723E-03	6.909E-03	6.139E-03		
Sb	1.763E+05	1.840E+02	1.109E+02	6.723E+01	1.929E+01	5.574E+00	1.648E+00	5.252E-01	2.038E-01	8.548E-02	7.578E-02	7.489E-02	7.479E-02		
	INITIAL	1.0YR	3.0YR	5.0YR	10.0YR	15.0YR	20.0YR	25.0YR	30.0YR	40.0YR	50.0YR	100.0YR	300.0YR		
Te	1.755E+05	2.034E+01	7.347E+00	4.407E+00	1.261E+00	3.607E-01	1.032E-01	2.954E-02	8.452E-03	6.921E-04	5.667E-05	2.086E-10	2.251E-15		
I	4.133E+05	8.951E-05	8.951E-05	8.951E-05	8.951E-05	8.951E-05	8.951E-05	8.951E-05	8.951E-05	8.951E-05	8.951E-05	8.951E-05	8.951E-05		
Xe	1.950E+05	7.845E-07	6.724E-13	6.143E-19	4.900E-34	0.000E+00	0.000E+00	0.000E+00	0.000E+00	0.000E+00	0.000E+00	0.000E+00	0.000E+00		
Cs	3.445E+05	4.894E+03	2.731E+03	1.616E+03	6.364E+02	4.174E+02	3.440E+02	3.013E+02	2.675E+02	2.121E+02	1.683E+02	5.302E+01	5.232E-01		
Ba	1.977E+05	1.754E+03	1.674E+03	1.599E+03	1.424E+03	1.269E+03	1.131E+03	1.007E+03	8.973E+02	7.122E+02	5.653E+02	1.780E+02	1.752E+00		
La	3.434E+05	1.915E-04	1.889E-12	1.889E-12	1.889E-12	1.889E-12	1.889E-12	1.889E-12	1.889E-12	1.889E-12	1.889E-12	1.889E-12	1.889E-12		
Ce	8.549E+04	7.808E+02	1.311E+02	2.208E+01	2.571E-01	2.993E-03	3.485E-05	4.056E-07	4.722E-09	6.399E-13	8.672E-17	0.000E+00	0.000E+00		
Pr	1.325E+05	8.632E+03	1.454E+03	2.449E+02	2.851E+00	3.319E-02	3.864E-04	4.498E-06	5.236E-08	7.095E-12	9.616E-16	0.000E+00	0.000E+00		
Nd	2.085E+04	4.234E-07	5.552E-27	0.000E+00	0.000E+00	0.000E+00	0.000E+00	0.000E+00	0.000E+00	0.000E+00	0.000E+00	0.000E+00	0.000E+00		
Pm	2.305E+04	1.923E+02	1.118E+02	6.590E+01	1.760E+01	4.705E+00	1.260E+00	3.386E-01	9.163E-02	7.063E-03	6.556E-04	3.746E-07	4.227E-18		
Eu	8.285E+03	5.112E+02	4.341E+02	3.687E+02	2.453E+02	1.634E+02	1.090E+02	7.274E+01	4.857E+01	2.168E+01	9.689E+00	1.758E-01	2.360E-07		
TOTAL FP	4.794E+06	3.500E+04	1.172E+04	6.037E+03	3.310E+03	2.684E+03	2.315E+03	2.027E+03	1.785E+03	1.395E+03	1.096E+03	3.385E+02	3.350E+00		
AP+FP	4.794E+06	3.500E+04	1.172E+04	6.037E+03	3.310E+03	2.684E+03	2.315E+03	2.027E+03	1.785E+03	1.395E+03	1.096E+03	3.385E+02	3.350E+00		
ACT+FP	5.092E+06	6.358E+04	2.826E+04	2.159E+04	1.774E+04	1.615E+04	1.493E+04	1.390E+04	1.301E+04	1.153E+04	1.037E+04	7.180E+03	3.802E+03		
TOTAL	5.092E+06	6.358E+04	2.826E+04	2.159E+04	1.774E+04	1.615E+04	1.493E+04	1.390E+04	1.301E+04	1.153E+04	1.037E+04	7.180E+03	3.802E+03		

Table N-XII presents the decay heat as a function of time separated into different fractions as described in Sec. 6, Table 6-I. The decay heat is normalized to initial metric tonnes of heavy metal.

Table N-XII. Decay Heat of Separated Fractions for MOX-Fueled LWR Fuel.

DECAY TIME, YR	DECAY HEAT, WATTS per INITIAL METRIC TONNE OF HEAVY METAL						
	SCENARIO						
	I	II	III	IV	V	VI	VII
INITIAL	1.52E+06	(a)	(a)	(a)	(a)	(a)	(a)
1	1.90E+04	(a)	(a)	(a)	(a)	(a)	(a)
3	8.46E+03	(a)	(a)	(a)	(a)	(a)	(a)
5	6.46E+03	(a)	(a)	(a)	(a)	(a)	(a)
10	5.31E+03	5.30E+03	4.41E+03	2.83E+03	3.72E+03	9.86E+02	9.66E+01
15	4.83E+03	4.83E+03	4.08E+03	2.56E+03	3.31E+03	7.99E+02	5.27E+01
20	4.47E+03	4.47E+03	3.81E+03	2.34E+03	3.00E+03	6.88E+02	3.23E+01
25	4.16E+03	4.16E+03	3.58E+03	2.16E+03	2.74E+03	6.03E+02	2.12E+01
30	3.89E+03	3.89E+03	3.37E+03	2.01E+03	2.52E+03	5.34E+02	1.58E+01
40	3.45E+03	3.45E+03	3.04E+03	1.76E+03	2.17E+03	4.17E+02	7.33E+00
50	3.10E+03	3.10E+03	2.78E+03	1.59E+03	1.91E+03	3.27E+02	2.66E+00
100	2.15E+03	2.15E+03	2.05E+03	1.19E+03	1.29E+03	1.01E+02	6.13E-02
300	1.14E+03	1.14E+03	1.14E+03	8.20E+02	8.21E+02	1.06E+00	1.02E-01
(a) Scenarios II-VII follow reprocessing at 10 years							

Table N-XIII presents the integrated decay heat as a function of time separated into different fractions as described in Sec. 6, Table 6-I. The integrated decay heat is normalized to initial metric tonnes of heavy metal.

Table N-XIII. Integrated Decay Heat of Separated Fractions for MOX-Fueled LWR Fuel.

TIME AFTER REPROCESSING YRS	INTEGRATED DECAY HEAT, JOULES per INITIAL METRIC TONNE OF HEAVY METAL						
	SCENARIO						
	I	II	III	IV	V	VI	VII
5	7.996E+11	7.988E+11	6.700E+11	4.252E+11	5.539E+11	1.403E+11	1.143E+10
10	1.533E+12	1.532E+12	1.292E+12	8.115E+11	1.051E+12	2.574E+11	1.801E+10
15	2.213E+12	2.212E+12	1.875E+12	1.166E+12	1.503E+12	3.592E+11	2.217E+10
20	2.849E+12	2.847E+12	2.423E+12	1.495E+12	1.918E+12	4.488E+11	2.508E+10
30	4.006E+12	4.004E+12	3.434E+12	2.089E+12	2.658E+12	5.981E+11	2.856E+10
40	5.039E+12	5.037E+12	4.351E+12	2.617E+12	3.301E+12	7.150E+11	3.001E+10
90	9.137E+12	9.134E+12	8.129E+12	4.789E+12	5.793E+12	1.019E+12	3.110E+10
290	1.917E+13	1.917E+13	1.790E+13	1.105E+13	1.234E+13	1.157E+12	3.160E+10

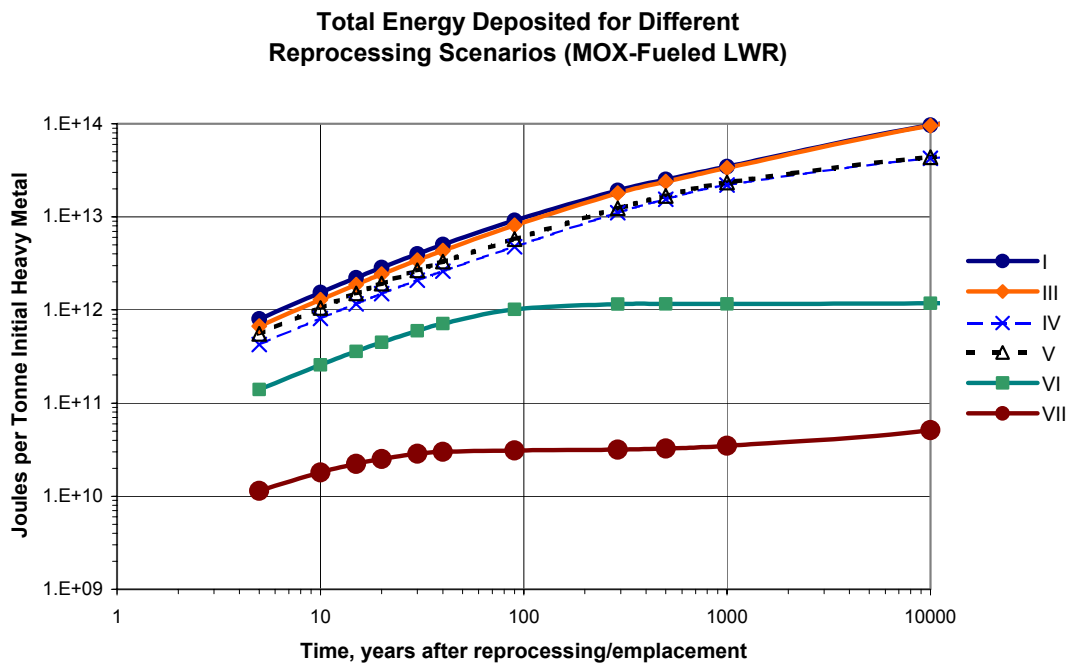


Figure N-3. Integrated decay heat of separated fractions for MOX-fueled LWR Fuel.

Table N-XIV presents the results of calculating the “repository capacity benefit ratio” for each of the three LWR fuel cases examined. The capacity benefit ratio compares the thermal load of fuel reprocessed in a given fashion (via Scenarios II-VII of Sec. 6, Table 6-I) to the thermal load of the unprocessed fuel. The thermal load of the MOX-fueled and Extended LWRs are both higher than that of the Standard LWR, so comparisons between these categories should be made with caution. Note, however, that Scenario VII is highly beneficial in all three cases.

Table N-XIV. Comparison of Repository Capacity Benefit Ratio for Standard, Extended, and MOX-Fueled LWR.

Scenario	Standard LWR (Note 1)						Extended LWR (Note 1)						MOX-Fueled LWR (Note 1)					
	Short Note 2	Long Note 3	WP Note 4	WF Note 5	LL Note 6		Short Note 2	Long Note 3	WP Note 4	WF Note 5	LL Note 6		Short Note 2	Long Note 3	WP Note 4	WF Note 5	LL Note 6	
II	1.00	1.00	1.01	6.75	1.00		1.00	1.00	1.01	4.46	1.00		1.00	1.00	1.00	2.72	1.00	
III	2.99	1.71	3.82	7.36	1.71		2.39	1.62	2.73	4.88	1.62		1.16	1.07	1.20	2.84	1.07	
IV	4.82	2.51	6.09	9.64	2.51		3.95	2.62	4.14	6.07	2.62		1.93	1.73	1.87	6.89	1.73	
V	1.15	1.23	1.12	8.62	1.12		1.20	1.31	1.15	5.44	1.15		1.53	1.55	1.43	6.19	1.43	
VI	1.48	2.7	1.30	8.95	1.30		1.61	2.89	1.51	5.66	1.51		7.05	16.6	5.39	7.20	5.39	
VII	82.2	218	26.9	10.1	10.1		82.3	215	30.5	6.35	6.35		168	607	55.0	8.18	8.18	

Note 1: Values should be compared only among Standard LWR, or among Extended LWR, or among MOX-fueled LWR. For comparison between these values, multiply Extended LWR values by 0.566, multiply MOX-fueled LWR values by 0.238

Note 2: Short-Term Benefit: Ratio of heat releases for Scenario 1 compared to Scenario nsc, integrated over first 40 years after separation/emplacement. This approximately reflects the drift tunnel wall (near field) temperature constraint.

Note 3: Long Term Benefit: Ratio of heat releases for Scenario 1 compared to Scenario nsc, integrated over first 290 years after separation/emplacement. This approximately reflects the zeolite layer (far field) temperature constraint.

Note 4: Waste Package Limit: Ratio of heat releases for Scenario 1 compared to Scenario nsc; instantaneous heat releasecontrolling waste package centerline temperature for vitrified HLW.

Note 5: Weight Fraction Limit: Limit assuming VHLLW is no more than 25% HLW by weight.

Note 6: Least Limit: Lesser of four limiting constraints listed in Notes 2-5.

This page is left blank intentionally.

Appendix O: Separations Processes and Error Analysis for Thermal Calculations

O.1 Separations Processes

Table O-I summarizes the sequence of solvent extractions assumed for each of the separation schemes I-VII described in Sec. 6, Table 6-I.

Table O-I. Separations Sequence for Each Scenario of Table 6-I.

Scenario	Separations Sequence	Waste Streams	Product Streams
I	None; direct disposal of SNF.	None	None
II	UREX, Vitrification	SE, Vol, U, VHLW	None
III	UREX, Cs, Sr, Vitrification	SE, Vol, U, VHLW, Cs, Sr	None
IV	PUREX, Cs, Sr, Vitrification	SE, Vol, U, VHLW, Cs, Sr	Pu
V	PUREX, Vitrification	SE, Vol, U, VHLW	Pu
VI	PUREX, TRUEX, Vitrification	SE, Vol, U, VHLW	Pu, MA ⁽
VII	PUREX, TRUEX, Cs, Sr, Vitrification	SE, Vol, U, VHLW, Cs, Sr	Pu, MA

UREX = Uranium Extraction process.
 Vitrification = drying followed by vitrification in borosilicate glass, 25 wt% heavy metal.
 Cs – cesium extraction with calixarene extractant (Dozol, 1997).
 Sr – strontium extraction with SREX process (Horwitz, 1991).
 PUREX = Plutonium, Uranium Extraction process.
 TRUEX = TRansUranic Extraction process (Schulz, 1988).
 SE – structural elements (clads, hulls, etc.). Released in any separation scheme.
 Vol – volatile elements hydrogen, carbon, krypton, xenon, bromine, iodine. Released in any separation scheme.
 MA – minor actinides neptunium, americium, curium.

Each separation is assumed to be 100% with no interfering elements. In practice, recoveries above 99.9% have been demonstrated for all extractions, however some interfering elements present in small quantity are partially extracted to the extent of a few percent. The quantitative effects of these interfering elements are evaluated below.

In addition to the separations performed for control of the decay heat of the SNF, it may be desirable to selectively extract from the waste certain other elements with long-lived isotopes (*e.g.*, ⁹⁹Tc) that strongly contribute to the radiotoxicity of the vitrified waste on long timescales (10⁵ - 10⁶) years. These elements can be encapsulated in waste forms optimized for each element, in long-lived waste forms that would not be cost-effective for direct disposal of SNF. In some cases (*e.g.*, ⁹⁹Tc, ¹²⁹I) these isotopes might be transmuted into stable species.

O.2 Error Analysis

In most cases, incomplete separations cause a negligible effect on the thermal analysis presented in Sec. 6. This follows from two reasons: 1) most extractions are of high efficiency, >99.9% with maximum co-extractants limited to a few percent of interfering elements, and 2) the interfering elements have negligible decay heat.

The worst-case error is found with Scenario VII, which has the lowest decay heat of the examined scenarios and is therefore most sensitive to errors (i.e. the small number is the difference between two large numbers). In Scenario VII, the actinides, plus cesium and strontium are extracted from the waste, and the repository capacity increase is thermally limited by the instantaneous heat release that controls the VHLW centerline temperature. Most of the remaining decay heat arises from the lanthanides, which are co-extracted with the actinides to the extent of a few percent. If the actinide recovery is assumed to be 100% and the lanthanides are (unintentionally) extracted to the extent of 5%, the decay heat in the remainder will be 5% low. The calculated repository capacity increase due to thermal effects (Sec. 6, Table 6-III) will be 5% higher than predicted. The waste fraction limit of 10.1 will still control the actual repository capacity increase.

If, on the other hand, 0.1% of the actinides remain in the waste stream (99.9% extraction efficiency, poorer performance than anticipated), the instantaneous decay heat at separation will be increased by 0.4% and the calculated repository capacity increase will be marginally lower than predicted (26.8 rather than 26.9). Alternatively, if as much as 1% of the cesium plus strontium remains in the waste (again, poorer performance than anticipated), the instantaneous decay heat will increase by ~19%, the calculated repository capacity increase will be reduced by ~16% from 26.9 to 22.6. Note that this error is opposite in sign to the error described in the previous paragraph, and the two will therefore partially cancel. Furthermore, the waste fraction factor of 10.1 will again limit the actual calculated repository capacity increase.

One objection that may arise to the analysis presented in Sec. 6, Appendix N, and this appendix is that the time variation of decay heat of reprocessed fuel will differ from that of SNF because of the different isotopic compositions that characterize the unprocessed and reprocessed fuel. If the time profile of the decay heat is sufficiently different for reprocessed SNF compared to unprocessed SNF, the peak temperature could shift to longer or shorter times and thereby invalidate the comparisons. Indeed, as shown in Figure O-1, the decay heat for unprocessed SNF (top curve) shows a gradual decrease with time, while the decay heat of waste from the Scenario VII reprocessing scheme (bottom curve) decreases rapidly between 10 and 100 years and closely follows the decay of the lanthanides that contribute to most of the remaining decay heat at “short” times. This behavior is the cause of the observation that the “repository benefit” calculated at short times is smaller than that calculated at long times (*i.e.*, Tables 6-III and N-XIV). This observation also suggests that the peak far-field (zeolite layer) temperature may occur at shorter times and at lower temperatures for (suitably concentrated) Scenario VII waste compared to raw SNF. It is not clear from the published thermal analyses whether

this different heat release profile would benefit or weaken the repository mission of delaying the release of radionuclides.

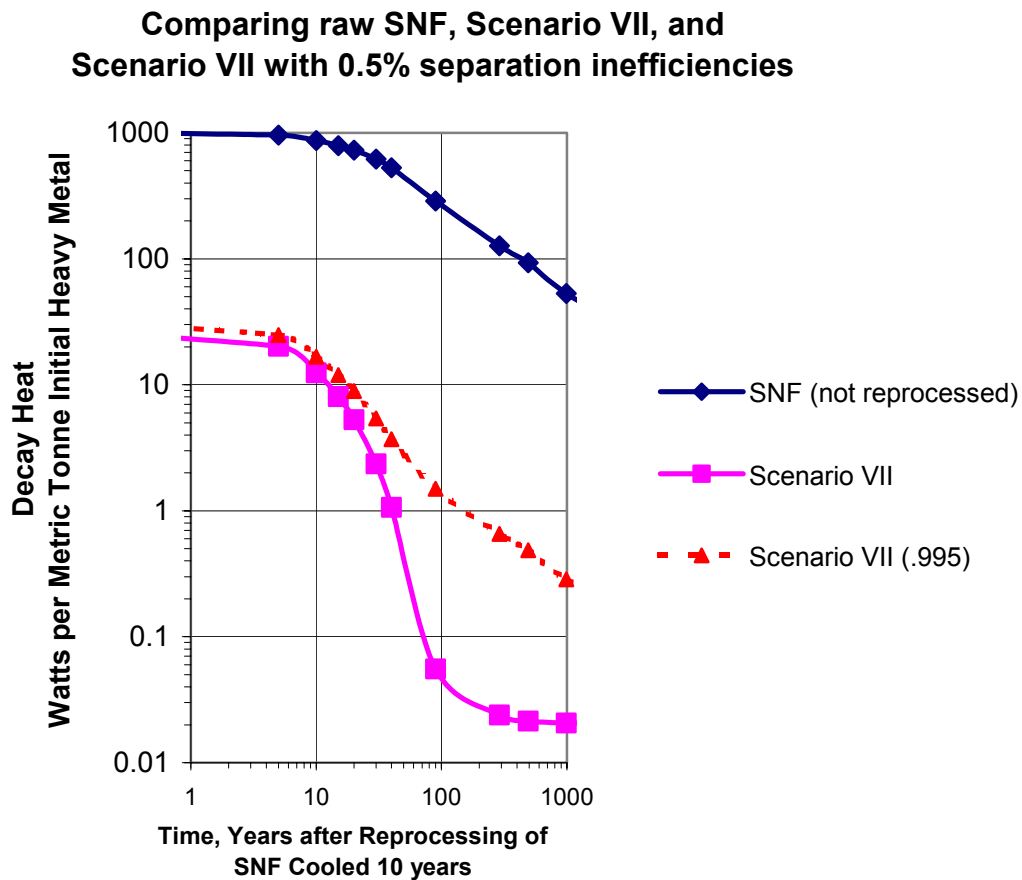


Figure O-1. Comparison of three decay heat profiles.

The decay-heat (time) profile, however, is also modified when separation inefficiencies are taken into account. The middle curve (dashed line) in Figure O-1 shows the decay heat of a modified Scenario VII, in which only 99.5% separations efficiency is assumed for removal of both short-term contributors to heat loads (caused primarily by Cs and Sr isotopes) and long-term contributors to heat loads (*e.g.*, primarily the actinides Pu, Am, and Cm). Note that the decay heat profile of the curve labeled “Scenario VII(0.995)” closely parallels that of the raw SNF; and indeed the ratio of decay heats is nearly constant; the change is less than 7% over the period 10-1,000 years after reprocessing, and is less than 2% over the period 15-500 years after reprocessing. It has previously been shown (Appendix M) that the assumption of reprocessing fuel cooled for only 10 years is not realistic if the existing (legacy) stores of SNF are considered and oldest fuel is reprocessed first (which has several benefits to the reprocessing plant, as well as mitigating related proliferation risks). Because the cooling time of reprocessed SNF will unlikely be less than 20 years during the “strawman” lifetime of YM (*i.e.*, emplacement starting 2010 until 63,000 MTIHM of SNF are emplaced at 3000 MTIHM/yr after a ramp-up period), only the period after 10 years shown on Figure O-1 (20 years cooling

corresponds to 10 years after the reprocessing assumed for the figure) should be considered. Estimates of increased repository capacity, therefore, can be made for heat release profiles [*e.g.*, the curve labeled ‘Scenario VII(0.995)’] that are essentially the same as that of raw SNF. The analysis presented in Sec. 6, therefore, is very likely to be representative of the results anticipated from the full 3-D, time-dependent thermal/hydraulic analyses that are planned to be undertaken in FY 2003.

Another source of error is our assumption that the limiting temperature constraints should be calculated by integrating the heat release for 40 years (tunnel wall temperature limits capacity of repository) or 300 years (zeolite layer temperature limits capacity of repository), rather than some other value of integration period. Figure O-2 shows the effect of varying the integration period for all separations schemes associated with Scenarios III-VII. The vertical dotted lines indicate the periods (40, 300 years) over which the integrations are performed. Changing the integration period from, *e.g.*, 40 years to 30 years decreases the repository benefit from 82 to 70-fold, still well above the waste package capacity limit of 26.9 and the (limiting) waste fraction limit of 10.1. For the cases where the limit is actually set by the integrated heat release, the slopes of the curves are much shallower and thus the percentage error is smaller (these scenarios are also not interesting because they would not be financially viable compared to Scenario VII).

Of course, time-dependent, 3-D finite element calculations should be performed for all the waste streams to determine a more accurate temperature profile, prior to accepting the conclusions of this report, and the “worst case” error due to separations inefficiency (or other error) should be propagated along with these calculations. But again, a simple analysis shows a small effect, and again the limiting constraint for the best performing separation scenario (Scenario VII) is set by the waste fraction in VHLW, not by the thermal constraint, and this is not affected by small errors in the thermal analysis.

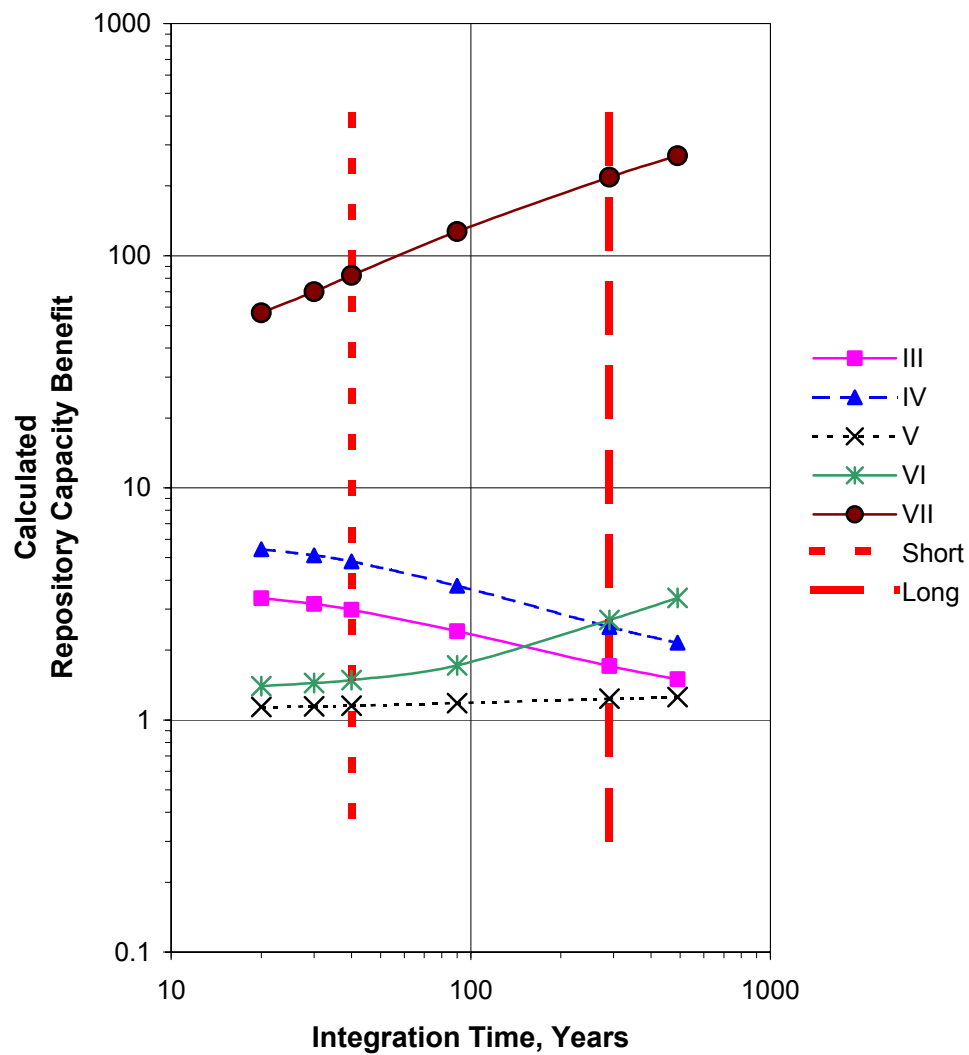


Figure O-2. Effect of Varying Integration Time on Repository Capacity Benefit for Standard LWR fuel.

